UNIVERSIDAD COMPLUTENSE DE MADRID
FACULTAD DE MEDICINA

TESIS DOCTORAL

Vesículas extracelulares derivadas de células madre mesenquimales: potencial terapéutico en el daño pulmonar agudo
Mesenchymal stem cell-derived extracellular vesicles: therapeutic potential in acute lung injury

MEMORIA PARA OPTAR AL GRADO DE DOCTOR

PRESENTADA POR

Sergio Antonio Esquivel Ruiz

Directores

Francisco Pérez Vizcaíno
Laura Moreno Gutiérrez

Madrid

UNIVERSIDAD COMPLUTENSE DE MADRID

Facultad de Medicina

Departamento de Farmacología y Toxicología

Vesículas extracelulares derivadas de células madre mesenquimales: potencial terapéutico en el daño pulmonar agudo

Mesenchymal stem cell-derived extracellular vesicles: therapeutic potential in acute lung injury

MEMORIA PARA OPTAR AL GRADO DE DOCTOR PRESENTADA POR

Sergio Antonio Esquivel Ruiz

DIRECTORES

Dr. Francisco Pérez Vizcaíno

Dra. Laura Moreno Gutiérrez

Madrid, 2022

INDEX

RESUMEN

El síndrome de distrés respiratorio agudo (SDRA) es una patología que se caracteriza por disfunción vascular pulmonar, fenómenos inflamatorios, alteraciones de la coagulación y edema pulmonar que produce colapso alveolar e hipoxemia arterial grave. Aunque las estrategias protectoras de soporte ventilatorio y hemodinámico han permitido mejorar el pronóstico, la mortalidad asociada se mantiene elevada por lo que el descubrimiento de nuevos tratamientos efectivos tendría un gran impacto en la supervivencia de los pacientes.

Las células madre mesenquimales (MSCs) se han propuesto como una posible terapia en diferentes patologías debido a su baja inmunogenicidad y a su capacidad de reparar el daño (debido a sus propiedades antiinflamatorias, antiapoptóticas, proangiogénicas y antifibróticas). Sin embargo, se ha demostrado que esta capacidad terapéutica se debe a la participación de mecanismos paracrinos, como puede ser la liberación de vesículas extracelulares (VEs). Varias evidencias han demostrado el potencial terapéutico de las vesículas extracelulares en diferentes modelos de daño pulmonar agudo e hipertensión pulmonar. Además, se ha demostrado que las MSCs presentan diferentes respuestas en función del ambiente en el que se encuentren, por lo que ha crecido el interés en la búsqueda de estrategias para incrementar sus efectos beneficiosos. Dentro de las estrategias de preacondicionamiento la hipoxia y la exposición a agonistas TLR3 han demostrado una mejora de la capacidad inmunomoduladora y angiogénica de las VEs.

HIPÓTESIS Y OBJETIVOS

La hipótesis general que nos planteamos en esta Tesis Doctoral es que la respuesta inflamatoria y disfunción vascular pulmonar asociada a SDRA puede ser revertida por el uso de EVs derivadas de MSCs.

El objetivo general de esta Tesis Doctoral es, por lo tanto, analizar el potencial terapéutico de EVs derivadas de MSCs y buscar estrategias de preacondicionamiento que sean capaces de incrementar este potencial.

MATERIALES Y MÉTODOS

MSCs de sangre de cordón umbilical fueron incubadas en ausencia o presencia del agonista TLR3 poly (I:C) (10 µg/mL) durante 1 hora y posteriormente se incubaron durante 72 horas en condiciones de normoxia (18.5 % O_2) o hipoxia (3% O_2). Tras esto, se llevó a cabo la purificación de vesículas extracelulares mediante ultracentrifugación y se procedió a su caracterización mediante microscopía electrónica de transmisión (TEM) y análisis de seguimiento de nanopartículas (NTA). El contenido proteico de las VEs se analizó mediante HPLC-MS y posterior análisis de enriquecimiento funcional.

Se ha utilizado un modelo de exposición *in vitro* a LPS en anillos de arteria pulmonar (AP), cultivos de células endoteliales de arterias pulmonares o cultivos primarios de células del músculo liso vascular humanas y de rata. Las células se incubaron durante 48 horas en medio DMEM en ausencia (control) o presencia de LPS (1 µg/mL) o vesículas extracelulares (5 µg/mL). Los anillos de AP se incubaron de igual manera durante 24 horas o se mantuvieron durante 48 horas en condiciones de normoxia o hipoxia más el antagonista de los receptores del factor de crecimiento endotelial vascular (VEGF, 10uM) en presencia de VEs hipóxicas. Después de los tratamientos se analizó la reactividad vascular (mediante el uso de miógrafos isométricos) y se determinaron los niveles de IL-6 o nitritos en los medios de cultivo (mediante ELISA o la reacción de Griess).

El potencial terapéutico de las vesículas extracelulares hipóxicas se evaluó en un modelo *in vivo* de SDRA inducido por la instilación intratraqueal de LPS. Este modelo consistió en la instilación de LPS (300 µg/Kg peso), VEs hipóxicas (0.1 µg/mL) o solución salina por vía intratraqueal. Cuatro horas después del tratamiento se midieron diversos parámetros hemodinámicos, la saturación de oxígeno y se recogieron muestras para el posterior análisis histológico pulmonar, la determinación de citoquinas o la medida de la actividad mieloperoxidasa.

RESULTADOS

El preacondicionamiento hipóxico indujo un incremento de la producción de VEs por las MSCs sin verse afectada la proliferación de estas. En cambio, no se

observaron diferencias en el tamaño medio y la moda. El análisis proteómico confirmó la expresión de marcadores vesiculares y de célula inmadura típicos, demostró que el protocolo de purificación era adecuado y que el protocolo de exposición a hipoxia utilizado no producía un proceso de diferenciación de las MSCs. El análisis bioinformático de las proteínas encontradas en las VEs (552) mostró que la exposición a hipoxia provoca el cambio en la expresión de 15 proteínas implicadas en la modulación de vías relacionadas con la adhesión celular, la señalización de las integrinas, la regulación del citoesqueleto y el desarrollo embrionario.

El LPS produce un incremento de la actividad iNOS, se traduce en la producción de niveles excesivos de óxido nítrico que provocan alteraciones funcionales entre las que destacan una hiporrespuesta a fenilefrina. Ninguna de las VEs fue capaz de revertir esta alteración, e incluso las vesículas expuestas al agonista TLR3 poly (I:C) (TLR3-VEs) o a ambas estrategias de preacondicionamiento (Hypo+TLR3-VEs) produjeron una disminución de la respuesta más pronunciada. Además de esta hiporrespuesta, el LPS produce hiperrespuesta a serotonina, disfunción endotelial y fracaso de la vasoconstricción pulmonar hipóxica (VPH). Las VEs hipóxicas (HypoVEs) fueron capaces de revertir todas estas alteraciones funcionales de manera significativa. Los niveles de IL-6 se vieron incrementados por el LPS y las HypoVEs fueron capaces de disminuir esta producción en cultivos de células musculares lisas de AP humanas y de rata pero no en células endoteliales de AP. Por el contrario, observamos un incremento en la liberación de IL-6 al medio de cultivo por parte de arterias aisladas, lo que podría reflejar los efectos de las VEs sobre otras células presentes en la pared vascular (por ejemplo, fibroblastos o pericitos). Además, aunque el LPS no afectó la viabilidad celular de las células endoteliales de AP, el tratamiento con las HypoVEs produjo un aumento significativo de su viabilidad.

En el modelo *in vivo* de ALI inducido por exposición a LPS se observó un incremento de la presión arterial pulmonar (PAP), una disminución de la saturación de oxígeno, formación de edema e incremento de los niveles de IL-1β, IL-6, TNF-α y ET-1 tanto a nivel pulmonar como sistémico. Las VEs hipóxicas

fueron capaces de normalizar los valores de la PAP y aumentar la saturación de oxígeno, sin modificar la frecuencia cardíaca. También se observó una disminución en el número y área de los edemas y en los niveles de IgM, células inmunitarias y citoquinas. Cabe destacar la buena correlación observada entre los niveles de citoquinas y la PAP media.

El modelo *in vitro* de HAP por exposición a hipoxia y el antagonista del receptor de VEGF SU5416 reprodujo las alteraciones funcionales de este modelo *in vivo* de HAP, incluyendo el desarrollo de disfunción endotelial y la hiperrespuesta a serotonina. En esta ocasión, las VEs hipóxicas solo fueron capaces de revertir parcialmente la respuesta a serotonina.

En cuanto al preacondicionamiento con el agonista TLR3, el tratamiento con las TLR3-VEs produjo una mejora parcial de la hiperrespuesta a serotonina y del fracaso de la VPH, pero provocó una disminución de la contracción a KCl. Los niveles de IL-6 en el medio de cultivo de las arterias también se vieron incrementados por la exposición a estas.

La combinación de ambas estrategias de preacondicionamiento se tradujo en la desaparición de los efectos beneficiosos observados por separado, por lo que se desaconseja su utilización.

CONCLUSIONES

1. La exposición a hipoxia de células madre mesenquimales (MSCs) derivadas de cordón umbilical aumenta la liberación de vesículas extracelulares, modificando su contenido proteico, pero sin alterar la expresión de marcadores específicos de vesículas extracelulares ni el tamaño de las vesículas liberadas.

2. Entre las 552 proteínas identificadas en el interior de estas VEs, el precondicionamiento hipóxico provoca el cambio en la expresión de 15 proteínas implicadas en la modulación de vías relacionadas con la adhesión celular, la señalización de las integrinas, la regulación del citoesqueleto y el desarrollo embrionario.

3. Las VEs liberadas por las MSCs en condiciones de hipoxia, pero no de normoxia, son capaces de prevenir la disfunción vascular pulmonar (disfunción endotelial, hiperrespuesta a serotonina, fracaso de la vasoconstricción pulmonar hipóxica) en modelos *in vitro* de SDRA e HAP.

4. La administración intratraqueal de VEs hipóxicas previene la respuesta inflamatoria, la alteración de la permeabilidad capilar pulmonar y el desarrollo de edema pulmonar y el aumento de la presión arterial pulmonar además de reducir parcialmente la hipoxemia al inducir una ligera mejora en el acoplamiento entre la ventilación y la perfusión en ratas sometidas a un modelo de daño pulmonar agudo inducido por la instilación intratraqueal de LPS.

5. La utilización de otras estrategias de precondicionamiento, como el empleo del agonista de TLR3 poly (I:C) combinado o no con hipoxia, provocó resultados insatisfactorios con una disminución de los efectos terapéuticos y un posible mayor riesgo de reacciones adversas. Nuestros datos desaconsejan, por tanto, la utilización de estas estrategias de precondicionamiento.

6. En conjunto, los resultados de esta Tesis Doctoral sugieren que el precondicionamiento hipóxico aumenta el potencial terapéutico de las VEs producidas por las MSCs y podría representar una nueva estrategia terapéutica para el tratamiento de enfermedades vasculares pulmonares asociadas con inflamación.

ABSTRACT

Abstract

Acute respiratory distress syndrome (ARDS) is a pathology characterized by pulmonary vascular dysfunction, inflammatory phenomena, coagulation disorders and pulmonary oedema leading to alveolar collapse and severe arterial hypoxaemia. Although protective ventilatory and haemodynamic support strategies have improved prognosis, the mortality associated remains high and the discovery of new effective treatments would have a major impact on patient survival.

Mesenchymal stem cells (MSCs) have been proposed as a possible therapy in different pathologies due to their low immunogenicity and their ability to repair damage (due to their anti-inflammatory, anti-apoptotic, proangiogenic and anti-fibrotic properties). However, this therapeutic capacity has been shown to be due to the involvement of paracrine mechanisms, such as the release of extracellular vesicles (EVs). Several studies have demonstrated the therapeutic potential of extracellular vesicles in different models of acute lung injury and pulmonary hypertension. In addition, MSCs have been shown to exhibit different responses depending on the environment in which they are found, which has led to a growing interest in the search for strategies to increase their beneficial effects. Among the preconditioning strategies, hypoxia and exposure to TLR3 agonists have been shown to enhance the immunomodulatory and angiogenic capacity of EVs.

HYPOTHESIS AND AIMS

The general hypothesis of this PhD thesis is that the lung inflammatory response and pulmonary vascular dysfunction associated with ARDS can be prevented by the use of MSC-derived extracellular vesicles (EVs).

The overall objective of this PhD thesis is, therefore, to analyse the therapeutic potential of MSC-derived EVs and to search for preconditioning strategies that are able to increase this potential.

MATERIALS AND METHODS

Cord umbilical blood MSCs were incubated in the absence or presence of TLR3 poly (I:C) agonist (10 µg/mL) for 1 hour and then incubated for 72 hours under

normoxic (18.5 % O_2) or hypoxic (3% O_2) conditions. After this, extracellular vesicles were purified by ultracentrifugation, followed by their characterisation by transmission-electronic microscopy (TEM) or nanoparticle tracking analysis (NTA). The protein cargo was analysed by HPLC-MS and functional enrichment analysis.

An *in vitro* LPS exposure model was used in pulmonary artery (PA) rings, pulmonary artery endothelial cell cultures or primary cultures of human and rat vascular smooth muscle cells. Cells were incubated for 48 hours in DMEM medium in the absence (control) or presence of LPS (1 µg/mL) or extracellular vesicles (5 µg/mL). PA rings were incubated under similar conditions for 24 hours or maintained for 48 hours under normoxic or hypoxic conditions plus a vascular endothelial growth factor receptor antagonist (VEGF, 10 µM) in the presence of hypoxic EVs. After treatments, vascular reactivity was analysed (using isometric myographs) and levels of IL-6 or nitrite in the culture media were determined (by ELISA or Griess reaction).

The therapeutic potential of hypoxic extracellular vesicles was evaluated in a model of ARDS induced by intratracheal instillation of LPS. This model consisted of instillation of LPS (300 µg/kg body weight), hypoxic EVs (0.1 µg/mL) or saline intratracheally. Four hours after treatment, haemodynamic parameters and oxygen saturation were measured and samples were collected for subsequent lung histological analysis, cytokine determination or measurement of myeloperoxidase activity.

RESULTS

Hypoxic preconditioning induced an increase in EV production without affecting the proliferation of MSCs. However, no differences in the mean size and mode were observed. Proteomic analysis confirmed the expression of classical vesicular and stem cell markers suggesting that the purification protocol was adequate and that protocol used for hypoxic preconditioning did not induce the differentiation of MSCs. Bioinformatic analysis of the proteins found in EVs (552) revealed that hypoxic preconditioning significantly modified the expression of

proteins involved in the modulation of pathways related to cell adhesion, integrin signaling, cytoskeleton regulation and embryonic development.

LPS leads to increased iNOS activity resulting in excessive production of nitric oxide (NO) causing functional alterations including a hyporesponsiveness to phenylephrine. None of the EVs was able to reverse this alteration, and vesicles exposed to the TLR3 poly (I:C) agonist (TLR3-EVs) or to both preconditioning strategies (Hypo+TLR3-EVs) even produced a more pronounced decrease in the contractile responses to phenylephrine. In addition to this hyporesponsiveness, LPS produces serotonin hyperresponsiveness, endothelial dysfunction and failure of hypoxic pulmonary vasoconstriction (HPV). Hypoxic EVs (HypoEVs) were able to significantly reverse all these functional alterations. IL-6 levels were increased by LPS and HypoEVs were able to decrease this production in cultured human and rat PA smooth muscle cells without affecting PA endothelial cells. In contrast, an increase in IL-6 released by whole PA in the culture medium of arteries was observed following incubation with hypoxic EVs, which may reflect the actions of these EVs in other cell types (e.g., fibroblasts or pericytes). Although LPS did not reduce the cell viability of PA endothelial cells, treatment with HypoEVs significantly increased it.

In the *in vivo* model of ALI induced by administration of LPS, increased pulmonary arterial pressure (PAP), decreased oxygen saturation, oedema formation and increased levels of IL-1β, IL-6, TNF-α and ET-1 were observed at both pulmonary and systemic levels. Hypoxic EVs were able to normalize PAP levels and increase oxygen saturation, without changing heart rate. A decrease in the number and area of oedema and in the levels of IgM, immune cells and cytokines was also observed. A strong correlation was observed between cytokine levels and mean PAP.

The *in vitro* model of PAH induced by exposure to hypoxia and the VEGF receptor antagonist SU5416 reproduced the functional alterations found in the *in vivo* model, including endothelial dysfunction and hyperresponsiveness to serotonin. Hypoxic EVs were only able to partially reverse the serotonin hyperresponsiveness in this model.

Finally, following preconditioning with the TLR3 agonist, TLR3-EVs produced partial improvements in serotonin hyperresponsiveness and HPV failure, but significantly reduced the contraction induced by KCl. IL-6 levels in the culture medium of the arteries were also increased following treatment with these vesicles.

The combination of both preconditioning strategies resulted in the disappearance of the beneficial effects observed separately, and their use is therefore discouraged.

CONCLUSIONS

1. Exposure of umbilical cord-derived mesenchymal stem cells (MSCs) to hypoxia increases the release of extracellular vesicles (EVs), modifying their protein content but without altering their size or the expression of specific markers of extracellular vesicles.

2. Among the 552 proteins identified within these EVs, hypoxic preconditioning significantly modified the expression of 15 proteins involved in the modulation of pathways related to cell adhesion, integrin signaling, cytoskeleton regulation and embryonic development.

3. EVs released by MSCs under hypoxic, but not normoxic, conditions were able to prevent pulmonary vascular dysfunction (endothelial dysfunction, hyperresponsiveness to serotonin, failure of hypoxic pulmonary vasoconstriction) in *in vitro* models of acute respiratory distress syndrome (ARDS) and pulmonary arterial hypertension (PAH).

4. Intratracheal administration of hypoxic EVs prevents the inflammatory response, the disruption of the pulmonary capillary barrier, the development of pulmonary oedema and the increase in pulmonary arterial pressure in rats exposed to a model of acute lung injury induced by intratracheal instillation of LPS. Furthermore, hypoxic EVs were able to

protect against the development of hypoxaemia by inducing a modest improvement in ventilation-perfusion coupling *in vivo*.

5. Evaluation of other preconditioning strategies, such as the TLR3 agonist poly (I:C) combined or not with hypoxia resulted in a reduction of their therapeutic potential.

6. In summary, the results of this PhD thesis suggest that hypoxic preconditioning enhances the therapeutic potential of EVs produced by MSCs and could represent a new therapeutic approach for the treatment of pulmonary vascular diseases associated with inflammation.

LIST OF ABBREVIATIONS

AECs = alveolar epithelial cells

AJ = adherens junctions

ALI = acute lung injury

AM = alveolar macrophages

Ang-1 = angiopoietin-1

APC = activated protein C

ARDS = acute respiratory distress syndrome

ATI/II = alveolar type I/II

BALF = bronchoalveolar lavage fluid

Bcl-2 = B-cell lymphoma 2

BM = bone marrow

CD = cluster of differentiation

CM = conditioned medium

CO_2 = carbon dioxide

COVID-19 = coronavirus disease 2019

CXC = chemokine (C-X-C motif)

$ECCO_2R$ = extracorporeal carbon dioxide removal

ECM = 21xtracelular matrix

EDHF = endothelium derived hyperpolarizing factor

eNOS = endothelial nitric oxide synthase

ESCRT = endosomal sorting complexes required for transport

ET-1 = endothelin-1

Evs = extracellular vesicles

FDR = false discovery rate

FGF2 = fibroblast growth factor 2

FiO_2 = fraction of inspired oxygen

FN = fibronectin

HCl = hydrochloric acid

HFOV = high-frequency oscillatory ventilation

HGF = hepatocyte growth factor

HLMVECs = human lung microvascular endothelial cells

HO-1 = heme oxygenase-1

HPLC-MS = high performance liquid chromatography-tandem mass spectrometry

HPV = hypoxic pulmonary vasoconstriction

ICAM-1 = intercellular cell adhesion molecule-1

ICUs = Intensive Care Units

IDO = indolamine 2,3 deoxygenase

IGF-1 = insulin-like growth factor 1

IFN-γ = interferon gamma

IL = interleukin

iNO = inhaled nitric oxide

iNOS = inducible nitric oxide synthase

I/R = ischemia/reperfusion

ISEV = International Society of Extracellular Vesicles

IT = intratracheal

IV = intravenous

KGF = keratinocyte growth factor

LBP = LPS binding protein

MIP = macrophage inflammatory protein

MPO = myeloperoxidase

MSCs = mesenchymal stem cells

mTOR = mammalian target of rapamycin

MVs = microvesicles

NMBA = neuromuscular blocking agents

NO = nitric oxide

NTA = nanoparticle tracking analysis

PaO_2 = partial pressure of arterial oxygen

PAP = pulmonary arterial pressure

PAR1 = protease-activated receptor-1

PBS = phosphate-buffered saline

PECAM-1 = platelet-endothelial cell adhesion molecule-1

PEEP = positive end-expiratory pressure

PGE = prostaglandin E

PGI2 = prostacyclin

PMNs = polymorphonuclear cells

PVD = pulmonary vascular dysfunction

RAGE = receptor for advanced glycation endproducts

RANTES = regulated on activation, normal T cell expressed and secreted

ROS = reactive oxygen species

RV = right ventricle

SaO_2 = oxygen saturation

SARS-CoV-2 = severe acute respiratory syndrome coronavirus-2

TEM = transmission electron microscopy

TF = tissue factor

TGF-β = transforming growth factor β

TJs = tight junctions

TLR = toll-like receptor

TNF-α = tumour necrosis factor α

TSG-101 = tumor susceptibility gene 101

TXA-2 = thromboxane A_2

UCB = umbilical cord blood

VCAM-1 = vascular cell adhesion molecule-1

VE-cadherin = vascular endothelial cadherin

VEGF = vascular endothelial growth factor

VILI = ventilator-induced lung injury

VSMCs = vascular smooth muscle cell

WHO = World Health Organization

INTRODUCTION

1. EXTRACELLULAR VESICLES

Extracellular vesicles (EVs) represent an heterogeneous set of membrane enclosed spheres of different sizes that are secreted by a variety of cell types, including T cells, B cells, dendritic cells, platelets, mast cells, epithelial cells, endothelial cells (ECs), neuronal cells, cancerous cells, oligodendrocytes, Schwann cells, embryonic cells, and mesenchymal stem cells (MSCs) (Raposo and Stoorvogel 2013, Borgovan, Crawford et al. 2019). They are shed or secreted from these cell types under various physiologic and pathologic conditions (Figure 1) into the circulation or surrounding body fluids, including blood or bronchoalveolar lavage fluid (BALF) (Witwer, Buzas et al. 2013, Cocucci and Meldolesi 2015, Konala, Mamidi et al. 2016, Borgovan, Crawford et al. 2019).

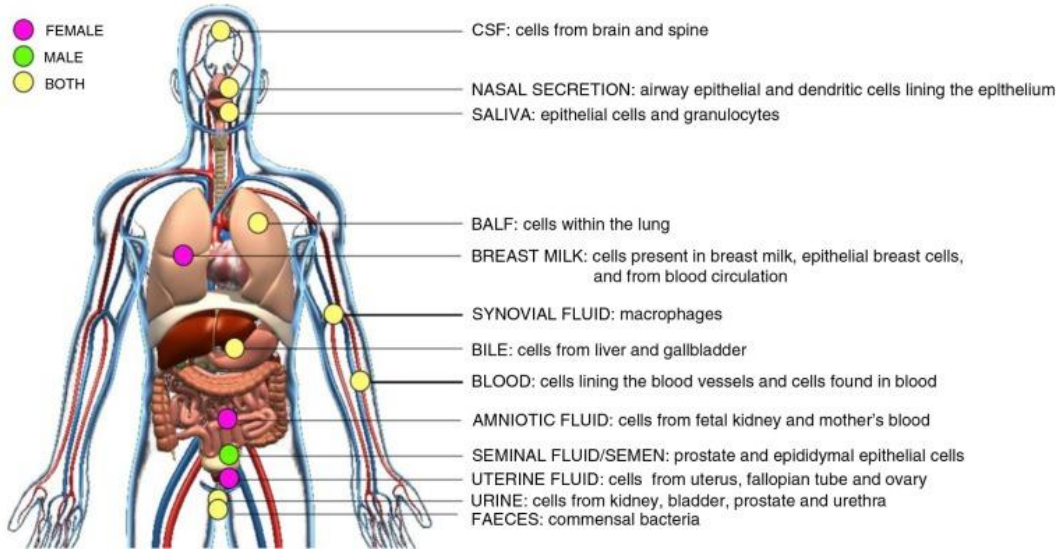

Figure 1. *EVs can be released by different cells and can be found in different biological fluids (Yanez-Mo, Siljander et al. 2015).*

The International Society of Extracellular Vesicles (ISEV) establishes the minimum requirements for the collection and pre-processing of samples and for the separation, concentration and characterization of EVs, as well as the steps to demonstrate that a function is associated specifically with EVs (Thery, Witwer et al. 2018, Nieuwland, Falcon-Perez et al. 2020). According to the ISEV, three main sub-groups of EVs have been classified based on their size, membrane composition and biogenesis (Raposo and Stoorvogel 2013, Witwer, Buzas et al.

2013), this classification is summarized in Table 1. Apoptotic bodies (50-5000 nm) are the largest EVs and are formed during cellular apoptosis by cell membrane-blebbing. Apoptotic bodies contain histones and genomic DNA. Microvesicles (MVs; 100-1000 nm) are shed via the outward blebbing of the plasma membrane, allowing retention of the membrane proteins of the parent cell. MVs are rich in the surface marker CD40, integrins and selectins as well as cholesterol, sphingomyelin, and ceramide. Exosomes (40-120 nm) are the smallest subgroup and are released after multiple vesicular bodies fuse with the plasma membrane. Exosomes may express distinct biomarkers, including tetraspanins (CD61, CD63 or CD81), ESCRT proteins (TSG101 and Alix), flotillin, and heat shock proteins, as well as high acetylcholinesterase activity (Crescitelli, Lässer et al. 2013, Raposo and Stoorvogel 2013, Cocucci and Meldolesi 2015, Yanez-Mo, Siljander et al. 2015, Borgovan, Crawford et al. 2019). Since exosomes and MVs can overlap in the size range and current methods are unable to separate these populations efficiently, the International Society of Extracellular Vesicles (ISEV) has encouraged using the generic term of "extracellular vesicles" (Thery, Witwer et al. 2018).

Characteristic	Exosomes	Microvesicles	Apoptotic bodies
Size	40-120 nm	100-1000 nm	50-5000 nm
Morphology	Cup-shaped	Heterogeneous	Heterogeneous
Formation mechanism	Multivesicular body	Plasma membrane	Plasma membrane
Pathways	1) ESCRT-dependent 2) Tetraspanin-dependent 3) Ceramide-dependent	1) Ca+2-dependent 2) Stimuli-dependent	Apoptosis-related pathways
Content	Proteins, lipids, and nucleic acids	Proteins, lipids, and nucleic acids	Nuclear fractions, cell organelles
Markers	Alix, Tsg101, tetraspanins (CD81, CD63, CD9), flotillin, heat shock proteins. High acetylcholinesterase activity	Integrins, selectins, CD40	Annexin V, phosphatidylserine
	Definitive markers for the different EV subpopulations do not exist.		

Table 1*. Types of extracellular vesicles based on their size and biogenesis pathways (Esquivel-Ruiz, Gonzalez-Rodriguez et al. 2021).*

EVs are carriers of biologically active molecules (nucleic acids, proteins and lipids), whose composition vary based on the parent cell phenotype and biological state (Keerthikumar, Chisanga et al. 2016, Pathan, Fonseka et al. 2019, Xie, Liu et al. 2020). Proteins carried by EVs include chemokines, and inflammatory cytokines, integrins, growth factors, enzymes or even cytoskeletal components (Gutierrez-Vazquez, Villarroya-Beltri et al. 2013, Keerthikumar, Chisanga et al. 2016, Maas, Breakefield et al. 2017, Mardpour, Hamidieh et al. 2019). Nucleic acid cargo in EVs comprise mitochondrial and genomic DNA, small non-coding RNA species (such as microRNA or tRNA, small nucleolar RNA, and small nuclear RNA) and long non-coding RNA species (Kalra, Simpson et al. 2012, Keerthikumar, Chisanga et al. 2016, Xie, Liu et al. 2020). EVs are also an important source of lipids, including sphingomyelin, ceramides, phosphatidylserine, cholesterol or saturated fatty acids (Gutierrez-Vazquez, Villarroya-Beltri et al. 2013, Chatterjee, Yang et al. 2020).

2. ACUTE LUNG INJURY (ALI) AND RESPIRATORY DISTRESS SYNDROME (ARDS)

2.1. Definition

Acute Lung Injury (ALI) and its more severe form, Acute Respiratory Distress Syndrome (ARDS), were first described in 1967 (Ashbaugh, Bigelow et al. 1967). According to the definition approved by the 1994 American-European Consensus Conference, ARDS was defined by: (1) the acute onset of bilateral infiltrates due to increased pulmonary vascular permeability on chest imaging, (2) the acute onset of hypoxaemia with a partial pressure of arterial oxygen (PaO_2) to fraction of inspired oxygen (FiO_2) ratio of <200, and (3) the absence of left heart failure (Bernard, Artigas et al. 1994). A similar definition was agreed for ALI, except for a higher limiting value of <300 mmHg for PaO_2/FiO_2 (Bernard, Artigas et al. 1994), which means that ARDS represent the more severe form of ALI.

In 2012 a new classification of ARDS, known as the Berlin classification, was published (Force, Ranieri et al. 2012). According to this classification, the ARDS

is classified as mild, moderate or severe by using a partial pressure of arterial oxygen (PaO_2) to fraction of inspired oxygen (FIO_2) threshold of 300, 200, and 100 mmHg respectively (Force, Ranieri et al. 2012). According to the Berlin definition, the term ALI was removed as a clinical entity since the committee felt that this term was used inappropriately in many contexts and hence was not helpful. However, the term ALI is still widely used in preclinical models.

2.2. Epidemiology

ARDS currently represents one of the leading causes of severe respiratory failure in Intensive Care Units (ICUs). The incidence of ARDS has been difficult to assess due to non-uniform definitions, aetiological and geographical variations, inadequate documentation and lack of awareness of the entity. In 2005, the annual incidence in the United States was estimated to be approximately 200,000 patients with a mortality rate of 40% (Rubenfeld, Caldwell et al. 2005, Villar, Blanco et al. 2011, Bellani, Laffey et al. 2016). The incidence of ARDS varies by age. In a multicenter prospective cohort study, the age-adjusted incidence estimates ranged from 64 to 86 per 100,000 person-years for moderate to severe ARDS (Rubenfeld, Caldwell et al. 2005). ARDS is associated with high mortality and morbidity rates, which increase with disease severity (Estenssoro, Dubin et al. 2002, MacCallum and Evans 2005, Bellani, Laffey et al. 2016). A multicenter prospective cohort study by Bellani *et al*. showed that 10.4% of those admitted to participating ICUs and 23.4% of those requiring mechanical ventilation exhibited ARDS criteria and reported that the rate of hospital mortality was 34.9% in patients with mild ARDS, 40.3% for those with moderate ARDS, and 46.1% for those with severe ARDS (Bellani, Laffey et al. 2016). The mortality rate of ARDS has decreased in recent years due to the use of protective mechanical ventilation strategies and other improvements in ICUs, including more effective treatment of sepsis (Maybauer, Maybauer et al. 2006, Seeley, McAuley et al. 2008, Zambon and Vincent 2008, Erickson, Martin et al. 2009).

ARDS can occur in the setting of either direct (pneumonia, aspiration, contusion) or indirect (sepsis, trauma, pancreatitis) lung insults (Ware and Matthay 2000, Wheeler and Bernard 2007, Bastarache and Blackwell 2009). The underlying

cause of ARDS is a critical determining factor of the mortality rate. Patients with ARDS rarely die due to respiratory failure alone. In the Bersten *et al*. study (Bersten, Edibam et al. 2002), pneumonia and sepsis were the most common causes of death, accounting for 30% and 32% of deaths, respectively. Other aetiologies of ARDS accounted for 38% of deaths, including aspiration (17%), trauma (13%), transfusion (3.3%), pancreatitis (2%), and drug overdose (0.7%) (Eisner, Thompson et al. 2001, Bersten, Edibam et al. 2002). The risk increases also in patients with multiple comorbidities, chronic lung disease or who suffer from chronic alcoholism (Ware and Matthay 2000).

As of 2020, a novel coronavirus, named as severe acute respiratory syndrome coronavirus-2 (SARS-CoV-2), emerged as one of the leading causes of ARDS worldwide (Kaye, Cornett et al. 2021, Pfortmueller, Spinetti et al. 2021). The World Health Organization (WHO) announced the official name for the epidemic disease caused by SARS-CoV-2 as coronavirus disease 2019 (COVID-19). Currently, COVID-19 has spread widely around the world, affecting to almost all countries (Russell, Wu et al. 2021). ARDS is the major cause of death in COVID-19 patients with an incidence of up to 68% in hospitalized patients (Tzotzos, Fischer et al. 2020). As of 21 November 2021, more than 257 million cases and 5.14 million deaths have been confirmed, making the pandemic one of the deadliest in history. The reported median age of patients was ranged from 41 to 57 years and male made up most patients with the proportion of 50–75% (Chen, Zhou et al. 2020, Huang, Wang et al. 2020, Xu, Wu et al. 2020). Approximately 25.2–50.5% SARS-CoV-2 infected patients had one or more underlying diseases, including hypertension, diabetes, chronic obstructive pulmonary disease, cardiovascular disease, and malignancy (Chen, Zhou et al. 2020, Huang, Wang et al. 2020, Xu, Wu et al. 2020). A study of early transmission dynamics of COVID-19 revealed that the mean incubation period was 5.2 days (95% confidence interval, 4.1-7.0), with the 95th percentile of the distribution at 12.5 days (Li, Guan et al. 2020, Zhai, Ding et al. 2020). Experts suggest 14 days for quarantine (Rahimi Pordanjani, Hasanpour et al. 2021). Human-to-human transmission occurs mainly via droplets from coughing or sneezing or direct contact (Chan, Yuan et al. 2020, Chen 2020, Ge, Wang et al. 2020, Rothe,

Schunk et al. 2020). Mortality for COVID-19 appears to be higher than that for influenza, especially seasonal influenza (Rahman, Montero et al. 2021).

2.3. Pathophysiology of ALI

The pathological hallmark of ARDS is diffuse alveolar damage with an early alveolar epithelial-capillary barrier disruption. ARDS is characterized by pulmonary oedema and alveolar collapse accompanied by ventilation-perfusion (V/Q) mismatch and severe arterial hypoxaemia (Thompson, Chambers et al. 2017, Kaku, Nguyen et al. 2020).

In the acute phase called exudative (Figure 2), there is inflammation with recruitment of neutrophils and macrophages in the alveolar space, release of pro-inflammatory mediators (TNF-α, IL-6, IL-1, IL-8), hyaline membrane formation, accumulation of protein-rich fluid in the pulmonary parenchymal interstitium, inactivation of surfactant, atelectasis and impaired gas exchange (Katzenstein, Bloor et al. 1976, Bachofen and Weibel 1977, Piantadosi and Schwartz 2004, Pierrakos, Karanikolas et al. 2012). Clinically, this early or exudative phase of ARDS is characterized by marked hypoxaemia and decreased lung compliance (Ashbaugh, Bigelow et al. 1967, Matthay, Zemans et al. 2019). This acute phase may resolve completely, or it may progress to the fibroproliferative phase with persistent hypoxaemia, increased dead space, further loss of lung compliance, lung fibrosis, and neovascularization of the lung (Figure 2) (Pierrakos, Karanikolas et al. 2012, Kaku, Nguyen et al. 2020). In some patients the proliferative process stops and rapid resolution is observed. In others, however, progressive diffuse fibrosis develops, with alveolar obliteration and destruction or collapse of pulmonary vessels (chronic phase) (Wheeler and Bernard 2007, Tsushima, King et al. 2009). The clinical course of ARDS is variable. Some patients recover within 1-2 weeks, while others suffer a more extended course and require prolonged mechanical ventilation. Resolution of lung injury involves suppression of apoptotic neutrophils, matrix remodelling, resolution of protein-rich alveolar fluid and activation of numerous distinct signalling pathways (Tsushima, King et al. 2009).

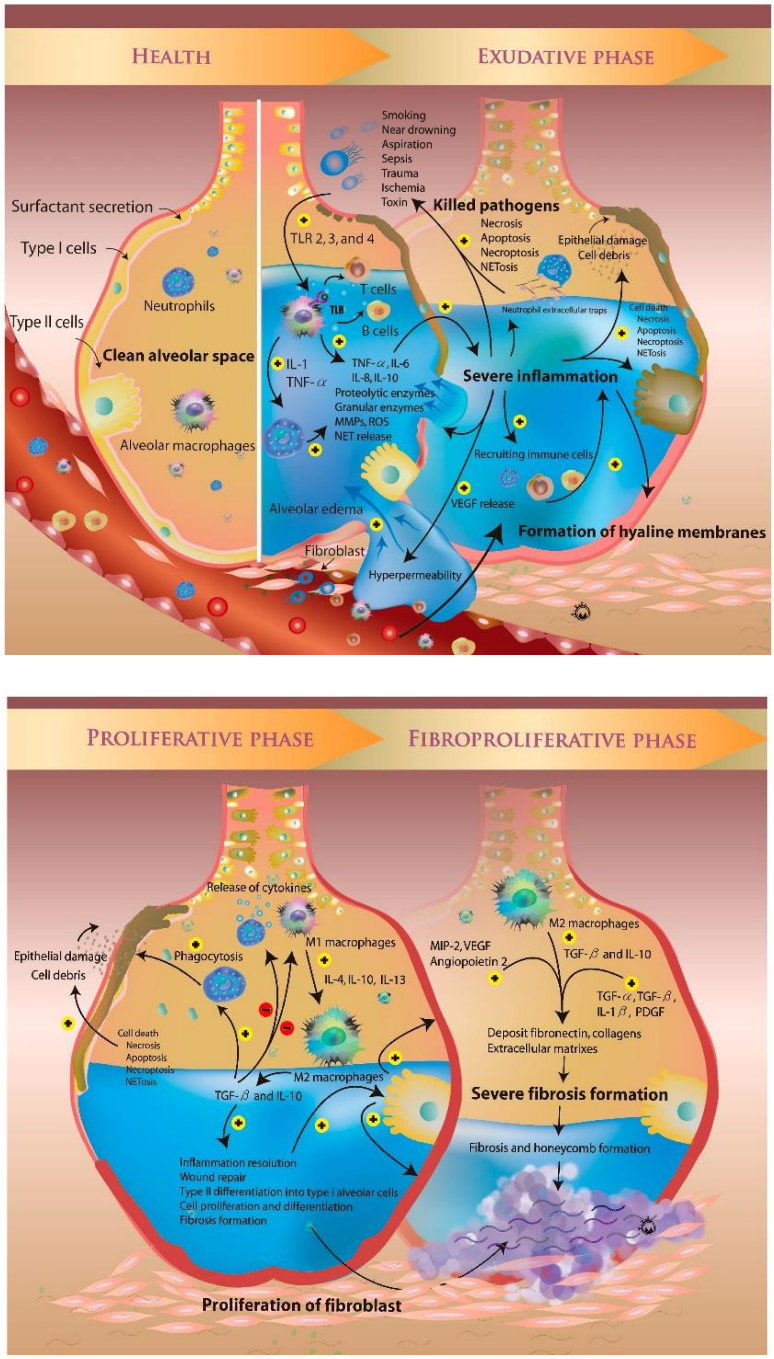

Figure 2. *The molecular regulation of the pathogenesis of acute respiratory distress syndrome (ARDS) in four major phases: health, exudative phase, proliferative phase and fibroproliferative phase (Yang, Chen et al. 2018).*

COVID-19 reveal the typical features of ARDS, including exudative and proliferative phases (Carsana, Sonzogni et al. 2020, Swenson, Ruoss et al. 2021). Possibly somewhat more pronounced in COVID-19 than in ARDS is a greater extent of vascular abnormalities, including macrothrombosis and microthrombosis, endothelial-cell injury, vascular dilation and aberrant angiogenesis (Ackermann, Verleden et al. 2020, Carsana, Sonzogni et al. 2020, Menter, Haslbauer et al. 2020, Ranucci, Ballotta et al. 2020). These vascular findings, also occurring in many other organs, have led to the idea that COVID-19 lung injury is part of a broader systemic vascular pathology differing from that of ARDS (Lang, Som et al. 2020, Mangalmurti, Reilly et al. 2020, Swenson, Ruoss et al. 2021). Also, preliminary reports suggest that severe COVID-19 can present as an atypical form of ARDS with significant dissociation between relatively well-preserved lung mechanics and severe hypoxaemia. Although controversial, it has been hypothesized that COVID-19 pneumonia may exist on a spectrum between two phenotypes. In the early phase, the less severe form (referred to as “type L”) may be associated with preserved lung mechanics with hypoxia (low elastance, low recruitability and low ventilation to perfusion ratio). In contrast, the more severe form (“type H”) reassembles more closely common ARDS characterized by high elastance, high right-to-left shunt and high recruitability, analogous to what is experienced in common acute respiratory distress (Gattinoni, Camporota et al. 2020).

2.3.1. Inflammation and coagulation

Inflammatory responses have key effects on every phase of ARDS (de Hemptinne, Remmelink et al. 2009). This can occur as a result of a direct injury to the lung (such as aspiration of gastric contents) or as a response to systemic inflammation and cytokine production. Mortality in ARDS correlates with increasing neutrophil number and increasing levels of circulating pro-inflammatory cytokines (Steinberg, Milberg et al. 1994, Headley, Tolley et al. 1997). An imbalance in pro- and antiinflammatory cytokines may promote ARDS as expression of pro-inflammatory cytokines (e.g. TNF-α and IL-1β) is increased while levels of antiinflammatory cytokines (IL-10) are lower in ARDS patients

compared to critically ill non-ARDS patients (Siler, Swierkosz et al. 1989, Armstrong and Millar 1997, Lo, Fu et al. 1998, Park, Goodman et al. 2001, Alcorn 2019).

Many cells and mediators are involved in the inflammatory response. The alveolar resident macrophages and the airway and alveolar epithelial cells (AECs) express pathogen recognition receptors whose stimulation produces secretion of pro-inflammatory cytokines (TNF-α, IL-1β, IL-6, IL-8, interferon gamma [IFN-γ] and granulocyte macrophage colony-stimulating factor), reactive oxygen radicals, platelet-activating factor, growth factors, chemokines and adhesion molecules to recruit inflammatory cells from the blood and surrounding tissue to the site of infection (Franke-Ullmann, Pfortner et al. 1996, Park, Goodman et al. 2001, Mariathasan and Monack 2007, Whitsett, Wert et al. 2010, Holtzman, Byers et al. 2014, Alcorn 2019). Neutrophils are recruited in response to these early release cytokines, which then induce expression of CXC chemokines to establish an extravascular neutrophil chemotactic gradient (Alcorn 2019). Neutrophils produce toxic oxygen radical species generated through the NADPH oxidase system and nitric oxide (NO) synthase (Lamb, Gutteridge et al. 1999) as well as proteolytic enzymes (such as elastase and lysozyme) (Fujishima, Morisaki et al. 2008) that can cause significant lung tissue damage because these mediators can be toxic when they are released in an uncontrolled manner (Kolaczkowska and Kubes 2013, Rebetz, Semple et al. 2018, Alcorn 2019, Zhang, He et al. 2021). In fact, the association between higher concentration of neutrophils and the development of more severe inflammation, hypoxia, higher permeability, and poor outcome was demonstrated thirty years ago (Miller, Cohen et al. 1992). Monocytes, macrophages, and lymphocytes are also recruited to the lung and produce large amounts of both pro- and anti-inflammatory cytokines (Larsen and Henson 1983, Zhang, He et al. 2021). Despite the predominance of inflammatory cells in the airspace in acute lung injury, ARDS occurs clinically even in the setting of neutropenia, as seen in patients who develop ARDS following bone marrow transplant, suggesting that inflammatory cells are not absolutely required for the induction of lung injury (Bastarache and Blackwell 2009). In this regard, a role for pathogen- or damage-associated molecular patterns (PAMPs or DAMPs) has

been proposed in the induction and persistence of inflammation through the activation of innate immune receptors such as Toll-like receptors (TLRs), NOD-like receptors (NLRs) or RIG-I-like receptors (RLRs) (Han and Mallampalli 2015).

Another key pathological feature of ARDS is the presence of hyaline membranes (Bachofen and Weibel 1982), which are a direct result of intra-alveolar fibrin polymerization. For decades it has been known that the alveolar compartment in ARDS has an increase in procoagulant protein activity and a decrease in fibrinolytic therapy, favoring fibrin formation (Idell 2003, Schultz, Haitsma et al. 2006). More recently, there is emerging evidence that resident lung cells, including AECs, actively modulate alveolar fibrin deposition through upregulation and activation of tissue factor (TF) (Bastarache, Wang et al. 2007), the most potent initiator of coagulation, and loss of the ability to activate protein C (Wang, Bastarache et al. 2007), a key anti-coagulant protein. Modulation of these pathways in patients with severe sepsis and ARDS by treatment with activated protein C (APC) reduced mortality (Bernard, Vincent et al. 2001) and was associated with a more rapid recovery of lung function in those with ARDS (Vincent, Angus et al. 2003). Furthermore, administration of recombinant APC improved the lung oedema and attenuated the increase in pulmonary artery pressure (Waerhaug, Kirov et al. 2008) and in another large clinical trial an improvement in dead space fraction was observed (Liu, Levitt et al. 2008). Indeed, a recombinant human Protein C marketed as Xigris became in 2001 the first biologic treatment approved for the treatment of severe sepsis (Bernard, Vincent et al. 2001). Unfortunately, the reduction of mortality observed in the original trial (PROWESS) was not replicated and Xigris was finally withdrawn from the market in 2011 (Lai and Thompson 2013). However, it is noteworthy that protein C plasma levels are reduced in patients with severe sepsis and in victims of ARDS, due to a greater consumption of this anticoagulant and anti-inflammatory protein, and it is associated with worse clinical outcomes (Yan, Helterbrand et al. 2001, Matthay and Ware 2004, McClintock, Zhuo et al. 2008). These findings provide further evidence for the central role of coagulation in the pathogenesis of ARDS. In addition to activation of coagulation in the airspace, systemic coagulation is also activated causing consumption of platelets and

resulting in microvascular thrombosis that, clinically, causes an increase in the dead space in the lungs due to an increase of pulmonary capillary permeability that contributes to lung oedema formation in ARDS (Zarbock, Singbartl et al. 2006, Bastarache and Blackwell 2009). Furthermore, activation of coagulation generates thrombin and fibrin, both of which are proinflammatory proteins that promote ongoing inflammation (Bastarache and Blackwell 2009). Furthermore, inflammation can modulate blood coagulation by activating C-reactive protein, which stimulates cells to generate TF (Idell, Koenig et al. 1991, Xue, Sun et al. 2015), and ECs to produce plasminogen activator inhibitor-1 (Prabhakaran, Ware et al. 2003). For example, IL-6 upregulates TF expression on ECs (Scarpati and Sadler 1989), and TNF-α attenuates fibrinolysis by stimulating the release of inhibitors of plasminogen activators (Levi, ten Cate et al. 2002). The linkage of inflammation and coagulation is further supported by studies where prevention of vascular injury by APC is dependent on inhibition of leukocyte activation (Uchiba, Okajima et al. 1996, Price, McAuley et al. 2012). The combined effects of all events can lead to disseminated intravascular coagulation (DIC) including formation of intravascular micro-thrombi and intra-alveolar fibrin deposits (Prabhakaran, Ware et al. 2003, Sapru, Curley et al. 2010, Xue, Sun et al. 2015, Ozolina, Sarkele et al. 2016), subsequently increasing both dead-space ventilation and intrapulmonary shunting, both characteristic features of ARDS (Brun-Buisson, Minelli et al. 2004).

The uncontrolled inflammation and coagulation abnormalities are also characteristic of COVID-19-associated ARDS. The massive release of inflammatory mediators (such as interleukin IL-1β, IL-6, IL-8 or TNF-α) cause the so-called “cytokine storm” which results in vascular inflammation, thrombosis and vasodilation and may lead to multiorgan dysfunction (Zheng 2020). Besides the formation of thrombi in the pulmonary microvasculature, disseminated intravascular coagulation (DIC) is also a frequent complication in COVID-19 patients that can be clinically expressed by excessive haemorrhage and ischemic necrosis of extremities and was associated with the severity and poor prognosis (Asakura and Ogawa 2021, Zhou, Cheng et al. 2021).

2.3.2. Pulmonary vascular permeability and oedema

In the lung, the alveolar-capillary membrane separates the alveolar airspace from the capillary lumen and comprises a complex architecture optimized to exert its multiple functions that include gas exchange (oxygen is diffused into the capillaries and carbon dioxide released from the capillaries into the air space) (Esquivel-Ruiz, Gonzalez-Rodriguez et al. 2021). The alveolar-capillary membrane has several layers: a lining fluid layer containing the surfactant, the epithelial barrier and its basement membrane, a thin interstitial space with a biologically active extracellular matrix (ECM), a capillary basement membrane and the capillary endothelium (Weibel 1973, Maina and West 2005, Knudsen and Ochs 2018). Between these epithelial and endothelial layers there are also resident and migratory leukocytes, as well as a population of mesenchymal stromal cells, such as pericytes and resident fibroblasts (Barron, Gharib et al. 2016).

One of the earliest abnormalities seen in injured lung is the loss of the alveolar-capillary barrier integrity. The alveolar epithelium is a tight barrier that restricts the passage of water, electrolytes, and small hydrophilic solutes from the insterstitium to the air spaces, allowing at the same time the diffusion of carbon dioxide and oxygen (Taylor and Gaar 1970, Weibel 2015). Thus, proper function of the channels of the alveolar epithelium is essential for the reabsorption of oedema and are key elements for a clear improvement of the disease in patients with sepsis and ARDS (Ware and Matthay 2001, Zeyed, Bastarache et al. 2012). Exudation from the plasma to the alveolar spaces decreases alveolar fluid clearance, leading to lung oedema (Yang, Chen et al. 2018). In this process the AECs downregulate ion transport machinery and the production of vascular endothelial growth factor (VEGF), also contributing to alveolar oedema. In addition, gas exchange is blocked by the accumulation of intra-alveolar fluid (Yang, Chen et al. 2018). Although more permeable than the epithelium, a healthy capillary endothelium in the alveoli forms a semipermeable barrier that limits the extravasation of plasma and its macromolecules from the vascular lumen to the instertitium. The severe inflammatory cascades are important

mediators that impaired the regulation of vascular endothelial barrier and vascular permeability (Larsen and Henson 1983, Yang, Chen et al. 2018). Severe inflammation causes losses of endothelial and epithelial cells by inducing apoptosis and necrosis (Yang, Chen et al. 2018). Both epithelial and endothelial barrier functions and permeability are governed by intercellular junctions (Herrero, Sanchez et al. 2018). These intercellular junctions between neighbouring cells in the epithelium and endothelium are mainly formed by apical tight junctions (TJs) and the underlying adherens junctions (AJ) and linked to the cellular cytoskeleton via numerous adaptor proteins. AJs are composed of cadherins, mainly vascular endothelial cadherin (VE-cadherin) that regulate the paracellular transport between blood and interstitium, consequently determine leukocyte migration and oedema formation during ARDS (Millar, Summers et al. 2016). In general, TJs control paracellular transport, maintain cellular polarity, establishing separate intercellular compartments, regulate a variety of intracellular signals, and control the transcellular transport. Occludins, claudins, and zonula occludens are essential components of TJs in the alveolar epithelium that constitute the main structure to regulate the passage of water and solute from the interstitial to the alveolar space, and to prevent the passage of pathogens and toxins from the air space into the systemic circulation (Zemans and Matthay 2004, Yanagi, Tsubouchi et al. 2015, Herrero, Sanchez et al. 2018). Thus, alteration of the epithelial TJs results in protein-rich oedema formation, and passage of infectious agents, exogenous toxins and endogenous products into the systemic circulation, exposing other organs and contributing to multiorgan failure (Denker and Nigam 1998, Schneeberger and Lynch 2004, Herrero, Sanchez et al. 2018). Endothelial junctional proteins also play important roles in tissue integrity as well as in vascular permeability, leukocyte extravasation, and angiogenesis (Wallez and Huber 2008). Specifically, intercellular cell adhesion molecule- 1 and vascular cell adhesion molecule-1 control the adhesion of leukocytes to ECs and facilitate their subsequent transendothelial migration via the platelet-endothelial cell adhesion molecule-1, contributing to the inflammatory process (Millar, Summers et al. 2016, Villar, Zhang et al. 2019).

The ECM, composed of a highly dynamic complex of fibrous proteins, glycoproteins, and proteoglycans, is crucial to maintain the epithelial and endothelial barrier function by regulating cell-cell interactions (Esquivel-Ruiz, Gonzalez-Rodriguez et al. 2021). Changes in the composition and mechanic properties of the ECM have been shown to modify the expression of TJs and the barrier function in alveolar epithelial and ECs, contributing to lung oedema formation (Rocco, Negri et al. 2001, Pelosi, Rocco et al. 2007, Koval, Ward et al. 2010, Mammoto, Mammoto et al. 2013). The oxidation of ECM proteins by ROS further modulates qualities of the ECM. It is well known that increased levels of ROS are present in the alveoli of patients with ARDS that may alter ECM properties, having an impact on cell-ECM interaction and alveolar permeability (Watson, Ritzenthaler et al. 2016). Other cells involved in the integrity of the epithelial-alveolar barrier are pericytes, fibroblasts and macrophages. The pericytes and fibroblasts are the main source of myofibroblasts in the lung during development and after injury, contributing in the latter to lung fibrosis (Rock, Barkauskas et al. 2011, Hung, Linn et al. 2013, Barron, Gharib et al. 2016). In pathological conditions, activated alveolar macrophages (AM) cause epithelial cells to produce anti-microbial peptides and a variety of mediators that not only modulate immune responses, but also contribute to epithelial barrier dysfunction via alteration of the TJ proteins (Bissonnette, Lauzon-Joset et al. 2020).

The loss of alveolar-capillary barrier integrity is seen both ultrastructurally on histological analysis (Riede, Joachim et al. 1978), radiographically with bilateral, fluffy alveolar infiltrates and clinically, as vascular leak with flooding of the alveolar space with protein-rich oedema fluid results in tachypnea and hypoxaemia (Bastarache and Blackwell 2009). Experimental evidence has shown that the alveolar-capillary leak allows bidirectional travel of fluid and proteins. In contrast to normal lungs, the lungs of ARDS patients who are administered with an intravenous (IV) injection of hydroxyethyl starch have an accumulation of this molecule in the airspaces (Wang, Oppenheimer et al. 1999). In addition, patients with ARDS have elevated plasma levels of surfactant proteins that are only produced by lung AECs (Doyle, Bersten et al. 1997). Although the oedema caused by vascular leak is crucial to the pathogenesis of ARDS, it should be

highlighted that lung oedema alone does not constitute ARDS (Bastarache and Blackwell 2009).

2.3.3. Alterations in the pulmonary circulation

The pulmonary circulation or “minor circulation” is normally a high flow, low resistance and low pressure system that carries blood into the pulmonary microcirculation whose main function is to facilitate gas exchange (Mandegar, Fung et al. 2004). The regulation of vascular tone in the pulmonary circulation is a complex and multifactorial process that involves the distensibility of the pulmonary vasculature, the function of the heart, the concentration of oxygen in the blood and the capacity of the endothelium to release vasoactive substances (Chester and Yacoub 2014). All these mechanisms together determine pulmonary vascular resistance and ensure that the pulmonary circulation is maintained as a low pressure and high blood flow circuit (Chester and Yacoub 2014, Olschewski, Papp et al. 2014).

Once ARDS develops, patients may present pulmonary vascular dysfunction (PVD) and pulmonary hypertension (PH) (Bull, Clark et al. 2010). The pulmonary vascular involvement in ARDS was first described more than 40 years ago (Zapol and Snider 1977). The term PVD encompasses the structural and functional pathophysiological changes affecting the vascular compartment and the right ventricle (RV) in ARDS. These changes include pulmonary vasoconstriction induced by hypoxia and/or the release of vasoactive inflammatory mediators, microvascular thrombosis, reduction in functional lung volume, direct inflammatory endothelial damage, endothelial dysfunction and vascular remodelling phenomena (Price, McAuley et al. 2012). The clinical expression of PVD is an increase in pulmonary arterial pressure (PAP), which contrasts with the lowered systemic vascular resistance that characterizes septic shock (Price, McAuley et al. 2012).

Despite advances in the management of ARDS, the prevalence of PH in ARDS patients remains high. Thus, A study established a prevalence of 92.2%, with 16.8% of ARDS patients having a mild form, 75.8% a moderate form and 7.4% a

severe form (Beiderlinden, Kuehl et al. 2006). However, most of the studies escribe a highly variable prevalence of PH ranging from 22 to 79% (Villar, Blazquez et al. 1989, Bull, Clark et al. 2010, Namendys-Silva, Santos-Martinez et al. 2014, Li, Mao et al. 2020) with pulmonary pressure values between 29 and 36 mmHg (Revercomb, Hanmandlu et al. 2020). In COVID-19 patients, PAH and right ventricular dysfunction are also common complications, being encountered after the recovery even in moderate cases (Lan, Liu et al. 2021, Suzuki, Nikolaienko et al. 2021, Tudoran, Tudoran et al. 2021). COVID-19 is considered a systemic disease that causes different pathologies that could lead to more than one group from the PH categories (Nabeh, Matter et al. 2021). A retrospective study reported 13.4% COVID-19 patients with signs of pulmonary hypertension. This is related to the severity of the infection, while 21% of patients with severe COVID-19 had evidence of pulmonary hypertension only 2% of patients with mild to moderate disease had pulmonary hypertension (Deng, Hu et al. 2020). Another study revealed that 7.69% of the COVID-19 patients had PH and 10.28% had right ventricular dysfunction (Tudoran, Tudoran et al. 2021). Among hospitalised non-ICU patients with COVID-19, the prevalence of PAH was 12% and was associated with signs of more severe COVID-19 with worse in-hospital clinical outcome (Pagnesi, Baldetti et al. 2020). A progressive increase in pulmonary pressures has been associated with a worse outcome (Zapol and Snider 1977, Bull, Clark et al. 2010, Price, McAuley et al. 2012). PVD should be considered as a continuum during the course of ARDS ranging from mild PH, invariably present in most ARDS patients, to more severe PH and ultimately RV failure (Figure 3) (Sipmann, Santos et al. 2018). In nearly 25% of patients PVD evolves to its most severe form acute *cor-pulmonale* with overt RV failure in which the reported associated mortality has been as high as 60–70% (Villar, Blazquez et al. 1989, Vieillard-Baron, Schmitt et al. 2001, Boissier, Katsahian et al. 2013).

The mechanisms leading the acute PH in these patients are complex and most likely depend on the underlying cause leading to ARDS. However, inflammation, endothelial dysfunction, hypoxia and disruption in the normal balance between endogenous vasoactive factors, with increased production of pulmonary vasoconstrictors (endothelin, thromboxane A_2 or serotonin) over vasodilators

(nitric oxide or prostacyclin), are thought to play a major role (Price, McAuley et al. 2012, Ryan, Frohlich et al. 2014, Pandolfi, Barreira et al. 2017).

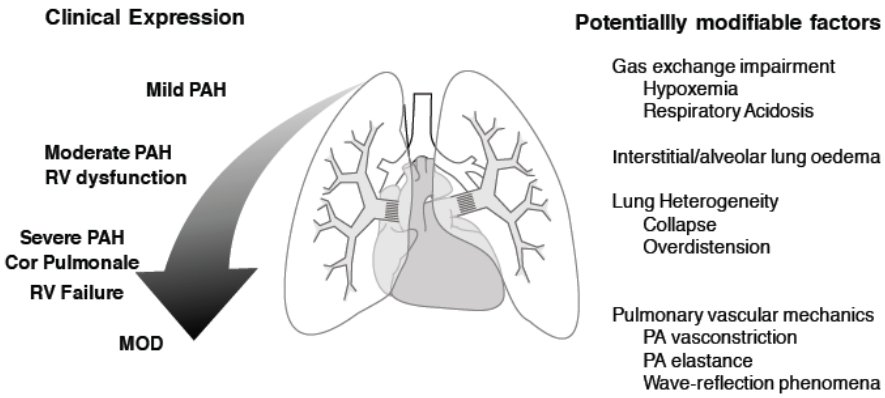

***Figure 3**. Pulmonary vascular dysfunction in ARDS (Sipmann, Santos et al. 2018).*

In addition to hypoxemia, ARDS patients also develop hypercapnia (Morales-Quinteros, Camprubi-Rimblas et al. 2019) and, as a consequence, respiratory acidosis (Repesse and Vieillard-Baron 2017, Patel and Sharma 2022). The pulmonary blood flow in ARDS is compromised to lung regions that remain well ventilated, the expected consequence would be an increase in the physiological dead space that represents an impaired ability to excrete carbon dioxide (CO_2). These alterations results in reduced CO_2 clearance which leads to hypercapnic acidosis (Gattinoni, Bombino et al. 1994, Nuckton, Alonso et al. 2002, Radermacher, Maggiore et al. 2017, Morales-Quinteros, Camprubi-Rimblas et al. 2019). In ARDS, the main effect of hypercapnia is exerted on the right ventricle, because of the huge increase in pulmonary arterial resistance, leading to right ventricular failure (acute cor pulmonale) (Jardin, Dubourg et al. 1997, Mekontso Dessap, Charron et al. 2009, Repesse and Vieillard-Baron 2017). Moreover, severe hypercapnia is associated with more circulatory failure and with higher ICU mortality (Mekontso Dessap, Boissier et al. 2016, Nin, Muriel et al. 2017).

ENDOTHELIAL DYSFUNCTION. As in the systemic circulation, the endothelium in the pulmonary circulation has a profound influence on vascular tone and remodelling. ECs release a variety of vasodilators such as nitric oxide (NO),

prostacyclin (PGI_2) or endothelium derived hyperpolarizing factor (EDHF), and vasoconstrictors, mainly endothelin-1 (ET-1) and thromboxane A_2 (TXA_2) (Cogolludo, Moreno et al. 2007). These mediators regulate the physical and biochemical properties of pulmonary vessels and affect vascular contractility and vascular smooth muscle cell (VSMCs) growth. Under physiological conditions, a balance between vasodilators and vasoconstrictors regulates pulmonary vascular tone, homeostasis, vascular damage repair and growth. Moreover, EC provide a smooth thromboresistant surface protecting the subendothelium from procoagulant factors and platelets (Maniatis and Orfanos 2008). Endothelial dysfunction involves an imbalance in the production of vasodilator and vasoconstrictor mediators and a transition to a prothrombotic phenotype (Price, McAuley et al. 2012). The disruption of this balance promotes vasoconstriction and proliferation of VSMCs, modifying the structure and contraction of pulmonary vessels. The resulting state is known as "pulmonary endothelial dysfunction" which is important during early and late ALI (Tomashefski, Davies et al. 1983, Tomashefski 2000). Histological characteristics of injury include EC swelling, the presence of enlarged mitochondria, dilated endoplasmic reticulum adjacent to the capillary lumens (Tomashefski, Davies et al. 1983), pinocytotic vesicle formation, and inter-endothelial cell separation (Schnells, Voigt et al. 1980). Additionally, there is evidence for altered production of endothelial-derived molecules including Von Willebrand's factor, angiotensin-converting enzyme and angiopoietin-2 (Price, McAuley et al. 2012). These molecules have been associated with increased pulmonary dead space fraction in experimental lung injury (Frank, McAuley et al. 2005) as well as with raised pulmonary vascular pressures (Calfee, Gallagher et al. 2012) and are considered biomarkers since their plasma levels predict the onset and increased mortality of patients with ALI (Casey, Krieger et al. 1981, Rubin, Wiener-Kronish et al. 1990, Sabharwal, Bajaj et al. 1995, Orfanos, Armaganidis et al. 2000, Ware, Eisner et al. 2004, Bhandari, Choo-Wing et al. 2006, Price, McAuley et al. 2012).

NO derived from endothelial nitric oxide synthase (eNOS) is an important vasodilator which has many functions, e.g. it modulates vascular tone, inhibits smooth muscle proliferation, platelet aggregation (Dinh-Xuan 1992), leukocyte

adhesion, negatively regulates ET-1 production (Smith, Demoncheaux et al. 2002, Mitchell, Ali et al. 2008) or protects against hypoxia-induced vasoconstriction in lungs (Perrella, Edell et al. 1992). For example, direct administration of LPS leads to acute increases in pulmonary vascular resistance, probably through inhibition of NO (Myers, Parker et al. 1994), a phenomenon that may be mediated by endothelin B receptors (Rossi, Persson et al. 2008, Price, McAuley et al. 2012) and overproduction of TXA_2. Moreover, the overexpression of eNOS in transgenic mice prevents hypoxia-induced PH (Ozaki, Kawashima et al. 2001). On the contrary, exposure to mild hypoxia results in severe PH in eNOS-deficient mice (Steudel, Ichinose et al. 1997, Fagan, Fouty et al. 1999). However, human studies have reported variable NO production in patients with idiopathic PH, with reduced eNOS expression in pulmonary vessels (Giaid and Saleh 1995) or increased expression in the endothelium of plexiform lesions (Mason, Springall et al. 1998). On the other hand, the production of NO by other routes (e.g. inducible nitric oxide synthase (iNOS)) can be harmful (Price, McAuley et al. 2012) and is believed to be responsible for the reduced vascular contractility in endotoxin shock (Murray, Wylam et al. 2000). However, PH develops despite iNOS induction in pulmonary arteries (PA) (Griffiths, Liu et al. 1995). However, PH develops despite iNOS is induced in both systemic and pulmonary vessel walls leading to the production of large quantities of vasoactive NO (Griffiths, Liu et al. 1995). Rather than increasing vasodilatation, however, these high NO levels may combine with reactive oxygen species (ROS) to form the highly damaging reactive nitrogen species peroxynitrite (Freeman 1994). Recently, our group has demonstrated that activation of iNOS pathway after TLR4 activation is responsible for the hyporesponsiveness to α-adrenoceptor activation and partly mediates endothelial dysfunction in rat PA (Pandolfi, Barreira et al. 2017). However, inhibition of iNOS activity limits septic shock, improving the general systemic hemodynamic situation, but at the cost of raised pulmonary vascular resistance (Avontuur, Biewenga et al. 1998, Morris, Beghetti et al. 2000) and increased mortality (Vender, Betancourt et al. 2014).

HYPOXIC PULMONARY VASOCONSTRICTION (HPV). Hypoxic pulmonary vasoconstriction (HPV) is a dynamic process predominantly mediated by precapillary arterioles (Brimioulle, LeJeune et al. 1996) that promotes ventilation/perfusion matching by diverting blood flow away from poorly ventilated (hypoxic) lung units, maximising oxygen saturation and thus its distribution to systemic tissues (Price, McAuley et al. 2012). Conversely, systemic arterioles dilate in response to reduced oxygen concentrations to maintain constant tissue oxygen levels.

Alterations in HPV are pathologically relevant (Marshall, Hanson et al. 1994, Ullrich, Bloch et al. 1999, Gierhardt, Pak et al. 2021). Indeed, generalised alveolar hypoxia associated with altitude, chronic obstructive pulmonary disease or sleep apnoea, produces HPV throughout the pulmonary vascular tree which, if persistent, can lead to PH and RV failure. In contrast, in ARDS and sepsis, failure of HPV results in ventilation-perfusion uncoupling and severe arterial hypoxaemia (Figure 4). Thus, HPV has a protective effect on gas exchange (Brimioulle, LeJeune et al. 1996) while also contributing to mild levels of PH (Marshall, Hanson et al. 1994, Brimioulle, Julien et al. 2002) in ARDS. In patients, hypoxaemia is mainly the result of intrapulmonary shunt, which occurs when lung areas are unventilated due to fluid accumulation in the alveoli (pulmonary oedema), but perfused, with consequent V/Q uncoupling (Dantzker, Brook et al. 1979, Price, McAuley et al. 2012), resulting in decreased PaO_2. In COVID-19 patients, a severe hypoxaemia also occurs in compliant lungs due to a loss of lung perfusion regulation and hypoxic vasoconstriction. Notably, hypoxaemia has been shown to be an independent prognostic factor for the severe form of COVID-19 and associated with in-hospital mortality (Habashi, Camporota et al. 2021, Kotwica, Knights et al. 2021, Perez-Vizcaino, Moreno et al. 2021). HPV is also affected in animal models of sepsis. Toll-like receptors (TLRs), which mediate inflammation, appear to play an important role in sepsis-induced respiratory failure. Since TLR activation is associated with the production of inflammatory mediators, including NO, vasodilation due to overproduction of NO released by iNOS has been proposed as a critical mediator for HPV impairment (Pandolfi, Barreira et al. 2017). NO has been shown to attenuate the response of pulmonary

arteries to hypoxia both in vitro and in vivo (Liu, Crawley et al. 1991). However, inhibition of iNOS only partly restores the HPV response, suggesting that the failure of HPV during endotoxaemia must be mediated, at least in part, by distinct mechanisms (Ullrich, Bloch et al. 1999, Spohr, Cornelissen et al. 2005).

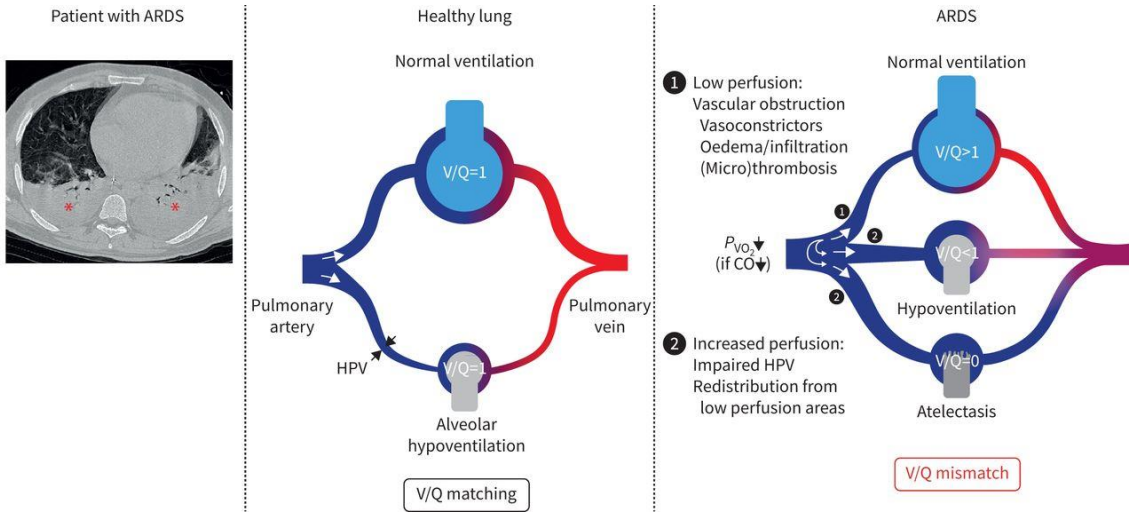

Figure 4. *Mechanism of ventilation/perfusion (V/Q) mismatch in acute respiratory distress syndrome (ARDS) (Gierhardt, Pak et al. 2021).*

In line with this, inflammatory cytokines have been shown to induce direct effects in the pulmonary vascular wall, leading to an increase in pulmonary vascular resistance (Price, Wort et al. 2012, Groth, Vrugt et al. 2014, Rabinovitch, Guignabert et al. 2014). Thus, IL-6, one of the most relevant cytokines in PH and ARDS (Soon, Holmes et al. 2010, Hashimoto-Kataoka, Hosen et al. 2015, Gierhardt, Pak et al. 2021), has been shown to increase the contractile responses to serotonin, to induce endothelial dysfunction and to inhibit HPV in isolated rodent and human pulmonary arteries (Pandolfi, Barreira et al. 2017, Voiriot, Razazi et al. 2017). We also observed that an antibody against IL-6 prevented the impairment of HPV induced by bacterial endotoxin in isolated rat pulmonary arteries (Pandolfi, Barreira et al. 2017) supporting the hypothesis that anti-inflammatory therapies could have beneficial effects on V/Q mismatch in ARDS (Horie, McNicholas et al. 2020, Gierhardt, Pak et al. 2021, Perez-Vizcaino, Moreno et al. 2021). Indeed, several studies have demonstrated a positive impact

of tozilizumab on arterial oxygenation in patients with severe COVID-19 (Xu, Han et al. 2020, Wang, Fu et al. 2021). In November 2021, the European Medicine Agency (EMA) recommended the approval of Tocilizumab, a monoclonal antibody against the IL-6 receptor, for the treatment of patients with severe Covid-19 who are receiving systemic treatment with corticosteroids and require supplemental oxygen or mechanical ventilation (https://www.ema.europa.eu/en/news/ema-recommends-approval-use-roactemra-adults-severe-covid-19)

2.4. Treatments

2.4.1. Conventional treatment

Lung protective ventilation strategies and prone position

One of the major advances in the management of ARDS has been the introduction of lung protective ventilation strategies which can be considered the first therapeutic intervention consistently improving outcomes (Amato, Barbas et al. 1998, Acute Respiratory Distress Syndrome, Brower et al. 2000). The goal of mechanical lung-protective ventilation in patients with ARDS is to rest the respiratory muscles, and maintain adequate gas exchange (Acute Respiratory Distress Syndrome, Brower et al. 2000). As mentioned in section 2.2 (Epidemiology), ARDS has an overall rate of death in the hospital of approximately 40% (Rubenfeld, Caldwell et al. 2005, Villar, Blanco et al. 2011, Bellani, Laffey et al. 2016) and lung-protective ventilation strategy decreased this mortality by 3-12% (Needham, Colantuoni et al. 2012, Esteban, Frutos-Vivar et al. 2013). Strategies to achieve these objectives have focused on limiting tidal stress (volutrauma) and cyclic tidal recruitment at the interface between collapsed and aerated lung regions (atelectrauma). The latter is based on the “open lung hypothesis,” which focuses on recruiting collapsed lung units and keeping them open throughout the ventilatory cycle (Lachmann 1992). Two strategies to achieve these goals were: high-frequency oscillatory ventilation (HFOV) and lung recruitment maneuvers (a sustained increase in airway pressure with the goal to open collapsed alveoli). Theoretically, HFOV represents an ideal lung protective strategy, delivering very small tidal volumes (limiting volutrauma) around a

relatively high mean airway pressure (limiting atelectrauma). A large body of experimental and clinical evidence supported the potential benefits of HFOV in ARDS (Sud, Sud et al. 2010, Sklar, Fan et al. 2017). However, HFOV treated patients showed an increased mortality due to the negative hemodynamic consequences (as evidenced using more vasoactive drugs in this group) due to higher mean airway pressures (Ferguson, Cook et al. 2013). After lung recruitment maneuvers, an important point is the positive end-expiratory pressure (PEEP), because a sufficient PEEP is applied to keep the lungs open. Patients who received mechanical ventilation with appropriate PEEP experienced improved oxygenation and reduced hypoperfusion due to the opening of collapsed alveoli and decreased intrapulmonary shunting. Low PEEP may also decrease ventilator-associated pneumonia and prevent pulmonary injury (Manzano, Fernandez-Mondejar et al. 2008). The major benefit in this population is the improvement in gas exchange by preventing alveolar collapse. High PEEP levels decrease repetitive alveolar opening and closing but could potentially promote pulmonary injury (Caironi, Cressoni et al. 2010). Current studies do not recommend the application of high PEEP as a routine initial treatment in the ARDS population (Brower, Lanken et al. 2004, Meade, Cook et al. 2008). The main adverse effect of ventilation is the ventilator-induced lung injury (VILI) (Grasso, Stripoli et al. 2007, Terragni, Rosboch et al. 2007, Fan, Brodie et al. 2018). Reduced tidal volume may cause less VILI, resulting in better patient outcomes (Needham, Colantuoni et al. 2012). Also, the limitation of tidal volumes and airway pressure can sometimes result in high partial pressure of CO_2 in arterial blood ($PaCO_2$) levels, this approach is accepted and is called “permissive hypercapnia” (Curley, Laffey et al. 2013, Morales-Quinteros, Camprubi-Rimblas et al. 2019). This has beneficial effects, including a reduction in pulmonary inflammation and alveolar oxidative stress (Laffey, Tanaka et al. 2000, Broccard, Hotchkiss et al. 2001, Peltekova, Engelberts et al. 2010, Kapetanakis, Siempos et al. 2011) and deleterious effects, such as impairments in tissue repair and decreased alveolar fluid clearance (Briva, Vadasz et al. 2007, O'Toole, Hassett et al. 2009). Extracorporeal CO_2 removal ($ECCO_2R$) takes CO_2 out of blood through an extracorporeal gas exchanger. Consequently, less CO_2 must be

removed by the lungs, reducing the intensity of ventilatory support (e.g., lower tidal volumes) facilitating the application of ultraprotective ventilation (Fitzgerald, Millar et al. 2014, Goligher, Amato et al. 2017, Morelli, Del Sorbo et al. 2017). VILI may also be reduced by placing patients in the prone position. Prone positioning facilitates more homogeneous lung inflation, resulting in a more uniform distribution of mechanical forces throughout the injured lung (Galiatsou, Kostanti et al. 2006, Gattinoni, Taccone et al. 2013, Beitler, Shaefi et al. 2014). The patients with severe ARDS should be placed in the prone position for at least 12 hours per day (Howell and Davis 2018). Based on the results from the Proning Severe ARDS Patients (PROSEVA) trial, prone positioning in patients with severe ARDS resulted in a significant diminution of the cardiovascular dysfunction and reduced 28-day mortality by more than 50% (Guerin, Reignier et al. 2013). Before endotracheal intubation, it is important to consider high-flow nasal oxygen for patients with moderately severe hypoxaemia because it may prevent ventilator-associated complications (e.g., ventilator-associated pneumonia), delirium, and the need for sedation, while potentially allowing patients to communicate and maintain oral feeding (Fan, Brodie et al. 2018, Matthay, Aldrich et al. 2020). This procedure might avoid the need for intubation and mechanical ventilation because it provides high concentrations of humidified oxygen, low levels of PEEP, and can facilitate the elimination of CO_2 (Frat, Thille et al. 2015, Matthay, Aldrich et al. 2020). WHO guidelines support the use of high-flow nasal oxygen in some patients, but they urge close monitoring for clinical deterioration that could result in the need for emergent intubations because such procedures might increase the risk of infection to health-care workers (Matthay, Aldrich et al. 2020).

Fluid management

Fluid management is important to consider as a measure to reduce pulmonary oedema (National Heart, Blood Institute Acute Respiratory Distress Syndrome Clinical Trials et al. 2006). In the absence of shock, fluid conservative therapy restricts the intake of fluids to achieve a negative fluid balance of 0.5 to 1 L per day. In the presence of shock, fluid balance might be achieved with renal

replacement therapy, especially if there is associated acute kidney injury and oliguria (Matthay, Aldrich et al. 2020). To determine the optimal fluid management a comparative study of conservative and liberal fluid management strategies was performed (National Heart, Blood Institute Acute Respiratory Distress Syndrome Clinical Trials et al. 2006). Although there was no significant difference in the primary outcome of 60-day mortality, the conservative strategy of fluid management improved lung function and shortened the duration of mechanical ventilation and intensive care without increasing nonpulmonary-organ failures (National Heart, Blood Institute Acute Respiratory Distress Syndrome Clinical Trials et al. 2006). However, among the limitations of this therapy is the different response of patients to these strategies. In two randomized controlled trial cohorts, with distinct natural histories, clinical and biomarker profiles, and differential response to therapy with PEEP, two ARDS subphenotypes with different response to the treatment were identified (Calfee, Delucchi et al. 2014, Famous, Delucchi et al. 2017).

Steroids therapies

The effects of anti-inflammatory treatments in ARDS in several clinical trials have been discouraging for many decades (Meduri, Carratu et al. 2003, Annane 2007, Matthay, Zemans et al. 2019, Zhang, Wang et al. 2021). For example, corticosteroid therapy has been studied in critically ill patients with ARDS with conflicting results. Thus, administration of corticosteroids controlled pulmonary inflammation and improved oxygenation (Meduri, Marik et al. 2008, Tang, Craig et al. 2009) or lung compliance in *in vitro* studies (Marik, Pastores et al. 2006, Belvitch and Dudek 2013, Lamontagne, Brower et al. 2013). In line with this protective effects, several studies showed that therapy with low-dose corticosteroids led to a reduction in duration of mechanical ventilation, length of stay, morbidity and mortality in ARDS (Meduri, Golden et al. 2007, Tang, Craig et al. 2009, Meduri, Bridges et al. 2016). However, in patients treated with high-dose steroids show no improvement in terms of duration of ventilation, level of PEEP, or FiO_2 and this therapy appears to result in worse clinical outcomes, including higher infection rates and higher mortality rates (Weigelt, Norcross et

al. 1985, Bone, Fisher et al. 1987, Steinberg, Hudson et al. 2006). Moderate-dose steroid therapy in ARDS is associated with improved oxygenation and more ventilator-free days but has no effect on mortality early in the course of the disease and increases mortality in patients with ARDS longer than 2 weeks (Steinberg, Hudson et al. 2006). More recently, a multicentre randomised trial showed that early administration of dexamethasone to patients with moderate-to-severe ARDS reduced the duration of mechanical ventilation and overall mortality (Villar, Ferrando et al. 2020).

Neuromuscular blocking agents (NMBA)

The NMBA in sedated ARDS patients significantly improved severe hypoxaemia by decreasing oxygen consumption and limiting the occurrence of potentially injurious phenomena during mechanical ventilation including reverse triggering (i.e., diaphragmatic muscle contractions triggered by controlled ventilator breaths) (Akoumianaki, Lyazidi et al. 2013), pendelluft (i.e., derived from the German words for pendulum and air, refers to the movement of air within the lung from nondependent to dependent regions without a change in tidal volume) (Yoshida, Torsani et al. 2013), and patient-ventilator dyssynchrony (i.e., in which the patient breathing efforts are not synchronized with the ventilator-initiated breaths) (Fan, Brodie et al. 2018). In a multicenter, double-blind trial (Papazian, Forel et al. 2010), ARDS patients were included and paralysis was induced. After receiving NMBA for 48 h, the hazard ratio for death at 90 days was reduced and the incidence of complications was not different between NMBA and placebo group (Papazian, Forel et al. 2010). In addition, it was demonstrated a decrease in the pro-inflammatory responses with the early use of NMB (Forel, Roch et al. 2006). However, NMBA-induced paralysis may increase the risk of acquired neuromuscular weakness leading to difficulty weaning from mechanical ventilation and increase mortality (Kim and Hong 2016, Sweeney and McAuley 2016, Umbrello, Formenti et al. 2016). Based on this evidence, NMB should not be used routinely in patients with moderate-severe ARDS, and when NMB is used by clinicians, it should be instituted early on in their course, but limited to no more than 48 hours of treatment (Yang, Chen et al. 2018).

Selective vasodilators

In some ARDS patients, diffuse pulmonary vasoconstriction was found and contributed to change vascular permeability and induce severe hypoxaemia. Administration of selective vasodilators, such as inhaled nitric oxide (iNO), seem to improve gas exchange in ARDS patients. iNO induces pulmonary vasodilation and redistribution of pulmonary blood flow. The inhaled form minimized the adverse systemic hemodynamic effects (Yang, Chen et al. 2018). Numerous case series and randomized trials of iNO in patients with ARDS have shown its benefit in improving PaO_2/FiO_2 ratios compared to conventional therapy, but this improvement is often transient and does not translate into improved clinical outcomes (e.g., survival, length of stay, duration of mechanical ventilation) (Johannigman, Davis et al. 1997, Dellinger, Zimmerman et al. 1998, Michael, Barton et al. 1998, Dupont, Le Corre et al. 1999, Kaku, Nguyen et al. 2020). The iNO may be a short-term therapy in severe ARDS patients, especially presenting hypoxaemia and respiratory failure. Another inhaled pulmonary vasodilator agents are the inhaled prostacyclin agonists (e.g., epoprostenol and iloprost), which also improve oxygenation and hemodynamics (Dunkley, Louzon et al. 2013, Sawheny, Ellis et al. 2013). Head-to-head comparisons of iNO and inhaled epoprostenol in patients with ARDS have shown equivalence in their effects on oxygenation and hemodynamics (Walmrath, Schneider et al. 1996, Torbic, Szumita et al. 2013). To sum up, pulmonary vasodilators such as iNO, prostacyclin and epoprostenol are attractive therapeutic options for PVD as they directly reduce PAP and pulmonary vascular resistance without systemic hemodynamic effects (Moloney and Evans 2003).

New therapies under study

In addition to the treatments described above, a number of therapies targeting different cellular or molecular pathways are currently being studied. Experimental data have shown that β2 agonists can increase sodium transport by activating β2 receptors on alveolar type I and type II cells, accelerating resolution of pulmonary edema (Bassford, Thickett et al. 2012, Fan, Brodie et al. 2018). This hypothesis was tested in a clinical trial demonstrating that a 7-day infusion of salbutamol

significantly reduced extravascular lung water (Perkins, McAuley et al. 2006). However, other clinical trials have demonstrated a lack of efficacy (National Heart, Blood Institute Acute Respiratory Distress Syndrome Clinical Trials et al. 2011, Gao Smith, Perkins et al. 2012, Perkins, Gates et al. 2014). Because injury to the alveolar epithelium is an important cause of ARDS, acceleration of alveolar epithelial repair may facilitate resolution of pulmonary oedema and lung injury. Keratinocyte growth factor (KGF) is important in alveolar epithelial repair, and experimental and human studies support the concept that KGF may be beneficial in patients with ARDS (Ware and Matthay 2002, Fan, Brodie et al. 2018). In a clinical trial, there was no significant difference in mean oxygenation index at day 7 in patients randomized to recombinant human KGF or placebo for 6 days (McAuley, Cross et al. 2017). However, there was evidence of harm from KGF, with those patients having significantly fewer ventilator-free days, longer duration of mechanical ventilation, and higher 28-day mortality (Fan, Brodie et al. 2018). Statins reduce inflammation and progression of lung injury in experimental models and were shown to be safe and to reduce nonpulmonary organ dysfunction (Jacobson, Barnard et al. 2005, Shyamsundar, McKeown et al. 2009, Craig, Duffy et al. 2011, Fan, Brodie et al. 2018). Two large clinical trials were conducted to examine the effect of statins in patients with ARDS. In the Statins for Acutely Injured Lungs from Sepsis (SAILS) trial there was no significant difference (rosuvastatin vs placebo) in 60-day in-hospital mortality (National Heart, Blood Institute et al. 2014). In the Hydroxymethylglutaryl-CoA Reductase Inhibition with Simvastatin in Acute Lung Injury to Reduce Pulmonary Dysfunction-2 (HARP-2) trial there was no significant difference (simvastatin vs placebo) in the ventilator-free days to day 28, nonpulmonary organ failure–free days or 28-day mortality (McAuley, Laffey et al. 2014). The role of surfactant to prevent alveolar collapse and its anti-inflammatory properties makes it a potential therapy for ARDS. Smaller studies have shown possible improvements in oxygenation without any mortality benefit (Weg, Balk et al. 1994, Anzueto, Baughman et al. 1996, Spragg, Lewis et al. 2004), whereas administration of surfactant in infants, children, and adolescents with ALI improved oxygenation and decreased mortality (Willson, Thomas et al. 2005). However, another study

of patients with ARDS showed that patients treated with porcine surfactant demonstrated a trend toward increased mortality and adverse effects (Kesecioglu, Beale et al. 2009).

Therapies in COVID-19 patients

With a high rate of transmission and mortality, the SARS-CoV-2 infection (COVID-19) has become a global threat which demands effective treatments beyond supportive therapies (Zheng 2020). Up to 33% of hospitalized patients with COVID-19 are mechanically ventilated (Wunsch 2020). In these patients, the use of low tidal volume (6 mL/kg per predicted bodyweight) with a plateau airway pressure of less than 30 cm H_2O, and increasing the respiratory rate to 35 breaths per min as needed, is the mainstay of lung protective ventilation (Matthay, Aldrich et al. 2020). Regarding PEEP, patients responded to initiation of invasive high PEEP ventilation with markedly improved oxygenation, which was accompanied by reduced pulmonary opacities within 6 h of mechanical ventilation (Mittermaier, Pickerodt et al. 2020). Decremental PEEP trials confirmed the need for high PEEP for optimal oxygenation. Prone positioning substantially increased oxygenation (Mittermaier, Pickerodt et al. 2020). A number of potential antiviral therapies against SARS-CoV-2 have been tested in clinical trials. Though oseltamivir had high application rate in the early cohort studies, its drug efficacy on COVID-19 was not obvious (Ge, Wang et al. 2020). Case report implied that lopinavir and ritonavir therapy may be beneficial for COVID-19 cases (Han, Quan et al. 2020, Lim, Jeon et al. 2020). Wang *et al.* (Wang, Cao et al. 2020) found that remdesivir and chloroquine were highly effective in the control of SARS-CoV-2 infection *in vitro*. Regarding glucocorticoids treatment, two COVID-19–related ARDS subgroups with differential outcomes, similar to previously described ARDS subphenotypes, and differential treatment responses to corticosteroids were identified (Sinha, Furfaro et al. 2021). In addition, a prospective meta-analysis of seven randomised trials enrolling 1703 critically ill COVID-19 patients has recently showed that administration of systemic corticoids resulted in lower 28-day all-cause mortality (Group, Sterne et al. 2020). However, glucocorticoids should be avoided in view of the evidence that they can be harmful in cases of

viral pneumonia and ARDS from influenza (Ni, Chen et al. 2019). Current interim guidance from WHO on clinical management of severe acute respiratory infection suggests not routinely using systemic corticosteroids unless indicated for another reason. According to pathological findings in COVID-19 patients, proper use of corticosteroid together with other support care should be considered for severe patients to prevent ARDS development (Xu, Shi et al. 2020). Currently, the following treatments have been authorised by the EMA (https://www.ema.europa.eu/en/human-regulatory/overview/public-health-threats/coronavirus-disease-covid-19/treatments-vaccines/treatments-covid-19/covid-19-treatments-authorised):

Regdanvimab (monoclonal antibody against the spike protein of SARS-CoV2). Marketing authorisation for adults who do not require supplemental oxygen and who are at increased risk of their disease becoming severe.

Combination of Casirivimab and imdevimab: Two monoclonal antibody against the spike protein of SARS-CoV2). Marketing authorisation also granted for adults and adolescents who do not require supplemental oxygen and who are at increased risk of their disease becoming severe.

Remdesivir: A nucleoside analog which inhibits the RNA-dependent RNA polymerase (RdRp) of coronaviruses including SARS-CoV-2. Conditional market authorization for adults and adolescents with pneumonia requiring supplemental oxygen (low- or high-flow oxygen or other non-invasive ventilation at the start of treatment).

In November 2021, the EMA also recommended the approval of Tocilizumab, a monoclonal antibody against the IL-6 receptor, for the treatment of patients with severe Covid-19 who are receiving systemic treatment with corticosteroids and require supplemental oxygen or mechanical ventilation (https://www.ema.europa.eu/en/news/ema-recommends-approval-use-roactemra-adults-severe-covid-19).

Precision medicine

One of the main problems in the search for new treatments is that new strategies are sought without taking into account the aetiology of ARDS or the specific characteristics of the patients. The lack of a common presentation highlights the need to take into account the characteristics of each patient, thus applying so-called precision medicine to find the optimal treatment (Beitler, Goligher et al. 2016, Matthay, Arabi et al. 2020, Bos, Artigas et al. 2021, Habashi, Camporota et al. 2021). Bos et al. establishes three domains that should be taken into account in the choice of treatments: aetiology, physiology and biology (Table 2). In general, the authors propose to systematically address the variations in these domains or the specific phenotypes in order to identify treatable traits that can be targeted in future clinical trials.

Domain	Subdomain	Trait	Interventions to be tested
Aetiology	Casual pathogen	COVID-19	Dexamethasone
	ARDS-mimic	Diffuse acute interstitial lung diseases	Immunosuppression
		Diffuse pulmonary infections	Antimicrobials
		Drug-induced diffuse lung disease	Withhold drug
	Amplifiers of lung injury	Fluid overload	Diuretics Vasopressors
		Ventilator-induced lung injury	Lower tidal volumes
	Nonresolving lung injury	Fibroproliferation	Corticosteroids Antifibrotics
		Secondary infection	Antimicrobials
Physiology	Shunt	PaO_2 /FiO_2	Prone positioning Adjust PEEP Lung recruitment
	Ventilation	Dead space ventilation	Adjust PEEP
	Mechanics	High mechanical power	Adjust PEEP, tidal volume and/or respiratory rate
		Driving pressure	Adjust PEEP

Biology	Systemic host response	Hyperinflammatory (or reactive)	High PEEP Restrictive fluid Simvastatin Immunomodulation
	Epithelial injury	Damaged epithelium	Epithelial protection
	Endothelial injury	Vascular permeability and endothelial injury	Endothelial protection Immunomodulation
	Angiopathy	Microthrombosis	Anticoagulation Immunomodulation
	Local host response	Pulmonary hyperinflamation	Immunomodulation

Table 2. *Potential treatable traits in ARDS across three domains (Modified by Bos et al., 2021)*

2.4.2. Cell therapy

2.4.2.1. Mesenchymal stem cells (MSCs)

Mesenchymal stem cells (MSCs) are multipotent progenitor cells that can be isolated from multiple tissues including bone marrow, adipose tissue, and umbilical cord tissue, blood and perivascular tissue. The source may impact the immunomodulatory effects, proliferation properties and therapeutic benefits of MSCs. Bone marrow-derived MSCs were the first type of MSCs isolated and are the most widely used for lung injury (Monsel, Zhu et al. 2016, Mohammadipoor, Antebi et al. 2018). Administration of MSCs induces potent anti-inflammatory and immunomodulatory effects and has been proven to decrease lung injury and increase survival in several preclinical models of ALI (Pati, Gerber et al. 2011, Curley, Hayes et al. 2012, Jackson, Morrison et al. 2016, Xiao, Hou et al. 2020). Thus, MSCs were able to maintain the integrity of the lung microvascular barrier (Li, Pan et al. 2019) and reduce the formation of pulmonary oedema (Gupta, Su et al. 2007) in several models of endotoxin-induced ALI due to a down-regulation of pro-inflammatory cytokines, such as TNF-α or MIP-2, and an increase in the production of the anti-inflammatory cytokine IL-10 (Gupta, Su et al. 2007). Moreover, MSCs also attenuated neutrophil-predominant inflammation and lung injury in an *in vivo* rat model of VILI (Lai, Wang et al. 2015). In Influenza mice models, MSCs also limited alveolar inflammation (Li, Xu et al. 2016) and

prevented the downregulation of sodium and chloride transported in infected cells, reducing the impairment of alveolar fluid clearance and attenuating lung injury (Chan, Kuok et al. 2016).

Despite these long-lasting therapeutic effects in a wide variety of *in vivo* experimental models, the engraftment rate of MSCs has been shown to be extremely low (Monsel, Zhu et al. 2016, Mastrolia, Foppiani et al. 2019). This unexpected low engraftment rate represented a major challenge in explaining the beneficial effects of MSCs (since in most cases, the cells were only temporarily resident in the host). Indeed, administration of MSC-derived conditioned medium (MSC-CM) recapitulates the therapeutic effects of MSCs in ARDS and other inflammatory lung diseases through activation of anti-inflammatory, pro-survival and anti-apoptotic pathways (Monsel, Zhu et al. 2016, Byrnes, Masterson et al. 2021). MSC-CM can mitigate the inflammatory response of the injured endothelium by preserving the integrity of the vascular barrier, restoring the normal status of membrane adhesion molecules β-catenin and VE-cadherin and preventing inflammatory cell binding to ECs (Pati, Gerber et al. 2011). Moreover, it has been demonstrated the capability of MSC-CM to reduce the secretion of TNF-α by macrophages mediated by IL-1ra (Ortiz, Dutreil et al. 2007). The administration of MSCs and MSC-CM improved lung endothelial barrier integrity and the rate of alveolar fluid clearance in an *ex vivo* model of perfused human lungs injured by endotoxin. This effect was, at least partially, mediated by the release of KGF which contributes to restore sodium dependent alveolar fluid transport (Lee, Fang et al. 2009). Administration of MSC-CM also exerted protective effects following VILI, decreasing lung inflammation (as evidenced by the reduction in alveolar inflammatory cell counts, the decrease in IL-6 and TNF-α production or the increase in IL-10), improving systemic oxygenation and enhancing alveolar fluid clearance through a mechanism which may also be mediated through KGF secretion (Curley, Hayes et al. 2012). Intratracheal (IT) administration of MSCs or MSC-CM also reduced the total number of infiltrated neutrophils in BALF and attenuated the formation of lung oedema in mice with endotoxin-induced ALI (Ionescu, Byrne et al. 2012). In contrast, in a rat model of *E. coli*-induced pneumonia administration of MSCs reduced the infiltration of

neutrophils and the total amount of protein in BALF, whereas MSC-CM was less effective, improving animal survival but without significant mitigation of the severity of lung injury or inflammation (Devaney, Horie et al. 2015).

Overall, we now have a large body of evidence suggesting that MSCs act through paracrine effects, rather than (trans)differentiating and incorporating into the host tissue. In this regard, the discovery that EVs released by MSCs act as carriers of bioactive molecules (Maas, Breakefield et al. 2017), opens the possibility to develop new therapies based on the use of stem cells but cell-free and therefore potentially safer and amenable to standardization (Mohammadipoor, Antebi et al. 2018, Lanyu and Feilong 2019). In line with this, administration of MSCs-derived EVs (MSC-EVs) are also showing promising results in experimental models of ALI from different aetiologies (Lee, Park et al. 2019), which are summarized in Table 3 and figure 5. Accordingly, administration of human MSC-EVs to mice model of ALI induced by IT administration of endotoxin attenuated the influx of inflammatory cells, decreased the total protein content in BALF and reduced the extravascular lung water content (Zhu, Feng et al. 2014). In this study, Zhu *et al.* demonstrated that IT administration of MSC-EVs was able to reduce inflammation and restore the barrier function in an endotoxin-induced ALI model through a mechanism which involved KGF. In a later study, these authors confirmed that IV administration of MSC-EVs also improved survival and reduced lung protein permeability in a model of *E. coli*-induced pneumonia through a mechanism also mediated by KGF (Monsel, Zhu et al. 2015). In addition, MSC-EVs were able to restore protein permeability in primary cultures of human alveolar epithelial type II cells, induce anti-inflammatory M2 polarization in a macrophage cell line (Zhu, Feng et al. 2014) and enhance bacterial phagocytosis by human monocytes (Monsel, Zhu et al. 2015).

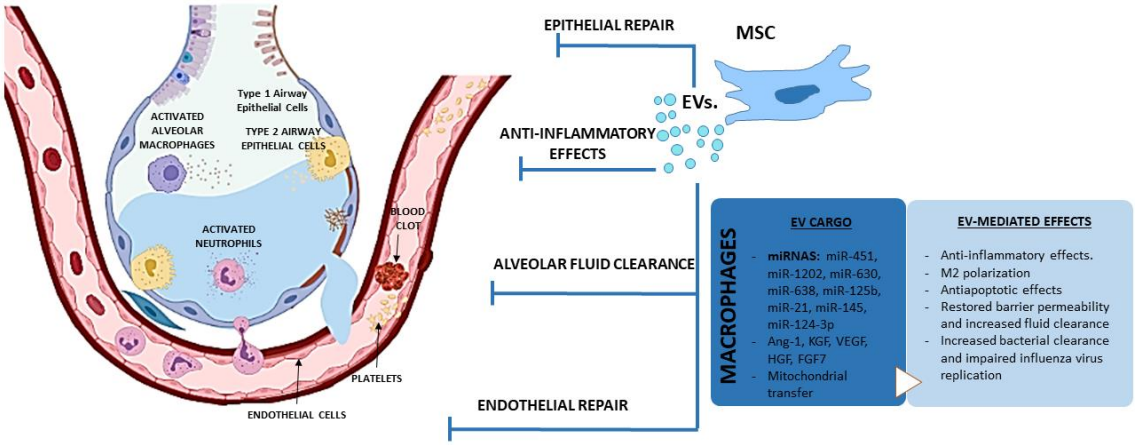

Figure 5. *Therapeutic potential of extracellular vesicles (EVs) derived from mesenchymal stem cells (MSCs) in acute respiratory distress syndrome (ARDS) (Esquivel-Ruiz, Gonzalez-Rodriguez et al. 2021).*

The direct effects of MSC-EVs on activated macrophages have also been confirmed in human monocyte–derived macrophages in the presence of BALF from ARDS patients and in murine AM (Morrison, Jackson et al. 2017). In this study, the authors found that EVs derived from MSCs can modulate macrophage polarization through a mechanism involving the transfer of functional mitochondria and upregulation of oxidative phosphorylation. Furthermore, administration of AM treated with MSC-EVs, but not control macrophages, protected against endotoxin-induced lung injury, significantly reducing the protein content and the total number of neutrophils in BALF (Morrison, Jackson et al. 2017). Phinney and colleagues also demonstrated that mitochondrial transfer by MSCs is facilitated by the simultaneous release of EVs containing microRNA which suppressed TLR signalling and desensitized macrophages to the ingested mitochondria. Using miRNA microarray analysis, the authors explored the content of MSC-derived EVs obtained from five human donors, identifying 156 microRNAs (45 upregulated; 111 down-regulated) that differed in abundance between EVs compared with their parent MSCs. The EVs were enriched in miR-451, miR-1202, miR-630 and miR-638, whereas miR-125b and miR-21 showed the largest reduction in MSC-EVs (Phinney, Di Giuseppe et al. 2015).

MSC-EVs also have protective effects on pulmonary structural cells. In a murine model of haemorrhagic shock, both MSCs and their EVs were shown to attenuate vascular permeability in injured lungs through inhibition of RhoA GTPase activity in lungs, but through differential activation of proteins and pathways (Potter, Miyazawa et al. 2018). In a swine model of influenza virus-induced ALI, MSC-EVs were able to inhibit the replication of influenza virus in epithelial cells and to significantly reduce the infiltration of inflammatory cells to the lungs, the thickening of alveolar walls and the number of collapsed alveoli in infected swine. (Khatri, Richardson et al. 2018). MSC-EVs were also effective on reducing the H_2O_2-induced epithelial cell death *in vitro* and hyperoxia-induced lung injuries *in vivo*, such as impaired alveolarization and angiogenesis, increased cell death and inflammatory responses. These protective effects against hyperoxic lung injury were apparently mediated by the transfer of vascular endothelial growth factor (VEGF) contained within these vesicles into pericytes, AM and ATII cells (Ahn, Park et al. 2018). In endotoxin-induced lung injury, the protective effects induced by MSC-EVs on pulmonary oedema were mediated partly by transfer of KGF mRNA to airway epithelial cells and angiopoietin-1 (Ang-1) mRNA to ECs (Zhu, Feng et al. 2014, Tang, Shi et al. 2017, Mahida, Matsumoto et al. 2020). In ECs stimulated with endotoxin *in vitro*, MSC-EVs augmented the expression of endothelial intercellular junction proteins, reduced EC apoptosis and inhibited the production of inflammatory cytokines through a mechanism involving the hepatocyte growth factor (HGF) gene carried inside the vesicles (Wang, Zheng et al. 2017). Increasing evidences suggest that MSC-EVs improve alveolar-capillary barrier properties through restoration of mitochondrial functions via mitochondrial transfer. In a model of severe pneumonia induced by *E. coli*, MSC-EVs also augmented intracellular ATP levels in injured AECs which is critical to restore fluid clearance and surfactant production (Monsel, Zhu et al. 2015). Although the mechanism was not elucidated in this study, the presence of mitochondria is critical for EV ability to reduce lung injury and restore mitochondrial respiration in the lung tissue (Dutra Silva, Su et al. 2021). Indeed, mitochondrial transfer by MSC-EVs has been shown to play a key role in the amelioration of lung injury by modulating the phenotype of macrophages

(Jackson, Morrison et al. 2016) or restoring bioenergetics functions in AECs, ECs and *ex vivo* cultured precision cut lung slices (Islam, Das et al. 2012, McVey, Maishan et al. 2019, Dutra Silva, Su et al. 2021). Another explanation for the barrier-enhancing effect of MSC-EVs can be attributed to an increased VE-cadherin expression and enhanced VE-cadherin and β-catenin interaction, supporting barrier integrity (Potter, Miyazawa et al. 2018, Simmons, Erfinanda et al. 2019). MSC-EVs restored protein permeability across human lung microvascular endothelial cells (HLMVECs) exposed to an inflammatory insult (a mixture of IL-1β, TNF-α, and IFN-γ) in part by maintaining inter-cellular junctions and preventing actin stress fiber formation. Incorporation of MSC-EVs into HLMVECs through the surface receptor CD44 was required for restoration of protein permeability. The therapeutic effect of MSC-EVs was associated with the transfer of Ang-1 from the EVs to the injured HLMVECs with subsequent secretion of the anti-permeability factor (Hu, Park et al. 2018).

MSC-EVs have been shown to restore alveolar fluid clearance and reduce oedema in *ex vivo* perfused human lungs rejected for transplantation and those injured by bacterial pneumonia (Gennai, Monsel et al. 2015, Park, Kim et al. 2019). Similarly, *E. coli*-induced pneumonia in mice was ameliorated by MSC EVs via the well-documented barrier-stabilizing and anti-inflammatory effects of KGF (Monsel, Zhu et al. 2015, McVey, Maishan et al. 2019). Prophylactic treatment with MSC-EVs increased survival in rats undergoing traumatic lung injury; inflammatory cytokines, infiltrating leukocytes and the degree of pulmonary oedema were all reduced (Li, Liang et al. 2019).

***IN VITRO* MODELS**			
MODEL	**EVs SOURCE**	**MAIN EFFECTS**	**REFERENCES**
Human macrophages stimulated with LPS or BALF from ARDS patients	Human BM-MSC	Decrease in inflammatory cytokines secretion and increase in M2 macrophage markers, IL-10 secretion and phagocytic capacity.	(Zhu, Feng et al. 2014, Monsel, Zhu et al. 2015, Morrison, Jackson et al. 2017, Tang, Shi et al. 2017)
Human endothelial cells stimulated with LPS, cytokines or plasma from ARDS patients	Human/mice BM-MSC	Increase in proliferation and IL-10 levels. Reduction in pulmonary capillary permeability, apoptosis, mitochondrial dysfunction and secretion of inflammatory cytokines and Ang-1 (EV cargo: HGF and mitochondria).	(Tang, Shi et al. 2017, Wang, Zheng et al. 2017, Hu, Park et al. 2018, Dutra Silva, Su et al. 2021)
Human alveolar epithelial type 2 cells stimulated with LPS, cytokines or plasma from ARDS patients	Human BM-MSC	Decrease in protein permeability, inflammatory cytokines and Ang-1 secretion and mitochondrial dysfunction (EV cargo: mitochondria).	(Monsel, Zhu et al. 2015, Morrison, Jackson et al. 2017, Dutra Silva, Su et al. 2021)
Human alveolar epithelial type 2 cells stimulated with *Influenza virus*	Swine BM-MSC	Reduction in replication and apoptosis.	(Khatri, Richardson et al. 2018)
***Ex vivo* perfused human lungs rejected for transplantation**	Human BM-MSC	Increase in alveolar fluid clearance and airway and hemodynamic parameters. Decrease in lung weight gain.	(Gennai, Monsel et al. 2015)
***Ex vivo* perfused human lungs injured with severe *E. coli* pneumonia**	Human BM-MSC	Increase in alveolar fluid clearance. Decrease in bacterial count, absolute neutrophil count and protein permeability.	(Park, Kim et al. 2019)
***Ex vivo* cultured human precision cut lung slices**	Human BM-MSC	Attenuation of mitochondrial dysfunction and downregulation of TNF-α, IL-8 and RAGE (EV cargo: mitochondria).	(Dutra Silva, Su et al. 2021)

IN VIVO MODELS			
MODEL	**EVs SOURCE**	**MAIN EFFECTS**	**REFERENCES**
Endotoxin-induced ALI in mice	Human BM-MSC	Improvement in lung mitochondrial bioenergetics and decrease in BALF total protein and cell count.	(Dutra Silva, Su et al. 2021)
		Reduction in the extravascular lung water and total protein levels in BALF, demonstrating a reduction in pulmonary edema and lung protein permeability. MVs also reduced the influx of neutrophils and macrophage inflammatory protein-2 levels in the BAL fluid (EV cargo: KGF mRNA).	(Zhu, Feng et al. 2014)
		Reduction in the influx of inflammatory cells in the injured alveoli, MIP-2 and albumin levels in BALF, pulmonary capillary permeability and histological injury (EV cargo: Ang-1 mRNA).	(Tang, Shi et al. 2017)
		Decrease in alveolar leukocytosis and protein leak, mitochondrial dysfunction and mortality and increase in surfactant secretion (EV cargo: mitochondria).	(Islam, Das et al. 2012)
		Improvement in survival and decrease in histological severity, influx of inflammatory cells, cytokines, protein and bacteria (EV cargo: KGF).	(Monsel, Zhu et al. 2015)

Hyperoxia-induced ALI in mice	Human UCB-MSC	Attenuation of impaired alveolarization and angiogenesis, increased cell death. Diminishment of activated macrophages and inflammatory cytokines secretion (EV cargo: VEGF).	(Ahn, Park et al. 2018)
Hemorrhagic shock-induced ALI in mice	Human BM-MSC	Significant decrease in lung vascular permeability (via decreased activation of the cytoskeletal GTPase RhoA).	(Potter, Miyazawa et al. 2018)
Traumatic-induced (weight-drop method) ALI in rats	Rat BM-MSC	Increase in survival and IL-10 level and decrease in oxidative stress, cell count, inflammatory cytokines secretion and protein in BALF (EV cargo: mitochondria).	(Li, Liang et al. 2019)
Influenza virus-induced ALI in pigs	Swine BM-MSC	Reduction in infiltration of inflammatory cells to the lungs, thickening of alveolar walls and number of collapsed alveoli.	(Khatri, Richardson et al. 2018)

Table 3*. Therapeutic potential of EVs derived from MSCs in ARDS .(Esquivel-Ruiz, Gonzalez-Rodriguez et al. 2021)*

Strategies for improving the therapeutic efficacy of MSCs in ALI

Although MSCs have an innate potential to induce and/or contribute to regeneration, this potential is now known to be greatly influenced by diverse extrinsic factors such as the tissue source of the MSCs, the health status and age of the MSCs donor, the batch/lot of serum used for the *in vitro* culture of the MSCs, passage number, oxygen concentration, and the presence/absence of a pro-inflammatory environment when the MSCs are infused. Indeed, after transplantation, MSCs must confront a harsh environment which limit their survival and compromise their ability to migrate towards damaged tissues leading to unsatisfactory therapeutic results. In the pursuit of strategies to enhance the therapeutic potential of MSCs, preconditioning strategies are gathering increasing attention. In this context, one of the major challenges in MSC-based

therapies is to develop methods that mimic the injury environment, without compromising cell quality and function. Thus, currently explored *in vitro* preconditioning strategies include environmental stimuli (such as exposure to hypoxia), treatment with cytokines or pharmacological agents or genetic engineering (Ferreira, Teixeira et al. 2018, Han, Li et al. 2019, Gorgun, Ceresa et al. 2021, Rolandsson Enes, Krasnodembskaya et al. 2021). The principal effects of preconditioning strategies in the therapeutic potential of MSCs are summarized in Table 4.

Hypoxia

MSCs are routinely cultured under standard oxygen conditions (ranging from the 18.5 % O_2 detected inside cell culture incubators to 21% O_2 in room air) despite the physiological environment in the bone marrow and other tissues is hypoxic, with oxygen tension ranging from 2 to 12% O_2. Furthermore, following transplantation, MSCs can confront severe hypoxic conditions in the ischemic tissues, even below 1% O_2, which often results in apoptosis (Rosová, Dao et al. 2008). Accordingly, it is well documented that culture under hypoxic conditions can promote the proliferation of MSCs, inhibit apoptosis and facilitate migration and chemotaxis, thereby improving the effectiveness of MSCs in treating ARDS/ALI (Bader, Klose et al. 2015, Beegle, Lakatos et al. 2015, Wang, Li et al. 2021).

Hypoxic preconditioning modulates the secretion of cytokines and other soluble factors enhancing the immunomodulatory properties of MSCs (Frazier, Gimble et al. 2013, Roemeling-van Rhijn, Mensah et al. 2013). For example, hypoxia markedly upregulated the expression of tryptophan-catabolizing enzyme indolamine 2,3 deoxygenase (IDO) or prostaglandin E (PGE) synthetase, two well-known activators of regulatory T cells, in human MSCs (Nemeth, Leelahavanichkul et al. 2009, Engela, Baan et al. 2013, English, Tonlorenzi et al. 2013, Roemeling-van Rhijn, Mensah et al. 2013). Moreover, it has been reported that hypoxia stimulates the production of anti-inflammatory cytokines (Jiang, Liu et al. 2015) and induces a metabolic switch from oxidative phosphorylation to glycolysis (Contreras-Lopez, Elizondo-Vega et al. 2020). Hypoxic preconditioning

also increases the angiogenic potential of MSCs (Leroux, Descamps et al. 2010, Liu, Hao et al. 2015, Ferreira, Teixeira et al. 2018, Han, Bai et al. 2018). Thus, hypoxia has been shown to increase the release of several factors involved in blood vessel formation such as VEGF, HGF, fibroblast growth factor 2 (FGF2), insulin-like growth factor 1 (IGF-1), Ang-1 or erythropoietin (Crisostomo, Wang et al. 2008, Kim, Noh et al. 2015). Notably, administration of EVs from MSCs cultured under hypoxic conditions has been shown to promote angiogenesis following acute myocardial infarction. Thus, injection of these EVs (80 μg of protein) thirty minutes after ligation of the coronary artery significantly reduced the infarct size and improved cardiac performance (Bian, Zhang et al. 2014). Similarly, IV administration of hypoxia – preconditioned EVs (50 μg of protein) immediately after the initiation of reperfusion also demonstrated cardioprotective effects in ischemia/reperfusion (I/R) injured hearts (Park, Park et al. 2018). Proteomic analysis of these EVs has identified the presence of Ang-1, VEGF, IGF-1, MCP-1, Tie-2/TEK and IL-6 as potential mediators for these hypoxia-augmented proangiogenic effects (Chen, Liu et al. 2014). In line with these evidences, hypoxic preconditioning has been shown to increase the protective effects of MSC-EVs in experimental models of lung injury (Table 4). Thus, hypoxic preconditioning potentiated the therapeutic effects of MSC-EVs in a model of endotoxin-induced ALI, facilitating the reduction of neutrophil influx, the decrease of TNF-α and the upregulation of IL-10 (Li, Jin et al. 2015). In line with this, acute lung transplantation of hypoxia-preconditioned MSCs also exerted better therapeutic effects in bleomycin-induced pulmonary fibrotic mice and enhanced the survival rate of engrafted MSCs, due to the increased expression of anti-apoptotic (HGF, Bcl-2), anti-oxidative (catalase, heme oxygenase 1 [HO-1]), and proangiogenic (VEGF) factors (Lan, Choo et al. 2015).

TLR ligands

MSCs sense the environment through various damage-associated and pathogen-associated cell surface receptors and respond differentially depending on the environmental requirements (Waterman, Tomchuck et al. 2010, Mastri, Shah et al. 2012, Rolandsson Enes, Krasnodembskaya et al. 2021). For example,

stimulation of TLR3 and TLR4 appeared to polarize MSCs into two different immune regulatory phenotypes. Whereas treatment with the TLR4 agonist LPS induced a polarization of MSCs towards a more pro-inflammatory phenotype (with increased release of IL-6 and IL-8), priming with the TLR3 agonist Poly (I:C) activated a immunosuppressive phenotype, with increased expression of IDO, PGE2 and RANTES (Waterman, Tomchuck et al. 2010, Fuenzalida, Kurte et al. 2016, Rolandsson Enes, Krasnodembskaya et al. 2021).

Treatment with endotoxin has been shown to increase the release of proangiogenic factors (such as VEGF, FGF2, IGF-1 or HGF) in MSCs (Crisostomo, Wang et al. 2008, Grote, Petri et al. 2013). The activation of TLR4 has also been demonstrated to be critical for MSCs survival and therapeutic effect in a pre-clinical model of *E. coli*-induced ALI. In this study, MSCs isolated from TLR4 deficient mice impaired survival under conditions of inflammatory stress *in vitro* and were not therapeutically active *in vivo*. Mechanistically, it was shown that TLR4 pathway regulates signalling through PAR1 on MSCs and TLR4 stimulation leads to expression and secretion of prothrombin (Gupta, Sinha et al. 2018). On the other hand, priming with the TLR-3 agonist Poly (I:C) was shown to increase the secretion of EVs with a higher content in KGF and to augment bacterial clearance in a murine model of *E.coli*-induced pneumonia (Monsel, Zhu et al. 2015). When examined *in vitro*, EVs from Poly (I:C)-primed MSCs were more effective in enhancing the anti-inflammatory and phagocytic activity of cultured macrophages, possibly by transferring COX-2 mRNA to activated monocytes resulting in an increase in production of PGE2 (Monsel, Zhu et al. 2015). Moreover, the preconditioning with the TLR-3 agonist MSC-EVs significantly reduced lung protein permeability, an effect which was attributed to its Ang-1 content, a protein with well-known anti-inflammatory, anti-permeability and endothelial protective characteristics (Park, Kim et al. 2019).

Preconditioning strategy		ARDS/ALI preclinical model	Effects	Referenc es
Hypoxia		**Endotoxin**	↓ Neutrophil influx ↓ TNF-α ↑ IL-10 level	(Li, Jin et al. 2015)
		Bleomycin	↑ Anti-apoptotic factors (HGF and Bcl-2) ↑ Antioxidative factors (catalase and HO-1) ↑ Proangiogenic factors (VEGF)	(Lan, Choo et al. 2015)
Cytokines	**IFN-γ**	***E. coli***	↑ Macrophages phagocytosis ↑ Capillary endothelial barrier function	(Varkouhi , Jerkic et al. 2019)
TLR ligands	**TLR4**	***E. coli***	↑ Survival ↓ Lung damage ↑ Bacterial clearance ↓ Influx of inflammatory cells in BALF ↓ MIP-2 in BALF ↓ Total level of protein in BALF	(Gupta, Sinha et al. 2018)
	TLR3	***E. coli***	↑ Bacterial clearance ↑ Phagocytic activity	(Monsel, Zhu et al. 2015)
		E. coli	↓ Lung protein permeability	(Park, Kim et al. 2019)
Genetic engineeri ng	**CXCR4**	**Endotoxin**	↑ MSC homing to injured lung tissue ↓ Lung protein permeability ↓ TNF-α levels ↑ IL-10 levels ↓ Lung pathology score ↓ Wet/dry ratio ↓ Total protein content in BALF	(Yang, Zhang et al. 2015)
	IL-10	***E. coli***	↓ Infiltrated neutrophils ↑ Phagocytic capacity ↓ Markers of structural lung injury	(Jerkic, Masterso n et al. 2019)
		HCl	↓ TGF-β1, FN and fibrinogen in BALF ↓ Inflammation scores and Ashcroft scores	(Islam, Huang et al. 2019)

	sST2	**Endotoxin**	↓ Lung airspace inflammation and vascular leakage ↑ Alveolar architecture	(Martinez-Gonzalez, Roca et al. 2013)
	HGF	**I/R**	↑ Oxygen saturation ↓ Lung oedema	(Chen, Chen et al. 2017)
		HCl	↓ TGF-β1, FN and fibrinogen in BALF ↓ Inflammation scores and Ashcroft scores	(Islam, Huang et al. 2019)
		Radiation	↓ TNF-α, IFN-γ, IL-6 and intercellular adhesion molecule-1 level ↑ IL-10 level ↓ Fibrosis progress	(Wang, Yang et al. 2013)
	Ang-1	**Endotoxin**	↑ Anti-inflammatory effects ↓ Capillary endothelial barrier function	(Mei, McCarter et al. 2007, Xu, Qu et al. 2008)
	PGE receptor 2	**Endotoxin**	↑ MSC homing to injured lung tissue ↓ Alveolar-capillary barrier permeability ↓ TNF-α and IL-1β level	(Han, Lu et al. 2016)
	HO-1	**Endotoxin**	↑ Survival ↓ Alveolar-capillary barrier permeability ↓ Inflammatory markers ↑ HGF, KGF and IL-10 levels in serum and lungs	(Chen, Wu et al. 2019)
	P130/E2F4	**Endotoxin**	↑ MSC homing to injured lung tissue ↑ Differentiation into AECs II ↓ Alveolar-capillary barrier permeability	(Zhang, Chen et al. 2019)
	miR-30b-3p	**Endotoxin**	↓ Histopathology ↓ Alveolar-capillary barrier permeability ↓ Neutrophil infiltration ↓ MPO activity ↓Alveolar inflammation	(Yi, Wei et al. 2019)

	miR-22-3p	**Endotoxin**	↓ Lung inflammation and oxidative stress ↓ Epithelial and endothelial apoptosis	(Zheng, Liu et al. 2021)

Table 4*. Strategies for improving the therapeutic efficacy of MSCs in ARDS/ALI preclinical models (Esquivel-Ruiz, Gonzalez-Rodriguez et al. 2021).*

2.4.2.2. Endothelial progenitor cells (EPCs)

EVs from endothelial progenitor cells (EPCs) have also been shown to have therapeutic potential. The IT delivery of EPC exosomes can mitigate lung injury enhancing EC proliferation, migration, angiogenesis, and trans-epithelial electrical resistance through the delivery of miR-126 to epithelial cells (Wu, Liu et al. 2018). Administration of EPC-EVs decreased lung injury, hypoxia, alveolar cell count, protein permeability, pulmonary edema, and inflammatory cytokines in the murine IT-endotoxin model (Zhou, Li et al. 2019). Furthermore, another work demonstrates that IV administration of EPC-EVs attenuate sepsis-related ALI and the increase in plasma levels of cytokines and chemokine (Zhou, Li et al. 2018).

2.5. Experimental models of ALI:

2.5.1. LPS-induced ALI model

LPS is a glycolipid present in the outer membrane of gram-negative bacteria that is composed of a polar lipid head group (lipid A) and a chain of repeating disaccharides (Raetz, Ulevitch et al. 1991). Most of the biological effects of LPS are reproduced by lipid A (Schromm, Brandenburg et al. 2000), although the presence or absence of the repeating oligosaccharide O antigen influences the magnitude of the response (Kelly, Young et al. 1991). In serum, LPS binds to a specific LPS binding protein (LBP) (Martin, Mathison et al. 1992), forming an LPS:LBP complex that activates the CD14/TLR4 receptor structure on monocytes, macrophages, and other cells, triggering the production of inflammatory mediators (Wright, Ramos et al. 1990, Schumann 1992, Tapping, Akashi et al. 2000).

In humans, pneumonia and sepsis are the two most common predisposing conditions for the development of ARDS (Quinlan and Evans 2000, Matthay,

Zemans et al. 2019, Kaku, Nguyen et al. 2020). The LPS-induced acute lung injury model is a reproducible model that resembles the inflammatory response and changes in alveolar-capillary permeability that occur in ARDS/ALI patients (Matute-Bello, Frevert et al. 2008). As a proinflammatory molecule, LPS directly activates the ECs by upregulating cytokines, adhesion molecules and tissue factors and, in addition, can induce EC apoptosis (Bannerman and Goldblum 2003, Wang, Bodenstein et al. 2008). In the LPS-induced secondary pathophysiological changes, activated neutrophils appear to play a central role (Abraham 2003), with other inflammatory cells (AMs and lymphocytes) and a large number of humoral mediators such as activated complement, metabolites of arachidonic acid, reactive oxygen/nitrogen species, proteolytic enzymes, diverse cytokines and chemokines and adhesion molecules (e.g. intercellular adhesion molecule-1), etc., being involved (Welbourn and Young 1992, Bhatia and Moochhala 2004, Wang, Bodenstein et al. 2008). In addition, other cells and factors are being studied (Wang, Bodenstein et al. 2008). Platelets have a critical role in the recruitment of polymorphonuclear cells (PMNs) to the lung through P-selectin, resulting in mutual cell activation and release of TXA2 (Kuebler 2006). High-mobility group box 1, a widely studied transcription factor and also growth factor, was found to act as a cytokine mediator and to play a major role in the pathogenesis of LPS-induced ALI (Wang, Yang et al. 2004).

LPS can be administered either directly to the lungs through IT injection or inhalation, or given intraperitoneally or intravenously to incite a systemic inflammatory response (Bastarache and Blackwell 2009). The IV administration produced a sequestration of PMNs in the alveolar septa, spaces and interstitium accompanied by congestion, hemorrhage and interstitial edema, all of which caused a marked thickening of alveolar walls (Nieman, Gatto et al. 1996, Lutz, Carney et al. 1998, Kemming, Flondor et al. 2005, Wang, Bodenstein et al. 2008). Another alteration was the dramatically increased number of AMs (Smith, Suffredini et al. 1994) and inflammation (Pittet, Mackersie et al. 1997, Thompson, Chambers et al. 2017, Kaku, Nguyen et al. 2020). Moreover, LPS infusion was also associated with minor or severe atelectasis (Nieman, Gatto et al. 1996), accumulation of detritus in the alveolar spaces (Kemming, Flondor et al. 2005),

alveolar proteinaceous edema and thrombosis (Da, Chen et al. 2007). The IT instillation of LPS is followed by an early phase characterized by increases in BAL fluid PMNs, albumin, and proinflammatory cytokines and a later phase 24–48 h after instillation characterized by normalization of the BALF cytokine concentrations and increases in the BAL fluid PMNs, monocyte, macrophage, and lymphocyte counts (O'Grady, Preas et al. 2001, Matute-Bello, Frevert et al. 2008). The hemodynamic response to intravenous LPS is characterized by an initial phase of leukopenia, decreased cardiac output, and a fall in arterial pressure. There is an increase in pulmonary arterial pressure, which is due mainly to an increase in the resistance of postcapillary veins (Kuida, Hinshaw et al. 1958). This initial phase is followed by slow improvement in leukocyte counts and the hemodynamic profile, over 4–6 h. Changes in the lungs become evident within 2–4 h and include hypoxaemia with an increase in the alveolar-arterial oxygen difference. In the lungs, the administration of LPS, either by IV or intra-alveolar routes, is followed by changes in PMN deformability and the entrapment of PMNs in the pulmonary capillaries (Reutershan, Cagnina et al. 2007, Matute-Bello, Frevert et al. 2008). The intraperitoneal administration activates systemic inflammation and is associated with a mild lung injury (Bastarache and Blackwell 2009). This injury can be augmented with either repeated injections of LPS or the implantation of an LPS pump in the peritoneal cavity to continually release LPS for hours, or even days (Everhart, Han et al. 2006, Cheng, Han et al. 2007).

LPS has some significant disadvantages. The treatment does not cause the severe endothelial and epithelial injury that occurs in humans with ARDS (Wiener-Kronish, Albertine et al. 1991). Bacteria produce exotoxins that are potent cellular toxins (Kudoh, Wiener-Kronish et al. 1994) and use effector systems such as the type III systems that cause direct cellular lysis (Roy-Burman, Savel et al. 2001). Thus, LPS by itself provides an incomplete picture of the effects of live bacteria in the lungs (Matute-Bello, Frevert et al. 2008).

2.5.2. Ventilator-induced lung injury (VILI) model

Despite its obvious benefits, several studies have shown that mechanical ventilation can inflict pulmonary structural damage (Grune, Tabuchi et al. 2019) and destabilize hemodynamics (Katira, Giesinger et al. 2017). The mechanism of VILI tissue damage involves mechanical stretch and activation of specific intracellular pathways involved in mechanotransduction (Gattinoni, Tonetti et al. 2016, Marini, Rocco et al. 2020). Damage was shown to be both magnitude- and duration-dependent (Tsuno, Miura et al. 1991, Dries, Adams et al. 2007, Yehya 2019). Deleterious effects of mechanical ventilation include inflammatory infiltration and vascular permeability, hyaline membrane formation, and pulmonary edema (Hughes and Beasley 2017). Excessive stretching of alveolar walls results in endothelial and epithelial rupture with formation of interstitial oedema (Fu, Costello et al. 1992). Furthermore, the development of hyaline membranes and increased permeability requires the presence of PMNs, suggesting that, in addition to mechanical damage, inflammatory damage is also necessary for mechanical ventilation to induce lung injury (Kawano, Mori et al. 1987). Mechanical cell deformation may induce the release of damage-associated molecular patterns (DAMPs) which can lead to activation innate immune receptors with subsequent production of proinflammatory cytokines and also changes in lipid trafficking, which could represent a mechanism for the maintenance of cellular integrity (Vlahakis and Hubmayr 2005, Matute-Bello, Frevert et al. 2008). In the animal model, low-injurious ventilation strategies such as high-frequency ventilation reduced pulmonary inflammation and increase the survival (Uhlig and Uhlig 2004)

The VILI model has advantages and disadvantages: the main advantages is its clinical relevance because it is the only model that has led to changes in clinical practice and induces a significant epithelial injury and impaired barrier function similar to what occurs in ARDS patients (Yehya 2019). The main disadvantage is the complexity of the model. Indeed, in small animals such as mice, damage occurs in relatively short periods of time, whereas patients require mechanical ventilation for days or weeks (Matute-Bello, Frevert et al. 2008).

2.5.3. Other models of ALI

- Bacteria. The intrapulmonary administration of live or attenuated bacteria increased permeability, interstitial edema, neutrophilic alveolitis (Fox-Dewhurst, Alberts et al. 1997). The administration of intravenous bacteria reproduces some of the alterations seen in ARDS patients, such as interstitial oedema, intravascular congestion and PMN sequestration. However, minimal neutrophilic alveolitis and no hyaline membrane formation is observed with these models (Asmussen, Ito et al. 2014).

- Acid aspiration. This model is characterised by a disruption of the alveolar/capillary barrier with neutrophilic infiltration. However, humans aspirate gastric contents, not pure acid and the difference between injurious and noninjurious doses is narrow (Modelska, Pittet et al. 1999).

- Saline lavage. Depletion of surfactant, decreased lung compliance and impaired gas exchange are observed, but without an additional stimulus there is minimal impairment of permeability and little PMN recruitment (Dos Santos and Slutsky 2000).

- Bleomycin. It is observed an acute inflammatory injury followed by reversible fibrosis with no formation of hyaline membranes (Moore and Hogaboam 2008).

- Oleic acid. This model presents acute and repair phases with similar histopathological and physiological features to human ARDS, but only a fraction of human ARDS is caused by fat embolism so it has a limited usefulness (Schuster 1994).

HYPOTHESIS AND AIMS

Acute respiratory distress syndrome (ARDS) is characterised by pulmonary oedema and alveolar collapse leading to severe arterial hypoxaemia. Although protective ventilatory support strategies have improved patient prognosis, associated mortality remains unacceptably high. In addition, the existence of pulmonary vascular dysfunction is an independent factor associated with a worse prognosis in these patients. The most frequent causes of ARDS have been sepsis and trauma but since 2020 a novel coronavirus, named as severe acute respiratory syndrome coronavirus-2 (SARS-CoV-2), emerged as one of the leading causes of ARDS worldwide.

Given that ARDS is one of the leading causes of death worldwide and that there are currently no effective treatments to reduce the mortality associated with ARDS, other than haemodynamic support and protective ventilatory support strategies, the discovery of new effective treatments would have a major impact on patient survival.

Mesenchymal stem cells (MSCs) are pluripotent stem cells that can easily be isolated from different tissues such as the bone marrow, adipose tissue and umbilical cord. Additionally, they can also be differentiated into a wide variety of cell types (such as muscle, bone, adipose tissue or cartilage). Administration of MSCs has been proposed as a possible therapy to many diseases, including inflammatory lung diseases or pulmonary hypertension, due to:

- Their low immunogenicity.

- Their intrinsic properties to respond, migrate and repair damaged tissues.

- And their potent anti-inflammatory, anti-apoptotic, pro-angiogenic and anti-fibrotic effects.

Although originally it was proposed that their therapeutic potential relied on their ability to regenerate the injured lung tissue due to their capacity to differentiate into distinct cell types, nowadays we know that the rate of cell engraftment is low and decrease over the time. For these reasons, now it is considered that the integration of these cells in the tissues is, in fact, a rare phenomenon and, possibly, clinically irrelevant. Besides, different groups have demonstrated that

the conditioned medium from MSCs is even more effective than the administration of the cells, which suggests the involvement of paracrine mechanisms such as exosomes.

The **general hypothesis** of this PhD thesis is that the lung inflammatory response and pulmonary vascular dysfunction associated with ARDS can be prevented by the use of MSC-derived extracellular vesicles (EVs).

The **overall objective** of this PhD thesis is, therefore, to analyse the therapeutic potential of MSC-derived EVs and to search for preconditioning strategies that are able to increase this potential.

The specific aims of this Thesis are:

a) To determine whether EVs derived from MSCs are able to prevent pulmonary vascular dysfunction induced by lipopolysaccharide (LPS) and hypoxia+Su5416 exposition in isolated pulmonary arteries.

b) To evaluate different concentrations of oxygen and TLR3 stimulation as preconditioning strategies to improve the therapeutic potential of these EVs.

c) To determine whether administration of any of these strategies increase the ability of EVs to prevent lung injury and pulmonary vascular dysfunction in an *in vivo* model of LPS-induced lung injury.

MATERIALS AND METHODS

The investigation conforms the Royal Decree 1201/2005 and 53/2013 on the Care and Use of Laboratory Animals and all procedures were approved by our institutional Ethical Committee and reported following ARRIVE guidelines(Kilkenny, Browne et al. 2010). Male Wistar rats (weight, 275 to 325 g; age, 12 weeks) were obtained from Envigo Laboratories (Barcelona, Spain). Animals were kept under standard conditions of temperature 22±1°C and 12:12 hour dark/light cycle with free access to food and water.

The Human Research Ethics Committee of the Hospital Universitario de Getafe (Madrid, Spain) approved the use, after informed consent, of lung tissue discarded by pathologists following thoracic surgery. Lung tissue was obtained from 4 adult patients with lung carcinoma surgery.

Normoxia and hypoxia

The techniques described in this section were used to evaluate the effects of different concentrations of oxygen with a double objective: 1) To evaluate preconditioning strategies to increase the therapeutic effects of MSCs and, 2) To replicate pathological conditions relevant to the pulmonary circulation.

We have evaluated the effect of different partial pressures of oxygen in either atmospheric conditions or aqueous solutions. Throughout the manuscript, oxygen tensions are either reported as a percentage (representing the volume fraction of oxygen in air) or as a partial pressure (mmHg or Torr).

When attempting to replicate either physiological or pathophysiological O_2 conditions, it is crucial to take into account the oxygen tensions to which human organs are typically exposed to and which ranges from 5 to 100 mmHg (or 1 to 13% O_2). In this regard, it should be noted that standard culture conditions (140 mm Hg O_2 ≈ 18.5% O_2) expose cells and tissues to a partial pressure of oxygen that is even higher than that experienced by the lung alveoli (~110 mm Hg ≈ 14% O_2), which are exposed to the highest partial pressure of oxygen of any site in the human body (Ast and Mootha 2019). In contrast, at the lower end of the spectrum we found the large intestine (3–11 mmHg), skeletal muscle during intense

exercise (7.5 mmHg O_2) or untreated cancer tissues (2 mmHg O_2) whereas pulmonary arteries are in the middle range (38-40 mm Hg ≈ 5% O_2).

In our attempt to evaluate different oxygen environments which could be relevant for MSCs and/or pulmonary arteries, the following protocols were performed and compared to standard culture conditions:

1. **Cell or tissue culture conditions:**
   - **A) Release of EVs by MSCs:** MSCs were grown under standard culture conditions or hypoxic conditions in a humidified CO_2 incubator.
     - Standard culture conditions, hereinafter referred to as “normoxic conditions”: The air in a humidified CO_2 cell culture incubator contains 18.5% O_2, equivalent to a partial pressure of 140 mmHg O_2.
     - “Hypoxic conditions”: Non-humidified pure N_2 gas was supplied to the CO_2 incubator to reach a 3% O_2, equivalent to a partial pressure of 23 mmHg O_2.
   - **B) *In vitro* model of PAH:** Isolated PAs were incubated under standard culture conditions (normoxic conditions: 18.5% O_2 or 140 mmHg) or hypoxic conditions (3% O_2; 23 mmHg O_2).

2. **Acute hypoxic pulmonary vasoconstriction:** To evaluate the effects of acute hypoxia in isolated pulmonary arteries, we performed experiments in an isometric microvascular myograph. For these in vitro experiments, hypoxia was induced by bubbling the Krebs solution with 95%N_2–5% CO_2 to achieve an oxygen concentration of 3%, equivalent to a partial pressure of oxygen (pO_2) of 23 mmHg (or Torr) in the chamber.

3. **Blood gasses:** We performed an *in vivo* model of acute lung injury. O_2 saturation (SaO_2) was measured using a pulse oximeter (MouseOx®Plus, Starr Life Sciences) and expressed as a percentage of O_2. It should be noted that normal values ranges between 95% and 100% (or PaO_2= 75-100 mmHg).

In summary, room air conditions are defined as 21% O_2 (=160 mmHg); normoxic culture conditions are 18.5 % O_2 (=140 mmHg) and our hypoxic conditions were set at 3% O_2 (= 23 mmHg O_2).

Production and purification of EVs

Isolated human umbilical cord blood mesenchymal stem cells (UCB-MSCs) were provided by Dr. Manuel Ramírez Orellana (Unit for Cell & Gene Therapies at Hospital Universitario Niño Jesús, Madrid). UCB-MSCs were cultured in complete Dulbecco's modified Eagle medium medium (DMEM) with Glutamax and 1mM pyruvate and supplemented with 10% (v/v) of fetal bovine serum (FBS), 0.1 mg/mL streptomycin, and 100 units/mL penicillin (GIBCO Life Technologies Inc.) in a humidified atmosphere of 5% CO_2 in air at 37°C. In order to ensure the collection of enough EVs for downstream analysis, cells were seed in four 150 cm^2 flasks for each condition tested. Briefly, upon reaching 70-80% of confluence, the cells were washed twice with Dulbecco's modified phosphate-buffered saline (PBS) and culture medium was replaced by DMEM supplemented with exosome-depleted FBS (from GIBCO), to avoid the interference of EVs present in conventional serum. Then, UCB-MSCs were incubated for 72 h under normoxia (18.5% O_2) or hypoxia (3% O_2) conditions. At the end of this period, conditioned medium was collected and cell viability was assessed by measuring the reduction of 3-[4,5-dimethylthiazol-2-yl]-2,5- diphenyltetrazolium bromide (MTT) to formazan. The isolation of EVs released by UCB-MSCs was performed using differentially ultracentrifugation (Figure 6), as previously described (Royo, Moreno et al. 2017). Briefly, the culture supernatant was centrifuged at 1,500×g for 10 min to remove cellular debris and large biomolecules. The resultant supernatant was subjected to ultracentrifugation at 10,000×g for 30 min. The pellet was resuspended in PBS and stored and the supernatant was submitted to a subsequent ultra-centrifuged at 100,000×g for 80 min. The final pellet of small EVs was resuspended in PBS and was performed a last ultracentrifugation at 100,000 × g for 80 min and the pellet was resuspended in 125 uL PBS and stored at −80 °C. Bradford assay, with BSA as a standard, was used for protein quantitation.

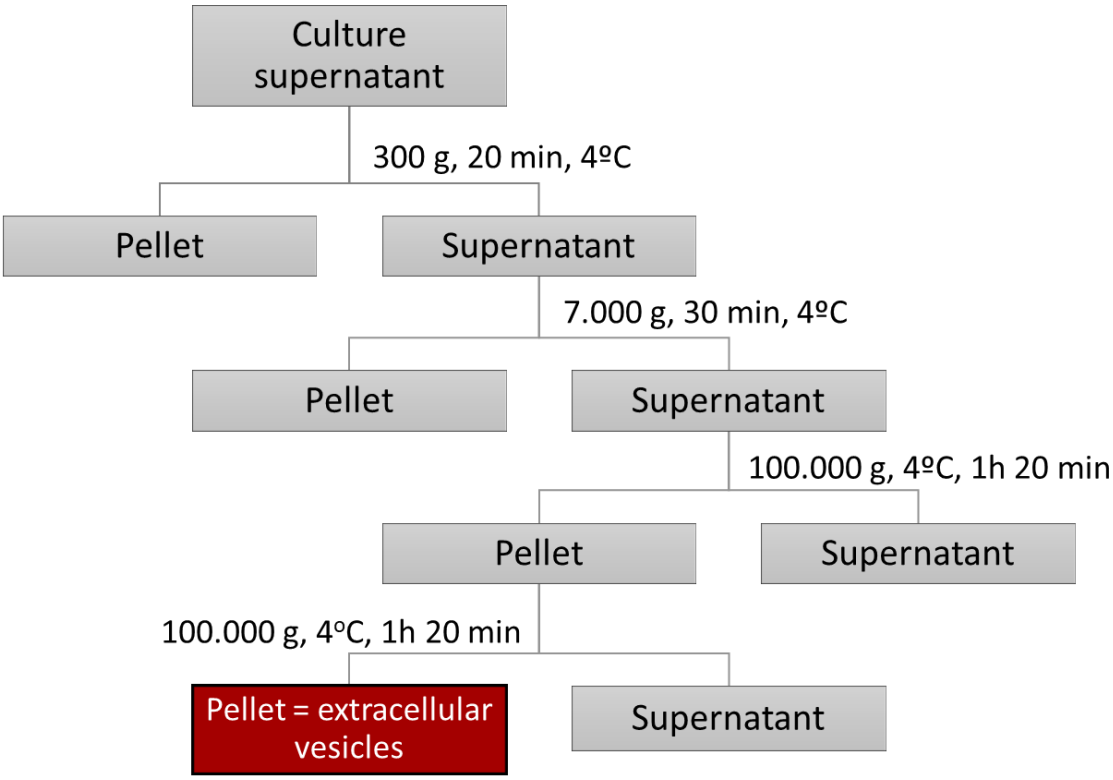

***Figure 6**. Extracellular vesicles purification via ultracentrifugation.*

Extracellular vesicles characterization

EVs were characterised by electron microscopy and nanoparticle tracking analysis. For the electron microscopy (EM) analysis, purified EVs fractions were applied onto freshly glow-discharged, carbon-coated, 300 or 400-mesh copper EM grids and incubated for 5 min at room temperature. The grids were placed consecutively on top of three distinct 50-µl drops of MilliQ water, laid on the top of a 50-µl drop of 2% uranyl acetate and stained for 1 min. Finally, the grids were rinsed gently and air dried. Grid visualization was performed on a JEOL JEM 1010 transmission electron microscope (TEM; Centro Nacional de Microscopía Electrónica, Madrid, Spain) at 100 KV. Images were recorded at 200K magnification with a Megaview II camera.

Size distribution within EV preparations was analysed using the nanoparticle-tracking analysis (NTA), by measuring the rate of Brownian motion in a NanoSight 300 system (Instituto de Investigación Sanitaria Gregorio Marañón). The system

was equipped with a fast video-capture and particle-tracking software. NTA post-acquisition settings were the same for all samples. Each video was analysed to calculate the mode and median vesicle size, as well as an estimate of the concentration (particles/mL).

The protein content of the extracellular vesicles was analysed by coupled high performance liquid chromatography - mass spectrometry (nLC MS/MS) at CIC BioGUNE, Bizkaia, Spain. Raw MS files were analyzed using MaxQuant v. 1.6.12.0 software. Proteins were identified matching to a human (Uniprot/Swissprot Homo sapiens) with a maximum of 2 missed cleavages and with precursor. Only proteins identified with at least one peptide at FDR < 1% were considered for further analysis. Comparative analysis was performed to identify proteins to be differentially expressed in EVs released by MSCs under hypoxic conditions as compared to those produced under normoxia (Filters applied: ±1.25 fold; FDR< 0.05).

DAVID tool from the NIH (https://david.ncifcrf.gov/) and ShinyGO v0.741 (http://bioinformatics.sdstate.edu/go/) were employed for Gene Ontology (GO) enrichment analysis (Huang da, Sherman et al. 2009, Huang da, Sherman et al. 2009, Ge, Jung et al. 2020). Functional annotation clustering was used for the selection of GO terms of interest. STRING software (https://string-db.org/) was used for the interaction analysis of a subset of hypoxia upregulated proteins. High-confidence results were specifically selected and used for the functional enrichment analysis and discussion.

Vessel isolation and *in vitro* models of ALI and PAH.

Pulmonary arteries (PA) were isolated from male Wistar rats in Krebs-Henseleit buffer solution of the following composition (in mmol/L): NaCl 118, KCl 4.75, $CaCl_2$ 2.0, $MgSO_4$ 1.2, $NaHCO_3$ 25, KH_2PO_4 1.2 and glucose 11 and cut into rings.

For ALI model, PA were incubated in DMEM supplemented with glucose (4.5 g/L), non-essential amino acid solution (1x), penicillin (100 U/ml), streptomycin (0.1 mg/ml), and amphotericin B (0.25 µg/ml) in the absence

(control) or presence of LPS (1 µg/mL) or EVs (5 µg/mL) for 24 hours in a normoxic incubator (18.5% O_2 and 5% CO_2). For in vitro models of PAH, the PA were maintained for 48 h in a normoxic incubator (18.5% O_2 and 5% CO_2) or a hypoxic incubator (3% O_2 and 5% CO_2) in the presence of the vascular endothelial growth factor receptor antagonist SUGEN 5416 (10 µM), as previously described (Mondejar-Parreno, Callejo et al. 2019).

Vascular reactivity

For contractile tension recording, distal resistance intrapulmonary artery (PA) rings (1.7–2 mm long, ~0.8 mm internal diameter) were mounted in a wire myograph with Krebs solution maintained at 37°C and bubbled with 21% O_2-5% CO_2-74% N_2 (normoxia). Vessels were stretched to an internal diameter of 500–800 µm to give an equivalent transmural pressure of 30 mmHg. This tension, although higher than that normally present *in vivo*, provides more reproducible responses with no other qualitative differences (Cogolludo, Moreno et al. 2003, Vankova, Snetkov et al. 2005, Cogolludo, Moreno et al. 2009, Strielkov, Krause et al. 2018). After equilibration, arterial rings were first stimulated with KCl (80 mM) and then every vessel was exposed to two hypoxic challenges (by bubbling the chambers with 95% N_2-5% CO_2 to achieve an oxygen concentration of 3–4%, or 24+1 mmHg, in the chamber) of 15 min duration each, with a 30 min recovering period in normoxia between hypoxic challenges (Cogolludo, Moreno et al. 2009, Pandolfi, Barreira et al. 2017). Afterwards, dose-response curves to serotonin (5-HT, $3x10^{-8}$ to $3x10^{-5}$ M) were performed and endothelial function was assessed by cumulative addition of acetylcholine (ACh, 10^{-9} to 10^{-5} M). After washing, a dose response curve to phenylephrine (Phe, 10^{-9} to 10^{-5} M) was performed by cumulative drug addition.

PASMCs isolation and culture

Rat and human PASMCs primary cell cultures were used in this study (Pandolfi, Barreira et al. 2017). Briefly, PASMCs were isolated from endothelium-denuded vessels dissected in Krebs-Henseleit buffer solution of the following composition (in mmol/L): NaCl 118, KCl 4.75, $CaCl_2$ 2.0, $MgSO_4$ 1.2, $NaHCO_3$ 25, KH_2PO_4 1.2 and glucose 11. Afterwards, PAs were digested in Ca2+-free PSS solution

containing (in mg/ml): collagenase 1.125, elastase 0.1, albumin 1. PAs were digested for 4 min at 4ºC followed by 1 min at 37ºC. Following digestion, tissues were washed in Ca2+- free PSS and disaggregated using a wide bore, smooth-tipped pipette, to make a cell suspension of PASMCs. Cell suspension was plated onto 35 mm petri dishes and incubated in a humidified atmosphere of 5% CO_2 in air at 37C in Dulbecco's modified Eagle's medium (DMEM) containing 20% heat-inactivated (FCS), pyruvate (0.11 mg/ml), 1% non-essential amino acids, streptomycin (0.1 mg/ml), penicillin (100 U/ml) and amphotericin B (250 ng/ml) for 1 week. Cells were subcultured in 75 cm2 sterile flasks in DMEM supplemented with 10% FCS and used within passages 2-3. PASMCs were seeded in 96 well plates at a seeding density of 25 x 103 cells / well. Cells were treated for 48 hours in 10% FBS DMEM in the absence (control) or presence of EVs (5 µg/mL) or LPS (1 µg/ml).

PAECs were kindly provided by Prof. María José Calzada (UAM).

Analysis of IL-6 release by whole PA or cultured cells.

Levels of IL-6 released into culture medium by PA, PAECs and PAMSCs were quantified by specific enzyme-linked immunosorbent assay (ELISA) (Rat and human IL-6 DuoSet ELISA Development Systems from R&D Systems, USA).

Determination of NO production.

NO production by PA rings was estimated by the accumulation of its oxidation product, nitrite, in culture medium of PA rings, using the Griess reaction (Figure 7), as previously described (Pandolfi, Barreira et al. 2017). Nitrite levels were quantified after incubation for 24 hours in the absence (control) or presence of EVs (5µg/ml) or LPS (1µg/ml).

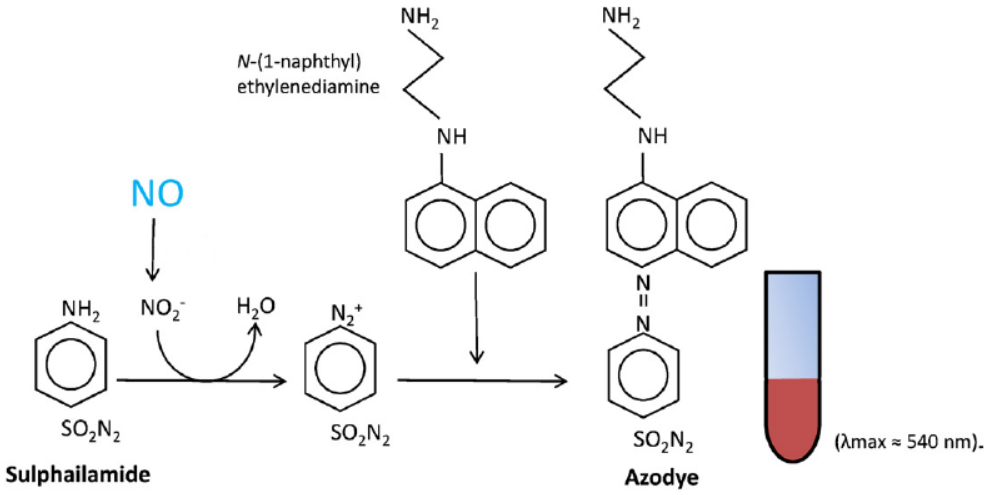

Figure 7. *Chemical reactions involved in the measurement of nitrite (NO_2^-) using the Griess Assay.*

Analysis of the incorporation of EVs into rat PASMCs.

EVs were labeled by using the liphophilic fluorescence dye, DiI (Molecular Probes) following the manufacture's instructions. Briefly, EVs were incubated with the dye at room temperature. After 30 minutes of incubation samples were ultracentrifuged at 100,000 × g for 75 min. Pellets were washed with PBS and centrifuged at 10000 × g for 5 min. Labelled-EVs were resuspended in PBS. In parallel same volume of the dye was incubated in the absence of EVs and subjected to same incubation periods, ultracentrifugation and wash steps previously described (Royo, Moreno et al. 2017). This latter sample was used to control the residual non-vesicular incorporated DiI label that could be co-purified during the ultracentrifugation process. Rat PASMCs were incubated with LPS, DiI-labeled EVs or residual-DiI control for 2 hours, then PBS-washed and mounted on DAPI and analyzed in a Leica Confocal Microscopy. All images were taken under same conditions and magnification.

Animal model of LPS-induced lung injury

Adult male Wistar rats (n=4-6) were anesthetized (80 mg/kg ketamine plus 8 mg/kg xylacine i.p.) and treated intratracheally with vehicle (saline solution) or

LPS (0.3 mg/kg) in the absence or the presence of hypoxic EVs (0.1 µg/kg of BW). Animals were randomly allocated to three experimental groups: (1) control group (saline solution); (2) LPS group and (3) HypoEVs-LPS group. 4 hours following instillation, rats were anaesthetised and ventilated with room air (tidal volume 9 ml/kg, 60 breaths/min, PEEP = 2 cm H2O). PAP was registered in open-chest rats with a pressure transducer via a catheter advanced through the right ventricle into the pulmonary artery. Heart rate, right ventricular systolic and diastolic pressure (sRVP) and systolic, diastolic and mean pulmonary arterial pressures (sPAP, dPAP and mPAP) were then measured and pulmonary pulse pressure, end diastolic pressure, contractility index and minimum and maximum dP/dt were calculated. Changes in oxygen saturation following partial airway occlusion by tracheal instillation of 100 µL of saline solution to induce ventilation-perfusion mismatching and oxygen saturation was monitored with a pulse oximeter (MouseOx®Plus, Starr Life Sciences) (Morales-Cano, Menendez et al. 2014, Pandolfi, Barreira et al. 2017, Morales-Cano, Callejo et al. 2019, Callejo, Mondejar-Parreno et al. 2020).

Histology

At the end of the hemodynamic measurements, the left lung was inflated *in situ* with paraformaldehyde saline solution (PFA 4%) through the left bronchus. Lung sections were stained with haematoxylin and eosin techniques and examined by light microscopy. The analysis were performed with ImageJ by a researcher unaware of the experimental groups allocation.

Mieloperoxidase activity assay.

Myeloperoxidase (MPO) activity was measured in frozen lung tissue, homogenized in phosphate buffer and centrifuged. As we have previously described (Pandolfi, Barreira et al. 2017) pellets were resuspended and subjected to three cycles of freezing and thawing prior to a final centrifugation step. The supernatants were collected and assayed in triplicate for MPO activity in a reaction buffer containing 50 mM potassium phosphate buffer, 0.167 mg/ml of O dianisidine dihydrochloride and 0.0006% H_2O_2 and using kinetic readings over 10 min at 450 nm.

Analysis of inflammatory cytokines.

Levels of IL-6, IL-1β, TNF-α or endothelin-1 present in plasma, BALF and whole lung homogenates were quantified by specific Rat DuoSet ELISA Development Systems (R&D System, USA) or by Quantikine ELISA Kit (R&D System, USA).

Statistical analysis.

Results are expressed as mean ± SEM. Technical replicates were combined to provide a single data point. Statistical analysis was performed using GraphPad Prism 7 as detailed in each figure legend. One-way ANOVA (for normally distributed data) followed by Bonferroni's post hoc test or the non-parametric Kruskal-Wallis test followed by Dunn´s test were used to compare three or more datasets. Repeated measures ANOVA was used to compare dose-response curves and one sample t test to evaluate normalized datasets. A value of $P < 0.05$ was considered statistically significant.

For the *in vivo* model, the primary end point variables were mean pulmonary pressure and inflammatory markers. Based on our previous data and considering a type I error $\alpha = 0.05$ (two tails), type 2 error $\beta = 0.8$, considering a variance of 6 mm Hg for mean arterial pressures, the calculated sample size to detect differences equal or greater than 5 mm Hg is 4. For pulmonary inflammatory markers, considering a variance of 10.000-15.000 pg for most cytokines, the calculated sample size to detect differences equal or greater than 250 pg was also 4.

RESULTS

1. EFFECTS OF HYPOXIC PRECONDITIONING ON EVs RELEASED BY MSCs.

1.1. Characterization of MSCs-derived EVs released under normoxic or hypoxic (3% O_2) conditions.

UCB-MSCs were grown under normoxic or hypoxic conditions for 72 hours (18.5 % and 3% O_2, respectively) before conditioned medium was collected and EVs isolated by ultracentrifugation (Royo, Moreno et al. 2017). The confirmation of the successful isolation of extracellular vesicles from UCB-MSCs was performed using well-established methods such as TEM, NTA and HPLC-MS (Thery, Witwer et al. 2018). TEM confirmed the presence of a population that exhibited the typical size and biconcave morphological features of extracellular vesicles (Figure 8).

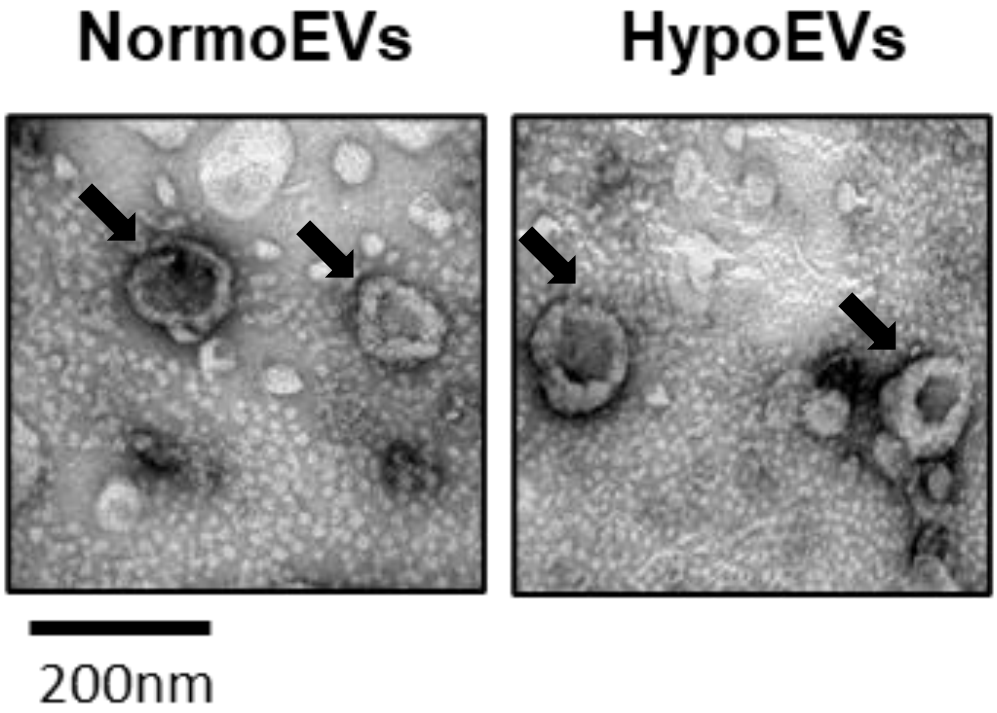

Figure 8. Representative transmission electron microscopy images showing a similar morphology between EVs released under normoxic (NormoEVs) and hypoxic (HypoEVs) conditions *(high magnification 200K; scale bars = 200 nm).*

NTA analysis revealed a heterogeneous EVs population but with a predominant peak corresponding to a diameter of 60-200 nm (Figures 9A). Comparative analysis of the concentration and the size of EVs released by MSCs following exposure to normoxic or hypoxic conditions found an increase in total protein concentration and a non-significant increase in the total number of particles (136 ± 19%) released under hypoxic conditions (Figures 9B-C). It should be noted that we found a strong correlation between these two quantification methods (i.e. determination of the number of particles by NTA vs protein concentration measured by Bradford assay (Figure 9D). These data suggest that hypoxia increases the release of EVs. However, it did not modify the proliferation rate of MSCs (Figure 9E). Moreover, no significant differences were found in terms of size parameters (Figures 9F-G) suggesting that hypoxia did not affect the population of EVs released by MSCs.

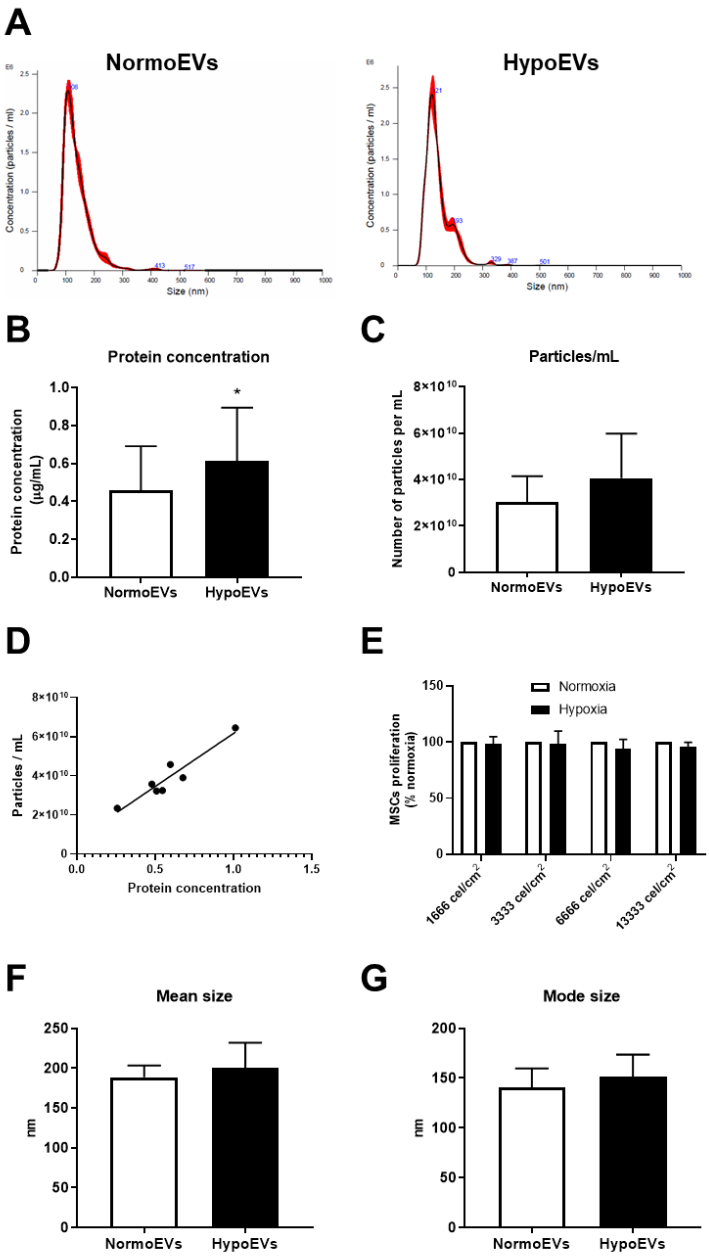

Figure 9. Characterization of mesenchymal stem cells (MSCs)-derived extracellular vesicles (EVs) released under normoxic or hypoxic (3% O_2) conditions. *(A) Representative histogram of nanoparticle tracking analysis (NTA) showing a similar particle size distribution between both preparations. (B) NTA also revealed that the number of particles was similar in NormoEVs and HypoEVs. (C) Total protein concentration (µg/mL) was significantly increased in the HypoEVs. (D) The protein concentration measured by the Bradford assay to perform the treatments correlates with the concentration of vesicles (particles/mL) as determined by NTA. (E) Exposure to hypoxia (3% O_2) does not increase the proliferation of umbilical cord blood derived mesenchymal stem cells. (F-G) Mean and mode sizes measured in NTA are similar in both preparations Data are shown as mean ± SEM (n = 4-6). * p <0.05 versus NormoEVs analysed with paired t-test.*

Proteome profiling was carried out in order to characterize and compare the protein cargo in normoxic and hypoxic EVs. Isolated EVs (n=4 in each group) were digested and analysed by HPLC-MS. As shown in Annex 1 (Table 1), 555 proteins were identified, most of them associated with extracellular vesicles or membranes (Figure 10D; Annex 1-Table 2). Among these proteins, we confirmed the expression of typical EV markers (CD63, CD9, CD81, TSG-101, Flotillin-1 and ALIX; Figures 10A-B) and the absence of negative markers (e.g. GM130, cytochrome C and Argonaute/RISC complex) (Thery, Witwer et al. 2018), further confirming the efficient isolation of EVs. Furthermore, EVs produced under normoxic or hypoxic conditions expressed typical MSC markers (CD73/5'-Nucleotidase, CD90/Thy1, CD105/Endoglin and CD44) and absence of mature cell markers such as CD34, CD45, CD11b/Integrin alpha M, CD14, CD79 alpha and CD19 alpha (Haynesworth, Baber et al. 1992, Dominici, Le Blanc et al. 2006, Varma, Breuls et al. 2007, Boxall and Jones 2012, Thery, Witwer et al. 2018) (Figure 10C). It should be noted that the expression pattern of EVs and MSCs markers was similar in both preparations suggesting that the exposure to hypoxia did not induce a differentiation process in the UCB-MSCs nor modify the identity of the vesicles released.

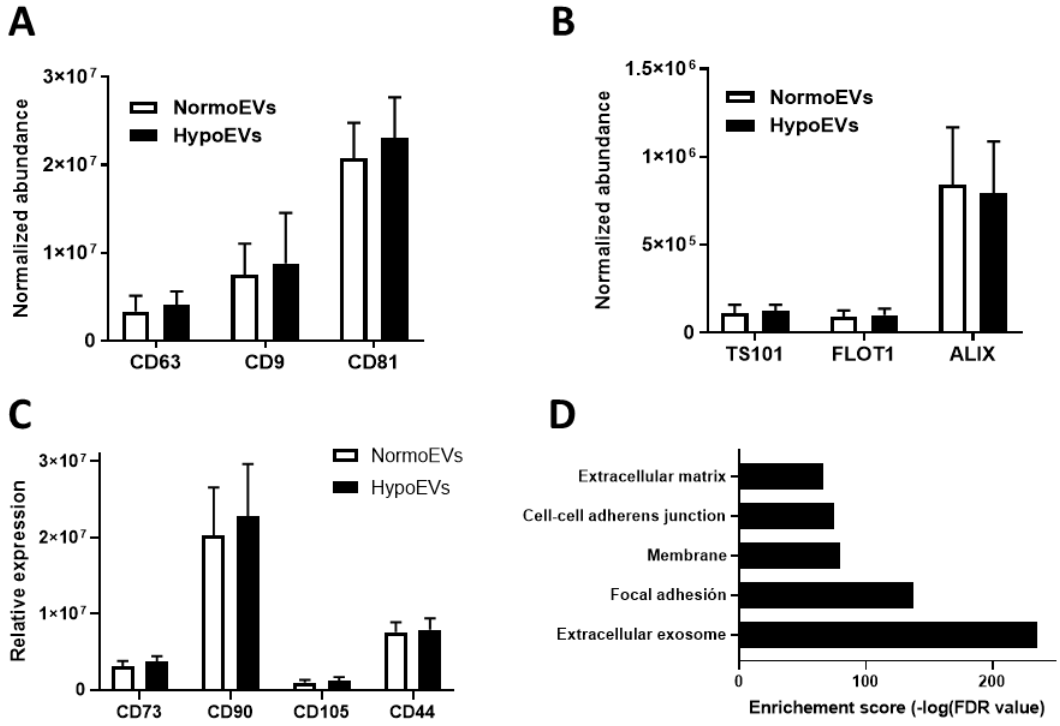

Figure 10. Expression of exosomal and MSCs markers in EVs released by MSCs under normoxic and hypoxic conditions. *(A-C) Quantification of the expression of markers of EVs (A-B) and MSCs (C) was similar in both preparations (D) The top 5 GO terms of cellular components for proteins identified in EVs are listed.*

Comparative analysis of the protein cargo identified in EVs released by MSCs under normoxic and hypoxic conditions, identified 15 proteins differentially expressed (±1.25 fold or more; FDR< 0.05) in hypoxic EVs vs normoxic EVs (Figure 11A; Annex 1-Table 1). To gain insights into the functional and biological processes, we performed a pathway and network analysis using DAVID Bioinformatics Resources 6.8 and ShinyGO v0.741 (Huang da, Sherman et al. 2009, Huang da, Sherman et al. 2009, Ge, Jung et al. 2020).

Top terms for the GO analysis in cellular components, molecular functions and biological process are represented in Figure 11B-D. Go enrichment analysis in cellular components confirmed that proteins differentially expressed in hypoxic EVs were mainly associated with extracellular organelles, extracellular vesicles, extracellular exosomes, extracellular space and focal adhesion confirming the origin of these proteins. For molecular processes, these proteins were mainly

involved in extracellular matrix structural constituent, cell adhesion molecule binding, integrin binding, structural molecule activity and cytoskeletal protein binding, suggesting that these proteins may modulate the ability of EVs to interact with other cells or the extracellular matrix and to modulate integrins, a large family of transmembrane receptors which play an important role in proliferation, inflammation, angiogenesis and fibrosis (Hood and Cheresh 2002). As for the GO analysis of biological process, these differentially expressed proteins were mainly involved in extracellular matrix organization, migration, cell adhesion and tissue development, suggesting again that these proteins may modulate adhesion and extracellular matrix remodelling. KEGG pathway analysis was also conducted for these 15 proteins reinforcing their involvement in modulating cell adhesion, cell-cell junction formation and cell polarity and unravelling the presence of several proteins involved in the immune response against several Gram negative bacterial infections (i.e., Salmonella or Shigella).

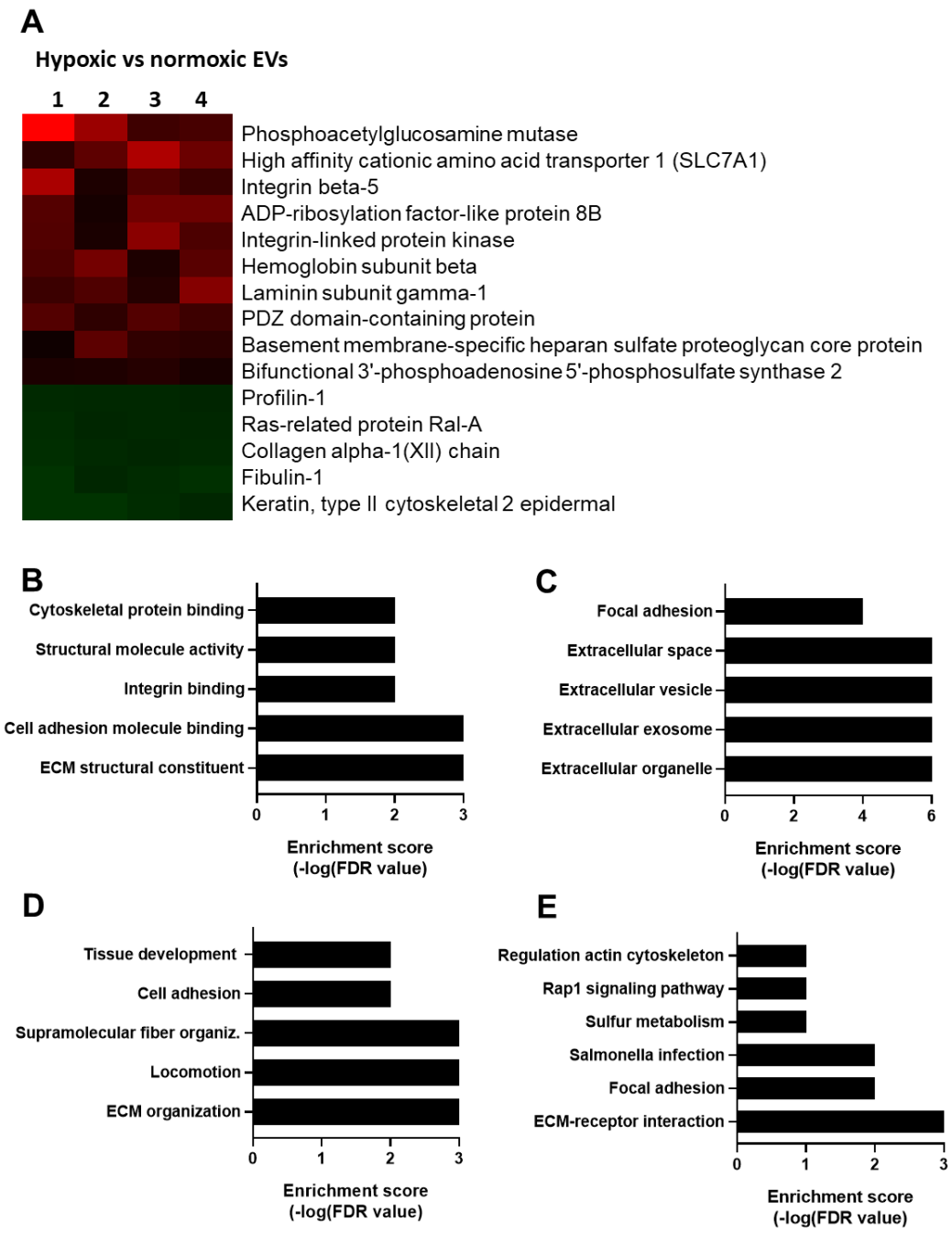

Figure 11. Comparative proteomic analysis of EVs released by MSCs under normoxic and hypoxic conditions. *A) Heatmap for paired samples (n=4) showing the fold change in expression of the fifteen proteins found to be differentially expressed in hypoxic EVs versus normoxic EVs. Fold change expression values are represented as colors and range from red (upregulation of protein expression) to green (downregulation of protein expression). (B-E) Top GO terms and KEGG pathways found following enrichment analysis. Top 5 GO (B) molecular function, (C) cellular component, and biological process (D) annotation, as well as (E) KEGG pathways for differentially expressed proteins in hypoxic EVs using DAVID Bioinformatics Resources 6.8 and ShinyGO v0.741.*

2. HYPOXIC PRECONDITIONING INCREASES THE POTENTIAL OF EVs DERIVED FROM MSCs TO LIMIT ACUTE LUNG INJURY INDUCED BY LPS

2.1. Induction of iNOS activity in rat PA by LPS is unaffected by the treatment with MSCs derived EVs.

Administration of MSCs induces potent anti-inflammatory and immunomodulatory effects and has been proven to decrease lung injury and increase survival in several preclinical models of ALI (Pati et al. 2011; Xiao et al. 2020; Jackson et al. 2016; Curley et al. 2012). Although initial research focused on their potential to regenerate the injured lung tissue, current evidence suggest that these protective effects are largely mediated by the EVs released by MSCs. In order to test the hypothesis that hypoxic preconditioning might increases the potential of EVs to ameliorate lung inflammation and prevent the development of pulmonary vascular dysfunction, we first assessed the effects of MSC-derived EVs produced under normoxic or hypoxic conditions on the inflammatory responses induced by lipopolysaccharide (LPS) *in vitro*.

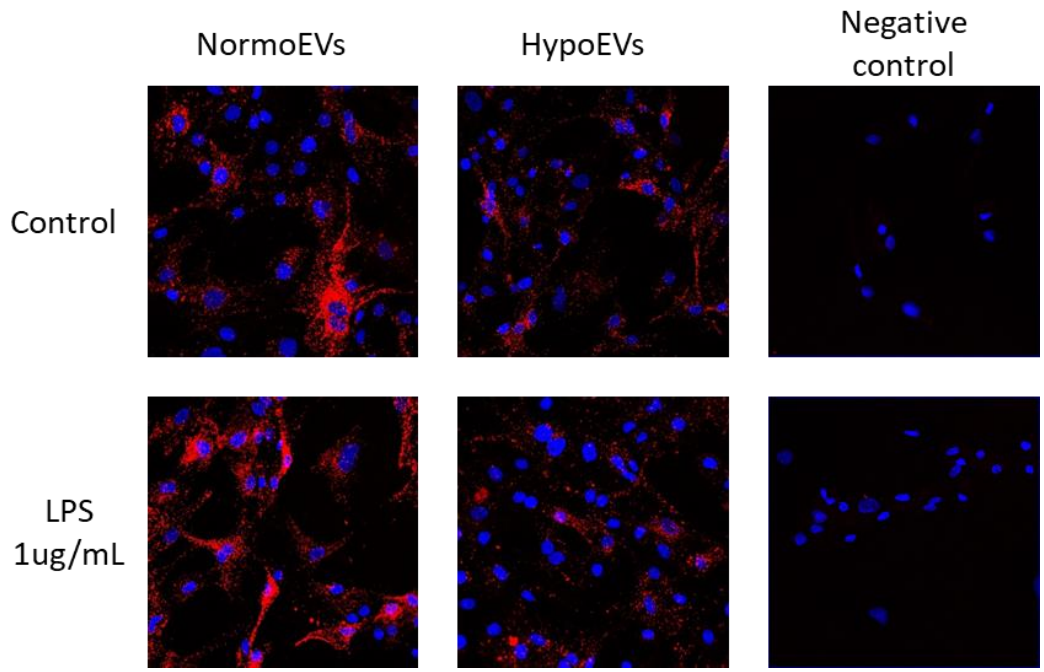

Figure 12. Incorporation of EVs into PASMCs in the presence or absence of LPS. *PASMCs were incubated with DiI-labeled EVs or residual non-vesicular DiI as described in* Materials and method section*. Representative confocal images showing DiI-label in red and DAPI (nucleus) in blue.*

Confocal microscopy employing fluorescently labelled EVs confirmed that, under our experimental conditions, both normoxic and hypoxic EVs are attached to PASMCs (Figure 12).

In isolated PA, LPS increased iNOS activity as evidenced by a robust increase in the levels of nitrites (Figure 13A). Accumulation of nitrite was unaffected by treatment with EVs released by MSCs regardless of hypoxic preconditioning (Figure 13B).

One of the main known functional consequences of vascular iNOS induction is a reduced contraction to α-adrenoceptor stimulation, a feature shared by pulmonary and systemic arteries (Murray, Wylam et al. 2000, Pandolfi, Barreira et al. 2017). Likewise, LPS markedly reduced the pulmonary vasoconstriction to phenylephrine (Figure 13C), an effect which is fully reversed by treatment with the selective iNOS inhibitor (Pandolfi, Barreira et al. 2017). In line with the lack of effects on nitrite production, neither NormoEVs nor HypoEVs were able to prevent LPS-induced hyporresponsiveness to phenylephrine (Figure 13C).

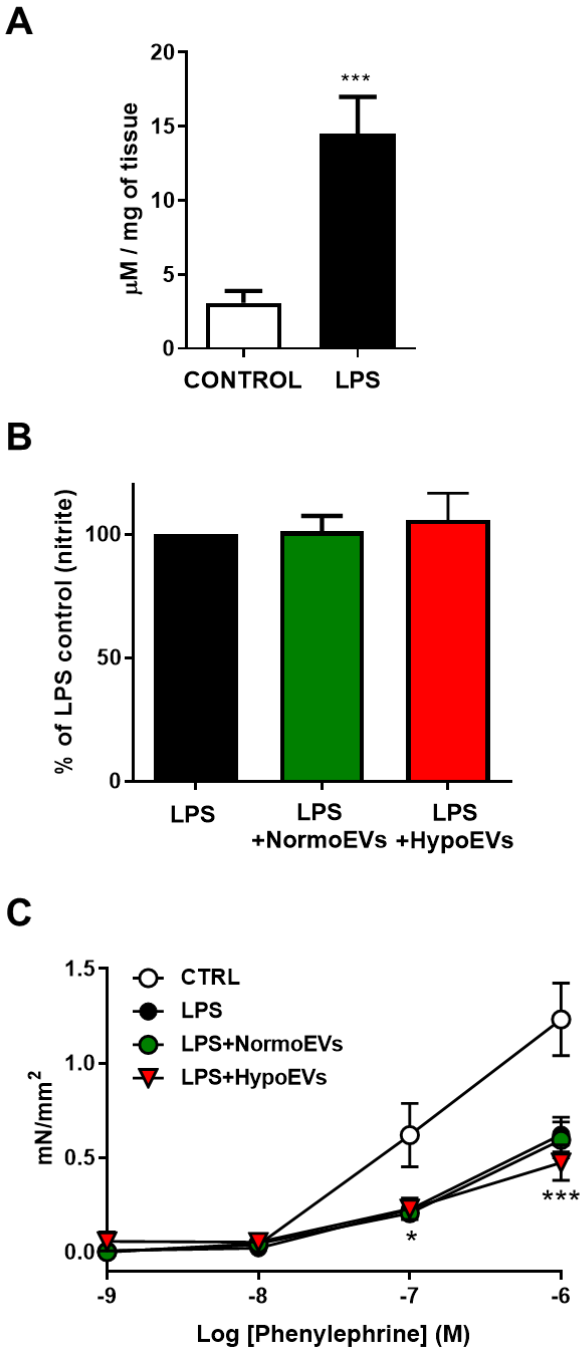

Figure 13. Effects of MSC-derived EVs on the induction of iNOS activity induced by LPS in whole pulmonary arteries (PA). *(A and B) Rat PA were incubated in the absence (Control; n=17) or in the presence of LPS (1 µg/mL; n=13) or EVs (5 µg/mL; n=4-9) for 24 hours before assessing iNOS activity by measurement of nitrite (breakdown product of NO) by the Griess assay. (C) Mean contractile responses to the α-adrenergic agonist phenylephrine in the absence (control; n=15) or presence of LPS (n=14) or EVs (n=9-12). Data are expressed as follows: µM per mg of wet weight tissue (A), percentage of the response induced by LPS (B) or active effective pressure (mN/mm^2; C). *** p<0.001 versus control analysed by one-way ANOVA followed by Bonferroni's post hoc test.*

2.2. Hypoxic EVs are able to prevent the hyperresponsiveness to serotonin, the failure of HPV and endothelial dysfunction induced by LPS in isolated PA.

As opposed to systemic vascular beds, hypoxia induces vasoconstriction in the pulmonary vasculature. In line with previous reports, (Ullrich, Bloch et al. 1999, Ichinose, Hataishi et al. 2003, Pandolfi, Barreira et al. 2017) incubation with LPS fully blocked HPV (Figure 14A). Notably, incubation with HypoEVs but not NormoEVs prevented the impairment of HPV induced by LPS (Figure 14A).

In contrast to the effects observed on adrenergic-induced pulmonary vasoconstriction, treatment with LPS markedly increased pulmonary vasoconstriction induced by serotonin (Figure 14B). Furthermore, hyperresponsiveness to serotonin was insensitive to treatment with NormoEVs but was prevented by HypoEVs (Figure 14B).

Treatment with LPS also induced a marked endothelial dysfunction (Figure 14C), a common feature in both systemic and PA exposed to endotoxin (Murray, Wylam et al. 2000, Price, McAuley et al. 2012, Pandolfi, Barreira et al. 2017). Treatment with HypoEVs partially prevented the endothelial dysfunction induced by LPS whereas in the presence of NormoEVs, ACh-induced relaxation remained blunted (Figure 14C).

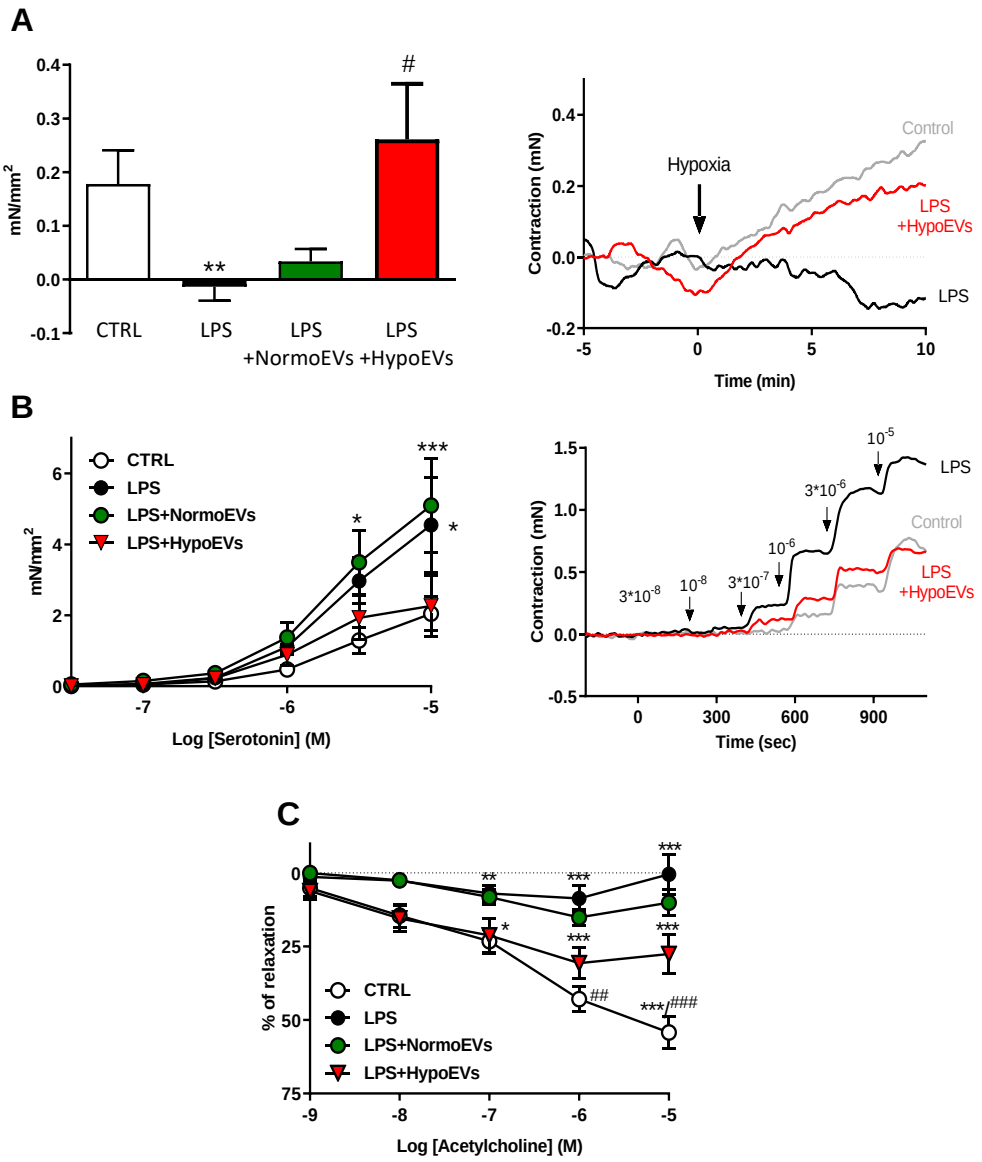

Figure 14. Hypoxic preconditioning increases the ability of MSC-derived EVs to prevent pulmonary vascular dysfunction induced by LPS in rat pulmonary arteries (PA). *(A) Mean contractile responses to hypoxia of PA incubated in the absence (control; n=18) or presence of LPS (1µg/mL; n=18) or EVs (5 µg/mL; n=7-16) and mounted in a wire myograph. Representative tracings showing the contractile responses of PAs exposed to hypoxia at time zero are shown in the right panel. (B) Mean contractile responses to serotonin and representative tracings in isolated PAs incubated for 24 hours in the absence (control; n=17) or presence of LPS (n=17) or EVs (n=7-14). (C) Concentration-dependent relaxation induced by the endothelium-dependent vasodilator acetylcholine in control (n=23) and LPS-treated (n=22) rat pulmonary artery (PA) rings incubated in the absence or the presence of EVs (n=12-17). Data in panels A and B are shown as active effective pressure (mN/mm^2), data in panel C are expressed as a percentage of the relaxation induced by acetylcholine. *, ** and *** p<0.05, p<0.01 and p<0.001 versus control and $^{\#}$, $^{\#\#}$ and $^{\#\#\#}$ p<0.05, p<0.01 and p<0.001 versus LPS (repeated measures ANOVA followed by Bonferroni's post hoc test).*

2.3. Hypoxic EVs induce different effects on IL-6 release induced by LPS in cultured PAECs, PASMCs and whole PA.

Our previous study (Pandolfi, Barreira et al. 2017) suggested that activation of the aSMase/IL-6 axis by LPS within pulmonary arteries contributes to the development of endothelial dysfunction, HPV impairment and hyperresponsiveness to serotonin. In order to test the possibility that HypoEVs were exerting their protective effects through the modulation of this pathway, we analysed the production of IL-6 in both isolated PA and primary cultured PASMCs.

LPS induced a strong increase in the production of IL-6 in both isolated rat PA (Figure 15A), PASMCs (Figure 15C and E) and human PAECs (Figure 15G). However, data shown in figure 12B revealed an increase in IL-6 released by whole PA following simultaneous treatment with both LPS and HypoEVs. By contrast, incubation with either NormoEVs or HypoEVs induced a modest but significant decrease in LPS-induced IL-6 production (Figure 15D). Similar findings were found in human PASMCs (Figure 15F). In contrast, HypoEVs did not modify secretion of IL-6 in human pulmonary artery endothelial cells (HPAECs) following stimulation with LPS (107 ± 4% of the response induced by LPS; 2 experimental runs performed in triplicate) (Figure 15H).

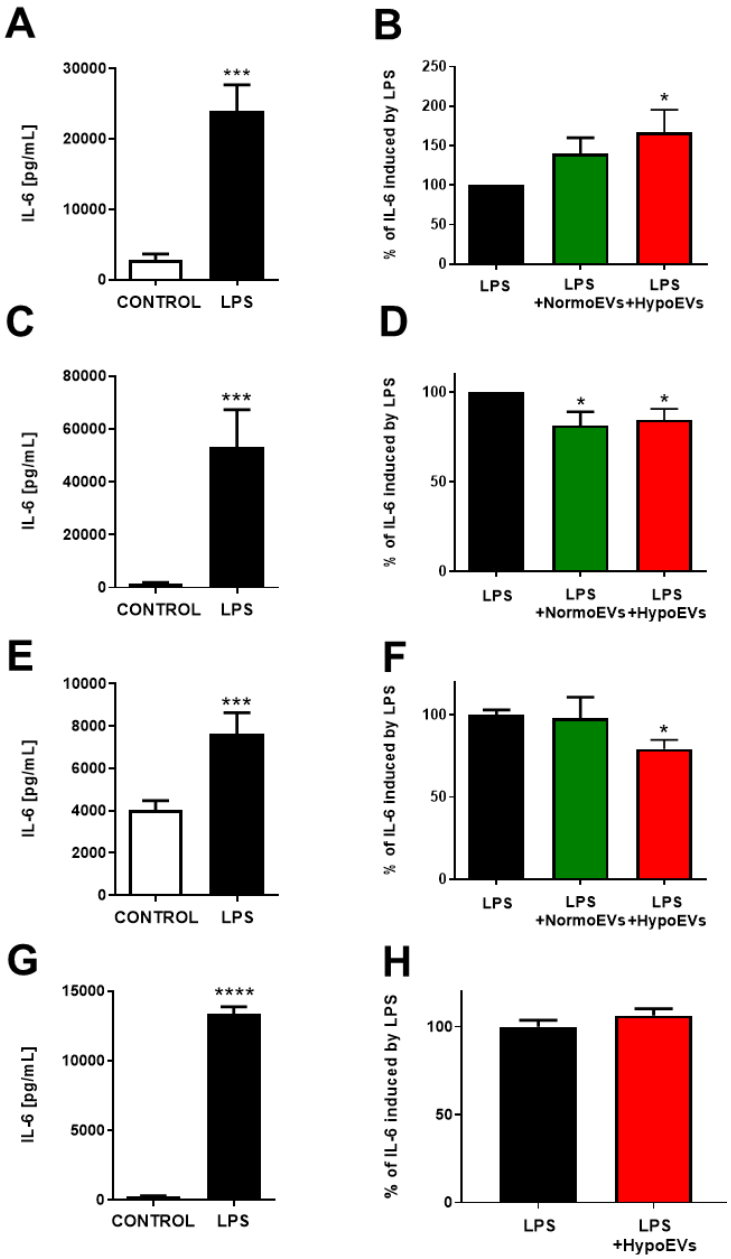

Figure 15. Effects of MSC-derived EVs on the release of IL-6 induced by LPS in whole pulmonary arteries (PA) and pulmonary arterial smooth muscle cells (PASMCs). *(A-B) Rat PA were incubated in the absence (Control; n=15) or in the presence of LPS (1 µg/mL; n=15) or EVs (5 µg/mL; n=6-11) for 24 hours before quantifying the release of IL-6 in the culture medium. Rat (C-D) and human (E-F) PASMCs (passage 2-3) were incubated in absence or in the presence of LPS (n=3-4) or EVs (5 µg/mL; n=3-4) for 48 hours and IL-6 production was assessed by ELISA. (G-H) PAECs (passage 2-3) were incubated in the absence or in the presence of LPS (n=2) or HypoEVs (n=2). Data shown in right panels are expressed as pg per mL of culture medium (A, C, E and G) and were analysed by paired Student´s t-test (*** p<0.001 versus control). Data shown in left panels are expressed as a percentage of the response induced by LPS, * p<0.05 versus control (One-way ANOVA followed by Bonferroni's post hoc test).*

2.4. HypoEVs increase the cell viability in cultured PAECs but not in PASMCs

Several studies show the ability of LPS to induce smooth muscle cell proliferation (Wort, Woods et al. 2001, Suda, Tsuruta et al. 2011, Jiang, Zeng et al. 2016) and endothelial cell loss by inducing apoptosis (Hamacher, Lucas et al. 2002, Luca, Lijnen et al. 2002, Wang, Akinci et al. 2007, Smith, Zimmerman et al. 2013, Chambers, Rounds et al. 2018) in animal models and ARDS patients. For the purpose of analysing the possible protective effect of extracellular vesicles against these processes, cell viability studies (i.e. the balance between proliferation and apoptosis/necrosis) were carried out in primary cultured PASMCs and human PAECs.

In our cultures, LPS had no clear effect on cell viability. Neither NormoEVs nor HypoEVs caused a change in PASMC proliferation (Figure 16A-B). Instead, HypoEVs were able to increase cell viability in human PAECs (Figure 16C).

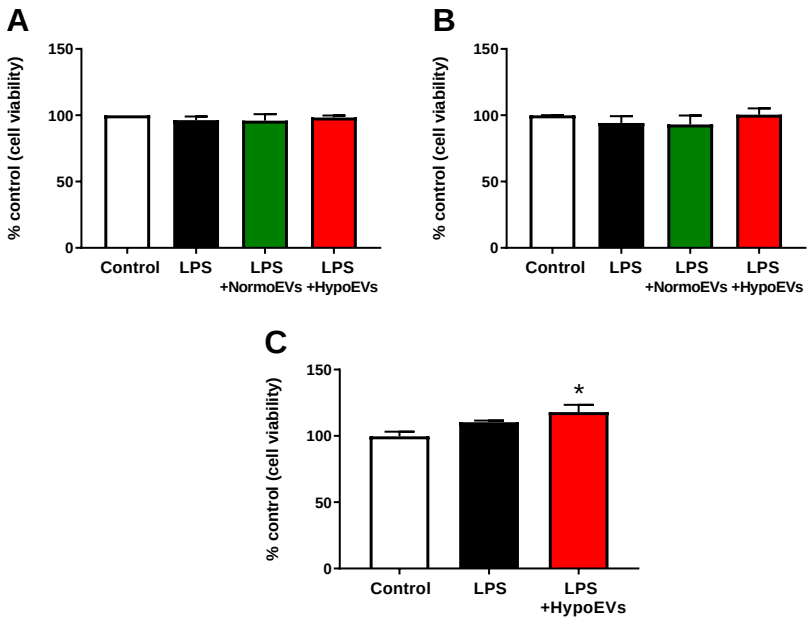

Figure 16. Effects of LPS and MSC-derived EVs on the cell viability in pulmonary arterial smooth muscle cells (PASMCs) and human pulmonary arterial endothelial cells (PAECs). *(A) Rat and (B) human PASMCs (passage 2-3) were incubated in absence or in the presence of LPS (n=3-4) or EVs (5 µg/mL; n=3-4) for 48 hours and cell viability was assessed by MTT. (C) Human PAECs (2 experimental runs performed in triplicate) were incubated and cell viability were measured. Data shown are expressed as a percentage of the response induced by LPS, * p<0.05 versus control (One-way ANOVA followed by Bonferroni's post hoc test)*

2.5. HypoEVs inhibits LPS-induced lung injury and pulmonary hypertension *in vivo*.

Vehicle (PBS) or HypoEVs (0.1 µg/Kg body weight) was intratracheally (I.T.) instilled 30 minutes before I.T. administration of LPS (300 µg/Kg body weight) or saline solution (control). All the animals survived to the procedures.

Intratracheal instillation of LPS resulted in an increase in heart rate and PAP (Figure 17A-F) and tend to decrease oxygen saturation (Figure 17G). Notably, administration of HypoEVs prevented the increase in PAP and the decrease in oxygen saturation despite having no direct effects in heart rate (Figure 17F). Finally, in order to test whether the impairment of HPV observed in vitro translated into ventilation-perfusion mismatching in vivo, we used a model of partial airway occlusion, as previously described (Pandolfi, Barreira et al. 2017). As shown in Figure 17H, intratracheal administration of 100 µl of saline solution induced a rapid but transient hypoxaemia. The maximum decline in oxygen saturation levels was similar among all the groups. By contrast, the recovery, which reflects blood redistribution away from the hypoxic/fluid filled alveoli (i.e. HPV) was significantly reduced in LPS-treated rats but not in animals treated with HypoEVs. Other haemodynamic parameters were not affected by treatment with LPS or HypoEVs, except for the contractility index which is significantly increased by HypoEVs (Figure 18).

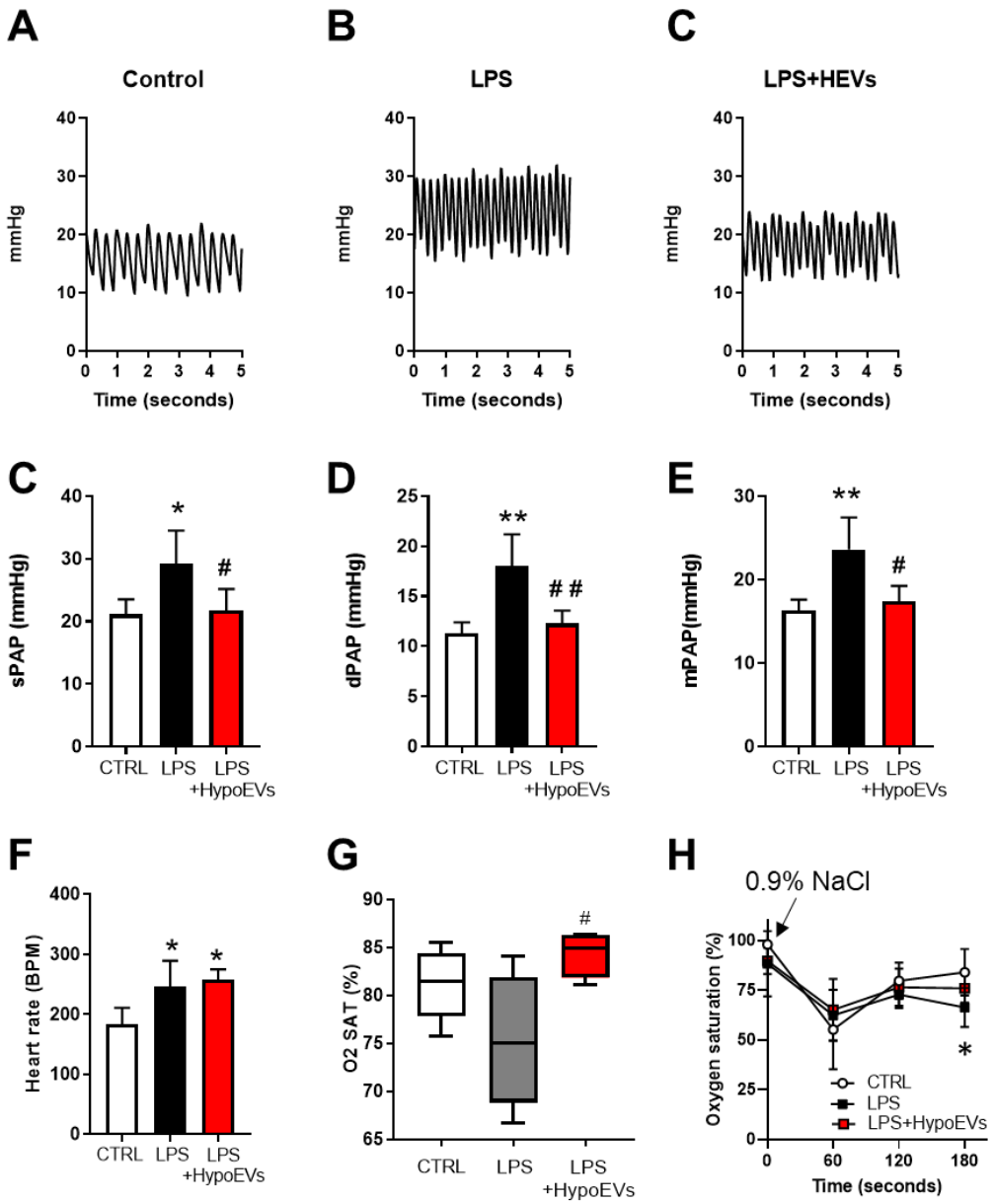

Figure 17. Treatment with EVs released by MSCs under hypoxic conditions (HypoEVs) limits LPS induced pulmonary hypertension in vivo. *(A-C) Representative recordings of pulmonary artery pressure (PAP) in control, LPS and HypoEVs plus LPS-treated rats (n=4-5). Averaged values of diastolic (C) systolic (D) and mean (E) PAP registered in vivo 4 hours after instilling intratracheally saline solution (control), LPS (1 mg/Kg) or HypoEVs (0.1 µg/kg of BW). (F) Changes in heart rate (F) and arterial oxygen (O_2) saturation (G) in the three experimental groups. (H) Time course of O_2 saturation (% of O2) following partial airway occlusion by intratracheal instillation of saline solution. Data are shown as the mean ± S.E.M. Data were analysed with the non-parametric Kruskal-Wallis test followed by Dunn´s test (G) or one-way ANOVA followed by Bonferroni's post hoc test for normally distributed data (C-F) * p<0.05 and ** p<0.01 versus control and $^{\#}$ p< 0,05 and $^{\#\#}$ p< 0,01 versus LPS. 7H: 2-way ANOVA.*

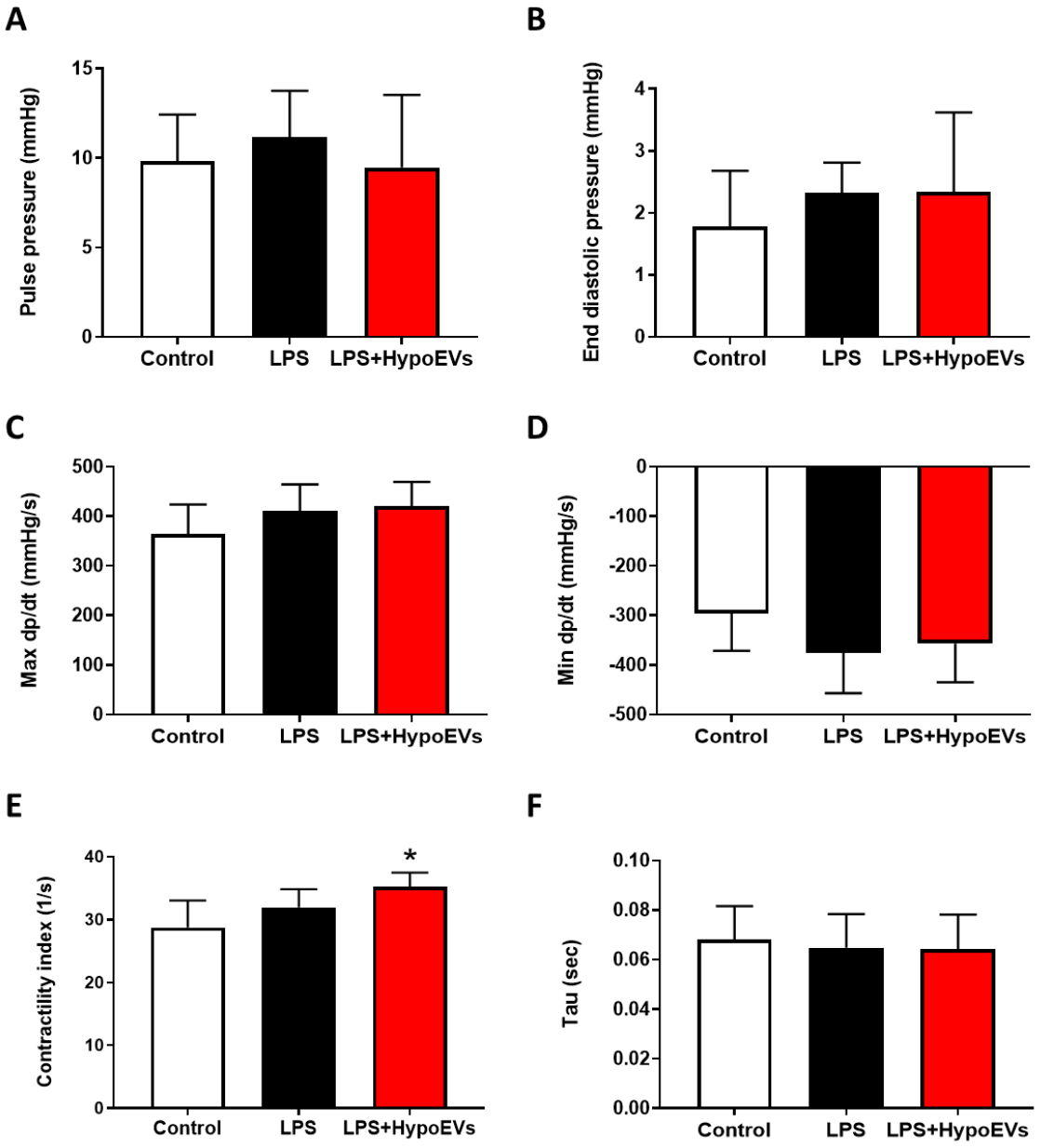

Figure 18. Effects of hypoxic extracellular vesicles (HypoEVs) on cardiac hemodynamics following intratracheal instillation of LPS. *(A) Pulse pressure, (B) end diastolic pressure, (C) dP/dt max, (D) dP/dt min, (E) contractility index and (F) tau in control, LPS and HypoEVs plus LPS-treated rats (n=4-5). Data are shown as the mean ± S.E.M (n=4-5). Data were analysed with one-way ANOVA followed by Bonferroni's post hoc test. *p> 0.05.*

Intratracheal instillation of LPS also induced an increase in pulmonary vascular permeability (as evidenced by the formation of perivascular edema and the increase in IgM content in BALF; Figure 19A-D) and promoted the recruitment of inflammatory cells to the lung, as evidenced by the increase in inflammatory cells found in BALF or the augmentation in lung myeloperoxidase activity (Figure 19E and F) and the increase in pro-inflammatory cytokines in BALF (Figure 19A, D and G). Notably, administration of HypoEVs significantly reduced ameliorated LPS-induced lung injury, by reducing the formation of perivascular lung edema and limiting the development of lung inflammation (Figures 19 and 20). Notably, a strong correlation between pulmonary but not systemic levels of inflammatory cytokines (IL-1β, IL-6 or TNF-α) and PAP leves were found (Figure 20C, F and I) suggesting that the protective effects of HypoEVs were due to direct anti-inflammatory effects in the lung. No significant associations were found between cytokine systemic levels and hemodynamic alterations. By contrast, the levels of endothelin-1, a key mediator of LPS-induced PH, were increased in the systemic circulation (Figure 16K) but not in BALF (Figure 20J). Moreover, despite direct delivery into the lung, HypoEVs significantly reduced the plasmatic levels of ET-1 (Figure 20K), revealing that the beneficial effects exerted by HypoEVs might exceed the lung tissue.

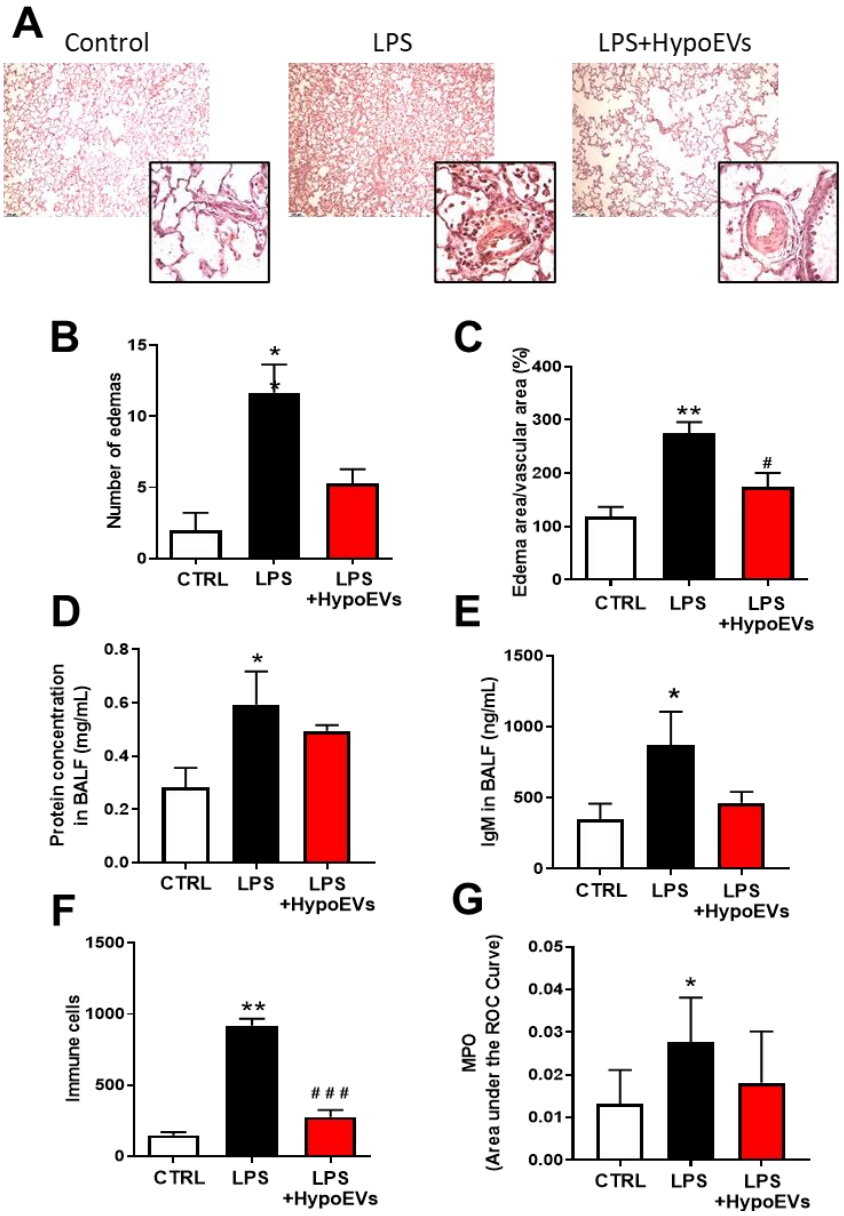

Figure 19. Treatment with EVs released by MSCs under hypoxic conditions (HypoEVs) ameliorates LPS-induced acute lung injury. *(A) Representative photomicrographs of lung sections stained with haematoxylin and eosin (10x; scale bar: 250 µm) and insets showing pulmonary arteries (40x; scale bar: 50 µm) from control, LPS and HypoEVs plus LPS-treated rats. Effects of intratracheal administration of HypoEVs (0.1 µg/kg of BW) on markers of inflammation and vascular permeability: number (B) and size (C) of perivascular oedema (measured as % of oedema area / total vascular area), total protein concentration (D) and levels of IgM (E) in bronchoalveolar Lavage Fluid (BALF), (F) number of immune cells and whole lung myeloperoxidase activity (MPO; G) following intratracheal administration of LPS (1 mg/Kg). Results are shown as the mean ± S.E.M. (n=4-6). Data were analysed with the non-parametric Kruskal-Wallis test followed by Dunn´s test (B) or one-way ANOVA followed by Bonferroni's post hoc test for normally distributed data (C-F). * p<0.05, ** p<0.01 and *** p<0.001 versus control and $^{\#}$ p< 0,05 and $^{\#\#\#}$ p< 0,001 versus LPS.*

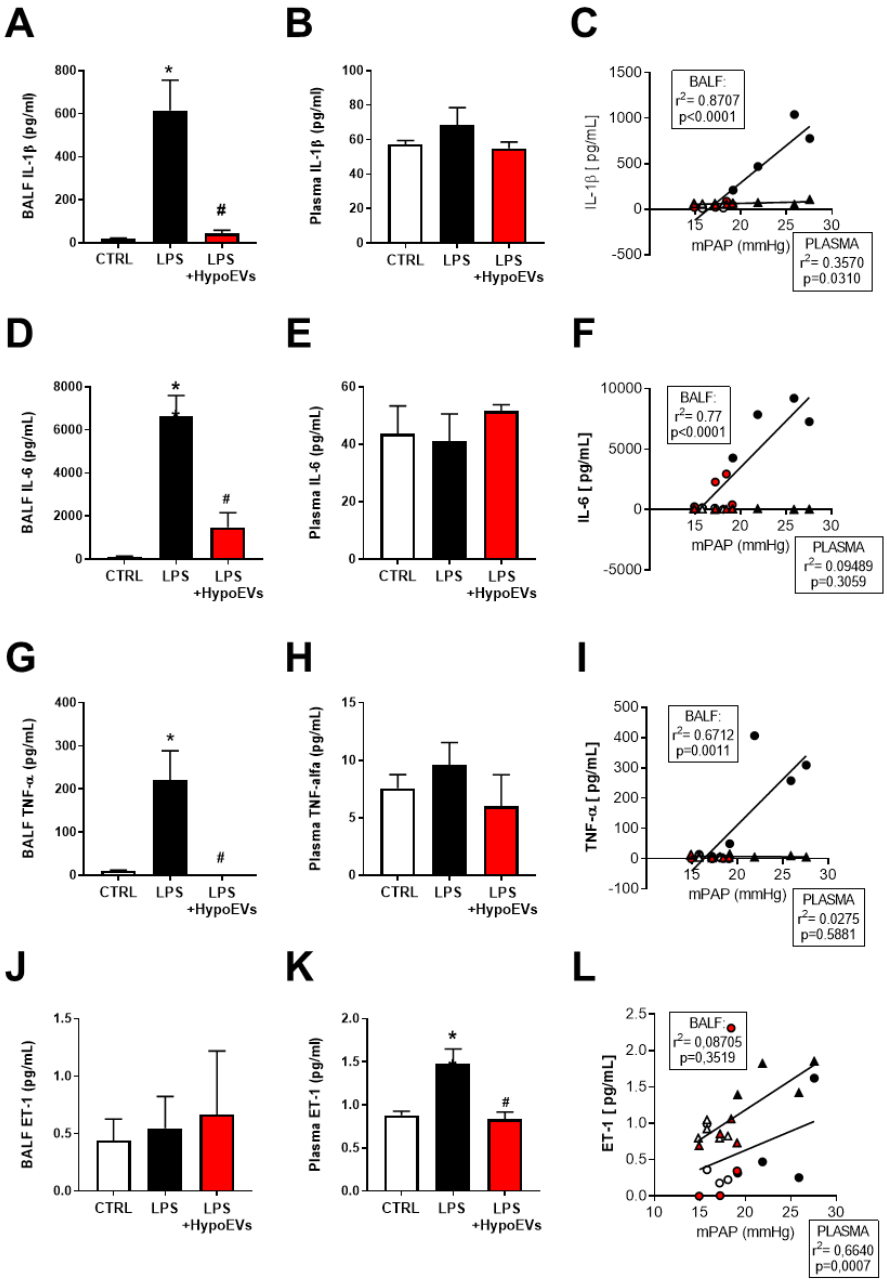

Figure 20. Effects of hypoxic extracellular vesicles (HypoEVs) on pulmonary and systemic levels of proinflammatory cytokines and endothelin-1 (ET-1) following intratracheal instillation of LPS. *(A-C) Levels of IL-1β in bronchoalveolar fluid lavage (BALF; A), plasma (B) and linear regression analysis between IL-1β levels and mean pulmonary artery pressure (PAP) in control, LPS and HypoEVs plus LPS-treated rats (n=4-5). (D-F) Concentration of IL-6 in BALF (D) and plasma (E) and linear analysis (F) between pulmonary or plasma IL-6 and mean PAP in the three experimental groups. (G-I) Levels of TNF-α in BALF (G), plasma (H) and linear analysis (I) between TNF-α levels and mean PAP. (J-L) Concentration of ET-1 in BALF (J) and plasma (K) and linear analysis (L) between pulmonary or plasma IL-6 and mean PAP in the three experimental groups. Data are shown as the mean ± S.E.M (n=4-5). Data were analysed with one-way ANOVA followed by Bonferroni's post hoc test.*

3. EFFECTS OF EVs RELEASED BY MSCs UNDER HYPOXIC CONDITIONS IN AN *IN VITRO* MODEL OF PULMONARY HYPERTENSION

3.1. Hypoxic EVs are able to partially prevent the hyperresponsiveness to serotonin, but not the endothelial dysfunction induced by hypoxia+Su5416 in isolated PA.

Data included in the previous section demonstrate that EVs released by MSCs following hypoxic preconditioning are able to limit acute PH induced by LPS. Based on these findings, we aimed to analyse whether these EVs would be also useful for the treatment of chronic pulmonary hypertension.

The combination of the VEGF antagonist SU5416 and chronic hypoxia is known to cause pronounced PH and angioobliterative lesions in the pulmonary arterioles that are similar to the "plexiform" lesions found in human idiopathic PAH (Taraseviciene-Stewart, Kasahara et al. 2001, Stenmark, Meyrick et al. 2009, Callejo, Mondejar-Parreno et al. 2020). More recently, our group has demonstrated that simultaneous incubation of isolated PA with SU5416 (10 µM) and hypoxia (3% O_2) for 48 hours is able to reproduce the vascular alterations found in the *in vivo* model (Mondejar-Parreno, Callejo et al. 2019). Since the results in the LPS model were promising, the therapeutic potential of HypoEVs was analysed in this model.

The Hpx+Su5416 model is characterised by a hyperresponsiveness to serotonin and endothelial dysfunction as shown in Figure 21. Treatment with HypoEVs partially reversed the hyperresponsiveness to serotonin (Figure 21A) but had not effect on the relaxant responses induced by acetylcholine (Figure 21B). Finally, the response to the endothelium-independent vasodilator sodium nitroprusside was not affected by the exposure to hypoxia+Su5416 nor the treatment with HypoEVs (Figure 21C).

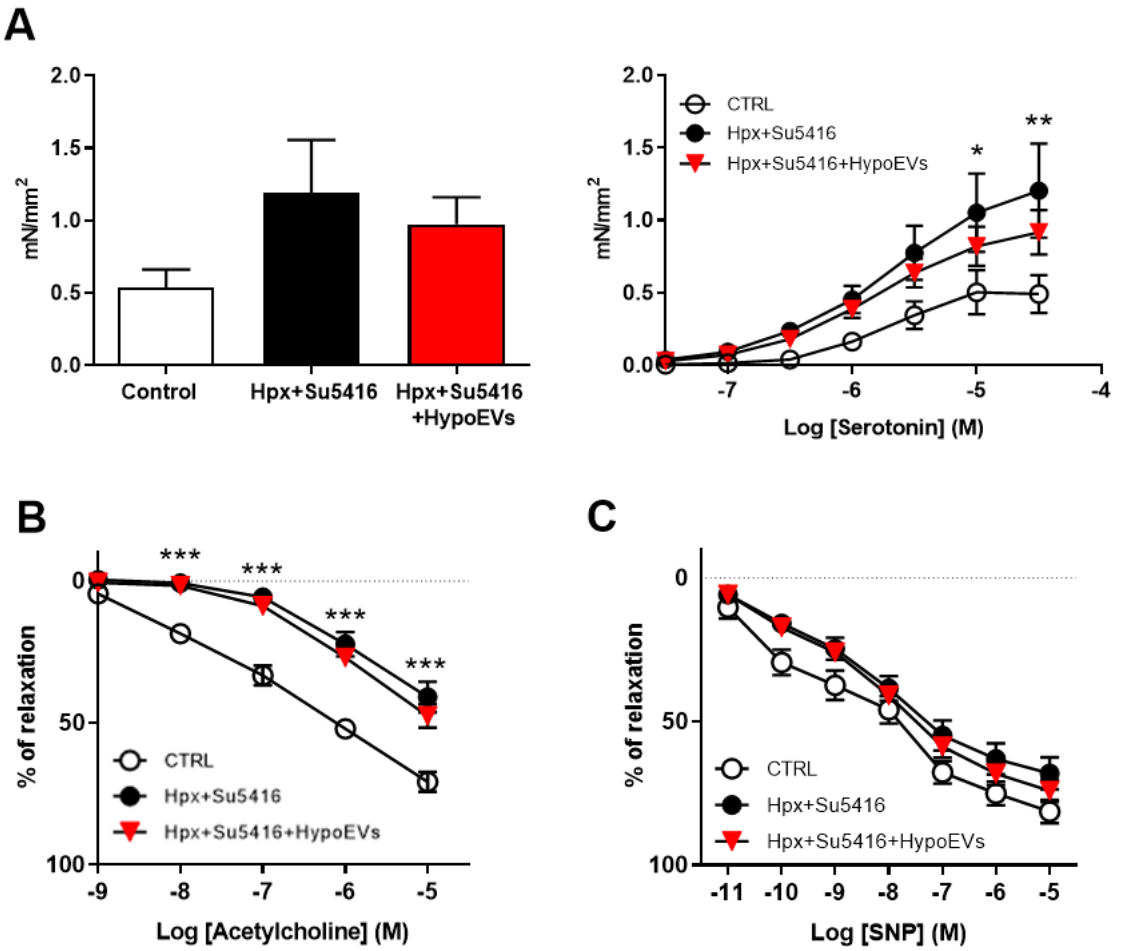

Figure 21. EVs released by MSCs under hypoxic conditions partially prevent the* hyperresponsiveness to serotonin *induced by Hpx+Su5416 exposition in rat pulmonary arteries (PA). *(A) Mean contractile responses to serotonin in isolated PAs incubated for 48 hours in the absence (control; n=18) or exposition to Hpx+Su5416 (n=15) or HypoEVs (n=24). (C) Concentration-dependent relaxation induced by the endothelium-dependent vasodilator acetylcholine in control (n=18) and Hpx+Su5416-exposed (n=16) rat PA rings incubated in the absence or the presence of HypoEVs (n=23). Data in panels A are shown as active effective pressure (mN/mm^2), data in panels B and C are expressed as a percentage of the relaxation induced by acetylcholine or sodium nitroprusside respectively. *, ** and *** p<0.05, p<0.01 and p<0.001 versus (repeated measures ANOVA followed by Bonferroni's post hoc test).*

4. EVALUATION OF OTHER PRECONDITIONING STRATEGIES:

4.1. Preconditioning MSCs with the TLR3 agonist Poly (I:C) reduces the contractile responses to KCl and serotonin in isolated PA.

Priming MSCs with the TLR3 agonist Poly (I:C) activates an immunosuppressive phenotype, with increased expression of IDO, PGE_2 and RANTES (Waterman, Tomchuck et al. 2010, Fuenzalida, Kurte et al. 2016, Rolandsson Enes, Krasnodembskaya et al. 2021). In ALI models, priming with Poly (I:C) increased secretion of EVs with a higher content in KGF and Ang-1 and augmented bacterial clearance, reduce lung protein permeability in a murine model of E.coli-induced pneumonia (Monsel, Zhu et al. 2015, Park, Kim et al. 2019) and was able to enhance the anti-inflammatory and phagocytic activity of cultured macrophages, possibly by transferring COX-2 mRNA to activated monocytes resulting in an increase in production of PGE_2 (Monsel, Zhu et al. 2015). In order to analyse the potential effects of this preconditioning strategy, MSCS-derived extracellular vesicles preconditioned with the TLR3 agonist Poly (I:C) were evaluated in the *in vitro* LPS model and vascular reactivity studies were carried out.

Rat resistance AP rings were stimulated with 80 mM KCl to obtain a contraction that served as a reference for the contractile capacity of the arteries. The contractile responses to hypoxia and serotonin and the endothelium-dependent relaxation induced by cumulative addition of acetylcholine were also analysed. Incubation with EVs released by MSCs following treatment with Poly (I:C) (10 µg/mL; TLR3-EVs) significantly decreased the contractile responses induced by KCl (Figure 22A). Notably, HPV failure was partially prevented by TLR3-EVs treatment (Figure 22B) and the hyperresponsiveness to serotonin was also reversed (Figure 22C). By contrast, the hyporesponsiveness to phenylephrine induced by LPS was even amplified following treatment with TLR3-EVs (Figure 22D).

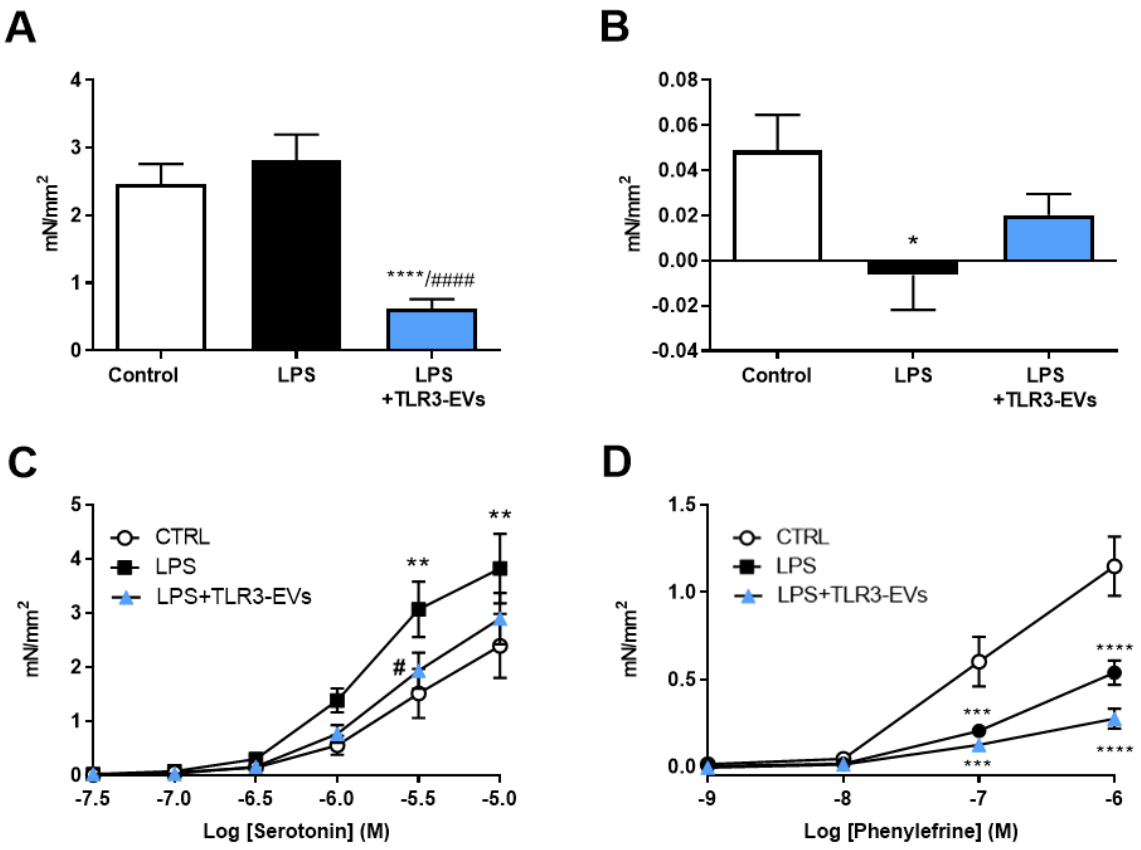

Figure 22. TLR3 preconditioning prevents the hyperresponsiveness to serotonin induced by LPS in rat pulmonary arteries (PA), but also decreases the contractile response to KCl. *(A) Mean contractile responses to KCl of PA incubated in the absence (control; n=16) or presence of LPS (1µg/mL; n=15) or TLR3-EVs (5µg/mL; n=20) and mounted in a wire myograph (B) Mean contractile responses to hypoxia in the absence (control; n=27) or presence of LPS (n=30) or TLR3-EVs (n=20). (C) Mean contractile to serotonin in the absence (control; n=13) or presence of LPS (n=13) or TLR3-EVs (n=12). (D) Mean contractile responses to the α-adrenergic agonist phenylephrine in the absence (control; n=18) or presence of LPS (n=19) or EVs (n=12) Data in all the panels are shown as active effective pressure (mN/mm^2. *, **, *** and **** p<0.05, p<0.01, p<0.001 and p<0.0001 versus control and $^{\#}$ and $^{\#\#\#\#}$ p<0.05 and p<0.0001 versus LPS (repeated measures ANOVA followed by Bonferroni's post hoc test).*

4.2. Simultaneous preconditioning with TLR3 and hypoxia do not increase the therapeutic potential of EVs on isolated PA

In order to analyse whether the combination of both preconditioning strategies could increase the therapeutic potential of MSC-derived EVs, vesicles were isolated following treatment with the TLR3 agonist Poly (I:C) under hypoxic conditions (Hypo-TLR3-EVs).

As described above, LPS induced a strong increase in the production of IL-6 in isolated rat PA (Figure 23A) and there is a striking increase in IL-6 released by whole PA following simultaneous treatment with both LPS and HypoEVs seen in Figure 23B. Exposure to the TLR3 agonist also causes an increase in IL-6 production. Combining both preconditioning strategies shows an additive effect on the increase in IL-6 production (Figure 23B).

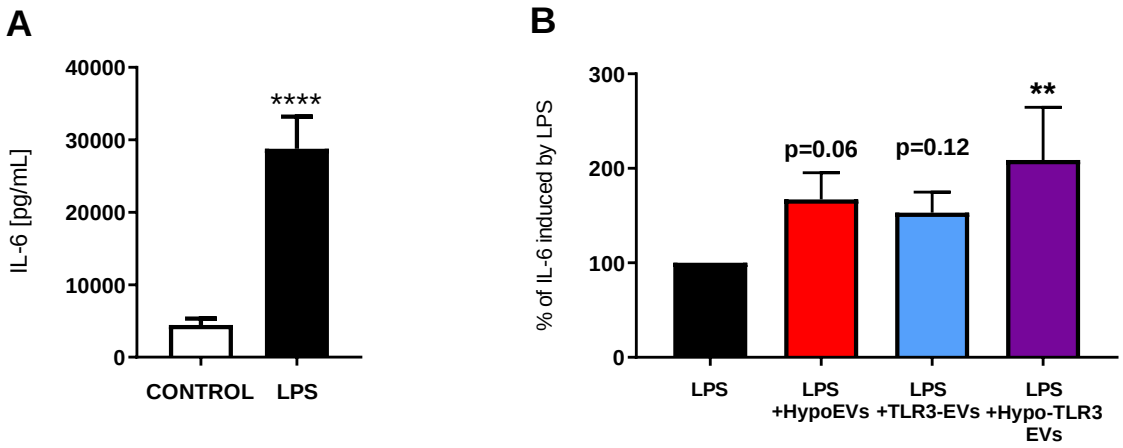

Figure 23. Effects of MSC-derived EVs preconditioned with hypoxia and/or TLR3 agonist on the release of IL-6 induced by LPS in whole pulmonary arteries (PA) *(A-B) Rat PA were incubated in the absence (Control; n=23) or in the presence of LPS (1 µg/mL; n=23) or EVs (5 µg/mL; n=4-9) for 24 hours before quantifying the release of IL-6 in the culture medium. Data shown in panel A is expressed as pg per mL of culture medium and were analysed by paired Student´s t-test (**** p<0.0001 versus control). Data shown in panel B is expressed as a percentage of the response induced by LPS, ** p<0.01 versus LPS (One-way ANOVA followed by Bonferroni's post hoc test).*

Evaluation of pulmonary vascular responses was performed following treatment with LPS in the presence or absence of Hypo-TLR3-EVs (5 µg/mL). In contrast with the effects observed with TLR3-EVs, treatment with Hypo-TLR3-EVs did not modify the contractile responses to KCl in isolated PA (Figure 24A). However, the protective effects exerted by either HypoEVs (Figure 14A) or TLR3-EVs (Figure 22B) on HPV failure disappeared when both stimulus were combined (Figure 24B), suggesting that this strategy of preconditioning would lead to a diminished therapeutic benefit. In line with this observation, the protective effects induced by EVs on the hyperresponsiveness to serotonin is also reduced as compared to EVs released following exposure to hypoxia or TLR3 agonist alone (Figure 24C). Finally, hyporesponsiveness to phenylephrine induced by LPS remains despite treatment with Hypo-TLR3-EVs (Figure 24D).

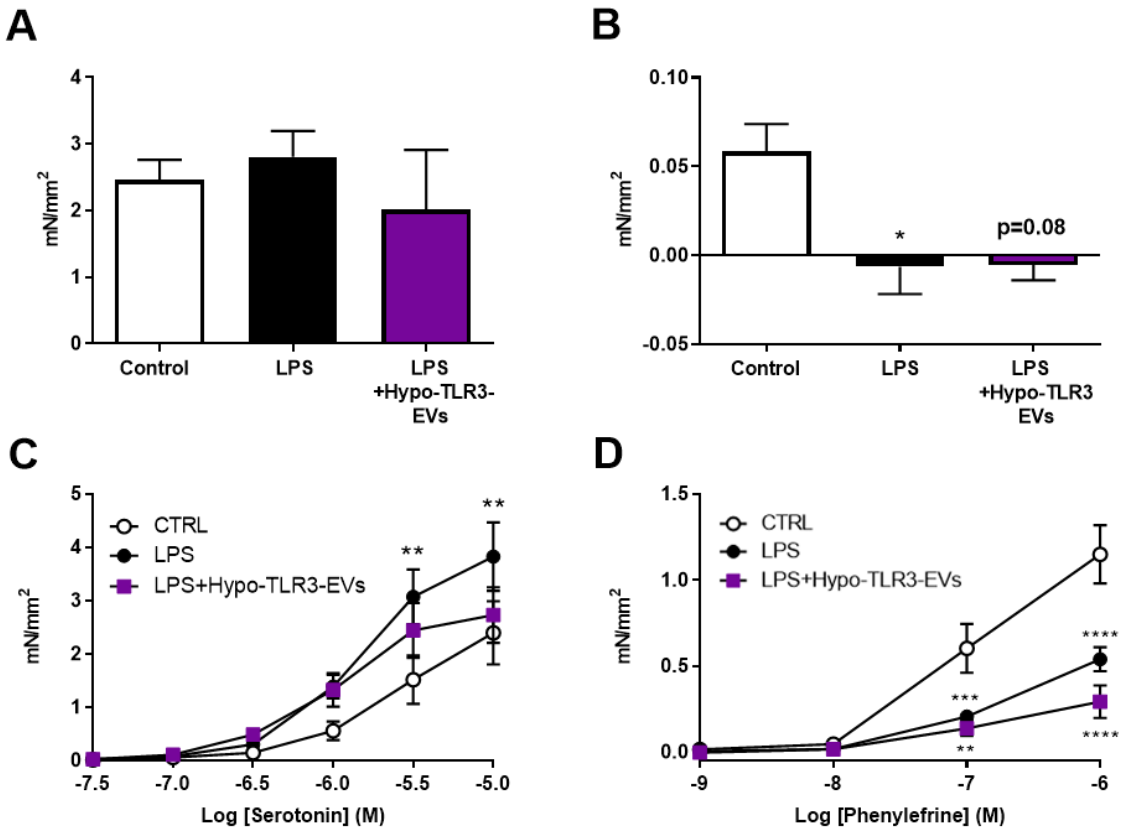

Figure 24. Preconditioning with TLR3 and hypoxia maintains the beneficial effect on the increased serotonin response but the prevention of HPV failure of HypoEVs disappears. *(A) Mean contractile responses to KCl of PA incubated in the absence (control; n=16) or presence of LPS (1µg/mL; n=15) or Hypo-TLR3-EVs (5µg/mL; n=11) and mounted in a wire myograph (B) Mean contractile responses to hypoxia in the absence (control; n=25) or presence of LPS (n=30) or TLR3-EVs (n=10). (C) Mean contractile to serotonin in the absence (control; n=13) or presence of LPS (n=13) or TLR3-EVs (n=8). (D) Mean contractile responses to the α-adrenergic agonist phenylephrine in the absence (control; n=18) or presence of LPS (n=19) or EVs (n=9) Data in all the panels are shown as active effective pressure (mN/mm^2. *, **, *** and **** p<0.05, p<0.01, p<0.001 and p<0.0001 versus (repeated measures ANOVA followed by Bonferroni's post hoc test).*

DISCUSSION

Mesenchymal stem cells and lung diseases

Mesenchymal stem cells (MSCs) are multipotent progenitor cells that can be isolated from multiple tissues including bone marrow, adipose tissue, and umbilical cord tissue, blood and perivascular tissue. A large number of preclinical studies have demonstrated that the administration of MSCs may be an effective strategy for several pulmonary diseases such as obstructive pulmonary disease (COPD), idiopathic pulmonary fibrosis (IPF), bronchopulmonary dysplasia (BPD), cystic fibrosis (CF) and acute respiratory distress syndrome (ARDS) (van Haaften, Byrne et al. 2009, Behnke, Kremer et al. 2020, Cruz and Rocco 2020, Sadeghian Chaleshtori, Mokhber Dezfouli et al. 2020, Rolandsson Enes, Krasnodembskaya et al. 2021). The mechanisms are thought to be mediated in part by paracrine release of several anti-inflammatory cytokines, keratinocyte growth factor, angiopoietin-1, as well as the release of antimicrobial peptides (Curley, Scott et al. 2014, Matthay 2015, Monsel, Zhu et al. 2016, Behnke, Kremer et al. 2020, Byrnes, Masterson et al. 2021, Gorman, Millar et al. 2021). Despite these therapeutic effects in a wide variety of *in vivo* experimental models, several studies have demonstrated that the engraftment rate of MSCs is extremely low (Monsel, Zhu et al. 2016, Mastrolia, Foppiani et al. 2019) suggesting the involvement of paracrine effects. In line with this hypothesis, administration of MSC-derived secretome (conditioned medium and extracellular vesicles) recapitulated the therapeutic effects of MSCs in ARDS and other inflammatory lung diseases (Kourembanas 2015, Phinney, Di Giuseppe et al. 2015, Monsel, Zhu et al. 2016, Park, Kim et al. 2019, Byrnes, Masterson et al. 2021). The discovery that EVs released by MSCs act as biotransporters of bioactive molecules and microRNAs (Maas, Breakefield et al. 2017), opens the possibility to develop new therapies based on the use of stem cells but cell-free and therefore potentially safer and amenable to standardization (Mohammadipoor, Antebi et al. 2018, Lanyu and Feilong 2019). Moreover, they have the potential to be used as vehicles of gene and drug delivery for clinical application.

Although MSCs and EVs have an innate potential to induce and/or contribute to regeneration, this potential is now known to be greatly influenced by diverse extrinsic factors such as the tissue source of the MSCs, the health status and age of the MSCs donor, the batch/lot of serum used for the *in vitro* culture of the MSCs, passage number, oxygen concentration, and the presence/absence of a pro-inflammatory environment when the MSCs are infused. In the pursuit of strategies to enhance the therapeutic potential of MSCs, preconditioning strategies such as exposure to hypoxia or treatment with cytokines or pharmacological agents are gathering increasing attention (Ferreira, Teixeira et al. 2018, Han, Li et al. 2019, Han, Li et al. 2019, Gorgun, Ceresa et al. 2021, Rolandsson Enes, Krasnodembskaya et al. 2021).

1. HYPOXIC PRECONDITIONING

1.1. Effect of hypoxia on MSC-derived extracellular vesicle production and size

Traditional methods for culturing mammalian cells results in the exposure to high oxygen partial pressure (approximately 18.5 %), which does not represent the physiological conditions of human organs and tissues (fluctuating between 1% in the dermis, 2% in the bone marrow or 14% in arterial blood) (Newby, Marks et al. 2005, Halliwell 2014, Horvath, Aulner et al. 2016). Traditional methods for culturing mammalian cells result in the exposure to uncontrolled O_2 levels which are often in range of 18-21% O_2 (i.e., hyperoxic as compared to the physiological normoxia). Despite the obvious impact on translation, MSCs are routinely cultured under ambient oxygen conditions (18.5% O_2).

However, culture under hypoxic conditions is thought to enhance proliferation and survival of MSCs improving their therapeutic potential (Rosová, Dao et al. 2008, Lan, Choo et al. 2015). In addition, several studies have demonstrated that hypoxia mediates an increases in EVs production (Bister, Pistono et al. 2020) under both pathophysiological and therapeutic conditions. Increase of EVs secretion under hypoxia is described in several inflammatory diseases, including

pulmonary arterial hypertension (Zhao, Luo et al. 2017), obesity (Sano, Izumi et al. 2014), and obstructive sleep apnoea (Khalyfa, Zhang et al. 2016). In various types of cancer, hypoxia has also been shown to increase the release of EVs (Hu, Chen et al. 2018, Park, Dutta et al. 2019, Walbrecq, Margue et al. 2020, Venturella, Criscuoli et al. 2021) and participate in the phenotype transformation of stromal cells and other tumour cells (Wang, Gilkes et al. 2014, Ramteke, Ting et al. 2015). On the other hand, the release by hypoxia can have a protective role,, we find examples in mature cells, e.g. renal epithelial cells (Borges, Melo et al. 2013) and renal proximal tubular cells (Zhang, Zhou et al. 2017), and mesenchymal stem cells (Gonzalez-King, Garcia et al. 2017, Zhu, Tian et al. 2018, Collino, Lopes et al. 2019). In this doctoral thesis, umbilical cord-derived mesenchymal stem cells were subjected to different preconditioning strategies, including incubation under hypoxia (3% O_2) or normoxia (18.5% O_2) for 72 hours. When extracellular vesicles were analysed, an increase in EVs production was observed following exposure to hypoxia despite no changes in cell viability were observed (Figure 9E). These data are consistent with the effects of hypoxia on the release of exosomes from MSCs described in previous studies (Zhang, Liu et al. 2012, Salomon, Ryan et al. 2013). Salomon et al. observed that the increase in the production of EVs is inversely correlated to oxygen tension while oxygen did not affect cell viability. This increase may be related to the activation of HIF-1 whose modulation has been shown to modify the release of extracellular vesicles (Bister, Pistono et al. 2020).

Regarding the effects of hypoxic preconditioning in the identity and content carried by EVs released by different type of cells, the results are contradictory. Thus, exposure to hypoxia has been shown to increase (Zhu, Tian et al. 2018), decrease (Ramteke, Ting et al. 2015) or not affect (Tadokoro, Umezu et al. 2013, Umezu, Tadokoro et al. 2014, Wang, Gilkes et al. 2014, Gonzalez-King, Garcia et al. 2017) the size of vesicles released by different type of cells. Patton MC *et al.* described that these changes in extracellular vesicle size (large EVs, medium EVs and small EVs) differed by the cell type used and by the intensity of the hypoxic stimulus employed (Patton, Zubair et al. 2020).

Based on these evidences, we first aimed to analyse the effect of different levels of oxygen on the therapeutic potential of EVs released by MSCs. Standard culture oxygen conditions (18.5% O_2) were compared to hypoxic conditions (3% O_2). Hypoxic conditions were selected based on preliminary studies performed at different O_2 levels to determine the optimal concentration for increasing the therapeutic potential of EVs without significantly affecting the viability of the cells. As shown in figure 9, we found an increase in total protein concentration and a non-significant increase in the total number of EVs released under hypoxic conditions. However, no significant differences were observed in either the mean or the mode sizes, indicating that there was a general increase in the production of EVs, with no specific effects in any particular subgroup of EVs.

Proteomic analysis however confirmed that the protein cargo of EVs was modified following exposure to hypoxia. More than five hundred proteins were identified, including exosomal markers (such as CD9, CD63, CD81, TSG-101, Flotlin-1 and ALIX) and MSCs markers (CD73/5'-Nucleotidase, CD90/Thy1, CD105/Endoglin and CD44) (Haynesworth, Baber et al. 1992, Dominici, Le Blanc et al. 2006, Varma, Breuls et al. 2007, Boxall and Jones 2012, Thery, Witwer et al. 2018). Importantly, the expression pattern of EVs and MSCs markers was similar in both preparations suggesting that the exposure to hypoxia did not induce a differentiation process in the UCB-MSCs nor modify the identity of the vesicles released.

Comparative analysis revealed that hypoxic preconditioning significantly modified the expression of 15 proteins, including an increase in haemoglobin β subunit, the high affinity cationic amino acid transporter 1 Slc7a1 or integrin-lined kinase. Pathway and GO analysis confirmed that these differentially expressed proteins were mainly related to extracellular vesicles and involved in the modulation of pathways related to cell adhesion, integrin signaling, cytoskeleton regulation, responses to Gram negative bacteria or even embryonic development (Figures 10 and 11; Annex 1).

Phosphoacetylglucosamine mutase (Pgm3), the top upregulated protein in hypoxic EVs, is a protein upregulated by erythropoietin and involved in the

synthesis of glucosamines and post-translational modification by protein glycosylation (Pang, Koda et al. 2002, Sassi, Lazaroski et al. 2014) Recently, a novel PGM3 mutation was identified (Pacheco-Cuellar, Gauthier et al. 2017) in two siblings with bone marrow failure, severe combined immunodeficiency, renal and intestinal malformations, and a skeletal dysplasia. Notably, both patients died soon after birth due to severe respiratory compromise secondary to lung hypoplasia and pulmonary hypertension and cardiac arrest.

PDZ domain-containing protein 8 (PDZD8) localizes at the endoplasmic reticulum (ER) fraction of the mitochondria-associated membranes, and the reduction of PDZD8 attenuates both mitochondria-ER contacts and $Ca2+$ flux into the mitochondria in HeLa cells (Hirabayashi, Kwon et al. 2017). PDZD8 is another protein carried by MSCs-derived EVs and upregulated by hypoxia. It is a crucial tethering protein that participates in $Ca2+$ dynamics between the endoplasmic reticulum (ER) and mitochondria (Hirabayashi, Kwon et al. 2017). In addition, PDZD8 has been shown to act as a moesin-interacting cytoskeletal regulatory protein that suppresses infection by herpes simplex virus type 1(Henning, Stiedl et al. 2011). Although its role in the pulmonary circulation is currently unknown, this proteins play a part in regulating $Ca2+$ buffering, lipid processing, mitochondrial fusion, and autophagy (Lee and Min 2018) and could therefore, have an impact on the regulation of vascular tone. In line with this hypothesis, levels of PDZD8 have been found to be significantly reduced in the lungs of two different models of PH (Baba, Shinjo et al. 2018).

Integrin-beta and integrin-linked protein kinase (ILK) were also found to be upregulated in the hypoxic EVs. Although the functional consequences of direct delivery of these two proteins is difficult to anticipate, ILK is known to act as a convergence point between integrins and growth factor signalling pathways, thereby modulating cell adhesion but also proliferation and angiogenesis through is ability to modulate Akt, GSK3B and VEGF signalling pathways (Lee, Youn et al. 2007, Urner, Planas-Paz et al. 2019).

Other proteins found to be upregulated in hypoxic EVs include Laminin and Basement membrane-specific heparan sulfate proteoglycan core protein

(HSPG2), proteins thought to mediate the attachment, migration and organization of cells into tissues during embryonic development by interacting with other extracellular matrix components. Notably, HSPG2 also plays essential roles in vascularization and has been shown to be critical for normal heart development and for regulating the vascular response to injury (Rienks, Papageorgiou et al. 2014).

1.2. Therapeutic potential in an *in vitro* model of LPS-induced vascular dysfunction in isolated PA

Administration of MSCs has been proven to reduce the formation of lung oedema and to limit lung injury in several preclinical models of ALI (Gupta, Su et al. 2007, Pati, Gerber et al. 2011, Curley, Hayes et al. 2012, Jackson, Morrison et al. 2016, Li, Pan et al. 2019, Xiao, Hou et al. 2020). Similarly, the therapeutic benefits of MSCs-derived EVs have also been demonstrated in preclinical models of ARDS, as shown in table 3, although the mechanisms involved are fairly unknown.

The results presented in this Doctoral Thesis demonstrate that hypoxic preconditioning increases the therapeutic potential of EVs in a model of LPS-induced pulmonary vascular dysfunction in vitro. As previously described (Pandolfi, Barreira et al. 2017), *in vitro* exposure to LPS recapitulates some of the vascular alterations found in the *in vivo* model, including endothelial dysfunction and dysregulation of vascular reactivity in isolated PA. Thus, while LPS is able to inhibit phenylephrine- or hypoxia-induced pulmonary vasoconstriction (which could lead to V/Q mismatch *in vivo*), it increases serotonin-induced vasoconstriction and produces marked endothelial dysfunction (which could contribute to the in vivo increase in the pulmonary arterial pressure) (Pandolfi, Barreira et al. 2017). The treatment with hypoxic exosomes (but not with normoxic exosomes) prevented the impairment of HPV, the hyper-responsiveness to serotonin and the development of endothelial dysfunction in isolated PA. These results suggest that hypoxic preconditioning of MSCs increase the therapeutic potential of EVs, conferring them the potential ability to reduce pulmonary arterial pressure and even improve oxygenation in vivo.

1.3. Effect of MSC-derived extracellular vesicles on the induction of iNOs activity by LPS

Studies in animal models seem to support the idea that high NO production by inducible nitric oxide synthase (iNOS) may aggravate lung injury, presumably through direct effects of highly reactive and toxic metabolites of NO on different proteins and lipids (Gow, Thom et al. 1998, Forstermann and Munzel 2006). One example is peroxynitrite, a highly harmful reactive species derived from the combination of NO and reactive oxygen species.

A large number of studies have shown that iNOS induction inhibits α-adrenergic agonist-mediated vasoconstriction and inhibits endothelial function, probably as a consequence of peroxynitrite formation, both in PA (Menendez, Martinez-Caro et al. 2013) and in systemic arteries (Cartwright, McMaster et al. 2007). In particular, the hyporesponsiveness to the a-adrenergic agonist phenylephrine is intimately related to iNOS induction. This is evidenced using the selective iNOS inhibitor 1400W, which causes a recovery of the adrenergic response (Fox, Paterson et al. 1994, Villamor, Perez-Vizcaino et al. 1995).

In addition, iNOS has been proposed as a critical mediator of HPV impairment. Inhibition of iNOS has been shown to be able to partially preserve HPV during endotoxaemia-associated processes (Ullrich, Bloch et al. 1999, Ichinose, Hataishi et al. 2003, Spohr, Cornelissen et al. 2005, Pandolfi, Barreira et al. 2017). However, this partial protection suggests that the failure of HPV during endotoxaemia must be mediated, at least in part, by mechanisms other than simple pulmonary vasodilation because of excess NO production (Ullrich, Bloch et al. 1999, Spohr, Cornelissen et al. 2005).

Our results show that LPS induces the expression of iNOS leading to increased nitrite production and hyporresponsiveness to the vasoconstrictor effects induced by phenylephrine. Neither normoxic nor hypoxic extracellular vesicles were able to reduce this production of nitrite or to restore the contractile responses to this α-adrenoceptor agonist. These findings suggest that that the beneficial effects on endothelial function and the response to hypoxia elicited by hypoxic EVs are independent of the direct effects on iNOS activity.

1.4. Modulation of IL-6 production by MSC-derived EVs

IL-6 is a cytokine that exhibits both proinflammatory and anti-inflammatory properties and is produced by various cell types, including T cells, B cells, monocytes, fibroblasts, smooth muscle cells, endothelial cells, and synovial cells. The observed pro- and anti-inflammatory effects of IL-6 make it difficult to know exactly the role of this interleukin in ARDS. Previous studies in mouse models of lung injury have shown model-specific responses related to IL-6, either protective or injurious (Ward, Waxman et al. 2000, Saito, Tasaka et al. 2008, Gurkan, He et al. 2011, Goldman, Sammani et al. 2014). For example, IL-6 was proinflammatory in a hydrochloric acid (HCl) and mechanical ventilation lung injury model (Gurkan, He et al. 2011), in a model of lung injury induced by acute kidney injury (Klein, Hoke et al. 2008) and in a model of LPS-induced lung injury (Pandolfi, Barreira et al. 2017) but was protective in a hyperoxia-induced lung injury model (Ward, Waxman et al. 2000) and another two models of LPS-induced lung injury (Xing, Gauldie et al. 1998, Bhargava, Janssen et al. 2013). Since IL-6 is a complex cytokine with both properties, it is likely that interactions of many variables in a complex disease such as ARDS will determine its ultimate effects (Goldman, Sammani et al. 2014). In PAH, it has been described that the difference between the two effects is due to the activation of classical (cis) or trans-signalling pathways. The classical pathway involves membrane-bound IL6R and therefore is relevant only in cells that express IL6R (PAH-SMC, macrophage and T cells). The trans-pathway involves binding of IL-6 to soluble IL6R and can be activated in all cells (vascular and non-vascular cells) (Pullamsetti, Seeger et al. 2018), being enhanced in PAH (Jasiewicz, Knapp et al. 2015). Importantly, each pathway regulates distinct biological effects of IL-6. Classical IL-6 signalling is particularly important for the acute-phase immunological response and promotes antiinflammatory activities, whereas IL-6 trans-signalling promotes proinflammatory activities (Pullamsetti, Seeger et al. 2018).

Recent studies show that IL-6 is elevated in plasma and BALF, both in experimental models and in critically ill patients with ARDS, and that elevated levels of IL-6 are associated with increased mortality (Meduri, Headley et al.

1995, Park, Goodman et al. 2001, Takala, Jousela et al. 2002, Cross and Matthay 2011). In addition, IL-6 appears to modulate the inflammatory response and pulmonary vascular remodelling in two experimental mouse models of hypoxia-induced PH (Golembeski, West et al. 2005, Savale, Tu et al. 2009) and its overexpression stimulates VSMC proliferation, reducing vessel lumen and producing PH (Steiner, Syrkina et al. 2009). Indeed, elevated circulating levels of IL-6 correlate with right ventricular function, worse clinical outcome, greater incidence of quality of life–related symptoms, and/or poorer survival in PAH patients (Humbert, Monti et al. 1995, Soon, Holmes et al. 2010, Cracowski, Chabot et al. 2014, Prins, Archer et al. 2018). Moreover, IL-6 can directly modulate vascular tone as it can inhibit eNOS (Hung, Cherng et al. 2010). It has also been observed that IL-6 can stimulate the production of serotonin, a major vasoconstrictor and stimulant of VSMC proliferation implicated in the development of PH, although this regulatory mechanism appears to be bidirectional (Ito, Ikeda et al. 2000, Miyata, Ito et al. 2001, Zhang, Terreni et al. 2001, Kubera, Maes et al. 2005).

Finally, a previous study of our group demonstrated that recombinant IL-6 was able to reproduce the effects of LPS on HPV, serotonin-induced contractile response and endothelial dysfunction but do not induce hyporesponsiveness to phenylephrine (Pandolfi, Barreira et al. 2017). This evidence led us to postulate that the beneficial effects on these functional alterations caused by hypoxic EVs may be due to their ability to reduce IL-6 production. In the present Doctoral Thesis, we have confirmed that LPS cause an increase in IL-6 levels in supernatants of whole PA, rat and human PASMCs and human PAECs. Hypoxic EVs have been able to reduce IL-6 production in PASMCs of both species, but did not modify the release of IL-6 by human PAECs. As for the whole PA, an increase in IL-6 was observed, which may reflect the stimulation of other cell types, such as fibroblasts (Zitnik, Whiting et al. 1994, Song and Kellum 2005) or pericytes (Rustenhoven, Aalderink et al. 2016, Li, Zhou et al. 2018). The increase in IL-6 in PA induced by HypoEVs indicates that the protective effects induced by these vesicles (i.e. restoring HPV, endothelial function and hyperresponsiveness to 5-HT) are not mediated by inihibiting IL-6 production.

1.5. Influence of MSC-derived EVs on cell viability of PASMCs and PAECs

There is increasing evidence that LPS can induce an inflammatory response by VSMCs via direct activation of TLR4-dependent mechanisms in these stromal cells (Yang, Coriolan et al. 2005, Moreno, McMaster et al. 2010, Jiang, Li et al. 2014, Yin, Jiang et al. 2017). Particular attention has been paid to the link between LPS-mediated inflammation and VSMCs proliferation, noting that LPS promotes VSMCs proliferation by different signalling pathways (Hattori, Hattori et al. 2003, Lin, Chen et al. 2006, Son, Jeong et al. 2008, Kim, Kim et al. 2010, Jain, Singh et al. 2015). In PAH and ARDS/ALI models, increased proliferation of PASMCs has been observed, participating in the vascular remodelling characteristic of these pathologies. Several factors are involved in this process. For example, in models of these pathologies there is an increase in the production of endothelin-1 (Jiang, Zeng et al. 2016), serotonin (MacLean and Dempsie 2009, Han, Chen et al. 2015) or thromboxane A2 (Cogolludo, Moreno et al. 2003) that promotes vasoconstriction and proliferation of PASMCs. In addition, as described in the previous section, IL-6 and serotonin have a bidirectional regulatory mechanism so that high levels of IL-6 are also involved (Ito, Ikeda et al. 2000, Miyata, Ito et al. 2001, Kubera, Maes et al. 2005). Finally, it is worth highlighting the influence of oxidative stress in these pathologies, involving both the increase of reactive oxygen species (Tabima, Frizzell et al. 2012) and the decrease of antioxidant mechanisms (Aggarwal, Gross et al. 2013).

In the previous sections we have shown that many of these mechanisms have been affected by LPS treatment (increased IL-6 production, ROS formation due to increased iNOS activity and pulmonary vascular alterations). Despite all this, the cell viability of human and rat PASMCs was not affected by LPS in our experimental conditions. On the other hand, neither hypoxic nor normoxic EVs modified the viability of PASMCs.

Apoptosis plays a major role in cellular homeostasis. maintaining the delicate balance between cell proliferation and cell death (Thompson 1995), but also contributes to diverse pathologic processes (Nicholson 2000), ranging from cancer and atherosclerosis to rheumatic and neurodegenerative diseases.

Endothelial cell apoptosis plays a critical role in physiologic and pathological vascular regression and remodeling (Alon, Hemo et al. 1995, Mallat and Tedgui 2000, Winn and Harlan 2005) and angiogenesis (Chavakis and Dimmeler 2002, Folkman 2003).

In contrast to PASMCs, LPS increases apoptosis and decreases cell survival in PAECs through TLR4 receptor binding (Ali, Nanchal et al. 2013). Moreover, LPS-induced cell damage appears to be related to endothelial cell apoptosis and develops rapidly after administration (Fujita, Kuwano et al. 1998, Wang, Akinci et al. 2007). Systemic treatment with the caspase inhibitor Z-VAD-fmk blocks apoptosis and improves survival in mice treated with intravenous LPS (Fujita, Kuwano et al. 1998).

One factor that appears to be actively involved in endothelial cell apoptosis is the level of ceramides. Ceramide levels are increased in patients with ARDS (Lin, Lin et al. 2011) and in animal models of acute lung injury (Haimovitz-Friedman, Cordon-Cardo et al. 1997, Goggel, Winoto-Morbach et al. 2004, Petrache, Natarajan et al. 2005, von Bismarck, Wistadt et al. 2008) as a consequence of increased SMase activity, leading to pulmonary endothelial cell apoptosis, increased vascular permeability and oedema formation. This increase in ceramide levels is a consequence of increased levels of reactive oxygen species (Andrieu-Abadie, Gouaze et al. 2001, Claus, Bunck et al. 2005, Dumitru and Gulbins 2006, Castillo, Levy et al. 2007) and is involved in the increased production of IL-6 by LPS (Pandolfi, Barreira et al. 2017). It would therefore be expected to observe a reduction in endothelial cell viability following treatment with LPS. However, the cell viability of PAECs was not affected by endotoxin whereas treatment with hypoxic MSC-derived EVs resulted in an increase in cell viability, which allows us to postulate that part of the improvement in functional alterations observed in isolated PA might be due to this effect. It should be noted that this increase in cell viability is in line with the superior angiogenic capacity of hypoxic EVs over normoxic EVs derived from MSCs reported by previous studies (Salomon, Ryan et al. 2013, Han, Bai et al. 2018, Xue, Shen et al. 2018, Collino, Lopes et al. 2019).

1.6. Effects of the treatment with hypoxic EVs in the in vivo LPS-induced ALI model

To investigate the molecular mechanisms of ALI, various experimental models of ALI have been used, being the two most common the mechanical ventilation- and LPS-induced lung injury models (Matute-Bello, Frevert et al. 2008). One of the most difficult aspects of modelling human ALI in humans is that the lungs of humans can be affected by the mechanisms involved in the primary illness (e.g., sepsis) and/or they can be affected by therapeutic modalities used for supportive care (e.g. mechanical ventilation) (Vlahakis and Hubmayr 2005). For this reason, the existing animal models are relevant for only limited aspects of the human disease (Matute-Bello, Frevert et al. 2008). For example, the LPS model has some similarities with ARDS such as a neutrophilic inflammatory response with increase in intrapulmonary cytokines, but also differs in other aspects, including that the changes in alveolar-capillary permeability are mild as compared to those changes found in patients with ARDS (Matute-Bello, Frevert et al. 2008).

The haemodynamic response to intravenously administered LPS is characterised by an initial phase of leukopenia, decreased cardiac output, and a fall in systemic arterial pressure accompanied by an increase in pulmonary arterial pressure (Taveira da Silva, Kaulbach et al. 1993). Intratracheal administration of LPS is characterised by a damage in the lung parenchyma caused by the generation and release of proteases and reactive oxygen and nitrogen species produced by activated lung macrophages and transmigrated neutrophils in the interstitial and alveolar compartments. Altogether they lead to microvascular injury and diffuse alveolar damage with intrapulmonary haemorrhage, oedema, fibrin deposition (Johnson and Ward 1974, Kabir, Gelinas et al. 2002, Reutershan and Ley 2004) and an increase in the levels of inflammatory cytokines and albumin in the BALF, mainly in the first 24 hours (Matute-Bello, Frevert et al. 2008). The oedema leads to hypoxaemia as lung areas are unventilated due to fluid accumulation in the alveoli, but perfused, with consequent V/Q uncoupling (Dantzker, Brook et al. 1979, Price, McAuley et al. 2012), resulting in decreased PaO_2.

The results presented in this Doctoral Thesis confirm that intratracheal instillation of LPS reproduces most of these alterations, including the recruitment of inflammatory cells (as evidenced by the number of cells present in BALF, MPO activity analysis or histological analysis), alterations in vascular permeability (development of oedema and increased IgM and protein concentrations in BALF), increased cytokine production (IL-1β, IL-6, TNF-a and ET-1) at pulmonary and systemic level, reduced oxygen saturation or increased systolic and diastolic PAP. On the other hand, our results demonstrate that hypoxic EVs are able to substantially restore to disruption of the alveolar epithelial-capillary barrier and to limit lung inflammation, as evidenced by the significant decrease in the formation of oedema, the reduction of IgM levels and number of inflammatory cells detected in BALF, the reduction of lung MPO activity and the decrease of pulmonary and systemic levels of proinflammatory cytokines. These results agree with those by Li et al. where hypoxic preconditioning potentiated the therapeutic effects of MSC-EVs in a model of LPS-induced ALI, facilitating the reduction of neutrophil influx and the decrease of TNFα (Li, Jin, and Zhang 2015). In line with our *in vitro* findings, administration of hypoxic EVs led to a significant decrease in PAP (reaching values similar to those registered in control animals) and an improvement in oxygen saturation. This evidence supports the beneficial effects of hypoxic EVs on LPS-induced vascular alterations discussed in previous sections, as the prevention of serotonin hyperresponsiveness and endothelial dysfunction would lead to a normalisation of PAP and reversal of HPV failure would translate to a recovery of oxygen saturation.

In addition to the effects observed in the lungs, intratracheal instillation of LPS also induced a systemic inflammatory response. However, the magnitude of the changes induced by LPS in the lung were found to exceed those in the peripheral circulation (around 100-fold). This gradient suggests that the production of these cytokines is mainly confined within the lungs. Furthermore, the lack of correlation between circulating levels of either IL-6, IL-1β or TNF-α and mean PAP suggests that the beneficial effects of hypoxic EVs on pulmonary pressure are due to direct effects on the lung. It should be noted, however, that despite direct delivery into the lung, the increase in ET-1 levels induced by LPS was of similar magnitude in

both lung tissue and plasma and that the increase in lung ET-1 levels was resistant to treatment with hypoxic EVs. Moreover, hypoxic EVs significantly reduced the plasmatic levels of ET-1 and this reduction showed a significant correlation with the decrease in PAP (Figures 20K-L). Although the origin of this circulating ET-1 is unclear, this findings reveal that the beneficial effects exerted by hypoxic EVs might exceed the lung tissue which warrants further research.

1.7. Therapeutic potential in an *in vitro* PAH model in isolated PA

Altogether, the data presented in this Doctoral Thesis suggest that administration of EVs derived from MSCs exposed to hypoxia could be an effective approach to limit endotoxin-induced PH and reduce pulmonary inflammation. Based on this promising results, our next aim was to analyse whether hypoxic extracellular vesicles could also be useful for the treatment of chronic PAH. In order to test this hypothesis, the effects of hypoxic EVs were analysed in an *in vitro* model of PAH induced by the combination of the VEGF antagonist SU5416 and chronic hypoxia in isolated PA. This model has been recently developed by our group and is able to reproduce some of the vascular alterations found in the *in vivo* model, including hyperresponsiveness to serotonin and the development of endothelial dysfunction (Mondejar-Parreno, Callejo et al. 2019).

PH is a progressive pathophysiological disorder characterized by vasoconstriction, vascular remodelling, thrombosis and inflammation, resulting in an increase of pulmonary pressure (<20 mmHg) (Galie, Humbert et al. 2015, Simonneau and Hoeper 2019). Vasoconstriction, as in ARDS-associated PH, is a result of an imbalance in tissue and circulating levels of vasoactive mediators. This imbalance includes a decrease in the production of vasodilators/growth inhibitors such as NO and PGI_2, while there is an increase in the production of the vasoconstrictor/pro-mitogens such as ET-1, TXA_2 and 5-HT (Morrell, Adnot et al. 2009, Rabinovitch 2012).

Several studies have demonstrated the therapeutic potential of MSC-derived EVs in different models of PH, including chronic exposure to hypoxia (Lee, Mitsialis et al. 2012), monocrotaline (Chen, An et al. 2014, Aliotta, Pereira et al. 2016, Liu, Liu et al. 2018) or the hypoxia/SU5416 model (Klinger, Pereira et al. 2020). In the

hypoxia/SU5416 model, it was demonstrated that MSC-EVs are effective at preventing and reversing increases in pulmonary artery pressure, right ventricular hypertrophy, and pulmonary vascular remodelling in rats (Klinger, Pereira et al. 2020). In contrast to these evidences,administration of hypoxic EVs only produced a partial improvement in serotonin hyperresponsiveness without affecting endothelial dysfunction in our *in vitro* model of PAH. This could be explained by several reasons, including the employment of an insufficient dose, differences in the hypoxic preconditioning strategy and source of MSCs or the involvement of other cell types (for examples, modulation of immune cells) which are not present in our *in vitro* model. However, the therapeutic potential of these vesicles warrants further research since a recent study suggest that the beneficial effects of MSCs-derived EVs in the hypoxia/SU5416 model appear when they are administered at lower doses and for longer dosing intervals than previously reported (Klinger, Pereira et al. 2021). Notably, hypoxic preconditioning did not improve the therapeutic potential of EVs.In fact, the Fulton ratio (measured as the ratio between the weight of the right ventricle to the weight of the left plus septum; RV/LV+S) tended to be higher in PH rats treated with hypoxic EVs as compared to normoxic EVs (Klinger, Pereira et al. 2021).

2. TLR3 PRECONDITIONING

2.1. Therapeutic potential in an *in vitro* model of LPS-induced vascular dysfunction in isolated PA

Besides hypoxic preconditioning, priming MSCs with inflammatory cytokines or TLR agonists have demonstrated to increase the therapeutic potential of EVs (Esquivel-Ruiz, Gonzalez-Rodriguez et al. 2021). Among these strategies, we aimed to analyse the potential effects of stimulating the MSCs with the TLR3 agonist Poly (I:C), an strategy which has been proven to increase the anti-inflammatory effects and the protective effects in barrier function in a murine model of E.coli-induced pneumonia (Monsel, Zhu et al. 2015, Park, Kim et al. 2019).

However, conflicting results were observed with this preconditioning strategy. EVs derived from TLR3-primed MSCs partially prevented the HPV failure and the hyperresponsiveness to serotonin in the *in vitro* model of LPS. However, a significant decrease in the contractile responses induced by KCl and phenylephrine was observed, suggesting a potential induction of iNOS by these EVs. In summary, our preliminary results suggest that although TLR3-EVs may have some beneficial effects, potential detrimental effects are also observed following its administration. This could be explained by the different behaviours of MSCs in response to TLR3 stimulation. On the one hand, preconditioning with the TLR3 agonist Poly (I:C) has been reported to polarise MSCs into an anti-inflammatory phenotype (Waterman, Tomchuck et al. 2010, Rolandsson Enes, Krasnodembskaya et al. 2021) and extracellular vesicles derived from these MSCs have been shown to enhance the beneficial effects when compared with untreated MSCs in ALI models (Monsel, Zhu et al. 2015, Park, Kim et al. 2019), as described in the Introduction and in table 4. On the other hand, Poly(I:C) elevated the levels of proinflammatory factors (e.g., IL-1β, lL-6, IL-8 and type I interferon) in MSCs compared to the untreated cells (Dumitru, Hemeda et al. 2014, Fuenzalida, Kurte et al. 2016). This increase in cytokines production appears to be mediated by changes in calcium homeostasis, involving mediators that may be transported by the vesicles and may explain the observed responses (Park, Kim et al. 2016). Our results are in line with these studies, since an increase in IL-6 production was detected following incubation of isolated PA. However, the increased in the contractile responses induced by serotonin, which is sensitive to IL-6 inhibition (Pandolfi, Barreira et al. 2017), was prevented by treatment with TLR3-EVs, suggesting the involvement of another unknown mechanisms.

3. SIMULTANEOUS PRECONDITIONING WITH TLR3 AND HYPOXIA

To analyse whether preconditioning with both strategies (hypoxia and TLR3) had a superior effect compared to individual preconditioning, vesicles were isolated following treatment with the TLR3 agonist Poly (I:C) under hypoxic conditions (Hypo-TLR3-EVs) and both contractile responses and IL-6 levels were analysed.

Unfortunately, the protective effects exerted by either hypoxic EVs or TLR3-EVs on HPV failure disappeared when both stimuli were combined, suggesting that this strategy of preconditioning would lead to a diminished therapeutic benefit. In line with this observation, the protective effects induced by EVs on the hyperresponsiveness to serotonin is also reduced as compared to EVs released following exposure to hypoxia or TLR3 agonist alone. This may be due to the significant increase in IL-6 production observed when both strategies are combined. Finally, hyporesponsiveness to phenylephrine induced by LPS remains despite treatment with Hypo-TLR3-EVs.

In summary, our results suggest that the combination of both preconditioning strategies is strongly discouraged as it leads to the disappearance of all the protective effects exerted by EVs released by MSCs under hypoxic conditions.

CONCLUSIONS

1. Exposure of umbilical cord-derived mesenchymal stem cells (MSCs) to hypoxia increases the release of extracellular vesicles (EVs), modifying their protein content but without altering their size or the expression of specific markers of EVs.

2. Among the 552 proteins identified within these EVs, hypoxic preconditioning significantly modified the expression of 15 proteins involved in the modulation of pathways related to cell adhesion, integrin signaling, cytoskeleton regulation and embryonic development.

3. EVs released by MSCs under hypoxic, but not normoxic, conditions were able to prevent pulmonary vascular dysfunction (endothelial dysfunction, hyperresponsiveness to serotonin, failure of hypoxic pulmonary vasoconstriction) in *in vitro* models of acute lung injury (ALI) and pulmonary arterial hypertension (PAH).

4. Intratracheal administration of hypoxic EVs prevents the inflammatory response, the disruption of the pulmonary capillary barrier, the development of pulmonary oedema and the increase in pulmonary arterial pressure in rats exposed to a model of acute lung injury induced by intratracheal instillation of LPS. Furthermore, hypoxic EVs were able to protect against the development of hypoxaemia by inducing a modest improvement in ventilation-perfusion coupling *in vivo*.

5. Evaluation of other preconditioning strategies, such as the TLR3 agonist poly (I:C) combined or not with hypoxia resulted in a reduction of their therapeutic potential.

6. In summary, the results of this PhD thesis suggest that hypoxic preconditioning enhances the therapeutic potential of EVs produced by MSCs and could represent a new therapeutic approach for the treatment of pulmonary vascular diseases associated with inflammation.

BIBLIOGRAPHY

Abraham, E. (2003). "Neutrophils and acute lung injury." Crit Care Med 31(4 Suppl): S195-199.

Ackermann, M., S. E. Verleden, M. Kuehnel, A. Haverich, T. Welte, F. Laenger, A. Vanstapel, C. Werlein, H. Stark, A. Tzankov, W. W. Li, V. W. Li, S. J. Mentzer and D. Jonigk (2020). "Pulmonary Vascular Endothelialitis, Thrombosis, and Angiogenesis in Covid-19." N Engl J Med 383(2): 120-128.

Acute Respiratory Distress Syndrome, N., R. G. Brower, M. A. Matthay, A. Morris, D. Schoenfeld, B. T. Thompson and A. Wheeler (2000). "Ventilation with lower tidal volumes as compared with traditional tidal volumes for acute lung injury and the acute respiratory distress syndrome." N Engl J Med 342(18): 1301-1308.

Aggarwal, S., C. M. Gross, S. Sharma, J. R. Fineman and S. M. Black (2013). "Reactive oxygen species in pulmonary vascular remodeling." Compr Physiol 3(3): 1011-1034.

Ahn, S. Y., W. S. Park, Y. E. Kim, D. K. Sung, S. I. Sung, J. Y. Ahn and Y. S. Chang (2018). "Vascular endothelial growth factor mediates the therapeutic efficacy of mesenchymal stem cell-derived extracellular vesicles against neonatal hyperoxic lung injury." Exp Mol Med 50(4): 1-12.

Akoumianaki, E., A. Lyazidi, N. Rey, D. Matamis, N. Perez-Martinez, R. Giraud, J. Mancebo, L. Brochard and J. M. Richard (2013). "Mechanical ventilation-induced reverse-triggered breaths: a frequently unrecognized form of neuromechanical coupling." Chest 143(4): 927-938.

Alcorn, J. L. (2019). Innate Immunity and Pulmonary Inflammation: A Balance Between Protection and Disease. Perspectives in Translational Cell Biology. J. K. Actor and K. C. Smith. Translational Inflammation: 153-175.

Ali, I., R. Nanchal, F. Husnain, S. Audi, G. G. Konduri, J. C. Densmore, M. Medhora and E. R. Jacobs (2013). "Hypoxia preconditioning increases survival and decreases expression of Toll-like receptor 4 in pulmonary artery endothelial cells exposed to lipopolysaccharide." Pulm Circ 3(3): 578-588.

Aliotta, J. M., M. Pereira, S. Wen, M. S. Dooner, M. Del Tatto, E. Papa, L. R. Goldberg, G. L. Baird, C. E. Ventetuolo, P. J. Quesenberry and J. R. Klinger (2016). "Exosomes induce and reverse monocrotaline-induced pulmonary hypertension in mice." Cardiovasc Res 110(3): 319-330.

Alon, T., I. Hemo, A. Itin, J. Pe'er, J. Stone and E. Keshet (1995). "Vascular endothelial growth factor acts as a survival factor for newly formed retinal vessels and has implications for retinopathy of prematurity." Nat Med 1(10): 1024-1028.

Amato, M. B., C. S. Barbas, D. M. Medeiros, R. B. Magaldi, G. P. Schettino, G. Lorenzi-Filho, R. A. Kairalla, D. Deheinzelin, C. Munoz, R. Oliveira, T. Y. Takagaki and C. R. Carvalho (1998). "Effect of a protective-ventilation strategy on mortality in the acute respiratory distress syndrome." N Engl J Med 338(6): 347-354.

Andrieu-Abadie, N., V. Gouaze, R. Salvayre and T. Levade (2001). "Ceramide in apoptosis signaling: relationship with oxidative stress." Free Radic Biol Med 31(6): 717-728.

Annane, D. (2007). "Glucocorticoids for ARDS: Just Do It!" Chest 131(4): 945-946.

Anzueto, A., R. P. Baughman, K. K. Guntupalli, J. G. Weg, H. P. Wiedemann, A. A. Raventos, F. Lemaire, W. Long, D. S. Zaccardelli and E. N. Pattishall (1996). "Aerosolized surfactant in adults with sepsis-induced acute respiratory distress syndrome. Exosurf Acute Respiratory Distress Syndrome Sepsis Study Group." N Engl J Med 334(22): 1417-1421.

Armstrong, L. and A. B. Millar (1997). "Relative production of tumour necrosis factor alpha and interleukin 10 in adult respiratory distress syndrome." Thorax 52(5): 442-446.

Asakura, H. and H. Ogawa (2021). "COVID-19-associated coagulopathy and disseminated intravascular coagulation." Int J Hematol 113(1): 45-57.

Ashbaugh, D. G., D. B. Bigelow, T. L. Petty and B. E. Levine (1967). "Acute respiratory distress in adults." Lancet 2(7511): 319-323.

Asmussen, S., H. Ito, D. L. Traber, J. W. Lee, R. A. Cox, H. K. Hawkins, D. F. McAuley, D. H. McKenna, L. D. Traber, H. Zhuo, J. Wilson, D. N. Herndon, D. S. Prough, K. D. Liu, M. A. Matthay and P. Enkhbaatar (2014). "Human mesenchymal stem cells reduce the severity of acute lung injury in a sheep model of bacterial pneumonia." Thorax 69(9): 819-825.

Ast, T. and V. K. Mootha (2019). "Oxygen and mammalian cell culture: are we repeating the experiment of Dr. Ox?" Nat Metab 1(9): 858-860.

Avontuur, J. A., M. Biewenga, S. L. Buijk, K. J. Kanhai and H. A. Bruining (1998). "Pulmonary hypertension and reduced cardiac output during inhibition of nitric oxide synthesis in human septic shock." Shock 9(6): 451-454.

Baba, S., S. Shinjo, M. Okada, Y. Fujimoto, T. Akaike, Y. Kusakari and S. Minamisawa (2018). "Downregulation of Endoplasmic Reticulum-Mitochondria Tethering Proteins in Monocrotaline-Induced Pulmonary Arterial Hypertension." Circulation 138.

Bachofen, M. and E. R. Weibel (1977). "Alterations of the gas exchange apparatus in adult respiratory insufficiency associated with septicemia." Am Rev Respir Dis 116(4): 589-615.

Bachofen, M. and E. R. Weibel (1982). "Structural alterations of lung parenchyma in the adult respiratory distress syndrome." Clin Chest Med 3(1): 35-56.

Bader, A. M., K. Klose, K. Bieback, D. Korinth, M. Schneider, M. Seifert, Y. H. Choi, A. Kurtz, V. Falk and C. Stamm (2015). "Hypoxic Preconditioning Increases Survival and Pro-Angiogenic Capacity of Human Cord Blood Mesenchymal Stromal Cells In Vitro." PLoS One 10(9): e0138477.

Bannerman, D. D. and S. E. Goldblum (2003). "Mechanisms of bacterial lipopolysaccharide-induced endothelial apoptosis." Am J Physiol Lung Cell Mol Physiol 284(6): L899-914.

Barron, L., S. A. Gharib and J. S. Duffield (2016). "Lung Pericytes and Resident Fibroblasts: Busy Multitaskers." Am J Pathol 186(10): 2519-2531.

Bassford, C. R., D. R. Thickett and G. D. Perkins (2012). "The rise and fall of beta-agonists in the treatment of ARDS." Crit Care 16(2): 208.

Bastarache, J. A. and T. S. Blackwell (2009). "Development of animal models for the acute respiratory distress syndrome." Dis Model Mech 2(5-6): 218-223.

Bastarache, J. A., L. Wang, T. Geiser, Z. Wang, K. H. Albertine, M. A. Matthay and L. B. Ware (2007). "The alveolar epithelium can initiate the extrinsic coagulation cascade through expression of tissue factor." Thorax 62(7): 608-616.

Beegle, J., K. Lakatos, S. Kalomoiris, H. Stewart, R. R. Isseroff, J. A. Nolta and F. A. Fierro (2015). "Hypoxic preconditioning of mesenchymal stromal cells induces metabolic changes, enhances survival, and promotes cell retention in vivo." Stem Cells 33(6): 1818-1828.

Behnke, J., S. Kremer, T. Shahzad, C. M. Chao, E. Bottcher-Friebertshauser, R. E. Morty, S. Bellusci and H. Ehrhardt (2020). "MSC Based Therapies-New Perspectives for the Injured Lung." J Clin Med 9(3).

Beiderlinden, M., H. Kuehl, T. Boes and J. Peters (2006). "Prevalence of pulmonary hypertension associated with severe acute respiratory distress syndrome: predictive value of computed tomography." Intensive Care Med 32(6): 852-857.

Beitler, J. R., E. C. Goligher, M. Schmidt, P. M. Spieth, A. Zanella, I. Martin-Loeches, C. S. Calfee, A. B. Cavalcanti and A. R. Investigators (2016). "Personalized medicine for ARDS: the 2035 research agenda." Intensive Care Med 42(5): 756-767.

Beitler, J. R., S. Shaefi, S. B. Montesi, A. Devlin, S. H. Loring, D. Talmor and A. Malhotra (2014). "Prone positioning reduces mortality from acute respiratory distress syndrome in the low tidal volume era: a meta-analysis." Intensive Care Med 40(3): 332-341.

Bellani, G., J. G. Laffey, T. Pham, E. Fan, L. Brochard, A. Esteban, L. Gattinoni, F. van Haren, A. Larsson, D. F. McAuley, M. Ranieri, G. Rubenfeld, B. T. Thompson, H. Wrigge, A. S. Slutsky, A. Pesenti, L. S. Investigators and E. T. Group (2016). "Epidemiology, Patterns of Care, and Mortality for Patients With Acute Respiratory Distress Syndrome in Intensive Care Units in 50 Countries." JAMA 315(8): 788-800.

Belvitch, P. and S. M. Dudek (2013). "Corticosteroids and acute respiratory distress syndrome: the debate continues." Crit Care Med 41(7): 1813-1814.

Bernard, G. R., A. Artigas, K. L. Brigham, J. Carlet, K. Falke, L. Hudson, M. Lamy, J. R. Legall, A. Morris and R. Spragg (1994). "The American-European Consensus Conference on ARDS. Definitions, mechanisms, relevant outcomes, and clinical trial coordination." Am J Respir Crit Care Med 149(3 Pt 1): 818-824.

Bernard, G. R., J. L. Vincent, P. F. Laterre, S. P. LaRosa, J. F. Dhainaut, A. Lopez-Rodriguez, J. S. Steingrub, G. E. Garber, J. D. Helterbrand, E. W. Ely, C. J. Fisher, Jr. and C. W. E. i. S. S. s. g. Recombinant human protein (2001). "Efficacy and safety of recombinant human activated protein C for severe sepsis." N Engl J Med 344(10): 699-709.

Bersten, A. D., C. Edibam, T. Hunt, J. Moran, Australian and G. New Zealand Intensive Care Society Clinical Trials (2002). "Incidence and mortality of

acute lung injury and the acute respiratory distress syndrome in three Australian States." Am J Respir Crit Care Med 165(4): 443-448.

Bhandari, V., R. Choo-Wing, C. G. Lee, Z. Zhu, J. H. Nedrelow, G. L. Chupp, X. Zhang, M. A. Matthay, L. B. Ware, R. J. Homer, P. J. Lee, A. Geick, A. R. de Fougerolles and J. A. Elias (2006). "Hyperoxia causes angiopoietin 2-mediated acute lung injury and necrotic cell death." Nat Med 12(11): 1286-1293.

Bhargava, R., W. Janssen, C. Altmann, A. Andres-Hernando, K. Okamura, R. W. Vandivier, N. Ahuja and S. Faubel (2013). "Intratracheal IL-6 protects against lung inflammation in direct, but not indirect, causes of acute lung injury in mice." PLoS One 8(5): e61405.

Bhatia, M. and S. Moochhala (2004). "Role of inflammatory mediators in the pathophysiology of acute respiratory distress syndrome." J Pathol 202(2): 145-156.

Bian, S., L. Zhang, L. Duan, X. Wang, Y. Min and H. Yu (2014). "Extracellular vesicles derived from human bone marrow mesenchymal stem cells promote angiogenesis in a rat myocardial infarction model." J Mol Med (Berl) 92(4): 387-397.

Bissonnette, E. Y., J. F. Lauzon-Joset, J. S. Debley and S. F. Ziegler (2020). "Cross-Talk Between Alveolar Macrophages and Lung Epithelial Cells is Essential to Maintain Lung Homeostasis." Front Immunol 11: 583042.

Bister, N., C. Pistono, B. Huremagic, J. Jolkkonen, R. Giugno and T. Malm (2020). "Hypoxia and extracellular vesicles: A review on methods, vesicular cargo and functions." J Extracell Vesicles 10(1): e12002.

Boissier, F., S. Katsahian, K. Razazi, A. W. Thille, F. Roche-Campo, R. Leon, E. Vivier, L. Brochard, A. Vieillard-Baron, C. Brun-Buisson and A. Mekontso Dessap (2013). "Prevalence and prognosis of cor pulmonale during protective ventilation for acute respiratory distress syndrome." Intensive Care Med 39(10): 1725-1733.

Bone, R. C., C. J. Fisher, Jr., T. P. Clemmer, G. J. Slotman and C. A. Metz (1987). "Early methylprednisolone treatment for septic syndrome and the adult respiratory distress syndrome." Chest 92(6): 1032-1036.

Borges, F. T., S. A. Melo, B. C. Ozdemir, N. Kato, I. Revuelta, C. A. Miller, V. H. Gattone, 2nd, V. S. LeBleu and R. Kalluri (2013). "TGF-beta1-containing exosomes from injured epithelial cells activate fibroblasts to initiate tissue regenerative responses and fibrosis." J Am Soc Nephrol 24(3): 385-392.

Borgovan, T., L. Crawford, C. Nwizu and P. Quesenberry (2019). "Stem cells and extracellular vesicles: biological regulators of physiology and disease." Am J Physiol Cell Physiol 317(2): C155-C166.

Bos, L. D. J., A. Artigas, J. M. Constantin, L. A. Hagens, N. Heijnen, J. G. Laffey, N. Meyer, L. Papazian, L. Pisani, M. J. Schultz, M. Shankar-Hari, M. R. Smit, C. Summers, L. B. Ware, R. Scala and C. S. Calfee (2021). "Precision medicine in acute respiratory distress syndrome: workshop report and recommendations for future research." Eur Respir Rev 30(159).

Boxall, S. A. and E. Jones (2012). "Markers for characterization of bone marrow multipotential stromal cells." Stem Cells Int 2012: 975871.

Brimioulle, S., V. Julien, R. Gust, J. K. Kozlowski, R. Naeije and D. P. Schuster (2002). "Importance of hypoxic vasoconstriction in maintaining oxygenation during acute lung injury." Crit Care Med 30(4): 874-880.

Brimioulle, S., P. LeJeune and R. Naeije (1996). "Effects of hypoxic pulmonary vasoconstriction on pulmonary gas exchange." J Appl Physiol (1985) 81(4): 1535-1543.

Briva, A., I. Vadasz, E. Lecuona, L. C. Welch, J. Chen, L. A. Dada, H. E. Trejo, V. Dumasius, Z. S. Azzam, P. M. Myrianthefs, D. Batlle, Y. Gruenbaum and J. I. Sznajder (2007). "High CO2 levels impair alveolar epithelial function independently of pH." PLoS One 2(11): e1238.

Broccard, A. F., J. R. Hotchkiss, C. Vannay, M. Markert, A. Sauty, F. Feihl and M. D. Schaller (2001). "Protective effects of hypercapnic acidosis on ventilator-induced lung injury." Am J Respir Crit Care Med 164(5): 802-806.

Brower, R. G., P. N. Lanken, N. MacIntyre, M. A. Matthay, A. Morris, M. Ancukiewicz, D. Schoenfeld, B. T. Thompson, L. National Heart and A. C. T. N. Blood Institute (2004). "Higher versus lower positive end-expiratory pressures in patients with the acute respiratory distress syndrome." N Engl J Med 351(4): 327-336.

Brun-Buisson, C., C. Minelli, G. Bertolini, L. Brazzi, J. Pimentel, K. Lewandowski, J. Bion, J. A. Romand, J. Villar, A. Thorsteinsson, P. Damas, A. Armaganidis, F. Lemaire and A. S. Group (2004). "Epidemiology and outcome of acute lung injury in European intensive care units. Results from the ALIVE study." Intensive Care Med 30(1): 51-61.

Bull, T. M., B. Clark, K. McFann and M. Moss (2010). "Pulmonary vascular dysfunction is associated with poor outcomes in patients with acute lung injury." Am J Respir Crit Care Med 182(9): 1123-1128.

Bull, T. M., B. Clark, K. McFann, M. Moss, L. National Institutes of Health/National Heart and A. N. Blood Institute (2010). "Pulmonary vascular dysfunction is associated with poor outcomes in patients with acute lung injury." Am J Respir Crit Care Med 182(9): 1123-1128.

Byrnes, D., C. H. Masterson, A. Artigas and J. G. Laffey (2021). "Mesenchymal Stem/Stromal Cells Therapy for Sepsis and Acute Respiratory Distress Syndrome." Semin Respir Crit Care Med 42(1): 20-39.

Caironi, P., M. Cressoni, D. Chiumello, M. Ranieri, M. Quintel, S. G. Russo, R. Cornejo, G. Bugedo, E. Carlesso, R. Russo, L. Caspani and L. Gattinoni (2010). "Lung opening and closing during ventilation of acute respiratory distress syndrome." Am J Respir Crit Care Med 181(6): 578-586.

Calfee, C. S., K. Delucchi, P. E. Parsons, B. T. Thompson, L. B. Ware, M. A. Matthay and N. A. Network (2014). "Subphenotypes in acute respiratory distress syndrome: latent class analysis of data from two randomised controlled trials." Lancet Respir Med 2(8): 611-620.

Calfee, C. S., D. Gallagher, J. Abbott, B. T. Thompson, M. A. Matthay and N. A. Network (2012). "Plasma angiopoietin-2 in clinical acute lung injury: prognostic and pathogenetic significance." Crit Care Med 40(6): 1731-1737.

Callejo, M., G. Mondejar-Parreno, D. Morales-Cano, B. Barreira, S. Esquivel-Ruiz, M. A. Olivencia, G. Manaud, F. Perros, J. Duarte, L. Moreno, A. Cogolludo and F. Perez-Vizcaino (2020). "Vitamin D deficiency downregulates TASK-1 channels and induces pulmonary vascular dysfunction." Am J Physiol Lung Cell Mol Physiol 319(4): L627-L640.

Carsana, L., A. Sonzogni, A. Nasr, R. S. Rossi, A. Pellegrinelli, P. Zerbi, R. Rech, R. Colombo, S. Antinori, M. Corbellino, M. Galli, E. Catena, A. Tosoni, A. Gianatti and M. Nebuloni (2020). "Pulmonary post-mortem findings in a series of COVID-19 cases from northern Italy: a two-centre descriptive study." Lancet Infect Dis 20(10): 1135-1140.

Cartwright, N., S. K. McMaster, R. Sorrentino, M. Paul-Clark, S. Sriskandan, B. Ryffel, V. F. Quesniaux, T. W. Evans and J. A. Mitchell (2007). "Elucidation of toll-like receptor and adapter protein signaling in vascular dysfunction induced by gram-positive Staphylococcus aureus or gram-negative Escherichia coli." Shock 27(1): 40-47.

Casey, L., B. Krieger, J. Kohler, C. Rice, S. Oparil and P. Szidon (1981). "Decreased serum angiotensin converting enzyme in adult respiratory distress syndrome associated with sepsis: a preliminary report." Crit Care Med 9(9): 651-654.

Castillo, S. S., M. Levy, J. V. Thaikoottathil and T. Goldkorn (2007). "Reactive nitrogen and oxygen species activate different sphingomyelinases to induce apoptosis in airway epithelial cells." Exp Cell Res 313(12): 2680-2686.

Chambers, E., S. Rounds and Q. Lu (2018). "Pulmonary Endothelial Cell Apoptosis in Emphysema and Acute Lung Injury." Adv Anat Embryol Cell Biol 228: 63-86.

Chan, J. F., S. Yuan, K. H. Kok, K. K. To, H. Chu, J. Yang, F. Xing, J. Liu, C. C. Yip, R. W. Poon, H. W. Tsoi, S. K. Lo, K. H. Chan, V. K. Poon, W. M. Chan, J. D. Ip, J. P. Cai, V. C. Cheng, H. Chen, C. K. Hui and K. Y. Yuen (2020). "A familial cluster of pneumonia associated with the 2019 novel coronavirus indicating person-to-person transmission: a study of a family cluster." Lancet 395(10223): 514-523.

Chan, M. C., D. I. Kuok, C. Y. Leung, K. P. Hui, S. A. Valkenburg, E. H. Lau, J. M. Nicholls, X. Fang, Y. Guan, J. W. Lee, R. W. Chan, R. G. Webster, M. A. Matthay and J. S. Peiris (2016). "Human mesenchymal stromal cells reduce influenza A H5N1-associated acute lung injury in vitro and in vivo." Proc Natl Acad Sci U S A 113(13): 3621-3626.

Chatterjee, V., X. Yang, Y. Ma, M. H. Wu and S. Y. Yuan (2020). "Extracellular vesicles: new players in regulating vascular barrier function." American Journal of Physiology-Heart and Circulatory Physiology 319(6): H1181-H1196.

Chavakis, E. and S. Dimmeler (2002). "Regulation of endothelial cell survival and apoptosis during angiogenesis." Arterioscler Thromb Vasc Biol 22(6): 887-893.

Chen, J. (2020). "Pathogenicity and transmissibility of 2019-nCoV-A quick overview and comparison with other emerging viruses." Microbes Infect 22(2): 69-71.

Chen, J., Z. Liu, M. M. Hong, H. Zhang, C. Chen, M. Xiao, J. Wang, F. Yao, M. Ba, J. Liu, Z. K. Guo and J. Zhong (2014). "Proangiogenic compositions of microvesicles derived from human umbilical cord mesenchymal stem cells." PLoS One 9(12): e115316.

Chen, J. Y., R. An, Z. J. Liu, J. J. Wang, S. Z. Chen, M. M. Hong, J. H. Liu, M. Y. Xiao and Y. F. Chen (2014). "Therapeutic effects of mesenchymal stem cell-derived microvesicles on pulmonary arterial hypertension in rats." Acta Pharmacol Sin 35(9): 1121-1128.

Chen, N., M. Zhou, X. Dong, J. Qu, F. Gong, Y. Han, Y. Qiu, J. Wang, Y. Liu, Y. Wei, J. Xia, T. Yu, X. Zhang and L. Zhang (2020). "Epidemiological and clinical characteristics of 99 cases of 2019 novel coronavirus pneumonia in Wuhan, China: a descriptive study." Lancet 395(10223): 507-513.

Chen, S., X. Chen, X. Wu, S. Wei, W. Han, J. Lin, M. Kang and L. Chen (2017). "Hepatocyte growth factor-modified mesenchymal stem cells improve ischemia/reperfusion-induced acute lung injury in rats." Gene Ther 24(1): 3-11.

Chen, X., S. Wu, L. Tang, L. Ma, F. Wang, H. Feng, J. Meng and Z. Han (2019). "Mesenchymal stem cells overexpressing heme oxygenase-1 ameliorate lipopolysaccharide-induced acute lung injury in rats." J Cell Physiol 234(5): 7301-7319.

Cheng, D. S., W. Han, S. M. Chen, T. P. Sherrill, M. Chont, G. Y. Park, J. R. Sheller, V. V. Polosukhin, J. W. Christman, F. E. Yull and T. S. Blackwell (2007). "Airway epithelium controls lung inflammation and injury through the NF-kappa B pathway." J Immunol 178(10): 6504-6513.

Chester, A. H. and M. H. Yacoub (2014). "The role of endothelin-1 in pulmonary arterial hypertension." Glob Cardiol Sci Pract 2014(2): 62-78.

Claus, R. A., A. C. Bunck, C. L. Bockmeyer, F. M. Brunkhorst, W. Losche, R. Kinscherf and H. P. Deigner (2005). "Role of increased sphingomyelinase activity in apoptosis and organ failure of patients with severe sepsis." FASEB J 19(12): 1719-1721.

Cocucci, E. and J. Meldolesi (2015). "Ectosomes and exosomes: shedding the confusion between extracellular vesicles." Trends Cell Biol 25(6): 364-372.

Cogolludo, A., L. Moreno, L. Bosca, J. Tamargo and F. Perez-Vizcaino (2003). "Thromboxane A2-induced inhibition of voltage-gated K+ channels and pulmonary vasoconstriction: role of protein kinase Czeta." Circ Res 93(7): 656-663.

Cogolludo, A., L. Moreno, G. Frazziano, J. Moral-Sanz, C. Menendez, J. Castaneda, C. Gonzalez, E. Villamor and F. Perez-Vizcaino (2009). "Activation of neutral sphingomyelinase is involved in acute hypoxic pulmonary vasoconstriction." Cardiovasc Res 82(2): 296-302.

Cogolludo, A., L. Moreno and E. Villamor (2007). "Mechanisms controlling vascular tone in pulmonary arterial hypertension: implications for vasodilator therapy." Pharmacology 79(2): 65-75.

Collino, F., J. A. Lopes, S. Correa, E. Abdelhay, C. M. Takiya, C. H. C. Wendt, K. R. de Miranda, A. Vieyra and R. S. Lindoso (2019). "Adipose-Derived Mesenchymal Stromal Cells Under Hypoxia: Changes in Extracellular Vesicles Secretion and Improvement of Renal Recovery after Ischemic Injury." Cell Physiol Biochem 52(6): 1463-1483.

Contreras-Lopez, R., R. Elizondo-Vega, M. J. Paredes, N. Luque-Campos, M. J. Torres, G. Tejedor, A. M. Vega-Letter, A. Figueroa-Valdes, C. Pradenas, K. Oyarce, C. Jorgensen, M. Khoury, M. L. A. Garcia-Robles, C. Altamirano, F. Djouad and P. Luz-Crawford (2020). "HIF1alpha-dependent metabolic reprogramming governs mesenchymal stem/stromal cell immunoregulatory functions." FASEB J 34(6): 8250-8264.

Cracowski, J. L., F. Chabot, J. Labarere, P. Faure, B. Degano, C. Schwebel, A. Chaouat, M. Reynaud-Gaubert, C. Cracowski, O. Sitbon, A. Yaici, G. Simonneau and M. Humbert (2014). "Proinflammatory cytokine levels are linked to death in pulmonary arterial hypertension." Eur Respir J 43(3): 915-917.

Craig, T. R., M. J. Duffy, M. Shyamsundar, C. McDowell, C. M. O'Kane, J. S. Elborn and D. F. McAuley (2011). "A randomized clinical trial of hydroxymethylglutaryl- coenzyme a reductase inhibition for acute lung injury (The HARP Study)." Am J Respir Crit Care Med 183(5): 620-626.

Crescitelli, R., C. Lässer, T. G. Szabó, A. Kittel, M. Eldh, I. Dianzani, E. I. Buzás and J. Lötvall (2013). "Distinct RNA profiles in subpopulations of extracellular vesicles: apoptotic bodies, microvesicles and exosomes." Journal of Extracellular Vesicles 2(1): 20677.

Crisostomo, P. R., Y. Wang, T. A. Markel, M. Wang, T. Lahm and D. R. Meldrum (2008). "Human mesenchymal stem cells stimulated by TNF-alpha, LPS, or hypoxia produce growth factors by an NF kappa B- but not JNK-dependent mechanism." Am J Physiol Cell Physiol 294(3): C675-682.

Cross, L. J. and M. A. Matthay (2011). "Biomarkers in acute lung injury: insights into the pathogenesis of acute lung injury." Crit Care Clin 27(2): 355-377.

Cruz, F. F. and P. R. M. Rocco (2020). "The potential of mesenchymal stem cell therapy for chronic lung disease." Expert Rev Respir Med 14(1): 31-39.

Curley, G. F., M. Hayes, B. Ansari, G. Shaw, A. Ryan, F. Barry, T. O'Brien, D. O'Toole and J. G. Laffey (2012). "Mesenchymal stem cells enhance recovery and repair following ventilator-induced lung injury in the rat." Thorax 67(6): 496-501.

Curley, G. F., J. G. Laffey and B. P. Kavanagh (2013). "CrossTalk proposal: there is added benefit to providing permissive hypercapnia in the treatment of ARDS." J Physiol 591(11): 2763-2765.

Curley, G. F., J. A. Scott and J. G. Laffey (2014). "Therapeutic potential and mechanisms of action of mesenchymal stromal cells for Acute Respiratory Distress Syndrome." Curr Stem Cell Res Ther 9(4): 319-329.

Da, J., L. Chen and G. Hedenstierna (2007). "Nitric oxide up-regulates the glucocorticoid receptor and blunts the inflammatory reaction in porcine endotoxin sepsis." Crit Care Med 35(1): 26-32.

Dantzker, D. R., C. J. Brook, P. Dehart, J. P. Lynch and J. G. Weg (1979). "Ventilation-perfusion distributions in the adult respiratory distress syndrome." Am Rev Respir Dis 120(5): 1039-1052.

de Hemptinne, Q., M. Remmelink, S. Brimioulle, I. Salmon and J. L. Vincent (2009). "ARDS: a clinicopathological confrontation." Chest 135(4): 944-949.

Dellinger, R. P., J. L. Zimmerman, R. W. Taylor, R. C. Straube, D. L. Hauser, G. J. Criner, K. Davis, Jr., T. M. Hyers and P. Papadakos (1998). "Effects of

inhaled nitric oxide in patients with acute respiratory distress syndrome: results of a randomized phase II trial. Inhaled Nitric Oxide in ARDS Study Group." Crit Care Med 26(1): 15-23.

Deng, Q., B. Hu, Y. Zhang, H. Wang, X. Zhou, W. Hu, Y. Cheng, J. Yan, H. Ping and Q. Zhou (2020). "Suspected myocardial injury in patients with COVID-19: Evidence from front-line clinical observation in Wuhan, China." Int J Cardiol 311: 116-121.

Denker, B. M. and S. K. Nigam (1998). "Molecular structure and assembly of the tight junction." Am J Physiol 274(1): F1-9.

Devaney, J., S. Horie, C. Masterson, S. Elliman, F. Barry, T. O'Brien, G. F. Curley, D. O'Toole and J. G. Laffey (2015). "Human mesenchymal stromal cells decrease the severity of acute lung injury induced by E. coli in the rat." Thorax 70(7): 625-635.

Dinh-Xuan, A. T. (1992). "Endothelial modulation of pulmonary vascular tone." Eur Respir J 5(6): 757-762.

Dominici, M., K. Le Blanc, I. Mueller, I. Slaper-Cortenbach, F. Marini, D. Krause, R. Deans, A. Keating, D. Prockop and E. Horwitz (2006). "Minimal criteria for defining multipotent mesenchymal stromal cells. The International Society for Cellular Therapy position statement." Cytotherapy 8(4): 315-317.

Dos Santos, C. C. and A. S. Slutsky (2000). "Invited review: mechanisms of ventilator-induced lung injury: a perspective." J Appl Physiol (1985) 89(4): 1645-1655.

Doyle, I. R., A. D. Bersten and T. E. Nicholas (1997). "Surfactant proteins-A and -B are elevated in plasma of patients with acute respiratory failure." Am J Respir Crit Care Med 156(4 Pt 1): 1217-1229.

Dries, D. J., A. B. Adams and J. J. Marini (2007). "Time course of physiologic variables in response to ventilator-induced lung injury." Respir Care 52(1): 31-37.

Dumitru, C. A. and E. Gulbins (2006). "TRAIL activates acid sphingomyelinase via a redox mechanism and releases ceramide to trigger apoptosis." Oncogene 25(41): 5612-5625.

Dumitru, C. A., H. Hemeda, M. Jakob, S. Lang and S. Brandau (2014). "Stimulation of mesenchymal stromal cells (MSCs) via TLR3 reveals a novel mechanism of autocrine priming." FASEB J 28(9): 3856-3866.

Dunkley, K. A., P. R. Louzon, J. Lee and S. Vu (2013). "Efficacy, safety, and medication errors associated with the use of inhaled epoprostenol for adults with acute respiratory distress syndrome: a pilot study." Ann Pharmacother 47(6): 790-796.

Dupont, H., F. Le Corre, L. Fierobe, C. Cheval, P. Moine and J. F. Timsit (1999). "Efficiency of inhaled nitric oxide as rescue therapy during severe ARDS: survival and factors associated with the first response." J Crit Care 14(3): 107-113.

Dutra Silva, J., Y. Su, C. S. Calfee, K. L. Delucchi, D. Weiss, D. F. McAuley, C. O'Kane and A. D. Krasnodembskaya (2021). "Mesenchymal stromal cell extracellular vesicles rescue mitochondrial dysfunction and improve barrier integrity in clinically relevant models of ARDS." Eur Respir J 58(1): 2002978.

Eisner, M. D., T. Thompson, L. D. Hudson, J. M. Luce, D. Hayden, D. Schoenfeld, M. A. Matthay and N. Acute Respiratory Distress Syndrome (2001). "Efficacy of low tidal volume ventilation in patients with different clinical risk factors for acute lung injury and the acute respiratory distress syndrome." Am J Respir Crit Care Med 164(2): 231-236.

Engela, A. U., C. C. Baan, A. M. Peeters, W. Weimar and M. J. Hoogduijn (2013). "Interaction between adipose tissue-derived mesenchymal stem cells and regulatory T-cells." Cell Transplant 22(1): 41-54.

English, K., R. Tonlorenzi, G. Cossu and K. J. Wood (2013). "Mesoangioblasts suppress T cell proliferation through IDO and PGE-2-dependent pathways." Stem Cells Dev 22(3): 512-523.

Erickson, S. E., G. S. Martin, J. L. Davis, M. A. Matthay, M. D. Eisner and N. N. A. Network (2009). "Recent trends in acute lung injury mortality: 1996-2005." Crit Care Med 37(5): 1574-1579.

Esquivel-Ruiz, S., P. Gonzalez-Rodriguez, J. A. Lorente, F. Perez-Vizcaino, R. Herrero and L. Moreno (2021). "Extracellular Vesicles and Alveolar Epithelial-Capillary Barrier Disruption in Acute Respiratory Distress Syndrome: Pathophysiological Role and Therapeutic Potential." Frontiers in Physiology 12: 1824.

Esteban, A., F. Frutos-Vivar, A. Muriel, N. D. Ferguson, O. Penuelas, V. Abraira, K. Raymondos, F. Rios, N. Nin, C. Apezteguia, D. A. Violi, A. W. Thille, L. Brochard, M. Gonzalez, A. J. Villagomez, J. Hurtado, A. R. Davies, B. Du, S. M. Maggiore, P. Pelosi, L. Soto, V. Tomicic, G. D'Empaire, D. Matamis, F. Abroug, R. P. Moreno, M. A. Soares, Y. Arabi, F. Sandi, M. Jibaja, P. Amin, Y. Koh, M. A. Kuiper, H. H. Bulow, A. A. Zeggwagh and A. Anzueto (2013). "Evolution of mortality over time in patients receiving mechanical ventilation." Am J Respir Crit Care Med 188(2): 220-230.

Estenssoro, E., A. Dubin, E. Laffaire, H. Canales, G. Saenz, M. Moseinco, M. Pozo, A. Gomez, N. Baredes, G. Jannello and J. Osatnik (2002). "Incidence, clinical course, and outcome in 217 patients with acute respiratory distress syndrome." Crit Care Med 30(11): 2450-2456.

Everhart, M. B., W. Han, T. P. Sherrill, M. Arutiunov, V. V. Polosukhin, J. R. Burke, R. T. Sadikot, J. W. Christman, F. E. Yull and T. S. Blackwell (2006). "Duration and intensity of NF-kappaB activity determine the severity of endotoxin-induced acute lung injury." J Immunol 176(8): 4995-5005.

Fagan, K. A., B. W. Fouty, R. C. Tyler, K. G. Morris, Jr., L. K. Hepler, K. Sato, T. D. LeCras, S. H. Abman, H. D. Weinberger, P. L. Huang, I. F. McMurtry and D. M. Rodman (1999). "The pulmonary circulation of homozygous or heterozygous eNOS-null mice is hyperresponsive to mild hypoxia." J Clin Invest 103(2): 291-299.

Famous, K. R., K. Delucchi, L. B. Ware, K. N. Kangelaris, K. D. Liu, B. T. Thompson, C. S. Calfee and A. Network (2017). "Acute Respiratory Distress Syndrome Subphenotypes Respond Differently to Randomized Fluid Management Strategy." Am J Respir Crit Care Med 195(3): 331-338.

Fan, E., D. Brodie and A. S. Slutsky (2018). "Acute Respiratory Distress Syndrome: Advances in Diagnosis and Treatment." JAMA 319(7): 698-710.

Ferguson, N. D., D. J. Cook, G. H. Guyatt, S. Mehta, L. Hand, P. Austin, Q. Zhou, A. Matte, S. D. Walter, F. Lamontagne, J. T. Granton, Y. M. Arabi, A. C. Arroliga, T. E. Stewart, A. S. Slutsky, M. O. Meade, O. T. Investigators and G. Canadian Critical Care Trials (2013). "High-frequency oscillation in early acute respiratory distress syndrome." N Engl J Med 368(9): 795-805.

Ferreira, J. R., G. Q. Teixeira, S. G. Santos, M. A. Barbosa, G. Almeida-Porada and R. M. Goncalves (2018). "Mesenchymal Stromal Cell Secretome: Influencing Therapeutic Potential by Cellular Pre-conditioning." Front Immunol 9: 2837.

Fitzgerald, M., J. Millar, B. Blackwood, A. Davies, S. J. Brett, D. F. McAuley and J. J. McNamee (2014). "Extracorporeal carbon dioxide removal for patients with acute respiratory failure secondary to the acute respiratory distress syndrome: a systematic review." Crit Care 18(3): 222.

Folkman, J. (2003). "Angiogenesis and apoptosis." Semin Cancer Biol 13(2): 159-167.

Force, A. D. T., V. M. Ranieri, G. D. Rubenfeld, B. T. Thompson, N. D. Ferguson, E. Caldwell, E. Fan, L. Camporota and A. S. Slutsky (2012). "Acute respiratory distress syndrome: the Berlin Definition." JAMA 307(23): 2526-2533.

Forel, J. M., A. Roch, V. Marin, P. Michelet, D. Demory, J. L. Blache, G. Perrin, M. Gainnier, P. Bongrand and L. Papazian (2006). "Neuromuscular blocking agents decrease inflammatory response in patients presenting with acute respiratory distress syndrome." Crit Care Med 34(11): 2749-2757.

Forstermann, U. and T. Munzel (2006). "Endothelial nitric oxide synthase in vascular disease: from marvel to menace." Circulation 113(13): 1708-1714.

Fox-Dewhurst, R., M. K. Alberts, O. Kajikawa, E. Caldwell, M. C. Johnson, 2nd, S. J. Skerrett, R. B. Goodman, J. T. Ruzinski, V. A. Wong, E. Y. Chi and T. R. Martin (1997). "Pulmonary and systemic inflammatory responses in rabbits with gram-negative pneumonia." Am J Respir Crit Care Med 155(6): 2030-2040.

Fox, G. A., N. A. Paterson and D. G. McCormack (1994). "Effect of inhibition of NO synthase on vascular reactivity in a rat model of hyperdynamic sepsis." Am J Physiol 267(4 Pt 2): H1377-1382.

Frank, J. A., D. F. McAuley, J. A. Gutierrez, B. M. Daniel, L. Dobbs and M. A. Matthay (2005). "Differential effects of sustained inflation recruitment maneuvers on alveolar epithelial and lung endothelial injury." Crit Care Med 33(1): 181-188; discussion 254-185.

Franke-Ullmann, G., C. Pfortner, P. Walter, C. Steinmuller, M. L. Lohmann-Matthes and L. Kobzik (1996). "Characterization of murine lung interstitial macrophages in comparison with alveolar macrophages in vitro." J Immunol 157(7): 3097-3104.

Frat, J. P., A. W. Thille, A. Mercat, C. Girault, S. Ragot, S. Perbet, G. Prat, T. Boulain, E. Morawiec, A. Cottereau, J. Devaquet, S. Nseir, K. Razazi, J. P. Mira, L. Argaud, J. C. Chakarian, J. D. Ricard, X. Wittebole, S. Chevalier, A. Herbland, M. Fartoukh, J. M. Constantin, J. M. Tonnelier, M. Pierrot, A. Mathonnet, G. Beduneau, C. Deletage-Metreau, J. C. Richard, L. Brochard, R. Robert, F. S. Group and R. Network (2015). "High-flow oxygen through nasal cannula in acute hypoxemic respiratory failure." N Engl J Med 372(23): 2185-2196.

Frazier, T. P., J. M. Gimble, I. Kheterpal and B. G. Rowan (2013). "Impact of low oxygen on the secretome of human adipose-derived stromal/stem cell primary cultures." Biochimie 95(12): 2286-2296.

Freeman, B. (1994). "Free radical chemistry of nitric oxide. Looking at the dark side." Chest 105(3 Suppl): 79S-84S.

Fu, Z., M. L. Costello, K. Tsukimoto, R. Prediletto, A. R. Elliott, O. Mathieu-Costello and J. B. West (1992). "High lung volume increases stress failure in pulmonary capillaries." J Appl Physiol (1985) 73(1): 123-133.

Fuenzalida, P., M. Kurte, C. Fernandez-O'ryan, C. Ibanez, M. Gauthier-Abeliuk, A. M. Vega-Letter, P. Gonzalez, C. Irarrazabal, N. Quezada, F. Figueroa and F. Carrion (2016). "Toll-like receptor 3 pre-conditioning increases the therapeutic efficacy of umbilical cord mesenchymal stromal cells in a dextran sulfate sodium-induced colitis model." Cytotherapy 18(5): 630-641.

Fujishima, S., H. Morisaki, A. Ishizaka, Y. Kotake, M. Miyaki, K. Yoh, K. Sekine, J. Sasaki, S. Tasaka, N. Hasegawa, Y. Kawai, J. Takeda and N. Aikawa (2008). "Neutrophil elastase and systemic inflammatory response syndrome in the initiation and development of acute lung injury among critically ill patients." Biomed Pharmacother 62(5): 333-338.

Fujita, M., K. Kuwano, R. Kunitake, N. Hagimoto, H. Miyazaki, Y. Kaneko, M. Kawasaki, T. Maeyama and N. Hara (1998). "Endothelial cell apoptosis in lipopolysaccharide-induced lung injury in mice." Int Arch Allergy Immunol 117(3): 202-208.

Galiatsou, E., E. Kostanti, E. Svarna, A. Kitsakos, V. Koulouras, S. C. Efremidis and G. Nakos (2006). "Prone position augments recruitment and prevents alveolar overinflation in acute lung injury." Am J Respir Crit Care Med 174(2): 187-197.

Galie, N., M. Humbert, J. L. Vachiery, S. Gibbs, I. Lang, A. Torbicki, G. Simonneau, A. Peacock, A. Vonk Noordegraaf, M. Beghetti, A. Ghofrani, M. A. Gomez Sanchez, G. Hansmann, W. Klepetko, P. Lancellotti, M. Matucci, T. McDonagh, L. A. Pierard, P. T. Trindade, M. Zompatori and M. Hoeper (2015). "2015 ESC/ERS Guidelines for the diagnosis and treatment of pulmonary hypertension: The Joint Task Force for the Diagnosis and Treatment of Pulmonary Hypertension of the European Society of Cardiology (ESC) and the European Respiratory Society (ERS): Endorsed by: Association for European Paediatric and Congenital Cardiology (AEPC), International Society for Heart and Lung Transplantation (ISHLT)." Eur Respir J 46(4): 903-975.

Gao Smith, F., G. D. Perkins, S. Gates, D. Young, D. F. McAuley, W. Tunnicliffe, Z. Khan, S. E. Lamb and B.-s. investigators (2012). "Effect of

intravenous beta-2 agonist treatment on clinical outcomes in acute respiratory distress syndrome (BALTI-2): a multicentre, randomised controlled trial." Lancet 379(9812): 229-235.

Gattinoni, L., M. Bombino, P. Pelosi, A. Lissoni, A. Pesenti, R. Fumagalli and M. Tagliabue (1994). "Lung structure and function in different stages of severe adult respiratory distress syndrome." JAMA 271(22): 1772-1779.

Gattinoni, L., L. Camporota and J. J. Marini (2020). "COVID-19 phenotypes: leading or misleading?" Eur Respir J 56(2).

Gattinoni, L., P. Taccone, E. Carlesso and J. J. Marini (2013). "Prone position in acute respiratory distress syndrome. Rationale, indications, and limits." Am J Respir Crit Care Med 188(11): 1286-1293.

Gattinoni, L., T. Tonetti, M. Cressoni, P. Cadringher, P. Herrmann, O. Moerer, A. Protti, M. Gotti, C. Chiurazzi, E. Carlesso, D. Chiumello and M. Quintel (2016). "Ventilator-related causes of lung injury: the mechanical power." Intensive Care Med 42(10): 1567-1575.

Ge, H., X. Wang, X. Yuan, G. Xiao, C. Wang, T. Deng, Q. Yuan and X. Xiao (2020). "The epidemiology and clinical information about COVID-19." Eur J Clin Microbiol Infect Dis 39(6): 1011-1019.

Ge, S. X., D. Jung and R. Yao (2020). "ShinyGO: a graphical gene-set enrichment tool for animals and plants." Bioinformatics 36(8): 2628-2629.

Gennai, S., A. Monsel, Q. Hao, J. Park, M. A. Matthay and J. W. Lee (2015). "Microvesicles Derived From Human Mesenchymal Stem Cells Restore Alveolar Fluid Clearance in Human Lungs Rejected for Transplantation." Am J Transplant 15(9): 2404-2412.

Giaid, A. and D. Saleh (1995). "Reduced expression of endothelial nitric oxide synthase in the lungs of patients with pulmonary hypertension." N Engl J Med 333(4): 214-221.

Gierhardt, M., O. Pak, D. Walmrath, W. Seeger, F. Grimminger, H. A. Ghofrani, N. Weissmann, M. Hecker and N. Sommer (2021). "Impairment of hypoxic pulmonary vasoconstriction in acute respiratory distress syndrome." Eur Respir Rev 30(161).

Goggel, R., S. Winoto-Morbach, G. Vielhaber, Y. Imai, K. Lindner, L. Brade, H. Brade, S. Ehlers, A. S. Slutsky, S. Schutze, E. Gulbins and S. Uhlig (2004). "PAF-mediated pulmonary edema: a new role for acid sphingomyelinase and ceramide." Nat Med 10(2): 155-160.

Goldman, J. L., S. Sammani, C. Kempf, L. Saadat, E. Letsiou, T. Wang, L. Moreno-Vinasco, A. N. Rizzo, J. D. Fortman and J. G. Garcia (2014). "Pleiotropic effects of interleukin-6 in a "two-hit" murine model of acute respiratory distress syndrome." Pulm Circ 4(2): 280-288.

Golembeski, S. M., J. West, Y. Tada and K. A. Fagan (2005). "Interleukin-6 causes mild pulmonary hypertension and augments hypoxia-induced pulmonary hypertension in mice." Chest 128(6 Suppl): 572S-573S.

Goligher, E. C., M. B. P. Amato and A. S. Slutsky (2017). "Applying Precision Medicine to Trial Design Using Physiology. Extracorporeal CO2 Removal for Acute Respiratory Distress Syndrome." Am J Respir Crit Care Med 196(5): 558-568.

Gonzalez-King, H., N. A. Garcia, I. Ontoria-Oviedo, M. Ciria, J. A. Montero and P. Sepulveda (2017). "Hypoxia Inducible Factor-1alpha Potentiates

Jagged 1-Mediated Angiogenesis by Mesenchymal Stem Cell-Derived Exosomes." Stem Cells 35(7): 1747-1759.

Gorgun, C., D. Ceresa, R. Lesage, F. Villa, D. Reverberi, C. Balbi, S. Santamaria, K. Cortese, P. Malatesta, L. Geris, R. Quarto and R. Tasso (2021). "Dissecting the effects of preconditioning with inflammatory cytokines and hypoxia on the angiogenic potential of mesenchymal stromal cell (MSC)-derived soluble proteins and extracellular vesicles (EVs)." Biomaterials 269: 120633.

Gorman, E., J. Millar, D. McAuley and C. O'Kane (2021). "Mesenchymal stromal cells for acute respiratory distress syndrome (ARDS), sepsis, and COVID-19 infection: optimizing the therapeutic potential." Expert Rev Respir Med 15(3): 301-324.

Gow, A. J., S. R. Thom and H. Ischiropoulos (1998). "Nitric oxide and peroxynitrite-mediated pulmonary cell death." Am J Physiol 274(1): L112-118.

Grasso, S., T. Stripoli, M. De Michele, F. Bruno, M. Moschetta, G. Angelelli, I. Munno, V. Ruggiero, R. Anaclerio, A. Cafarelli, B. Driessen and T. Fiore (2007). "ARDSnet ventilatory protocol and alveolar hyperinflation: role of positive end-expiratory pressure." Am J Respir Crit Care Med 176(8): 761-767.

Griffiths, M. J., S. Liu, N. P. Curzen, M. Messent and T. W. Evans (1995). "In vivo treatment with endotoxin induces nitric oxide synthase in rat main pulmonary artery." Am J Physiol 268(3 Pt 1): L509-518.

Grote, K., M. Petri, C. Liu, P. Jehn, S. Spalthoff, H. Kokemuller, M. Luchtefeld, T. Tschernig, C. Krettek, C. Haasper and M. Jagodzinski (2013). "Toll-like receptor 2/6-dependent stimulation of mesenchymal stem cells promotes angiogenesis by paracrine factors." Eur Cell Mater 26: 66-79; discussion 79.

Groth, A., B. Vrugt, M. Brock, R. Speich, S. Ulrich and L. C. Huber (2014). "Inflammatory cytokines in pulmonary hypertension." Respir Res 15: 47.

Group, W. H. O. R. E. A. f. C.-T. W., J. A. C. Sterne, S. Murthy, J. V. Diaz, A. S. Slutsky, J. Villar, D. C. Angus, D. Annane, L. C. P. Azevedo, O. Berwanger, A. B. Cavalcanti, P. F. Dequin, B. Du, J. Emberson, D. Fisher, B. Giraudeau, A. C. Gordon, A. Granholm, C. Green, R. Haynes, N. Heming, J. P. T. Higgins, P. Horby, P. Juni, M. J. Landray, A. Le Gouge, M. Leclerc, W. S. Lim, F. R. Machado, C. McArthur, F. Meziani, M. H. Moller, A. Perner, M. W. Petersen, J. Savovic, B. Tomazini, V. C. Veiga, S. Webb and J. C. Marshall (2020). "Association Between Administration of Systemic Corticosteroids and Mortality Among Critically Ill Patients With COVID-19: A Meta-analysis." JAMA 324(13): 1330-1341.

Grune, J., A. Tabuchi and W. M. Kuebler (2019). "Alveolar dynamics during mechanical ventilation in the healthy and injured lung." Intensive Care Med Exp 7(Suppl 1): 34.

Guerin, C., J. Reignier, J. C. Richard, P. Beuret, A. Gacouin, T. Boulain, E. Mercier, M. Badet, A. Mercat, O. Baudin, M. Clavel, D. Chatellier, S. Jaber, S. Rosselli, J. Mancebo, M. Sirodot, G. Hilbert, C. Bengler, J. Richecoeur, M. Gainnier, F. Bayle, G. Bourdin, V. Leray, R. Girard, L. Baboi, L. Ayzac

and P. S. Group (2013). "Prone positioning in severe acute respiratory distress syndrome." N Engl J Med 368(23): 2159-2168.

Gupta, N., R. Sinha, A. Krasnodembskaya, X. Xu, V. Nizet, M. A. Matthay and J. H. Griffin (2018). "The TLR4-PAR1 Axis Regulates Bone Marrow Mesenchymal Stromal Cell Survival and Therapeutic Capacity in Experimental Bacterial Pneumonia." Stem Cells 36(5): 796-806.

Gupta, N., X. Su, B. Popov, J. W. Lee, V. Serikov and M. A. Matthay (2007). "Intrapulmonary delivery of bone marrow-derived mesenchymal stem cells improves survival and attenuates endotoxin-induced acute lung injury in mice." J Immunol 179(3): 1855-1863.

Gurkan, O. U., C. He, R. Zielinski, H. Rabb, L. S. King, J. M. Dodd-o, F. R. D'Alessio, N. Aggarwal, D. Pearse and P. M. Becker (2011). "Interleukin-6 mediates pulmonary vascular permeability in a two-hit model of ventilator-associated lung injury." Exp Lung Res 37(10): 575-584.

Gutierrez-Vazquez, C., C. Villarroya-Beltri, M. Mittelbrunn and F. Sanchez-Madrid (2013). "Transfer of extracellular vesicles during immune cell-cell interactions." Immunol Rev 251(1): 125-142.

Habashi, N. M., L. Camporota, L. A. Gatto and G. Nieman (2021). "Functional pathophysiology of SARS-CoV-2-induced acute lung injury and clinical implications." J Appl Physiol (1985) 130(3): 877-891.

Haimovitz-Friedman, A., C. Cordon-Cardo, S. Bayoumy, M. Garzotto, M. McLoughlin, R. Gallily, C. K. Edwards, 3rd, E. H. Schuchman, Z. Fuks and R. Kolesnick (1997). "Lipopolysaccharide induces disseminated endothelial apoptosis requiring ceramide generation." J Exp Med 186(11): 1831-1841.

Halliwell, B. (2014). "Cell culture, oxidative stress, and antioxidants: avoiding pitfalls." Biomed J 37(3): 99-105.

Hamacher, J., R. Lucas, H. R. Lijnen, S. Buschke, Y. Dunant, A. Wendel, G. E. Grau, P. M. Suter and B. Ricou (2002). "Tumor necrosis factor-alpha and angiostatin are mediators of endothelial cytotoxicity in bronchoalveolar lavages of patients with acute respiratory distress syndrome." Am J Respir Crit Care Med 166(5): 651-656.

Han, J., Y. Li and Y. Li (2019). "Strategies to Enhance Mesenchymal Stem Cell-Based Therapies for Acute Respiratory Distress Syndrome." Stem Cells Int 2019: 5432134.

Han, J., Y. Li and Y. Li (2019). "Strategies to Enhance Mesenchymal Stem Cell-Based Therapies for Acute Respiratory Distress Syndrome." Stem Cells International 2019: 5432134.

Han, J., X. Lu, L. Zou, X. Xu and H. Qiu (2016). "E-Prostanoid 2 Receptor Overexpression Promotes Mesenchymal Stem Cell Attenuated Lung Injury." Hum Gene Ther 27(8): 621-630.

Han, S. and R. K. Mallampalli (2015). "The acute respiratory distress syndrome: from mechanism to translation." J Immunol 194(3): 855-860.

Han, W., B. Quan, Y. Guo, J. Zhang, Y. Lu, G. Feng, Q. Wu, F. Fang, L. Cheng, N. Jiao, X. Li and Q. Chen (2020). "The course of clinical diagnosis and treatment of a case infected with coronavirus disease 2019." J Med Virol 92(5): 461-463.

Han, X., C. Chen, G. Cheng, L. Liang, X. Yao, G. Yang, P. You and X. Shou (2015). "Peroxisome proliferator-activated receptor gamma attenuates serotonin-induced pulmonary artery smooth muscle cell proliferation and apoptosis inhibition involving ERK1/2 pathway." Microvasc Res 100: 17-24.

Han, Y. D., Y. Bai, X. L. Yan, J. Ren, Q. Zeng, X. D. Li, X. T. Pei and Y. Han (2018). "Co-transplantation of exosomes derived from hypoxia-preconditioned adipose mesenchymal stem cells promotes neovascularization and graft survival in fat grafting." Biochem Biophys Res Commun 497(1): 305-312.

Hashimoto-Kataoka, T., N. Hosen, T. Sonobe, Y. Arita, T. Yasui, T. Masaki, M. Minami, T. Inagaki, S. Miyagawa, Y. Sawa, M. Murakami, A. Kumanogoh, K. Yamauchi-Takihara, M. Okumura, T. Kishimoto, I. Komuro, M. Shirai, Y. Sakata and Y. Nakaoka (2015). "Interleukin-6/interleukin-21 signaling axis is critical in the pathogenesis of pulmonary arterial hypertension." Proc Natl Acad Sci U S A 112(20): E2677-2686.

Hattori, Y., S. Hattori and K. Kasai (2003). "Lipopolysaccharide activates Akt in vascular smooth muscle cells resulting in induction of inducible nitric oxide synthase through nuclear factor-kappa B activation." Eur J Pharmacol 481(2-3): 153-158.

Haynesworth, S. E., M. A. Baber and A. I. Caplan (1992). "Cell surface antigens on human marrow-derived mesenchymal cells are detected by monoclonal antibodies." Bone 13(1): 69-80.

Headley, A. S., E. Tolley and G. U. Meduri (1997). "Infections and the inflammatory response in acute respiratory distress syndrome." Chest 111(5): 1306-1321.

Henning, M. S., P. Stiedl, D. S. Barry, R. McMahon, S. G. Morham, D. Walsh and M. H. Naghavi (2011). "PDZD8 is a novel moesin-interacting cytoskeletal regulatory protein that suppresses infection by herpes simplex virus type 1." Virology 415(2): 114-121.

Herrero, R., G. Sanchez and J. A. Lorente (2018). "New insights into the mechanisms of pulmonary edema in acute lung injury." Ann Transl Med 6(2): 32.

Hirabayashi, Y., S. K. Kwon, H. Paek, W. M. Pernice, M. A. Paul, J. Lee, P. Erfani, A. Raczkowski, D. S. Petrey, L. A. Pon and F. Polleux (2017). "ER-mitochondria tethering by PDZD8 regulates Ca(2+) dynamics in mammalian neurons." Science 358(6363): 623-630.

Holtzman, M. J., D. E. Byers, J. Alexander-Brett and X. Wang (2014). "The role of airway epithelial cells and innate immune cells in chronic respiratory disease." Nat Rev Immunol 14(10): 686-698.

Hood, J. D. and D. A. Cheresh (2002). "Role of integrins in cell invasion and migration." Nat Rev Cancer 2(2): 91-100.

Horie, S., B. McNicholas, E. Rezoagli, T. Pham, G. Curley, D. McAuley, C. O'Kane, A. Nichol, C. Dos Santos, P. R. M. Rocco, G. Bellani and J. G. Laffey (2020). "Emerging pharmacological therapies for ARDS: COVID-19 and beyond." Intensive Care Med 46(12): 2265-2283.

Horvath, P., N. Aulner, M. Bickle, A. M. Davies, E. D. Nery, D. Ebner, M. C. Montoya, P. Ostling, V. Pietiainen, L. S. Price, S. L. Shorte, G. Turcatti, C.

von Schantz and N. O. Carragher (2016). "Screening out irrelevant cell-based models of disease." Nat Rev Drug Discov 15(11): 751-769.
Howell, M. D. and A. M. Davis (2018). "Management of ARDS in Adults." JAMA 319(7): 711-712.
Hu, C., M. Chen, R. Jiang, Y. Guo, M. Wu and X. Zhang (2018). "Exosome-related tumor microenvironment." J Cancer 9(17): 3084-3092.
Hu, S., J. Park, A. Liu, J. Lee, X. Zhang, Q. Hao and J. W. Lee (2018). "Mesenchymal Stem Cell Microvesicles Restore Protein Permeability Across Primary Cultures of Injured Human Lung Microvascular Endothelial Cells." Stem Cells Transl Med 7(8): 615-624.
Huang, C., Y. Wang, X. Li, L. Ren, J. Zhao, Y. Hu, L. Zhang, G. Fan, J. Xu, X. Gu, Z. Cheng, T. Yu, J. Xia, Y. Wei, W. Wu, X. Xie, W. Yin, H. Li, M. Liu, Y. Xiao, H. Gao, L. Guo, J. Xie, G. Wang, R. Jiang, Z. Gao, Q. Jin, J. Wang and B. Cao (2020). "Clinical features of patients infected with 2019 novel coronavirus in Wuhan, China." Lancet 395(10223): 497-506.
Huang da, W., B. T. Sherman and R. A. Lempicki (2009). "Bioinformatics enrichment tools: paths toward the comprehensive functional analysis of large gene lists." Nucleic Acids Res 37(1): 1-13.
Huang da, W., B. T. Sherman and R. A. Lempicki (2009). "Systematic and integrative analysis of large gene lists using DAVID bioinformatics resources." Nat Protoc 4(1): 44-57.
Hughes, K. T. and M. B. Beasley (2017). "Pulmonary Manifestations of Acute Lung Injury: More Than Just Diffuse Alveolar Damage." Arch Pathol Lab Med 141(7): 916-922.
Humbert, M., G. Monti, F. Brenot, O. Sitbon, A. Portier, L. Grangeot-Keros, P. Duroux, P. Galanaud, G. Simonneau and D. Emilie (1995). "Increased interleukin-1 and interleukin-6 serum concentrations in severe primary pulmonary hypertension." Am J Respir Crit Care Med 151(5): 1628-1631.
Hung, C., G. Linn, Y. H. Chow, A. Kobayashi, K. Mittelsteadt, W. A. Altemeier, S. A. Gharib, L. M. Schnapp and J. S. Duffield (2013). "Role of lung pericytes and resident fibroblasts in the pathogenesis of pulmonary fibrosis." Am J Respir Crit Care Med 188(7): 820-830.
Hung, M. J., W. J. Cherng, M. Y. Hung, H. T. Wu and J. H. Pang (2010). "Interleukin-6 inhibits endothelial nitric oxide synthase activation and increases endothelial nitric oxide synthase binding to stabilized caveolin-1 in human vascular endothelial cells." J Hypertens 28(5): 940-951.
Ichinose, F., R. Hataishi, J. C. Wu, N. Kawai, A. C. Rodrigues, C. Mallari, J. M. Post, J. F. Parkinson, M. H. Picard, K. D. Bloch and W. M. Zapol (2003). "A selective inducible NOS dimerization inhibitor prevents systemic, cardiac, and pulmonary hemodynamic dysfunction in endotoxemic mice." Am J Physiol Heart Circ Physiol 285(6): H2524-2530.
Idell, S. (2003). "Coagulation, fibrinolysis, and fibrin deposition in acute lung injury." Crit Care Med 31(4 Suppl): S213-220.
Idell, S., K. B. Koenig, D. S. Fair, T. R. Martin, J. McLarty and R. J. Maunder (1991). "Serial abnormalities of fibrin turnover in evolving adult respiratory distress syndrome." Am J Physiol 261(4 Pt 1): L240-248.
Ionescu, L., R. N. Byrne, T. van Haaften, A. Vadivel, R. S. Alphonse, G. J. Rey-Parra, G. Weissmann, A. Hall, F. Eaton and B. Thebaud (2012). "Stem cell

conditioned medium improves acute lung injury in mice: in vivo evidence for stem cell paracrine action." Am J Physiol Lung Cell Mol Physiol 303(11): L967-977.

Islam, D., Y. Huang, V. Fanelli, L. Delsedime, S. Wu, J. Khang, B. Han, A. Grassi, M. Li, Y. Xu, A. Luo, J. Wu, X. Liu, M. McKillop, J. Medin, H. Qiu, N. Zhong, M. Liu, J. Laffey, Y. Li and H. Zhang (2019). "Identification and Modulation of Microenvironment Is Crucial for Effective Mesenchymal Stromal Cell Therapy in Acute Lung Injury." Am J Respir Crit Care Med 199(10): 1214-1224.

Islam, M. N., S. R. Das, M. T. Emin, M. Wei, L. Sun, K. Westphalen, D. J. Rowlands, S. K. Quadri, S. Bhattacharya and J. Bhattacharya (2012). "Mitochondrial transfer from bone-marrow-derived stromal cells to pulmonary alveoli protects against acute lung injury." Nat Med 18(5): 759-765.

Ito, T., U. Ikeda, M. Shimpo, K. Yamamoto and K. Shimada (2000). "Serotonin increases interleukin-6 synthesis in human vascular smooth muscle cells." Circulation 102(20): 2522-2527.

Jackson, M. V., T. J. Morrison, D. F. Doherty, D. F. McAuley, M. A. Matthay, A. Kissenpfennig, C. M. O'Kane and A. D. Krasnodembskaya (2016). "Mitochondrial Transfer via Tunneling Nanotubes is an Important Mechanism by Which Mesenchymal Stem Cells Enhance Macrophage Phagocytosis in the In Vitro and In Vivo Models of ARDS." Stem Cells 34(8): 2210-2223.

Jacobson, J. R., J. W. Barnard, D. N. Grigoryev, S. F. Ma, R. M. Tuder and J. G. Garcia (2005). "Simvastatin attenuates vascular leak and inflammation in murine inflammatory lung injury." Am J Physiol Lung Cell Mol Physiol 288(6): L1026-1032.

Jain, M., A. Singh, V. Singh and M. K. Barthwal (2015). "Involvement of interleukin-1 receptor-associated kinase-1 in vascular smooth muscle cell proliferation and neointimal formation after rat carotid injury." Arterioscler Thromb Vasc Biol 35(6): 1445-1455.

Jardin, F., O. Dubourg and J. P. Bourdarias (1997). "Echocardiographic pattern of acute cor pulmonale." Chest 111(1): 209-217.

Jasiewicz, M., M. Knapp, E. Waszkiewicz, K. Ptaszynska-Kopczynska, A. Szpakowicz, B. Sobkowicz, W. J. Musial and K. A. Kaminski (2015). "Enhanced IL-6 trans-signaling in pulmonary arterial hypertension and its potential role in disease-related systemic damage." Cytokine 76(2): 187-192.

Jerkic, M., C. Masterson, L. Ormesher, S. Gagnon, S. Goyal, R. Rabani, G. Otulakowski, H. Zhang, B. P. Kavanagh and J. G. Laffey (2019). "Overexpression of IL-10 Enhances the Efficacy of Human Umbilical-Cord-Derived Mesenchymal Stromal Cells in E. coli Pneumosepsis." J Clin Med 8(6): 847.

Jiang, C. M., J. Liu, J. Y. Zhao, L. Xiao, S. An, Y. C. Gou, H. X. Quan, Q. Cheng, Y. L. Zhang, W. He, Y. T. Wang, W. J. Yu, Y. F. Huang, Y. T. Yi, Y. Chen and J. Wang (2015). "Effects of hypoxia on the immunomodulatory properties of human gingiva-derived mesenchymal stem cells." J Dent Res 94(1): 69-77.

Jiang, D., D. Li, L. Cao, L. Wang, S. Zhu, T. Xu, C. Wang and D. Pan (2014). "Positive feedback regulation of proliferation in vascular smooth muscle cells stimulated by lipopolysaccharide is mediated through the TLR 4/Rac1/Akt pathway." PLoS One 9(3): e92398.

Jiang, H. N., B. Zeng, G. L. Chen, B. Lai, S. H. Lu and J. M. Qu (2016). "Lipopolysaccharide potentiates endothelin-1-induced proliferation of pulmonary arterial smooth muscle cells by upregulating TRPC channels." Biomed Pharmacother 82: 20-27.

Johannigman, J. A., K. Davis, Jr., R. S. Campbell, F. Luchette, J. M. Hurst and R. D. Branson (1997). "Inhaled nitric oxide in acute respiratory distress syndrome." J Trauma 43(6): 904-909; discussion 909-910.

Johnson, K. J. and P. A. Ward (1974). "Acute immunologic pulmonary alveolitis." J Clin Invest 54(2): 349-357.

Kabir, K., J. P. Gelinas, M. Chen, D. Chen, D. Zhang, X. Luo, J. H. Yang, D. Carter and R. Rabinovici (2002). "Characterization of a murine model of endotoxin-induced acute lung injury." Shock 17(4): 300-303.

Kaku, S., C. D. Nguyen, N. N. Htet, D. Tutera, J. Barr, H. S. Paintal and W. G. Kuschner (2020). "Acute Respiratory Distress Syndrome: Etiology, Pathogenesis, and Summary on Management." J Intensive Care Med 35(8): 723-737.

Kalra, H., R. J. Simpson, H. Ji, E. Aikawa, P. Altevogt, P. Askenase, V. C. Bond, F. E. Borras, X. Breakefield, V. Budnik, E. Buzas, G. Camussi, A. Clayton, E. Cocucci, J. M. Falcon-Perez, S. Gabrielsson, Y. S. Gho, D. Gupta, H. C. Harsha, A. Hendrix, A. F. Hill, J. M. Inal, G. Jenster, E. M. Kramer-Albers, S. K. Lim, A. Llorente, J. Lotvall, A. Marcilla, L. Mincheva-Nilsson, I. Nazarenko, R. Nieuwland, E. N. Nolte-'t Hoen, A. Pandey, T. Patel, M. G. Piper, S. Pluchino, T. S. Prasad, L. Rajendran, G. Raposo, M. Record, G. E. Reid, F. Sanchez-Madrid, R. M. Schiffelers, P. Siljander, A. Stensballe, W. Stoorvogel, D. Taylor, C. Thery, H. Valadi, B. W. van Balkom, J. Vazquez, M. Vidal, M. H. Wauben, M. Yanez-Mo, M. Zoeller and S. Mathivanan (2012). "Vesiclepedia: a compendium for extracellular vesicles with continuous community annotation." PLoS Biol 10(12): e1001450.

Kapetanakis, T., Siempos, II, E. I. Metaxas, P. Kopterides, G. Agrogiannis, E. Patsouris, A. C. Lazaris, K. G. Stravodimos, C. Roussos and A. Armaganidis (2011). "Metabolic acidosis may be as protective as hypercapnic acidosis in an ex-vivo model of severe ventilator-induced lung injury: a pilot study." BMC Anesthesiol 11: 8.

Katira, B. H., R. E. Giesinger, D. Engelberts, D. Zabini, A. Kornecki, G. Otulakowski, T. Yoshida, W. M. Kuebler, P. J. McNamara, K. A. Connelly and B. P. Kavanagh (2017). "Adverse Heart-Lung Interactions in Ventilator-induced Lung Injury." Am J Respir Crit Care Med 196(11): 1411-1421.

Katzenstein, A. L., C. M. Bloor and A. A. Leibow (1976). "Diffuse alveolar damage--the role of oxygen, shock, and related factors. A review." Am J Pathol 85(1): 209-228.

Kawano, T., S. Mori, M. Cybulsky, R. Burger, A. Ballin, E. Cutz and A. C. Bryan (1987). "Effect of granulocyte depletion in a ventilated surfactant-depleted lung." J Appl Physiol (1985) 62(1): 27-33.

Kaye, A. D., E. M. Cornett, K. C. Brondeel, Z. I. Lerner, H. E. Knight, A. Erwin, K. Charipova, K. L. Gress, I. Urits, R. D. Urman, C. J. Fox and C. G. Kevil (2021). "Biology of COVID-19 and related viruses: Epidemiology, signs, symptoms, diagnosis, and treatment." Best Pract Res Clin Anaesthesiol 35(3): 269-292.

Keerthikumar, S., D. Chisanga, D. Ariyaratne, H. Al Saffar, S. Anand, K. Zhao, M. Samuel, M. Pathan, M. Jois, N. Chilamkurti, L. Gangoda and S. Mathivanan (2016). "ExoCarta: A Web-Based Compendium of Exosomal Cargo." J Mol Biol 428(4): 688-692.

Kelly, N. M., L. Young and A. S. Cross (1991). "Differential induction of tumor necrosis factor by bacteria expressing rough and smooth lipopolysaccharide phenotypes." Infect Immun 59(12): 4491-4496.

Kemming, G. I., M. Flondor, A. Hanser, S. Pallivathukal, M. Holtmannspotter, F. F. Kneisel, D. A. Reuter, H. Kisch-Wedel and B. Zwissler (2005). "Effects of perfluorohexan vapor on gas exchange, respiratory mechanics, and lung histology in pigs with lung injury after endotoxin infusion." Anesthesiology 103(3): 585-594.

Kesecioglu, J., R. Beale, T. E. Stewart, G. P. Findlay, J. J. Rouby, L. Holzapfel, P. Bruins, E. J. Steenken, O. K. Jeppesen and B. Lachmann (2009). "Exogenous natural surfactant for treatment of acute lung injury and the acute respiratory distress syndrome." Am J Respir Crit Care Med 180(10): 989-994.

Khalyfa, A., C. Zhang, A. A. Khalyfa, G. E. Foster, A. E. Beaudin, J. Andrade, P. J. Hanly, M. J. Poulin and D. Gozal (2016). "Effect on Intermittent Hypoxia on Plasma Exosomal Micro RNA Signature and Endothelial Function in Healthy Adults." Sleep 39(12): 2077-2090.

Khatri, M., L. A. Richardson and T. Meulia (2018). "Mesenchymal stem cell-derived extracellular vesicles attenuate influenza virus-induced acute lung injury in a pig model." Stem Cell Res Ther 9(1): 17.

Kilkenny, C., W. J. Browne, I. C. Cuthill, M. Emerson and D. G. Altman (2010). "Improving bioscience research reporting: the ARRIVE guidelines for reporting animal research." PLoS Biol 8(6): e1000412.

Kim, H. J., M. Y. Kim, J. S. Hwang, H. J. Kim, J. H. Lee, K. C. Chang, J. H. Kim, C. W. Han, J. H. Kim and H. G. Seo (2010). "PPARdelta inhibits IL-1beta-stimulated proliferation and migration of vascular smooth muscle cells via up-regulation of IL-1Ra." Cell Mol Life Sci 67(12): 2119-2130.

Kim, W. Y. and S. B. Hong (2016). "Sepsis and Acute Respiratory Distress Syndrome: Recent Update." Tuberc Respir Dis (Seoul) 79(2): 53-57.

Kim, Y. S., M. Y. Noh, K. A. Cho, H. Kim, M. S. Kwon, K. S. Kim, J. Kim, S. H. Koh and S. H. Kim (2015). "Hypoxia/Reoxygenation-Preconditioned Human Bone Marrow-Derived Mesenchymal Stromal Cells Rescue Ischemic Rat Cortical Neurons by Enhancing Trophic Factor Release." Mol Neurobiol 52(1): 792-803.

Klein, C. L., T. S. Hoke, W. F. Fang, C. J. Altmann, I. S. Douglas and S. Faubel (2008). "Interleukin-6 mediates lung injury following ischemic acute kidney injury or bilateral nephrectomy." Kidney Int 74(7): 901-909.

Klinger, J., M. Pereira, M. Del Tatto, M. Dooner, S. Wen, P. Quesenberry and O. D. Liang (2021). "Effect of dose, dosing intervals, and hypoxic stress on the reversal of pulmonary hypertension by mesenchymal stem cell extracellular vesicles." Pulmonary Circulation 11(4).

Klinger, J. R., M. Pereira, M. Del Tatto, A. S. Brodsky, K. Q. Wu, M. S. Dooner, T. Borgovan, S. Wen, L. R. Goldberg, J. M. Aliotta, C. E. Ventetuolo, P. J. Quesenberry and O. D. Liang (2020). "Mesenchymal Stem Cell Extracellular Vesicles Reverse Sugen/Hypoxia Pulmonary Hypertension in Rats." Am J Respir Cell Mol Biol 62(5): 577-587.

Knudsen, L. and M. Ochs (2018). "The micromechanics of lung alveoli: structure and function of surfactant and tissue components." Histochem Cell Biol 150(6): 661-676.

Kolaczkowska, E. and P. Kubes (2013). "Neutrophil recruitment and function in health and inflammation." Nat Rev Immunol 13(3): 159-175.

Konala, V. B., M. K. Mamidi, R. Bhonde, A. K. Das, R. Pochampally and R. Pal (2016). "The current landscape of the mesenchymal stromal cell secretome: A new paradigm for cell-free regeneration." Cytotherapy 18(1): 13-24.

Kotwica, A., H. Knights, N. Mayor, E. Russell-Jones, T. Dassios and D. Russell-Jones (2021). "Intrapulmonary shunt measured by bedside pulse oximetry predicts worse outcomes in severe COVID-19." Eur Respir J 57(4).

Kourembanas, S. (2015). "Exosomes: vehicles of intercellular signaling, biomarkers, and vectors of cell therapy." Annu Rev Physiol 77: 13-27.

Koval, M., C. Ward, M. K. Findley, S. Roser-Page, M. N. Helms and J. Roman (2010). "Extracellular matrix influences alveolar epithelial claudin expression and barrier function." Am J Respir Cell Mol Biol 42(2): 172-180.

Kubera, M., M. Maes, G. Kenis, Y. K. Kim and W. Lason (2005). "Effects of serotonin and serotonergic agonists and antagonists on the production of tumor necrosis factor alpha and interleukin-6." Psychiatry Res 134(3): 251-258.

Kudoh, I., J. P. Wiener-Kronish, S. Hashimoto, J. F. Pittet and D. Frank (1994). "Exoproduct secretions of Pseudomonas aeruginosa strains influence severity of alveolar epithelial injury." Am J Physiol 267(5 Pt 1): L551-556.

Kuebler, W. M. (2006). "Selectins revisited: the emerging role of platelets in inflammatory lung disease." J Clin Invest 116(12): 3106-3108.

Kuida, H., L. B. Hinshaw, R. P. Gilbert and M. B. Visscher (1958). "Effect of gram-negative endotoxin on pulmonary circulation." Am J Physiol 192(2): 335-344.

Lachmann, B. (1992). "Open up the lung and keep the lung open." Intensive Care Med 18(6): 319-321.

Laffey, J. G., M. Tanaka, D. Engelberts, X. Luo, S. Yuan, A. K. Tanswell, M. Post, T. Lindsay and B. P. Kavanagh (2000). "Therapeutic hypercapnia reduces pulmonary and systemic injury following in vivo lung reperfusion." Am J Respir Crit Care Med 162(6): 2287-2294.

Lai, P. S. and B. T. Thompson (2013). "Why activated protein C was not successful in severe sepsis and septic shock: are we still tilting at windmills?" Curr Infect Dis Rep 15(5): 407-412.

Lai, T. S., Z. H. Wang and S. X. Cai (2015). "Mesenchymal stem cell attenuates neutrophil-predominant inflammation and acute lung injury in an in vivo rat model of ventilator-induced lung injury." Chin Med J (Engl) 128(3): 361-367.

Lamb, N. J., J. M. Gutteridge, C. Baker, T. W. Evans and G. J. Quinlan (1999). "Oxidative damage to proteins of bronchoalveolar lavage fluid in patients with acute respiratory distress syndrome: evidence for neutrophil-mediated hydroxylation, nitration, and chlorination." Crit Care Med 27(9): 1738-1744.

Lamontagne, F., R. Brower and M. Meade (2013). "Corticosteroid therapy in acute respiratory distress syndrome." CMAJ 185(3): 216-221.

Lan, Y., W. Liu and Y. Zhou (2021). "Right Ventricular Damage in COVID-19: Association Between Myocardial Injury and COVID-19." Front Cardiovasc Med 8: 606318.

Lan, Y. W., K. B. Choo, C. M. Chen, T. H. Hung, Y. B. Chen, C. H. Hsieh, H. P. Kuo and K. Y. Chong (2015). "Hypoxia-preconditioned mesenchymal stem cells attenuate bleomycin-induced pulmonary fibrosis." Stem Cell Res Ther 6: 97.

Lang, M., A. Som, D. Carey, N. Reid, D. P. Mendoza, E. J. Flores, M. D. Li, J. O. Shepard and B. P. Little (2020). "Pulmonary Vascular Manifestations of COVID-19 Pneumonia." Radiol Cardiothorac Imaging 2(3): e200277.

Lanyu, Z. and H. Feilong (2019). "Emerging role of extracellular vesicles in lung injury and inflammation." Biomed Pharmacother 113: 108748.

Larsen, G. L. and P. M. Henson (1983). "Mediators of inflammation." Annu Rev Immunol 1: 335-359.

Lee, C., S. A. Mitsialis, M. Aslam, S. H. Vitali, E. Vergadi, G. Konstantinou, K. Sdrimas, A. Fernandez-Gonzalez and S. Kourembanas (2012). "Exosomes mediate the cytoprotective action of mesenchymal stromal cells on hypoxia-induced pulmonary hypertension." Circulation 126(22): 2601-2611.

Lee, J. H., J. Park and J.-W. Lee (2019). "Therapeutic use of mesenchymal stem cell–derived extracellular vesicles in acute lung injury." Transfusion 59(S1): 876-883.

Lee, J. W., X. Fang, N. Gupta, V. Serikov and M. A. Matthay (2009). "Allogeneic human mesenchymal stem cells for treatment of E. coli endotoxin-induced acute lung injury in the ex vivo perfused human lung." Proc Natl Acad Sci U S A 106(38): 16357-16362.

Lee, S. and K. T. Min (2018). "The Interface Between ER and Mitochondria: Molecular Compositions and Functions." Mol Cells 41(12): 1000-1007.

Lee, S. P., S. W. Youn and H. S. Kim (2007). "Integrin-Linked Kinase: It's Role in the Vascular System." Int J Biomed Sci 3(1): 1-8.

Leroux, L., B. Descamps, N. F. Tojais, B. Seguy, P. Oses, C. Moreau, D. Daret, Z. Ivanovic, J. M. Boiron, J. M. Lamaziere, P. Dufourcq, T. Couffinhal and C. Duplaa (2010). "Hypoxia preconditioned mesenchymal stem cells improve vascular and skeletal muscle fiber regeneration after ischemia through a Wnt4-dependent pathway." Mol Ther 18(8): 1545-1552.

Levi, M., H. ten Cate and T. van der Poll (2002). "Endothelium: interface between coagulation and inflammation." Crit Care Med 30(5 Suppl): S220-224.

Li, C., J. Pan, L. Ye, H. Xu, B. Wang, H. Xu, L. Xu, T. Hou and D. Zhang (2019). "Autophagy regulates the therapeutic potential of adipose-derived stem cells in LPS-induced pulmonary microvascular barrier damage." Cell Death Dis 10(11): 804.

Li, D. K., J. Y. Mao, Y. Long, D. W. Liu and X. T. Wang (2020). "Pulmonary hypertension with adult respiratory distress syndrome: prevalence, clinical impact, and association with central venous pressure." Pulm Circ 10(3): 2045894020933087.

Li, L., S. Jin and Y. Zhang (2015). "Ischemic preconditioning potentiates the protective effect of mesenchymal stem cells on endotoxin-induced acute lung injury in mice through secretion of exosome." Int J Clin Exp Med 8(3): 3825-3832.

Li, P., Y. Zhou, A. J. Goodwin, J. A. Cook, P. V. Halushka, X. K. Zhang, C. L. Wilson, L. M. Schnapp, B. Zingarelli and H. Fan (2018). "Fli-1 Governs Pericyte Dysfunction in a Murine Model of Sepsis." J Infect Dis 218(12): 1995-2005.

Li, Q., X. Guan, P. Wu, X. Wang, L. Zhou, Y. Tong, R. Ren, K. S. M. Leung, E. H. Y. Lau, J. Y. Wong, X. Xing, N. Xiang, Y. Wu, C. Li, Q. Chen, D. Li, T. Liu, J. Zhao, M. Liu, W. Tu, C. Chen, L. Jin, R. Yang, Q. Wang, S. Zhou, R. Wang, H. Liu, Y. Luo, Y. Liu, G. Shao, H. Li, Z. Tao, Y. Yang, Z. Deng, B. Liu, Z. Ma, Y. Zhang, G. Shi, T. T. Y. Lam, J. T. Wu, G. F. Gao, B. J. Cowling, B. Yang, G. M. Leung and Z. Feng (2020). "Early Transmission Dynamics in Wuhan, China, of Novel Coronavirus-Infected Pneumonia." N Engl J Med 382(13): 1199-1207.

Li, Q. C., Y. Liang and Z. B. Su (2019). "Prophylactic treatment with MSC-derived exosomes attenuates traumatic acute lung injury in rats." Am J Physiol Lung Cell Mol Physiol 316(6): L1107-L1117.

Li, Y., J. Xu, W. Shi, C. Chen, Y. Shao, L. Zhu, W. Lu and X. Han (2016). "Mesenchymal stromal cell treatment prevents H9N2 avian influenza virus-induced acute lung injury in mice." Stem Cell Res Ther 7(1): 159.

Lim, J., S. Jeon, H. Y. Shin, M. J. Kim, Y. M. Seong, W. J. Lee, K. W. Choe, Y. M. Kang, B. Lee and S. J. Park (2020). "Case of the Index Patient Who Caused Tertiary Transmission of COVID-19 Infection in Korea: the Application of Lopinavir/Ritonavir for the Treatment of COVID-19 Infected Pneumonia Monitored by Quantitative RT-PCR." J Korean Med Sci 35(6): e79.

Lin, F. Y., Y. H. Chen, J. S. Tasi, J. W. Chen, T. L. Yang, H. J. Wang, C. Y. Li, Y. L. Chen and S. J. Lin (2006). "Endotoxin induces toll-like receptor 4 expression in vascular smooth muscle cells via NADPH oxidase activation and mitogen-activated protein kinase signaling pathways." Arterioscler Thromb Vasc Biol 26(12): 2630-2637.

Lin, W. C., C. F. Lin, C. L. Chen, C. W. Chen and Y. S. Lin (2011). "Inhibition of neutrophil apoptosis via sphingolipid signaling in acute lung injury." J Pharmacol Exp Ther 339(1): 45-53.

Liu, J., H. Hao, L. Xia, D. Ti, H. Huang, L. Dong, C. Tong, Q. Hou, Y. Zhao, H. Liu, X. Fu and W. Han (2015). "Hypoxia pretreatment of bone marrow mesenchymal stem cells facilitates angiogenesis by improving the function of endothelial cells in diabetic rats with lower ischemia." PLoS One 10(5): e0126715.

Liu, K. D., J. Levitt, H. Zhuo, R. H. Kallet, S. Brady, J. Steingrub, M. Tidswell, M. D. Siegel, G. Soto, M. W. Peterson, M. S. Chesnutt, C. Phillips, A. Weinacker, B. T. Thompson, M. D. Eisner and M. A. Matthay (2008). "Randomized clinical trial of activated protein C for the treatment of acute lung injury." Am J Respir Crit Care Med 178(6): 618-623.

Liu, S. F., D. E. Crawley, P. J. Barnes and T. W. Evans (1991). "Endothelium-derived relaxing factor inhibits hypoxic pulmonary vasoconstriction in rats." Am Rev Respir Dis 143(1): 32-37.

Liu, Z., J. Liu, M. Xiao, J. Wang, F. Yao, W. Zeng, L. Yu, Y. Guan, W. Wei, Z. Peng, K. Zhu, J. Wang, Z. Yang, J. Zhong and J. Chen (2018). "Mesenchymal stem cell-derived microvesicles alleviate pulmonary arterial hypertension by regulating renin-angiotensin system." J Am Soc Hypertens 12(6): 470-478.

Lo, C. J., M. Fu and H. G. Cryer (1998). "Interleukin 10 inhibits alveolar macrophage production of inflammatory mediators involved in adult respiratory distress syndrome." J Surg Res 79(2): 179-184.

Luca, R., H. R. Lijnen, A. F. Suffredini, M. S. Pepper, K. P. Steinberg, T. R. Martin and J. Pugin (2002). "Increased angiostatin levels in bronchoalveolar lavage fluids from ARDS patients and from human volunteers after lung instillation of endotoxin." Thromb Haemost 87(6): 966-971.

Lutz, C., D. Carney, C. Finck, A. Picone, L. A. Gatto, A. Paskanik, E. Langenback and G. Nieman (1998). "Aerosolized surfactant improves pulmonary function in endotoxin-induced lung injury." Am J Respir Crit Care Med 158(3): 840-845.

Maas, S. L. N., X. O. Breakefield and A. M. Weaver (2017). "Extracellular Vesicles: Unique Intercellular Delivery Vehicles." Trends Cell Biol 27(3): 172-188.

MacCallum, N. S. and T. W. Evans (2005). "Epidemiology of acute lung injury." Curr Opin Crit Care 11(1): 43-49.

MacLean, M. R. and Y. Dempsie (2009). "Serotonin and pulmonary hypertension--from bench to bedside?" Curr Opin Pharmacol 9(3): 281-286.

Mahida, R. Y., S. Matsumoto and M. A. Matthay (2020). "Extracellular Vesicles: A New Frontier for Research in Acute Respiratory Distress Syndrome." Am J Respir Cell Mol Biol 63(1): 15-24.

Maina, J. N. and J. B. West (2005). "Thin and strong! The bioengineering dilemma in the structural and functional design of the blood-gas barrier." Physiol Rev 85(3): 811-844.

Mallat, Z. and A. Tedgui (2000). "Apoptosis in the vasculature: mechanisms and functional importance." Br J Pharmacol 130(5): 947-962.

Mammoto, A., T. Mammoto, M. Kanapathipillai, C. Wing Yung, E. Jiang, A. Jiang, K. Lofgren, E. P. Gee and D. E. Ingber (2013). "Control of lung

vascular permeability and endotoxin-induced pulmonary oedema by changes in extracellular matrix mechanics." Nat Commun 4: 1759.

Mandegar, M., Y. C. Fung, W. Huang, C. V. Remillard, L. J. Rubin and J. X. Yuan (2004). "Cellular and molecular mechanisms of pulmonary vascular remodeling: role in the development of pulmonary hypertension." Microvasc Res 68(2): 75-103.

Mangalmurti, N. S., J. P. Reilly, D. B. Cines, N. J. Meyer, C. A. Hunter and A. E. Vaughan (2020). "COVID-19-associated Acute Respiratory Distress Syndrome Clarified: A Vascular Endotype?" Am J Respir Crit Care Med 202(5): 750-753.

Maniatis, N. A. and S. E. Orfanos (2008). "The endothelium in acute lung injury/acute respiratory distress syndrome." Curr Opin Crit Care 14(1): 22-30.

Manzano, F., E. Fernandez-Mondejar, M. Colmenero, M. E. Poyatos, R. Rivera, J. Machado, I. Catalan and A. Artigas (2008). "Positive-end expiratory pressure reduces incidence of ventilator-associated pneumonia in nonhypoxemic patients." Crit Care Med 36(8): 2225-2231.

Mardpour, S., A. A. Hamidieh, S. Taleahmad, F. Sharifzad, A. Taghikhani and H. Baharvand (2019). "Interaction between mesenchymal stromal cell-derived extracellular vesicles and immune cells by distinct protein content." J Cell Physiol 234(6): 8249-8258.

Mariathasan, S. and D. M. Monack (2007). "Inflammasome adaptors and sensors: intracellular regulators of infection and inflammation." Nat Rev Immunol 7(1): 31-40.

Marik, P., S. Pastores and D. Annane (2006). "Corticosteroids in ARDS." N Engl J Med 355(3): 316-317; author reply 318-319.

Marini, J. J., P. R. M. Rocco and L. Gattinoni (2020). "Static and Dynamic Contributors to Ventilator-induced Lung Injury in Clinical Practice. Pressure, Energy, and Power." Am J Respir Crit Care Med 201(7): 767-774.

Marshall, B. E., C. W. Hanson, F. Frasch and C. Marshall (1994). "Role of hypoxic pulmonary vasoconstriction in pulmonary gas exchange and blood flow distribution. 2. Pathophysiology." Intensive Care Med 20(5): 379-389.

Martin, T. R., J. C. Mathison, P. S. Tobias, D. J. Leturcq, A. M. Moriarty, R. J. Maunder and R. J. Ulevitch (1992). "Lipopolysaccharide binding protein enhances the responsiveness of alveolar macrophages to bacterial lipopolysaccharide. Implications for cytokine production in normal and injured lungs." J Clin Invest 90(6): 2209-2219.

Martinez-Gonzalez, I., O. Roca, J. R. Masclans, R. Moreno, M. T. Salcedo, V. Baekelandt, M. J. Cruz, J. Rello and J. M. Aran (2013). "Human mesenchymal stem cells overexpressing the IL-33 antagonist soluble IL-1 receptor-like-1 attenuate endotoxin-induced acute lung injury." Am J Respir Cell Mol Biol 49(4): 552-562.

Mason, N. A., D. R. Springall, M. Burke, J. Pollock, G. Mikhail, M. H. Yacoub and J. M. Polak (1998). "High expression of endothelial nitric oxide synthase in plexiform lesions of pulmonary hypertension." J Pathol 185(3): 313-318.

Mastri, M., Z. Shah, T. McLaughlin, C. J. Greene, L. Baum, G. Suzuki and T. Lee (2012). "Activation of Toll-like receptor 3 amplifies mesenchymal stem cell trophic factors and enhances therapeutic potency." Am J Physiol Cell Physiol 303(10): C1021-1033.

Mastrolia, I., E. M. Foppiani, A. Murgia, O. Candini, A. V. Samarelli, G. Grisendi, E. Veronesi, E. M. Horwitz and M. Dominici (2019). "Challenges in Clinical Development of Mesenchymal Stromal/Stem Cells: Concise Review." Stem Cells Transl Med 8(11): 1135-1148.

Matthay, M. A. (2015). "Therapeutic potential of mesenchymal stromal cells for acute respiratory distress syndrome." Ann Am Thorac Soc 12 Suppl 1: S54-57.

Matthay, M. A., J. M. Aldrich and J. E. Gotts (2020). "Treatment for severe acute respiratory distress syndrome from COVID-19." Lancet Respir Med 8(5): 433-434.

Matthay, M. A., Y. M. Arabi, E. R. Siegel, L. B. Ware, L. D. J. Bos, P. Sinha, J. R. Beitler, K. D. Wick, M. A. Q. Curley, J. M. Constantin, J. E. Levitt and C. S. Calfee (2020). "Phenotypes and personalized medicine in the acute respiratory distress syndrome." Intensive Care Med 46(12): 2136-2152.

Matthay, M. A. and L. B. Ware (2004). "Plasma protein C levels in patients with acute lung injury: prognostic significance." Crit Care Med 32(5 Suppl): S229-232.

Matthay, M. A., R. L. Zemans, G. A. Zimmerman, Y. M. Arabi, J. R. Beitler, A. Mercat, M. Herridge, A. G. Randolph and C. S. Calfee (2019). "Acute respiratory distress syndrome." Nat Rev Dis Primers 5(1): 18.

Matute-Bello, G., C. W. Frevert and T. R. Martin (2008). "Animal models of acute lung injury." Am J Physiol Lung Cell Mol Physiol 295(3): L379-399.

Maybauer, M. O., D. M. Maybauer and D. N. Herndon (2006). "Incidence and outcomes of acute lung injury." N Engl J Med 354(4): 416-417; author reply 416-417.

McAuley, D. F., L. M. Cross, U. Hamid, E. Gardner, J. S. Elborn, K. M. Cullen, A. Dushianthan, M. P. Grocott, M. A. Matthay and C. M. O'Kane (2017). "Keratinocyte growth factor for the treatment of the acute respiratory distress syndrome (KARE): a randomised, double-blind, placebo-controlled phase 2 trial." Lancet Respir Med 5(6): 484-491.

McAuley, D. F., J. G. Laffey, C. M. O'Kane, G. D. Perkins, B. Mullan, T. J. Trinder, P. Johnston, P. A. Hopkins, A. J. Johnston, C. McDowell, C. McNally, H.-. Investigators and G. Irish Critical Care Trials (2014). "Simvastatin in the acute respiratory distress syndrome." N Engl J Med 371(18): 1695-1703.

McClintock, D., H. Zhuo, N. Wickersham, M. A. Matthay and L. B. Ware (2008). "Biomarkers of inflammation, coagulation and fibrinolysis predict mortality in acute lung injury." Crit Care 12(2): R41.

McVey, M. J., M. Maishan, K. E. C. Blokland, N. Bartlett and W. M. Kuebler (2019). "Extracellular vesicles in lung health, disease, and therapy." Am J Physiol Lung Cell Mol Physiol 316(6): L977-L989.

Meade, M. O., D. J. Cook, G. H. Guyatt, A. S. Slutsky, Y. M. Arabi, D. J. Cooper, A. R. Davies, L. E. Hand, Q. Zhou, L. Thabane, P. Austin, S. Lapinsky, A. Baxter, J. Russell, Y. Skrobik, J. J. Ronco, T. E. Stewart and

I. Lung Open Ventilation Study (2008). "Ventilation strategy using low tidal volumes, recruitment maneuvers, and high positive end-expiratory pressure for acute lung injury and acute respiratory distress syndrome: a randomized controlled trial." JAMA 299(6): 637-645.

Meduri, G. U., L. Bridges, M. C. Shih, P. E. Marik, R. A. C. Siemieniuk and M. Kocak (2016). "Prolonged glucocorticoid treatment is associated with improved ARDS outcomes: analysis of individual patients' data from four randomized trials and trial-level meta-analysis of the updated literature." Intensive Care Med 42(5): 829-840.

Meduri, G. U., P. Carratu and A. X. Freire (2003). "Evidence of biological efficacy for prolonged glucocorticoid treatment in patients with unresolving ARDS." Eur Respir J Suppl 42: 57s-64s.

Meduri, G. U., E. Golden, A. X. Freire, E. Taylor, M. Zaman, S. J. Carson, M. Gibson and R. Umberger (2007). "Methylprednisolone infusion in early severe ARDS: results of a randomized controlled trial." Chest 131(4): 954-963.

Meduri, G. U., S. Headley, G. Kohler, F. Stentz, E. Tolley, R. Umberger and K. Leeper (1995). "Persistent elevation of inflammatory cytokines predicts a poor outcome in ARDS. Plasma IL-1 beta and IL-6 levels are consistent and efficient predictors of outcome over time." Chest 107(4): 1062-1073.

Meduri, G. U., P. E. Marik, G. P. Chrousos, S. M. Pastores, W. Arlt, A. Beishuizen, F. Bokhari, G. Zaloga and D. Annane (2008). "Steroid treatment in ARDS: a critical appraisal of the ARDS network trial and the recent literature." Intensive Care Med 34(1): 61-69.

Mei, S. H., S. D. McCarter, Y. Deng, C. H. Parker, W. C. Liles and D. J. Stewart (2007). "Prevention of LPS-induced acute lung injury in mice by mesenchymal stem cells overexpressing angiopoietin 1." PLoS Med 4(9): e269.

Mekontso Dessap, A., F. Boissier, C. Charron, E. Begot, X. Repesse, A. Legras, C. Brun-Buisson, P. Vignon and A. Vieillard-Baron (2016). "Acute cor pulmonale during protective ventilation for acute respiratory distress syndrome: prevalence, predictors, and clinical impact." Intensive Care Med 42(5): 862-870.

Mekontso Dessap, A., C. Charron, J. Devaquet, J. Aboab, F. Jardin, L. Brochard and A. Vieillard-Baron (2009). "Impact of acute hypercapnia and augmented positive end-expiratory pressure on right ventricle function in severe acute respiratory distress syndrome." Intensive Care Med 35(11): 1850-1858.

Menendez, C., L. Martinez-Caro, L. Moreno, N. Nin, J. Moral-Sanz, D. Morales, A. Cogolludo, A. Esteban, J. A. Lorente and F. Perez-Vizcaino (2013). "Pulmonary vascular dysfunction induced by high tidal volume mechanical ventilation." Crit Care Med 41(8): e149-155.

Menter, T., J. D. Haslbauer, R. Nienhold, S. Savic, H. Hopfer, N. Deigendesch, S. Frank, D. Turek, N. Willi, H. Pargger, S. Bassetti, J. D. Leuppi, G. Cathomas, M. Tolnay, K. D. Mertz and A. Tzankov (2020). "Postmortem examination of COVID-19 patients reveals diffuse alveolar damage with severe capillary congestion and variegated findings in lungs and other organs suggesting vascular dysfunction." Histopathology 77(2): 198-209.

Michael, J. R., R. G. Barton, J. R. Saffle, M. Mone, B. A. Markewitz, K. Hillier, M. R. Elstad, E. J. Campbell, B. E. Troyer, R. E. Whatley, T. G. Liou, W. M. Samuelson, H. J. Carveth, D. M. Hinson, S. E. Morris, B. L. Davis and R. W. Day (1998). "Inhaled nitric oxide versus conventional therapy: effect on oxygenation in ARDS." Am J Respir Crit Care Med 157(5 Pt 1): 1372-1380.

Millar, F. R., C. Summers, M. J. Griffiths, M. R. Toshner and A. G. Proudfoot (2016). "The pulmonary endothelium in acute respiratory distress syndrome: insights and therapeutic opportunities." Thorax 71(5): 462-473.

Miller, E. J., A. B. Cohen, S. Nagao, D. Griffith, R. J. Maunder, T. R. Martin, J. P. Weiner-Kronish, M. Sticherling, E. Christophers and M. A. Matthay (1992). "Elevated levels of NAP-1/interleukin-8 are present in the airspaces of patients with the adult respiratory distress syndrome and are associated with increased mortality." Am Rev Respir Dis 146(2): 427-432.

Mitchell, J. A., F. Ali, L. Bailey, L. Moreno and L. S. Harrington (2008). "Role of nitric oxide and prostacyclin as vasoactive hormones released by the endothelium." Exp Physiol 93(1): 141-147.

Mittermaier, M., P. Pickerodt, F. Kurth, L. B. de Jarcy, A. Uhrig, C. Garcia, F. Machleidt, P. Pergantis, S. Weber, Y. Li, A. Breitbart, F. Bremer, P. Knape, M. Dewey, F. Doellinger, S. Weber-Carstens, A. S. Slutsky, W. M. Kuebler, N. Suttorp and H. Muller-Redetzky (2020). "Evaluation of PEEP and prone positioning in early COVID-19 ARDS." EClinicalMedicine 28: 100579.

Miyata, M., M. Ito, T. Sasajima, H. Ohira and R. Kasukawa (2001). "Effect of a serotonin receptor antagonist on interleukin-6-induced pulmonary hypertension in rats." Chest 119(2): 554-561.

Modelska, K., J. F. Pittet, H. G. Folkesson, V. Courtney Broaddus and M. A. Matthay (1999). "Acid-induced lung injury. Protective effect of anti-interleukin-8 pretreatment on alveolar epithelial barrier function in rabbits." Am J Respir Crit Care Med 160(5 Pt 1): 1450-1456.

Mohammadipoor, A., B. Antebi, A. I. Batchinsky and L. C. Cancio (2018). "Therapeutic potential of products derived from mesenchymal stem/stromal cells in pulmonary disease." Respir Res 19(1): 218.

Moloney, E. D. and T. W. Evans (2003). "Pathophysiology and pharmacological treatment of pulmonary hypertension in acute respiratory distress syndrome." Eur Respir J 21(4): 720-727.

Mondejar-Parreno, G., M. Callejo, B. Barreira, D. Morales-Cano, S. Esquivel-Ruiz, L. Moreno, A. Cogolludo and F. Perez-Vizcaino (2019). "miR-1 is increased in pulmonary hypertension and downregulates Kv1.5 channels in rat pulmonary arteries." J Physiol 597(4): 1185-1197.

Monsel, A., Y. G. Zhu, S. Gennai, Q. Hao, S. Hu, J. J. Rouby, M. Rosenzwajg, M. A. Matthay and J. W. Lee (2015). "Therapeutic Effects of Human Mesenchymal Stem Cell-derived Microvesicles in Severe Pneumonia in Mice." Am J Respir Crit Care Med 192(3): 324-336.

Monsel, A., Y. G. Zhu, V. Gudapati, H. Lim and J. W. Lee (2016). "Mesenchymal stem cell derived secretome and extracellular vesicles for acute lung injury and other inflammatory lung diseases." Expert Opin Biol Ther 16(7): 859-871.

Moore, B. B. and C. M. Hogaboam (2008). "Murine models of pulmonary fibrosis." Am J Physiol Lung Cell Mol Physiol 294(2): L152-160.

Morales-Cano, D., M. Callejo, B. Barreira, G. Mondejar-Parreno, S. Esquivel-Ruiz, S. Ramos, M. A. Martin, A. Cogolludo, L. Moreno and F. Perez-Vizcaino (2019). "Elevated pulmonary arterial pressure in Zucker diabetic fatty rats." PLoS One 14(1): e0211281.

Morales-Cano, D., C. Menendez, E. Moreno, J. Moral-Sanz, B. Barreira, P. Galindo, R. Pandolfi, R. Jimenez, L. Moreno, A. Cogolludo, J. Duarte and F. Perez-Vizcaino (2014). "The flavonoid quercetin reverses pulmonary hypertension in rats." PLoS One 9(12): e114492.

Morales-Quinteros, L., M. Camprubi-Rimblas, J. Bringue, L. D. Bos, M. J. Schultz and A. Artigas (2019). "The role of hypercapnia in acute respiratory failure." Intensive Care Med Exp 7(Suppl 1): 39.

Morelli, A., L. Del Sorbo, A. Pesenti, V. M. Ranieri and E. Fan (2017). "Extracorporeal carbon dioxide removal (ECCO2R) in patients with acute respiratory failure." Intensive Care Med 43(4): 519-530.

Moreno, L., S. K. McMaster, T. Gatheral, L. K. Bailey, L. S. Harrington, N. Cartwright, P. C. Armstrong, T. D. Warner, M. Paul-Clark and J. A. Mitchell (2010). "Nucleotide oligomerization domain 1 is a dominant pathway for NOS2 induction in vascular smooth muscle cells: comparison with Toll-like receptor 4 responses in macrophages." Br J Pharmacol 160(8): 1997-2007.

Morrell, N. W., S. Adnot, S. L. Archer, J. Dupuis, P. Lloyd Jones, M. R. MacLean, I. F. McMurtry, K. R. Stenmark, P. A. Thistlethwaite, N. Weissmann, J. X. Yuan and E. K. Weir (2009). "Cellular and molecular basis of pulmonary arterial hypertension." J Am Coll Cardiol 54(1 Suppl): S20-S31.

Morris, K., M. Beghetti, A. Petros, I. Adatia and D. Bohn (2000). "Comparison of hyperventilation and inhaled nitric oxide for pulmonary hypertension after repair of congenital heart disease." Crit Care Med 28(8): 2974-2978.

Morrison, T. J., M. V. Jackson, E. K. Cunningham, A. Kissenpfennig, D. F. McAuley, C. M. O'Kane and A. D. Krasnodembskaya (2017). "Mesenchymal Stromal Cells Modulate Macrophages in Clinically Relevant Lung Injury Models by Extracellular Vesicle Mitochondrial Transfer." Am J Respir Crit Care Med 196(10): 1275-1286.

Murray, P. T., M. E. Wylam and J. G. Umans (2000). "Nitric oxide and septic vascular dysfunction." Anesth Analg 90(1): 89-101.

Myers, P. R., J. L. Parker, M. A. Tanner and H. R. Adams (1994). "Effects of cytokines tumor necrosis factor alpha and interleukin 1 beta on endotoxin-mediated inhibition of endothelium-derived relaxing factor bioactivity and nitric oxide production in vascular endothelium." Shock 1(1): 73-78.

Nabeh, O. A., L. M. Matter, M. A. Khattab and M. Esraa (2021). ""The possible implication of endothelin in the pathology of COVID-19-induced pulmonary hypertension"." Pulm Pharmacol Ther 71: 102082.

Namendys-Silva, S. A., L. E. Santos-Martinez, T. Pulido, E. Rivero-Sigarroa, J. A. Baltazar-Torres, G. Dominguez-Cherit and J. Sandoval (2014). "Pulmonary hypertension due to acute respiratory distress syndrome." Braz J Med Biol Res 47(10): 904-910.

National Heart, L., A. C. T. N. Blood Institute, J. D. Truwit, G. R. Bernard, J. Steingrub, M. A. Matthay, K. D. Liu, T. E. Albertson, R. G. Brower, C. Shanholtz, P. Rock, I. S. Douglas, B. P. deBoisblanc, C. L. Hough, R. D. Hite and B. T. Thompson (2014). "Rosuvastatin for sepsis-associated acute respiratory distress syndrome." N Engl J Med 370(23): 2191-2200.

National Heart, L., N. Blood Institute Acute Respiratory Distress Syndrome Clinical Trials, M. A. Matthay, R. G. Brower, S. Carson, I. S. Douglas, M. Eisner, D. Hite, S. Holets, R. H. Kallet, K. D. Liu, N. MacIntyre, M. Moss, D. Schoenfeld, J. Steingrub and B. T. Thompson (2011). "Randomized, placebo-controlled clinical trial of an aerosolized beta(2)-agonist for treatment of acute lung injury." Am J Respir Crit Care Med 184(5): 561-568.

National Heart, L., N. Blood Institute Acute Respiratory Distress Syndrome Clinical Trials, H. P. Wiedemann, A. P. Wheeler, G. R. Bernard, B. T. Thompson, D. Hayden, B. deBoisblanc, A. F. Connors, Jr., R. D. Hite and A. L. Harabin (2006). "Comparison of two fluid-management strategies in acute lung injury." N Engl J Med 354(24): 2564-2575.

Needham, D. M., E. Colantuoni, P. A. Mendez-Tellez, V. D. Dinglas, J. E. Sevransky, C. R. Dennison Himmelfarb, S. V. Desai, C. Shanholtz, R. G. Brower and P. J. Pronovost (2012). "Lung protective mechanical ventilation and two year survival in patients with acute lung injury: prospective cohort study." BMJ 344: e2124.

Nemeth, K., A. Leelahavanichkul, P. S. Yuen, B. Mayer, A. Parmelee, K. Doi, P. G. Robey, K. Leelahavanichkul, B. H. Koller, J. M. Brown, X. Hu, I. Jelinek, R. A. Star and E. Mezey (2009). "Bone marrow stromal cells attenuate sepsis via prostaglandin E(2)-dependent reprogramming of host macrophages to increase their interleukin-10 production." Nat Med 15(1): 42-49.

Newby, D., L. Marks and F. Lyall (2005). "Dissolved oxygen concentration in culture medium: assumptions and pitfalls." Placenta 26(4): 353-357.

Ni, Y. N., G. Chen, J. Sun, B. M. Liang and Z. A. Liang (2019). "The effect of corticosteroids on mortality of patients with influenza pneumonia: a systematic review and meta-analysis." Crit Care 23(1): 99.

Nicholson, D. W. (2000). "From bench to clinic with apoptosis-based therapeutic agents." Nature 407(6805): 810-816.

Nieman, G. F., L. A. Gatto, A. M. Paskanik, B. Yang, R. Fluck and A. Picone (1996). "Surfactant replacement in the treatment of sepsis-induced adult respiratory distress syndrome in pigs." Crit Care Med 24(6): 1025-1033.

Nieuwland, R., J. M. Falcon-Perez, C. Thery and K. W. Witwer (2020). "Rigor and standardization of extracellular vesicle research: Paving the road towards robustness." J Extracell Vesicles 10(2): e12037.

Nin, N., A. Muriel, O. Penuelas, L. Brochard, J. A. Lorente, N. D. Ferguson, K. Raymondos, F. Rios, D. A. Violi, A. W. Thille, M. Gonzalez, A. J. Villagomez, J. Hurtado, A. R. Davies, B. Du, S. M. Maggiore, L. Soto, G. D'Empaire, D. Matamis, F. Abroug, R. P. Moreno, M. A. Soares, Y. Arabi, F. Sandi, M. Jibaja, P. Amin, Y. Koh, M. A. Kuiper, H. H. Bulow, A. A. Zeggwagh, A. Anzueto, J. I. Sznajder, A. Esteban and V. Group (2017). "Severe hypercapnia and outcome of mechanically ventilated patients with

moderate or severe acute respiratory distress syndrome." Intensive Care Med 43(2): 200-208.

Nuckton, T. J., J. A. Alonso, R. H. Kallet, B. M. Daniel, J. F. Pittet, M. D. Eisner and M. A. Matthay (2002). "Pulmonary dead-space fraction as a risk factor for death in the acute respiratory distress syndrome." N Engl J Med 346(17): 1281-1286.

O'Grady, N. P., H. L. Preas, J. Pugin, C. Fiuza, M. Tropea, D. Reda, S. M. Banks and A. F. Suffredini (2001). "Local inflammatory responses following bronchial endotoxin instillation in humans." Am J Respir Crit Care Med 163(7): 1591-1598.

O'Toole, D., P. Hassett, M. Contreras, B. D. Higgins, S. T. McKeown, D. F. McAuley, T. O'Brien and J. G. Laffey (2009). "Hypercapnic acidosis attenuates pulmonary epithelial wound repair by an NF-kappaB dependent mechanism." Thorax 64(11): 976-982.

Olschewski, A., R. Papp, C. Nagaraj and H. Olschewski (2014). "Ion channels and transporters as therapeutic targets in the pulmonary circulation." Pharmacol Ther 144(3): 349-368.

Orfanos, S. E., A. Armaganidis, C. Glynos, E. Psevdi, P. Kaltsas, P. Sarafidou, J. D. Catravas, U. G. Dafni, D. Langleben and C. Roussos (2000). "Pulmonary capillary endothelium-bound angiotensin-converting enzyme activity in acute lung injury." Circulation 102(16): 2011-2018.

Ortiz, L. A., M. Dutreil, C. Fattman, A. C. Pandey, G. Torres, K. Go and D. G. Phinney (2007). "Interleukin 1 receptor antagonist mediates the antiinflammatory and antifibrotic effect of mesenchymal stem cells during lung injury." Proc Natl Acad Sci U S A 104(26): 11002-11007.

Ozaki, M., S. Kawashima, T. Yamashita, Y. Ohashi, Y. Rikitake, N. Inoue, K. I. Hirata, Y. Hayashi, H. Itoh and M. Yokoyama (2001). "Reduced hypoxic pulmonary vascular remodeling by nitric oxide from the endothelium." Hypertension 37(2): 322-327.

Ozolina, A., M. Sarkele, O. Sabelnikovs, A. Skesters, I. Jaunalksne, J. Serova, T. Ievins, L. J. Bjertnaes and I. Vanags (2016). "Activation of Coagulation and Fibrinolysis in Acute Respiratory Distress Syndrome: A Prospective Pilot Study." Front Med (Lausanne) 3: 64.

Pacheco-Cuellar, G., J. Gauthier, V. Desilets, C. Lachance, M. Lemire-Girard, F. Rypens, F. Le Deist, H. Decaluwe, M. Duval, D. Bouron-Dal Soglio, V. Kokta, E. Haddad and P. M. Campeau (2017). "A Novel PGM3 Mutation Is Associated With a Severe Phenotype of Bone Marrow Failure, Severe Combined Immunodeficiency, Skeletal Dysplasia, and Congenital Malformations." J Bone Miner Res 32(9): 1853-1859.

Pagnesi, M., L. Baldetti, A. Beneduce, F. Calvo, M. Gramegna, V. Pazzanese, G. Ingallina, A. Napolano, R. Finazzi, A. Ruggeri, S. Ajello, G. Melisurgo, P. G. Camici, P. Scarpellini, M. Tresoldi, G. Landoni, F. Ciceri, A. M. Scandroglio, E. Agricola and A. M. Cappelletti (2020). "Pulmonary hypertension and right ventricular involvement in hospitalised patients with COVID-19." Heart 106(17): 1324-1331.

Pandolfi, R., B. Barreira, E. Moreno, V. Lara-Acedo, D. Morales-Cano, A. Martinez-Ramas, B. de Olaiz Navarro, R. Herrero, J. A. Lorente, A. Cogolludo, F. Perez-Vizcaino and L. Moreno (2017). "Role of acid

sphingomyelinase and IL-6 as mediators of endotoxin-induced pulmonary vascular dysfunction." Thorax 72(5): 460-471.

Pang, H., Y. Koda, M. Soejima and H. Kimura (2002). "Identification of human phosphoglucomutase 3 (PGM3) as N-acetylglucosamine-phosphate mutase (AGM1)." Ann Hum Genet 66(Pt 2): 139-144.

Papazian, L., J. M. Forel, A. Gacouin, C. Penot-Ragon, G. Perrin, A. Loundou, S. Jaber, J. M. Arnal, D. Perez, J. M. Seghboyan, J. M. Constantin, P. Courant, J. Y. Lefrant, C. Guerin, G. Prat, S. Morange, A. Roch and A. S. Investigators (2010). "Neuromuscular blockers in early acute respiratory distress syndrome." N Engl J Med 363(12): 1107-1116.

Park, H., H. Park, D. Mun, J. Kang, H. Kim, M. Kim, S. Cui, S. H. Lee and B. Joung (2018). "Extracellular Vesicles Derived from Hypoxic Human Mesenchymal Stem Cells Attenuate GSK3beta Expression via miRNA-26a in an Ischemia-Reperfusion Injury Model." Yonsei Med J 59(6): 736-745.

Park, J., S. Kim, H. Lim, A. Liu, S. Hu, J. Lee, H. Zhuo, Q. Hao, M. A. Matthay and J. W. Lee (2019). "Therapeutic effects of human mesenchymal stem cell microvesicles in an ex vivo perfused human lung injured with severe E. coli pneumonia." Thorax 74(1): 43-50.

Park, J. E., B. Dutta, S. W. Tse, N. Gupta, C. F. Tan, J. K. Low, K. W. Yeoh, O. L. Kon, J. P. Tam and S. K. Sze (2019). "Hypoxia-induced tumor exosomes promote M2-like macrophage polarization of infiltrating myeloid cells and microRNA-mediated metabolic shift." Oncogene 38(26): 5158-5173.

Park, K. S., S. H. Kim, A. Das, S. N. Yang, K. H. Jung, M. K. Kim, P. O. Berggren, Y. Lee, J. C. Chai, H. J. Kim and Y. G. Chai (2016). "TLR3-/4-Priming Differentially Promotes Ca(2+) Signaling and Cytokine Expression and Ca(2+)-Dependently Augments Cytokine Release in hMSCs." Sci Rep 6: 23103.

Park, W. Y., R. B. Goodman, K. P. Steinberg, J. T. Ruzinski, F. Radella, 2nd, D. R. Park, J. Pugin, S. J. Skerrett, L. D. Hudson and T. R. Martin (2001). "Cytokine balance in the lungs of patients with acute respiratory distress syndrome." Am J Respir Crit Care Med 164(10 Pt 1): 1896-1903.

Patel, S. and S. Sharma (2022). Respiratory Acidosis. StatPearls. Treasure Island (FL).

Pathan, M., P. Fonseka, S. V. Chitti, T. Kang, R. Sanwlani, J. Van Deun, A. Hendrix and S. Mathivanan (2019). "Vesiclepedia 2019: a compendium of RNA, proteins, lipids and metabolites in extracellular vesicles." Nucleic Acids Res 47(D1): D516-D519.

Pati, S., M. H. Gerber, T. D. Menge, K. A. Wataha, Y. Zhao, J. A. Baumgartner, J. Zhao, P. A. Letourneau, M. P. Huby, L. A. Baer, J. R. Salsbury, R. A. Kozar, C. E. Wade, P. A. Walker, P. K. Dash, C. S. Cox, Jr., M. F. Doursout and J. B. Holcomb (2011). "Bone marrow derived mesenchymal stem cells inhibit inflammation and preserve vascular endothelial integrity in the lungs after hemorrhagic shock." PLoS One 6(9): e25171.

Patton, M. C., H. Zubair, M. A. Khan, S. Singh and A. P. Singh (2020). "Hypoxia alters the release and size distribution of extracellular vesicles in pancreatic cancer cells to support their adaptive survival." J Cell Biochem 121(1): 828-839.

Pelosi, P., P. R. Rocco, D. Negrini and A. Passi (2007). "The extracellular matrix of the lung and its role in edema formation." An Acad Bras Cienc 79(2): 285-297.

Peltekova, V., D. Engelberts, G. Otulakowski, S. Uematsu, M. Post and B. P. Kavanagh (2010). "Hypercapnic acidosis in ventilator-induced lung injury." Intensive Care Med 36(5): 869-878.

Perez-Vizcaino, F., L. Moreno and J. A. Lorente (2021). "Interleukin-6 and intrapulmonary shunt." Eur Respir J 58(2).

Perkins, G. D., S. Gates, D. Park, F. Gao, C. Knox, B. Holloway, D. F. McAuley, J. Ryan, J. Marzouk, M. W. Cooke, S. E. Lamb, D. R. Thickett and B. A.-P. Collaborators (2014). "The beta agonist lung injury trial prevention. A randomized controlled trial." Am J Respir Crit Care Med 189(6): 674-683.

Perkins, G. D., D. F. McAuley, D. R. Thickett and F. Gao (2006). "The beta-agonist lung injury trial (BALTI): a randomized placebo-controlled clinical trial." Am J Respir Crit Care Med 173(3): 281-287.

Perrella, M. A., E. S. Edell, M. J. Krowka, D. A. Cortese and J. C. Burnett, Jr. (1992). "Endothelium-derived relaxing factor in pulmonary and renal circulations during hypoxia." Am J Physiol 263(1 Pt 2): R45-50.

Petrache, I., V. Natarajan, L. Zhen, T. R. Medler, A. T. Richter, C. Cho, W. C. Hubbard, E. V. Berdyshev and R. M. Tuder (2005). "Ceramide upregulation causes pulmonary cell apoptosis and emphysema-like disease in mice." Nat Med 11(5): 491-498.

Pfortmueller, C. A., T. Spinetti, R. D. Urman, M. M. Luedi and J. C. Schefold (2021). "COVID-19-associated acute respiratory distress syndrome (CARDS): Current knowledge on pathophysiology and ICU treatment - A narrative review." Best Pract Res Clin Anaesthesiol 35(3): 351-368.

Phinney, D. G., M. Di Giuseppe, J. Njah, E. Sala, S. Shiva, C. M. St Croix, D. B. Stolz, S. C. Watkins, Y. P. Di, G. D. Leikauf, J. Kolls, D. W. Riches, G. Deiuliis, N. Kaminski, S. V. Boregowda, D. H. McKenna and L. A. Ortiz (2015). "Mesenchymal stem cells use extracellular vesicles to outsource mitophagy and shuttle microRNAs." Nat Commun 6: 8472.

Piantadosi, C. A. and D. A. Schwartz (2004). "The acute respiratory distress syndrome." Ann Intern Med 141(6): 460-470.

Pierrakos, C., M. Karanikolas, S. Scolletta, V. Karamouzos and D. Velissaris (2012). "Acute respiratory distress syndrome: pathophysiology and therapeutic options." J Clin Med Res 4(1): 7-16.

Pittet, J. F., R. C. Mackersie, T. R. Martin and M. A. Matthay (1997). "Biological markers of acute lung injury: prognostic and pathogenetic significance." Am J Respir Crit Care Med 155(4): 1187-1205.

Potter, D. R., B. Y. Miyazawa, S. L. Gibb, X. Deng, P. P. Togaratti, R. H. Croze, A. K. Srivastava, A. Trivedi, M. Matthay, J. B. Holcomb, M. A. Schreiber and S. Pati (2018). "Mesenchymal stem cell-derived extracellular vesicles attenuate pulmonary vascular permeability and lung injury induced by hemorrhagic shock and trauma." J Trauma Acute Care Surg 84(2): 245-256.

Prabhakaran, P., L. B. Ware, K. E. White, M. T. Cross, M. A. Matthay and M. A. Olman (2003). "Elevated levels of plasminogen activator inhibitor-1 in

pulmonary edema fluid are associated with mortality in acute lung injury." Am J Physiol Lung Cell Mol Physiol 285(1): L20-28.

Price, L. C., D. F. McAuley, P. S. Marino, S. J. Finney, M. J. Griffiths and S. J. Wort (2012). "Pathophysiology of pulmonary hypertension in acute lung injury." Am J Physiol Lung Cell Mol Physiol 302(9): L803-815.

Price, L. C., S. J. Wort, F. Perros, P. Dorfmuller, A. Huertas, D. Montani, S. Cohen-Kaminsky and M. Humbert (2012). "Inflammation in pulmonary arterial hypertension." Chest 141(1): 210-221.

Prins, K. W., S. L. Archer, M. Pritzker, L. Rose, E. K. Weir, A. Sharma and T. Thenappan (2018). "Interleukin-6 is independently associated with right ventricular function in pulmonary arterial hypertension." J Heart Lung Transplant 37(3): 376-384.

Pullamsetti, S. S., W. Seeger and R. Savai (2018). "Classical IL-6 signaling: a promising therapeutic target for pulmonary arterial hypertension." J Clin Invest 128(5): 1720-1723.

Quinlan, G. J. and T. W. Evans (2000). "Acute respiratory distress syndrome in adults." Hosp Med 61(8): 561-563.

Rabinovitch, M. (2012). "Molecular pathogenesis of pulmonary arterial hypertension." J Clin Invest 122(12): 4306-4313.

Rabinovitch, M., C. Guignabert, M. Humbert and M. R. Nicolls (2014). "Inflammation and immunity in the pathogenesis of pulmonary arterial hypertension." Circ Res 115(1): 165-175.

Radermacher, P., S. M. Maggiore and A. Mercat (2017). "Fifty Years of Research in ARDS. Gas Exchange in Acute Respiratory Distress Syndrome." Am J Respir Crit Care Med 196(8): 964-984.

Raetz, C. R., R. J. Ulevitch, S. D. Wright, C. H. Sibley, A. Ding and C. F. Nathan (1991). "Gram-negative endotoxin: an extraordinary lipid with profound effects on eukaryotic signal transduction." FASEB J 5(12): 2652-2660.

Rahimi Pordanjani, S., A. Hasanpour, H. Askarpour, D. Bastam, M. Rafiee, Z. Khazaei, E. Mazaheri, M. H. Vaziri and S. Sabour (2021). "Aspects of Epidemiology, Pathology, Virology, Immunology, Transmission, Prevention, Prognosis, Diagnosis, and Treatment of COVID-19 Pandemic: A Narrative Review." Int J Prev Med 12: 38.

Rahman, S., M. T. V. Montero, K. Rowe, R. Kirton and F. Kunik, Jr. (2021). "Epidemiology, pathogenesis, clinical presentations, diagnosis and treatment of COVID-19: a review of current evidence." Expert Rev Clin Pharmacol 14(5): 601-621.

Ramteke, A., H. Ting, C. Agarwal, S. Mateen, R. Somasagara, A. Hussain, M. Graner, B. Frederick, R. Agarwal and G. Deep (2015). "Exosomes secreted under hypoxia enhance invasiveness and stemness of prostate cancer cells by targeting adherens junction molecules." Mol Carcinog 54(7): 554-565.

Ranucci, M., A. Ballotta, U. Di Dedda, E. Baryshnikova, M. Dei Poli, M. Resta, M. Falco, G. Albano and L. Menicanti (2020). "The procoagulant pattern of patients with COVID-19 acute respiratory distress syndrome." J Thromb Haemost 18(7): 1747-1751.

Raposo, G. and W. Stoorvogel (2013). "Extracellular vesicles: exosomes, microvesicles, and friends." J Cell Biol 200(4): 373-383.

Rebetz, J., J. W. Semple and R. Kapur (2018). "The Pathogenic Involvement of Neutrophils in Acute Respiratory Distress Syndrome and Transfusion-Related Acute Lung Injury." Transfus Med Hemother 45(5): 290-298.

Repesse, X. and A. Vieillard-Baron (2017). "Hypercapnia during acute respiratory distress syndrome: the tree that hides the forest!" J Thorac Dis 9(6): 1420-1425.

Reutershan, J., R. E. Cagnina, D. Chang, J. Linden and K. Ley (2007). "Therapeutic anti-inflammatory effects of myeloid cell adenosine receptor A2a stimulation in lipopolysaccharide-induced lung injury." J Immunol 179(2): 1254-1263.

Reutershan, J. and K. Ley (2004). "Bench-to-bedside review: acute respiratory distress syndrome - how neutrophils migrate into the lung." Crit Care 8(6): 453-461.

Revercomb, L., A. Hanmandlu, N. Wareing, B. Akkanti and H. Karmouty-Quintana (2020). "Mechanisms of Pulmonary Hypertension in Acute Respiratory Distress Syndrome (ARDS)." Front Mol Biosci 7: 624093.

Riede, U. N., H. Joachim, J. Hassenstein, U. Costabel, W. Sandritter, P. Augustin and C. Mittermayer (1978). "The pulmonary air-blood barrier of human shock lungs (a clinical, ultrastructural and morphometric study)." Pathol Res Pract 162(1): 41-72.

Rienks, M., A. P. Papageorgiou, N. G. Frangogiannis and S. Heymans (2014). "Myocardial extracellular matrix: an ever-changing and diverse entity." Circ Res 114(5): 872-888.

Rocco, P. R., E. M. Negri, P. M. Kurtz, F. P. Vasconcellos, G. H. Silva, V. L. Capelozzi, P. V. Romero and W. A. Zin (2001). "Lung tissue mechanics and extracellular matrix remodeling in acute lung injury." Am J Respir Crit Care Med 164(6): 1067-1071.

Rock, J. R., C. E. Barkauskas, M. J. Cronce, Y. Xue, J. R. Harris, J. Liang, P. W. Noble and B. L. Hogan (2011). "Multiple stromal populations contribute to pulmonary fibrosis without evidence for epithelial to mesenchymal transition." Proc Natl Acad Sci U S A 108(52): E1475-1483.

Roemeling-van Rhijn, M., F. K. Mensah, S. S. Korevaar, M. J. Leijs, G. J. van Osch, J. N. Ijzermans, M. G. Betjes, C. C. Baan, W. Weimar and M. J. Hoogduijn (2013). "Effects of Hypoxia on the Immunomodulatory Properties of Adipose Tissue-Derived Mesenchymal Stem cells." Front Immunol 4: 203.

Rolandsson Enes, S., A. D. Krasnodembskaya, K. English, C. C. Dos Santos and D. J. Weiss (2021). "Research Progress on Strategies that can Enhance the Therapeutic Benefits of Mesenchymal Stromal Cells in Respiratory Diseases With a Specific Focus on Acute Respiratory Distress Syndrome and Other Inflammatory Lung Diseases." Front Pharmacol 12: 647652.

Rosová, I., M. Dao, B. Capoccia, D. Link and J. A. Nolta (2008). "Hypoxic preconditioning results in increased motility and improved therapeutic potential of human mesenchymal stem cells." Stem cells (Dayton, Ohio) 26(8): 2173-2182.

Rossi, P., B. Persson, P. J. Boels, A. Arner, E. Weitzberg and A. Oldner (2008). "Endotoxemic pulmonary hypertension is largely mediated by endothelin-induced venous constriction." Intensive Care Med 34(5): 873-880.

Rothe, C., M. Schunk, P. Sothmann, G. Bretzel, G. Froeschl, C. Wallrauch, T. Zimmer, V. Thiel, C. Janke, W. Guggemos, M. Seilmaier, C. Drosten, P. Vollmar, K. Zwirglmaier, S. Zange, R. Wolfel and M. Hoelscher (2020). "Transmission of 2019-nCoV Infection from an Asymptomatic Contact in Germany." N Engl J Med 382(10): 970-971.

Roy-Burman, A., R. H. Savel, S. Racine, B. L. Swanson, N. S. Revadigar, J. Fujimoto, T. Sawa, D. W. Frank and J. P. Wiener-Kronish (2001). "Type III protein secretion is associated with death in lower respiratory and systemic Pseudomonas aeruginosa infections." J Infect Dis 183(12): 1767-1774.

Royo, F., L. Moreno, J. Mleczko, L. Palomo, E. Gonzalez, D. Cabrera, A. Cogolludo, F. P. Vizcaino, S. van-Liempd and J. M. Falcon-Perez (2017). "Hepatocyte-secreted extracellular vesicles modify blood metabolome and endothelial function by an arginase-dependent mechanism." Sci Rep 7: 42798.

Rubenfeld, G. D., E. Caldwell, E. Peabody, J. Weaver, D. P. Martin, M. Neff, E. J. Stern and L. D. Hudson (2005). "Incidence and outcomes of acute lung injury." N Engl J Med 353(16): 1685-1693.

Rubin, D. B., J. P. Wiener-Kronish, J. F. Murray, D. R. Green, J. Turner, J. M. Luce, A. B. Montgomery, J. D. Marks and M. A. Matthay (1990). "Elevated von Willebrand factor antigen is an early plasma predictor of acute lung injury in nonpulmonary sepsis syndrome." J Clin Invest 86(2): 474-480.

Russell, T. W., J. T. Wu, S. Clifford, W. J. Edmunds, A. J. Kucharski, M. Jit and C.-w. g. Centre for the Mathematical Modelling of Infectious Diseases (2021). "Effect of internationally imported cases on internal spread of COVID-19: a mathematical modelling study." Lancet Public Health 6(1): e12-e20.

Rustenhoven, J., M. Aalderink, E. L. Scotter, R. L. Oldfield, P. S. Bergin, E. W. Mee, E. S. Graham, R. L. Faull, M. A. Curtis, T. I. Park and M. Dragunow (2016). "TGF-beta1 regulates human brain pericyte inflammatory processes involved in neurovasculature function." J Neuroinflammation 13: 37.

Ryan, D., S. Frohlich and P. McLoughlin (2014). "Pulmonary vascular dysfunction in ARDS." Ann Intensive Care 4: 28.

Sabharwal, A. K., S. P. Bajaj, A. Ameri, S. M. Tricomi, T. M. Hyers, T. E. Dahms, F. B. Taylor, Jr. and M. S. Bajaj (1995). "Tissue factor pathway inhibitor and von Willebrand factor antigen levels in adult respiratory distress syndrome and in a primate model of sepsis." Am J Respir Crit Care Med 151(3 Pt 1): 758-767.

Sadeghian Chaleshtori, S., M. R. Mokhber Dezfouli and M. Jabbari Fakhr (2020). "Mesenchymal stem/stromal cells: the therapeutic effects in animal models of acute pulmonary diseases." Respir Res 21(1): 110.

Saito, F., S. Tasaka, K. Inoue, K. Miyamoto, Y. Nakano, Y. Ogawa, W. Yamada, Y. Shiraishi, N. Hasegawa, S. Fujishima, H. Takano and A. Ishizaka

(2008). "Role of interleukin-6 in bleomycin-induced lung inflammatory changes in mice." Am J Respir Cell Mol Biol 38(5): 566-571.

Salomon, C., J. Ryan, L. Sobrevia, M. Kobayashi, K. Ashman, M. Mitchell and G. E. Rice (2013). "Exosomal signaling during hypoxia mediates microvascular endothelial cell migration and vasculogenesis." PLoS One 8(7): e68451.

Sano, S., Y. Izumi, T. Yamaguchi, T. Yamazaki, M. Tanaka, M. Shiota, M. Osada-Oka, Y. Nakamura, M. Wei, H. Wanibuchi, H. Iwao and M. Yoshiyama (2014). "Lipid synthesis is promoted by hypoxic adipocyte-derived exosomes in 3T3-L1 cells." Biochem Biophys Res Commun 445(2): 327-333.

Sapru, A., M. A. Curley, S. Brady, M. A. Matthay and H. Flori (2010). "Elevated PAI-1 is associated with poor clinical outcomes in pediatric patients with acute lung injury." Intensive Care Med 36(1): 157-163.

Sassi, A., S. Lazaroski, G. Wu, S. M. Haslam, M. Fliegauf, F. Mellouli, T. Patiroglu, E. Unal, M. A. Ozdemir, Z. Jouhadi, K. Khadir, L. Ben-Khemis, M. Ben-Ali, I. Ben-Mustapha, L. Borchani, D. Pfeifer, T. Jakob, M. Khemiri, A. C. Asplund, M. O. Gustafsson, K. E. Lundin, E. Falk-Sorqvist, L. N. Moens, H. E. Gungor, K. R. Engelhardt, M. Dziadzio, H. Stauss, B. Fleckenstein, R. Meier, K. Prayitno, A. Maul-Pavicic, S. Schaffer, M. Rakhmanov, P. Henneke, H. Kraus, H. Eibel, U. Kolsch, S. Nadifi, M. Nilsson, M. Bejaoui, A. A. Schaffer, C. I. Smith, A. Dell, M. R. Barbouche and B. Grimbacher (2014). "Hypomorphic homozygous mutations in phosphoglucomutase 3 (PGM3) impair immunity and increase serum IgE levels." J Allergy Clin Immunol 133(5): 1410-1419, 1419 e1411-1413.

Savale, L., L. Tu, D. Rideau, M. Izziki, B. Maitre, S. Adnot and S. Eddahibi (2009). "Impact of interleukin-6 on hypoxia-induced pulmonary hypertension and lung inflammation in mice." Respir Res 10: 6.

Sawheny, E., A. L. Ellis and G. T. Kinasewitz (2013). "Iloprost improves gas exchange in patients with pulmonary hypertension and ARDS." Chest 144(1): 55-62.

Scarpati, E. M. and J. E. Sadler (1989). "Regulation of endothelial cell coagulant properties. Modulation of tissue factor, plasminogen activator inhibitors, and thrombomodulin by phorbol 12-myristate 13-acetate and tumor necrosis factor." J Biol Chem 264(34): 20705-20713.

Schneeberger, E. E. and R. D. Lynch (2004). "The tight junction: a multifunctional complex." Am J Physiol Cell Physiol 286(6): C1213-1228.

Schnells, G., W. H. Voigt, H. Redl, G. Schlag and A. Glatzl (1980). "Electron-microscopic investigation of lung biopsies in patients with post-traumatic respiratory insufficiency." Acta Chir Scand Suppl 499: 9-20.

Schromm, A. B., K. Brandenburg, H. Loppnow, A. P. Moran, M. H. Koch, E. T. Rietschel and U. Seydel (2000). "Biological activities of lipopolysaccharides are determined by the shape of their lipid A portion." Eur J Biochem 267(7): 2008-2013.

Schultz, M. J., J. J. Haitsma, H. Zhang and A. S. Slutsky (2006). "Pulmonary coagulopathy as a new target in therapeutic studies of acute lung injury or pneumonia--a review." Crit Care Med 34(3): 871-877.

Schumann, R. R. (1992). "Function of lipopolysaccharide (LPS)-binding protein (LBP) and CD14, the receptor for LPS/LBP complexes: a short review." Res Immunol 143(1): 11-15.

Schuster, D. P. (1994). "ARDS: clinical lessons from the oleic acid model of acute lung injury." Am J Respir Crit Care Med 149(1): 245-260.

Seeley, E., D. F. McAuley, M. Eisner, M. Miletin, M. A. Matthay and R. H. Kallet (2008). "Predictors of mortality in acute lung injury during the era of lung protective ventilation." Thorax 63(11): 994-998.

Shyamsundar, M., S. T. McKeown, C. M. O'Kane, T. R. Craig, V. Brown, D. R. Thickett, M. A. Matthay, C. C. Taggart, J. T. Backman, J. S. Elborn and D. F. McAuley (2009). "Simvastatin decreases lipopolysaccharide-induced pulmonary inflammation in healthy volunteers." Am J Respir Crit Care Med 179(12): 1107-1114.

Siler, T. M., J. E. Swierkosz, T. M. Hyers, A. A. Fowler and R. O. Webster (1989). "Immunoreactive interleukin-1 in bronchoalveolar lavage fluid of high-risk patients and patients with the adult respiratory distress syndrome." Exp Lung Res 15(6): 881-894.

Simmons, S., L. Erfinanda, C. Bartz and W. M. Kuebler (2019). "Novel mechanisms regulating endothelial barrier function in the pulmonary microcirculation." J Physiol 597(4): 997-1021.

Simonneau, G. and M. M. Hoeper (2019). "The revised definition of pulmonary hypertension: exploring the impact on patient management." Eur Heart J Suppl 21(Suppl K): K4-K8.

Sinha, P., D. Furfaro, M. J. Cummings, D. Abrams, K. Delucchi, M. V. Maddali, J. He, A. Thompson, M. Murn, J. Fountain, A. Rosen, S. Y. Robbins-Juarez, M. A. Adan, T. Satish, M. Madhavan, A. Gupta, A. K. Lyashchenko, C. Agerstrand, N. H. Yip, K. M. Burkart, J. R. Beitler, M. R. Baldwin, C. S. Calfee, D. Brodie and M. R. O'Donnell (2021). "Latent Class Analysis Reveals COVID-19-related ARDS Subgroups with Differential Responses to Corticosteroids." Am J Respir Crit Care Med.

Sipmann, F. S., A. Santos and G. Tusman (2018). "Heart-lung interactions in acute respiratory distress syndrome: pathophysiology, detection and management strategies." Ann Transl Med 6(2): 27.

Sklar, M. C., E. Fan and E. C. Goligher (2017). "High-Frequency Oscillatory Ventilation in Adults With ARDS: Past, Present, and Future." Chest 152(6): 1306-1317.

Smith, A. P., E. A. Demoncheaux and T. W. Higenbottam (2002). "Nitric oxide gas decreases endothelin-1 mRNA in cultured pulmonary artery endothelial cells." Nitric Oxide 6(2): 153-159.

Smith, L. S., J. J. Zimmerman and T. R. Martin (2013). "Mechanisms of acute respiratory distress syndrome in children and adults: a review and suggestions for future research." Pediatr Crit Care Med 14(6): 631-643.

Smith, P. D., A. F. Suffredini, J. B. Allen, L. M. Wahl, J. E. Parrillo and S. M. Wahl (1994). "Endotoxin administration to humans primes alveolar macrophages for increased production of inflammatory mediators." J Clin Immunol 14(2): 141-148.

Son, Y. H., Y. T. Jeong, K. A. Lee, K. H. Choi, S. M. Kim, B. Y. Rhim and K. Kim (2008). "Roles of MAPK and NF-kappaB in interleukin-6 induction by

lipopolysaccharide in vascular smooth muscle cells." J Cardiovasc Pharmacol 51(1): 71-77.

Song, M. and J. A. Kellum (2005). "Interleukin-6." Crit Care Med 33(12 Suppl): S463-465.

Soon, E., A. M. Holmes, C. M. Treacy, N. J. Doughty, L. Southgate, R. D. Machado, R. C. Trembath, S. Jennings, L. Barker, P. Nicklin, C. Walker, D. C. Budd, J. Pepke-Zaba and N. W. Morrell (2010). "Elevated levels of inflammatory cytokines predict survival in idiopathic and familial pulmonary arterial hypertension." Circulation 122(9): 920-927.

Spohr, F., A. J. Cornelissen, C. Busch, M. M. Gebhard, J. Motsch, E. O. Martin and J. Weimann (2005). "Role of endogenous nitric oxide in endotoxin-induced alteration of hypoxic pulmonary vasoconstriction in mice." Am J Physiol Heart Circ Physiol 289(2): H823-831.

Spragg, R. G., J. F. Lewis, H. D. Walmrath, J. Johannigman, G. Bellingan, P. F. Laterre, M. C. Witte, G. A. Richards, G. Rippin, F. Rathgeb, D. Hafner, F. J. Taut and W. Seeger (2004). "Effect of recombinant surfactant protein C-based surfactant on the acute respiratory distress syndrome." N Engl J Med 351(9): 884-892.

Steinberg, K. P., L. D. Hudson, R. B. Goodman, C. L. Hough, P. N. Lanken, R. Hyzy, B. T. Thompson, M. Ancukiewicz, L. National Heart and N. Blood Institute Acute Respiratory Distress Syndrome Clinical Trials (2006). "Efficacy and safety of corticosteroids for persistent acute respiratory distress syndrome." N Engl J Med 354(16): 1671-1684.

Steinberg, K. P., J. A. Milberg, T. R. Martin, R. J. Maunder, B. A. Cockrill and L. D. Hudson (1994). "Evolution of bronchoalveolar cell populations in the adult respiratory distress syndrome." Am J Respir Crit Care Med 150(1): 113-122.

Steiner, M. K., O. L. Syrkina, N. Kolliputi, E. J. Mark, C. A. Hales and A. B. Waxman (2009). "Interleukin-6 overexpression induces pulmonary hypertension." Circ Res 104(2): 236-244, 228p following 244.

Stenmark, K. R., B. Meyrick, N. Galie, W. J. Mooi and I. F. McMurtry (2009). "Animal models of pulmonary arterial hypertension: the hope for etiological discovery and pharmacological cure." Am J Physiol Lung Cell Mol Physiol 297(6): L1013-1032.

Steudel, W., F. Ichinose, P. L. Huang, W. E. Hurford, R. C. Jones, J. A. Bevan, M. C. Fishman and W. M. Zapol (1997). "Pulmonary vasoconstriction and hypertension in mice with targeted disruption of the endothelial nitric oxide synthase (NOS 3) gene." Circ Res 81(1): 34-41.

Strielkov, I., N. C. Krause, N. Sommer, R. T. Schermuly, H. A. Ghofrani, F. Grimminger, T. Gudermann, A. Dietrich and N. Weissmann (2018). "Hypoxic pulmonary vasoconstriction in isolated mouse pulmonary arterial vessels." Exp Physiol 103(9): 1185-1191.

Sud, S., M. Sud, J. O. Friedrich, M. O. Meade, N. D. Ferguson, H. Wunsch and N. K. Adhikari (2010). "High frequency oscillation in patients with acute lung injury and acute respiratory distress syndrome (ARDS): systematic review and meta-analysis." BMJ 340: c2327.

Suda, K., M. Tsuruta, J. Eom, C. Or, T. Mui, J. E. Jaw, Y. Li, N. Bai, J. Kim, J. Man, D. Ngan, J. Lee, S. Hansen, S. W. Lee, S. Tam, S. P. Man, S. Van

Eeden and D. D. Sin (2011). "Acute lung injury induces cardiovascular dysfunction: effects of IL-6 and budesonide/formoterol." Am J Respir Cell Mol Biol 45(3): 510-516.

Suzuki, Y. J., S. I. Nikolaienko, N. V. Shults and S. G. Gychka (2021). "COVID-19 patients may become predisposed to pulmonary arterial hypertension." Med Hypotheses 147: 110483.

Sweeney, R. M. and D. F. McAuley (2016). "Acute respiratory distress syndrome." Lancet 388(10058): 2416-2430.

Swenson, K. E., S. J. Ruoss and E. R. Swenson (2021). "The Pathophysiology and Dangers of Silent Hypoxemia in COVID-19 Lung Injury." Ann Am Thorac Soc 18(7): 1098-1105.

Tabima, D. M., S. Frizzell and M. T. Gladwin (2012). "Reactive oxygen and nitrogen species in pulmonary hypertension." Free Radic Biol Med 52(9): 1970-1986.

Tadokoro, H., T. Umezu, K. Ohyashiki, T. Hirano and J. H. Ohyashiki (2013). "Exosomes derived from hypoxic leukemia cells enhance tube formation in endothelial cells." J Biol Chem 288(48): 34343-34351.

Takala, A., I. Jousela, O. Takkunen, H. Kautiainen, S. E. Jansson, A. Orpana, S. L. Karonen and H. Repo (2002). "A prospective study of inflammation markers in patients at risk of indirect acute lung injury." Shock 17(4): 252-257.

Tang, B. M., J. C. Craig, G. D. Eslick, I. Seppelt and A. S. McLean (2009). "Use of corticosteroids in acute lung injury and acute respiratory distress syndrome: a systematic review and meta-analysis." Crit Care Med 37(5): 1594-1603.

Tang, X. D., L. Shi, A. Monsel, X. Y. Li, H. L. Zhu, Y. G. Zhu and J. M. Qu (2017). "Mesenchymal Stem Cell Microvesicles Attenuate Acute Lung Injury in Mice Partly Mediated by Ang-1 mRNA." Stem Cells 35(7): 1849-1859.

Tapping, R. I., S. Akashi, K. Miyake, P. J. Godowski and P. S. Tobias (2000). "Toll-like receptor 4, but not toll-like receptor 2, is a signaling receptor for Escherichia and Salmonella lipopolysaccharides." J Immunol 165(10): 5780-5787.

Taraseviciene-Stewart, L., Y. Kasahara, L. Alger, P. Hirth, G. Mc Mahon, J. Waltenberger, N. F. Voelkel and R. M. Tuder (2001). "Inhibition of the VEGF receptor 2 combined with chronic hypoxia causes cell death-dependent pulmonary endothelial cell proliferation and severe pulmonary hypertension." FASEB J 15(2): 427-438.

Taveira da Silva, A. M., H. C. Kaulbach, F. S. Chuidian, D. R. Lambert, A. F. Suffredini and R. L. Danner (1993). "Brief report: shock and multiple-organ dysfunction after self-administration of Salmonella endotoxin." N Engl J Med 328(20): 1457-1460.

Taylor, A. E. and K. A. Gaar, Jr. (1970). "Estimation of equivalent pore radii of pulmonary capillary and alveolar membranes." Am J Physiol 218(4): 1133-1140.

Terragni, P. P., G. Rosboch, A. Tealdi, E. Corno, E. Menaldo, O. Davini, G. Gandini, P. Herrmann, L. Mascia, M. Quintel, A. S. Slutsky, L. Gattinoni and V. M. Ranieri (2007). "Tidal hyperinflation during low tidal volume

ventilation in acute respiratory distress syndrome." Am J Respir Crit Care Med 175(2): 160-166.

Thery, C., K. W. Witwer, E. Aikawa, M. J. Alcaraz, J. D. Anderson, R. Andriantsitohaina, A. Antoniou, T. Arab, F. Archer, G. K. Atkin-Smith, D. C. Ayre, J. M. Bach, D. Bachurski, H. Baharvand, L. Balaj, S. Baldacchino, N. N. Bauer, A. A. Baxter, M. Bebawy, C. Beckham, A. Bedina Zavec, A. Benmoussa, A. C. Berardi, P. Bergese, E. Bielska, C. Blenkiron, S. Bobis-Wozowicz, E. Boilard, W. Boireau, A. Bongiovanni, F. E. Borras, S. Bosch, C. M. Boulanger, X. Breakefield, A. M. Breglio, M. A. Brennan, D. R. Brigstock, A. Brisson, M. L. Broekman, J. F. Bromberg, P. Bryl-Gorecka, S. Buch, A. H. Buck, D. Burger, S. Busatto, D. Buschmann, B. Bussolati, E. I. Buzas, J. B. Byrd, G. Camussi, D. R. Carter, S. Caruso, L. W. Chamley, Y. T. Chang, C. Chen, S. Chen, L. Cheng, A. R. Chin, A. Clayton, S. P. Clerici, A. Cocks, E. Cocucci, R. J. Coffey, A. Cordeiro-da-Silva, Y. Couch, F. A. Coumans, B. Coyle, R. Crescitelli, M. F. Criado, C. D'Souza-Schorey, S. Das, A. Datta Chaudhuri, P. de Candia, E. F. De Santana, O. De Wever, H. A. Del Portillo, T. Demaret, S. Deville, A. Devitt, B. Dhondt, D. Di Vizio, L. C. Dieterich, V. Dolo, A. P. Dominguez Rubio, M. Dominici, M. R. Dourado, T. A. Driedonks, F. V. Duarte, H. M. Duncan, R. M. Eichenberger, K. Ekstrom, S. El Andaloussi, C. Elie-Caille, U. Erdbrugger, J. M. Falcon-Perez, F. Fatima, J. E. Fish, M. Flores-Bellver, A. Forsonits, A. Frelet-Barrand, F. Fricke, G. Fuhrmann, S. Gabrielsson, A. Gamez-Valero, C. Gardiner, K. Gartner, R. Gaudin, Y. S. Gho, B. Giebel, C. Gilbert, M. Gimona, I. Giusti, D. C. Goberdhan, A. Gorgens, S. M. Gorski, D. W. Greening, J. C. Gross, A. Gualerzi, G. N. Gupta, D. Gustafson, A. Handberg, R. A. Haraszti, P. Harrison, H. Hegyesi, A. Hendrix, A. F. Hill, F. H. Hochberg, K. F. Hoffmann, B. Holder, H. Holthofer, B. Hosseinkhani, G. Hu, Y. Huang, V. Huber, S. Hunt, A. G. Ibrahim, T. Ikezu, J. M. Inal, M. Isin, A. Ivanova, H. K. Jackson, S. Jacobsen, S. M. Jay, M. Jayachandran, G. Jenster, L. Jiang, S. M. Johnson, J. C. Jones, A. Jong, T. Jovanovic-Talisman, S. Jung, R. Kalluri, S. I. Kano, S. Kaur, Y. Kawamura, E. T. Keller, D. Khamari, E. Khomyakova, A. Khvorova, P. Kierulf, K. P. Kim, T. Kislinger, M. Klingeborn, D. J. Klinke, 2nd, M. Kornek, M. M. Kosanovic, A. F. Kovacs, E. M. Kramer-Albers, S. Krasemann, M. Krause, I. V. Kurochkin, G. D. Kusuma, S. Kuypers, S. Laitinen, S. M. Langevin, L. R. Languino, J. Lannigan, C. Lasser, L. C. Laurent, G. Lavieu, E. Lazaro-Ibanez, S. Le Lay, M. S. Lee, Y. X. F. Lee, D. S. Lemos, M. Lenassi, A. Leszczynska, I. T. Li, K. Liao, S. F. Libregts, E. Ligeti, R. Lim, S. K. Lim, A. Line, K. Linnemannstons, A. Llorente, C. A. Lombard, M. J. Lorenowicz, A. M. Lorincz, J. Lotvall, J. Lovett, M. C. Lowry, X. Loyer, Q. Lu, B. Lukomska, T. R. Lunavat, S. L. Maas, H. Malhi, A. Marcilla, J. Mariani, J. Mariscal, E. S. Martens-Uzunova, L. Martin-Jaular, M. C. Martinez, V. R. Martins, M. Mathieu, S. Mathivanan, M. Maugeri, L. K. McGinnis, M. J. McVey, D. G. Meckes, Jr., K. L. Meehan, I. Mertens, V. R. Minciacchi, A. Moller, M. Moller Jorgensen, A. Morales-Kastresana, J. Morhayim, F. Mullier, M. Muraca, L. Musante, V. Mussack, D. C. Muth, K. H. Myburgh, T. Najrana, M. Nawaz, I. Nazarenko, P. Nejsum, C. Neri, T. Neri, R. Nieuwland, L.

Nimrichter, J. P. Nolan, E. N. Nolte-'t Hoen, N. Noren Hooten, L. O'Driscoll, T. O'Grady, A. O'Loghlen, T. Ochiya, M. Olivier, A. Ortiz, L. A. Ortiz, X. Osteikoetxea, O. Ostergaard, M. Ostrowski, J. Park, D. M. Pegtel, H. Peinado, F. Perut, M. W. Pfaffl, D. G. Phinney, B. C. Pieters, R. C. Pink, D. S. Pisetsky, E. Pogge von Strandmann, I. Polakovicova, I. K. Poon, B. H. Powell, I. Prada, L. Pulliam, P. Quesenberry, A. Radeghieri, R. L. Raffai, S. Raimondo, J. Rak, M. I. Ramirez, G. Raposo, M. S. Rayyan, N. Regev-Rudzki, F. L. Ricklefs, P. D. Robbins, D. D. Roberts, S. C. Rodrigues, E. Rohde, S. Rome, K. M. Rouschop, A. Rughetti, A. E. Russell, P. Saa, S. Sahoo, E. Salas-Huenuleo, C. Sanchez, J. A. Saugstad, M. J. Saul, R. M. Schiffelers, R. Schneider, T. H. Schoyen, A. Scott, E. Shahaj, S. Sharma, O. Shatnyeva, F. Shekari, G. V. Shelke, A. K. Shetty, K. Shiba, P. R. Siljander, A. M. Silva, A. Skowronek, O. L. Snyder, 2nd, R. P. Soares, B. W. Sodar, C. Soekmadji, J. Sotillo, P. D. Stahl, W. Stoorvogel, S. L. Stott, E. F. Strasser, S. Swift, H. Tahara, M. Tewari, K. Timms, S. Tiwari, R. Tixeira, M. Tkach, W. S. Toh, R. Tomasini, A. C. Torrecilhas, J. P. Tosar, V. Toxavidis, L. Urbanelli, P. Vader, B. W. van Balkom, S. G. van der Grein, J. Van Deun, M. J. van Herwijnen, K. Van Keuren-Jensen, G. van Niel, M. E. van Royen, A. J. van Wijnen, M. H. Vasconcelos, I. J. Vechetti, Jr., T. D. Veit, L. J. Vella, E. Velot, F. J. Verweij, B. Vestad, J. L. Vinas, T. Visnovitz, K. V. Vukman, J. Wahlgren, D. C. Watson, M. H. Wauben, A. Weaver, J. P. Webber, V. Weber, A. M. Wehman, D. J. Weiss, J. A. Welsh, S. Wendt, A. M. Wheelock, Z. Wiener, L. Witte, J. Wolfram, A. Xagorari, P. Xander, J. Xu, X. Yan, M. Yanez-Mo, H. Yin, Y. Yuana, V. Zappulli, J. Zarubova, V. Zekas, J. Y. Zhang, Z. Zhao, L. Zheng, A. R. Zheutlin, A. M. Zickler, P. Zimmermann, A. M. Zivkovic, D. Zocco and E. K. Zuba-Surma (2018). "Minimal information for studies of extracellular vesicles 2018 (MISEV2018): a position statement of the International Society for Extracellular Vesicles and update of the MISEV2014 guidelines." J Extracell Vesicles 7(1): 1535750.

Thompson, B. T., R. C. Chambers and K. D. Liu (2017). "Acute Respiratory Distress Syndrome." N Engl J Med 377(6): 562-572.

Thompson, B. T., R. C. Chambers and K. D. Liu (2017). "Acute Respiratory Distress Syndrome." N Engl J Med 377(19): 1904-1905.

Thompson, C. B. (1995). "Apoptosis in the pathogenesis and treatment of disease." Science 267(5203): 1456-1462.

Tomashefski, J. F., Jr. (2000). "Pulmonary pathology of acute respiratory distress syndrome." Clin Chest Med 21(3): 435-466.

Tomashefski, J. F., Jr., P. Davies, C. Boggis, R. Greene, W. M. Zapol and L. M. Reid (1983). "The pulmonary vascular lesions of the adult respiratory distress syndrome." Am J Pathol 112(1): 112-126.

Torbic, H., P. M. Szumita, K. E. Anger, P. Nuccio, S. LaGambina and G. Weinhouse (2013). "Inhaled epoprostenol vs inhaled nitric oxide for refractory hypoxemia in critically ill patients." J Crit Care 28(5): 844-848.

Tsuno, K., K. Miura, M. Takeya, T. Kolobow and T. Morioka (1991). "Histopathologic pulmonary changes from mechanical ventilation at high peak airway pressures." Am Rev Respir Dis 143(5 Pt 1): 1115-1120.

Tsushima, K., L. S. King, N. R. Aggarwal, A. De Gorordo, F. R. D'Alessio and K. Kubo (2009). "Acute lung injury review." Intern Med 48(9): 621-630.

Tudoran, C., M. Tudoran, V. E. Lazureanu, A. R. Marinescu, G. N. Pop, A. S. Pescariu, A. Enache and T. G. Cut (2021). "Evidence of Pulmonary Hypertension after SARS-CoV-2 Infection in Subjects without Previous Significant Cardiovascular Pathology." J Clin Med 10(2).

Tzotzos, S. J., B. Fischer, H. Fischer and M. Zeitlinger (2020). "Incidence of ARDS and outcomes in hospitalized patients with COVID-19: a global literature survey." Crit Care 24(1): 516.

Uchiba, M., K. Okajima, K. Murakami, M. Johno, H. Okabe and K. Takatsuki (1996). "Recombinant thrombomodulin prevents endotoxin-induced lung injury in rats by inhibiting leukocyte activation." Am J Physiol 271(3 Pt 1): L470-475.

Uhlig, S. and U. Uhlig (2004). "Pharmacological interventions in ventilator-induced lung injury." Trends Pharmacol Sci 25(11): 592-600.

Ullrich, R., K. D. Bloch, F. Ichinose, W. Steudel and W. M. Zapol (1999). "Hypoxic pulmonary blood flow redistribution and arterial oxygenation in endotoxin-challenged NOS2-deficient mice." J Clin Invest 104(10): 1421-1429.

Umbrello, M., P. Formenti, L. Bolgiaghi and D. Chiumello (2016). "Current Concepts of ARDS: A Narrative Review." Int J Mol Sci 18(1).

Umezu, T., H. Tadokoro, K. Azuma, S. Yoshizawa, K. Ohyashiki and J. H. Ohyashiki (2014). "Exosomal miR-135b shed from hypoxic multiple myeloma cells enhances angiogenesis by targeting factor-inhibiting HIF-1." Blood 124(25): 3748-3757.

Urner, S., L. Planas-Paz, L. S. Hilger, C. Henning, A. Branopolski, M. Kelly-Goss, L. Stanczuk, B. Pitter, E. Montanez, S. M. Peirce, T. Makinen and E. Lammert (2019). "Identification of ILK as a critical regulator of VEGFR3 signalling and lymphatic vascular growth." EMBO J 38(2).

van Haaften, T., R. Byrne, S. Bonnet, G. Y. Rochefort, J. Akabutu, M. Bouchentouf, G. J. Rey-Parra, J. Galipeau, A. Haromy, F. Eaton, M. Chen, K. Hashimoto, D. Abley, G. Korbutt, S. L. Archer and B. Thebaud (2009). "Airway delivery of mesenchymal stem cells prevents arrested alveolar growth in neonatal lung injury in rats." Am J Respir Crit Care Med 180(11): 1131-1142.

Vankova, M., V. A. Snetkov, G. A. Knock, P. I. Aaronson and J. P. Ward (2005). "Euhydric hypercapnia increases vasoreactivity of rat pulmonary arteries via HCO3- transport and depolarisation." Cardiovasc Res 65(2): 505-512.

Varkouhi, A. K., M. Jerkic, L. Ormesher, S. Gagnon, S. Goyal, R. Rabani, C. Masterson, C. Spring, P. Z. Chen, F. X. Gu, C. C. Dos Santos, G. F. Curley and J. G. Laffey (2019). "Extracellular Vesicles from Interferon-gamma-primed Human Umbilical Cord Mesenchymal Stromal Cells Reduce Escherichia coli-induced Acute Lung Injury in Rats." Anesthesiology 130(5): 778-790.

Varma, M. J., R. G. Breuls, T. E. Schouten, W. J. Jurgens, H. J. Bontkes, G. J. Schuurhuis, S. M. van Ham and F. J. van Milligen (2007). "Phenotypical and functional characterization of freshly isolated adipose tissue-derived stem cells." Stem Cells Dev 16(1): 91-104.

Vender, R. L., M. F. Betancourt, E. B. Lehman, C. Harrell, D. Galvan and D. C. Frankenfield (2014). "Prediction equation to estimate dead space to tidal volume fraction correlates with mortality in critically ill patients." J Crit Care 29(2): 317 e311-313.

Venturella, M., M. Criscuoli, F. Carraro, A. Naldini and D. Zocco (2021). "Interplay between Hypoxia and Extracellular Vesicles in Cancer and Inflammation." Biology (Basel) 10(7).

Vieillard-Baron, A., J. M. Schmitt, R. Augarde, J. L. Fellahi, S. Prin, B. Page, A. Beauchet and F. Jardin (2001). "Acute cor pulmonale in acute respiratory distress syndrome submitted to protective ventilation: incidence, clinical implications, and prognosis." Crit Care Med 29(8): 1551-1555.

Villamor, E., F. Perez-Vizcaino, T. Ruiz, J. C. Leza, M. Moro and J. Tamargo (1995). "Group B Streptococcus and E. coli LPS-induced NO-dependent hyporesponsiveness to noradrenaline in isolated intrapulmonary arteries of neonatal piglets." Br J Pharmacol 115(2): 261-266.

Villar, J., J. Blanco, J. M. Anon, A. Santos-Bouza, L. Blanch, A. Ambros, F. Gandia, D. Carriedo, F. Mosteiro, S. Basaldua, R. L. Fernandez, R. M. Kacmarek and A. Network (2011). "The ALIEN study: incidence and outcome of acute respiratory distress syndrome in the era of lung protective ventilation." Intensive Care Med 37(12): 1932-1941.

Villar, J., M. A. Blazquez, S. Lubillo, J. Quintana and J. L. Manzano (1989). "Pulmonary hypertension in acute respiratory failure." Crit Care Med 17(6): 523-526.

Villar, J., C. Ferrando, D. Martinez, A. Ambros, T. Munoz, J. A. Soler, G. Aguilar, F. Alba, E. Gonzalez-Higueras, L. A. Conesa, C. Martin-Rodriguez, F. J. Diaz-Dominguez, P. Serna-Grande, R. Rivas, J. Ferreres, J. Belda, L. Capilla, A. Tallet, J. M. Anon, R. L. Fernandez, J. M. Gonzalez-Martin and A. n. dexamethasone in (2020). "Dexamethasone treatment for the acute respiratory distress syndrome: a multicentre, randomised controlled trial." Lancet Respir Med 8(3): 267-276.

Villar, J., H. Zhang and A. S. Slutsky (2019). "Lung Repair and Regeneration in ARDS: Role of PECAM1 and Wnt Signaling." Chest 155(3): 587-594.

Vincent, J. L., D. C. Angus, A. Artigas, A. Kalil, B. R. Basson, H. H. Jamal, G. Johnson, 3rd, G. R. Bernard and C. W. E. i. S. S. S. G. Recombinant Human Activated Protein (2003). "Effects of drotrecogin alfa (activated) on organ dysfunction in the PROWESS trial." Crit Care Med 31(3): 834-840.

Vlahakis, N. E. and R. D. Hubmayr (2005). "Cellular stress failure in ventilator-injured lungs." Am J Respir Crit Care Med 171(12): 1328-1342.

Voiriot, G., K. Razazi, V. Amsellem, J. Tran Van Nhieu, S. Abid, S. Adnot, A. Mekontso Dessap and B. Maitre (2017). "Interleukin-6 displays lung anti-inflammatory properties and exerts protective hemodynamic effects in a double-hit murine acute lung injury." Respir Res 18(1): 64.

von Bismarck, P., C. F. Wistadt, K. Klemm, S. Winoto-Morbach, U. Uhlig, S. Schutze, D. Adam, B. Lachmann, S. Uhlig and M. F. Krause (2008). "Improved pulmonary function by acid sphingomyelinase inhibition in a newborn piglet lavage model." Am J Respir Crit Care Med 177(11): 1233-1241.

Waerhaug, K., M. Y. Kirov, V. V. Kuzkov, V. N. Kuklin and L. J. Bjertnaes (2008). "Recombinant human activated protein C ameliorates oleic acid-induced lung injury in awake sheep." Crit Care 12(6): R146.

Walbrecq, G., C. Margue, I. Behrmann and S. Kreis (2020). "Distinct Cargos of Small Extracellular Vesicles Derived from Hypoxic Cells and Their Effect on Cancer Cells." Int J Mol Sci 21(14).

Wallez, Y. and P. Huber (2008). "Endothelial adherens and tight junctions in vascular homeostasis, inflammation and angiogenesis." Biochim Biophys Acta 1778(3): 794-809.

Walmrath, D., T. Schneider, R. Schermuly, H. Olschewski, F. Grimminger and W. Seeger (1996). "Direct comparison of inhaled nitric oxide and aerosolized prostacyclin in acute respiratory distress syndrome." Am J Respir Crit Care Med 153(3): 991-996.

Wang, D., B. Fu, Z. Peng, D. Yang, M. Han, M. Li, Y. Yang, T. Yang, L. Sun, W. Li, W. Shi, X. Yao, Y. Ma, F. Xu, X. Wang, J. Chen, D. Xia, Y. Sun, L. Dong, J. Wang, X. Zhu, M. Zhang, Y. Zhou, A. Pan, X. Hu, X. Mei, H. Wei and X. Xu (2021). "Tocilizumab in patients with moderate or severe COVID-19: a randomized, controlled, open-label, multicenter trial." Front Med 15(3): 486-494.

Wang, H., H. Yang and K. J. Tracey (2004). "Extracellular role of HMGB1 in inflammation and sepsis." J Intern Med 255(3): 320-331.

Wang, H., Y. F. Yang, L. Zhao, F. J. Xiao, Q. W. Zhang, M. L. Wen, C. T. Wu, R. Y. Peng and L. S. Wang (2013). "Hepatocyte growth factor gene-modified mesenchymal stem cells reduce radiation-induced lung injury." Hum Gene Ther 24(3): 343-353.

Wang, H., R. Zheng, Q. Chen, J. Shao, J. Yu and S. Hu (2017). "Mesenchymal stem cells microvesicles stabilize endothelial barrier function partly mediated by hepatocyte growth factor (HGF)." Stem Cell Res Ther 8(1): 211.

Wang, H. L., I. O. Akinci, C. M. Baker, D. Urich, A. Bellmeyer, M. Jain, N. S. Chandel, G. M. Mutlu and G. R. Budinger (2007). "The intrinsic apoptotic pathway is required for lipopolysaccharide-induced lung endothelial cell death." J Immunol 179(3): 1834-1841.

Wang, H. M., M. Bodenstein and K. Markstaller (2008). "Overview of the pathology of three widely used animal models of acute lung injury." Eur Surg Res 40(4): 305-316.

Wang, J., L. Oppenheimer, P. Fata, J. Pintin, R. Stimpson and H. H. Mantsch (1999). "Spectroscopic approach to capillary-alveolar membrane damage induced acute lung injury." Can Respir J 6(6): 499-506.

Wang, L., J. A. Bastarache, N. Wickersham, X. Fang, M. A. Matthay and L. B. Ware (2007). "Novel role of the human alveolar epithelium in regulating intra-alveolar coagulation." Am J Respir Cell Mol Biol 36(4): 497-503.

Wang, M., R. Cao, L. Zhang, X. Yang, J. Liu, M. Xu, Z. Shi, Z. Hu, W. Zhong and G. Xiao (2020). "Remdesivir and chloroquine effectively inhibit the recently emerged novel coronavirus (2019-nCoV) in vitro." Cell Res 30(3): 269-271.

Wang, T., D. M. Gilkes, N. Takano, L. Xiang, W. Luo, C. J. Bishop, P. Chaturvedi, J. J. Green and G. L. Semenza (2014). "Hypoxia-inducible

factors and RAB22A mediate formation of microvesicles that stimulate breast cancer invasion and metastasis." Proc Natl Acad Sci U S A 111(31): E3234-3242.

Wang, Y., H. Li, X. Li, X. Su, H. Xiao and J. Yang (2021). "Hypoxic Preconditioning of Human Umbilical Cord Mesenchymal Stem Cells Is an Effective Strategy for Treating Acute Lung Injury." Stem Cells Dev 30(3): 128-134.

Ward, N. S., A. B. Waxman, R. J. Homer, L. L. Mantell, O. Einarsson, Y. Du and J. A. Elias (2000). "Interleukin-6-induced protection in hyperoxic acute lung injury." Am J Respir Cell Mol Biol 22(5): 535-542.

Ware, L. B., M. D. Eisner, B. T. Thompson, P. E. Parsons and M. A. Matthay (2004). "Significance of von Willebrand factor in septic and nonseptic patients with acute lung injury." Am J Respir Crit Care Med 170(7): 766-772.

Ware, L. B. and M. A. Matthay (2000). "The acute respiratory distress syndrome." N Engl J Med 342(18): 1334-1349.

Ware, L. B. and M. A. Matthay (2001). "Alveolar fluid clearance is impaired in the majority of patients with acute lung injury and the acute respiratory distress syndrome." Am J Respir Crit Care Med 163(6): 1376-1383.

Ware, L. B. and M. A. Matthay (2002). "Keratinocyte and hepatocyte growth factors in the lung: roles in lung development, inflammation, and repair." Am J Physiol Lung Cell Mol Physiol 282(5): L924-940.

Waterman, R. S., S. L. Tomchuck, S. L. Henkle and A. M. Betancourt (2010). "A new mesenchymal stem cell (MSC) paradigm: polarization into a pro-inflammatory MSC1 or an Immunosuppressive MSC2 phenotype." PLoS One 5(4): e10088.

Watson, W. H., J. D. Ritzenthaler and J. Roman (2016). "Lung extracellular matrix and redox regulation." Redox Biol 8: 305-315.

Weg, J. G., R. A. Balk, R. S. Tharratt, S. G. Jenkinson, J. B. Shah, D. Zaccardelli, J. Horton and E. N. Pattishall (1994). "Safety and potential efficacy of an aerosolized surfactant in human sepsis-induced adult respiratory distress syndrome." JAMA 272(18): 1433-1438.

Weibel, E. R. (1973). "Morphological basis of alveolar-capillary gas exchange." Physiol Rev 53(2): 419-495.

Weibel, E. R. (2015). "On the tricks alveolar epithelial cells play to make a good lung." Am J Respir Crit Care Med 191(5): 504-513.

Weigelt, J. A., J. F. Norcross, K. R. Borman and W. H. Snyder, 3rd (1985). "Early steroid therapy for respiratory failure." Arch Surg 120(5): 536-540.

Welbourn, C. R. and Y. Young (1992). "Endotoxin, septic shock and acute lung injury: neutrophils, macrophages and inflammatory mediators." Br J Surg 79(10): 998-1003.

Wheeler, A. P. and G. R. Bernard (2007). "Acute lung injury and the acute respiratory distress syndrome: a clinical review." Lancet 369(9572): 1553-1564.

Whitsett, J. A., S. E. Wert and T. E. Weaver (2010). "Alveolar surfactant homeostasis and the pathogenesis of pulmonary disease." Annu Rev Med 61: 105-119.

Wiener-Kronish, J. P., K. H. Albertine and M. A. Matthay (1991). "Differential responses of the endothelial and epithelial barriers of the lung in sheep to Escherichia coli endotoxin." J Clin Invest 88(3): 864-875.

Willson, D. F., N. J. Thomas, B. P. Markovitz, L. A. Bauman, J. V. DiCarlo, S. Pon, B. R. Jacobs, L. S. Jefferson, M. R. Conaway, E. A. Egan, I. Pediatric Acute Lung and I. Sepsis (2005). "Effect of exogenous surfactant (calfactant) in pediatric acute lung injury: a randomized controlled trial." JAMA 293(4): 470-476.

Winn, R. K. and J. M. Harlan (2005). "The role of endothelial cell apoptosis in inflammatory and immune diseases." J Thromb Haemost 3(8): 1815-1824.

Witwer, K. W., E. I. Buzas, L. T. Bemis, A. Bora, C. Lasser, J. Lotvall, E. N. Nolte-'t Hoen, M. G. Piper, S. Sivaraman, J. Skog, C. Thery, M. H. Wauben and F. H. Hochberg (2013). "Standardization of sample collection, isolation and analysis methods in extracellular vesicle research." Journal of Extracellular Vesicles 2(1): 20360.

Wort, S. J., M. Woods, T. D. Warner, T. W. Evans and J. A. Mitchell (2001). "Endogenously released endothelin-1 from human pulmonary artery smooth muscle promotes cellular proliferation: relevance to pathogenesis of pulmonary hypertension and vascular remodeling." Am J Respir Cell Mol Biol 25(1): 104-110.

Wright, S. D., R. A. Ramos, P. S. Tobias, R. J. Ulevitch and J. C. Mathison (1990). "CD14, a receptor for complexes of lipopolysaccharide (LPS) and LPS binding protein." Science 249(4975): 1431-1433.

Wu, X., Z. Liu, L. Hu, W. Gu and L. Zhu (2018). "Exosomes derived from endothelial progenitor cells ameliorate acute lung injury by transferring miR-126." Exp Cell Res 370(1): 13-23.

Wunsch, H. (2020). "Mechanical Ventilation in COVID-19: Interpreting the Current Epidemiology." Am J Respir Crit Care Med 202(1): 1-4.

Xiao, K., F. Hou, X. Huang, B. Li, Z. R. Qian and L. Xie (2020). "Mesenchymal stem cells: current clinical progress in ARDS and COVID-19." Stem Cell Res Ther 11(1): 305.

Xie, F., S. Liu, J. Wang, J. Xuan, X. Zhang, L. Qu, L. Zheng and J. Yang (2020). "deepBase v3.0: expression atlas and interactive analysis of ncRNAs from thousands of deep-sequencing data." Nucleic Acids Research 49(D1): D877-D883.

Xing, Z., J. Gauldie, G. Cox, H. Baumann, M. Jordana, X. F. Lei and M. K. Achong (1998). "IL-6 is an antiinflammatory cytokine required for controlling local or systemic acute inflammatory responses." J Clin Invest 101(2): 311-320.

Xu, J., J. Qu, L. Cao, Y. Sai, C. Chen, L. He and L. Yu (2008). "Mesenchymal stem cell-based angiopoietin-1 gene therapy for acute lung injury induced by lipopolysaccharide in mice." J Pathol 214(4): 472-481.

Xu, X., M. Han, T. Li, W. Sun, D. Wang, B. Fu, Y. Zhou, X. Zheng, Y. Yang, X. Li, X. Zhang, A. Pan and H. Wei (2020). "Effective treatment of severe COVID-19 patients with tocilizumab." Proc Natl Acad Sci U S A 117(20): 10970-10975.

Xu, X. W., X. X. Wu, X. G. Jiang, K. J. Xu, L. J. Ying, C. L. Ma, S. B. Li, H. Y. Wang, S. Zhang, H. N. Gao, J. F. Sheng, H. L. Cai, Y. Q. Qiu and L. J. Li

(2020). "Clinical findings in a group of patients infected with the 2019 novel coronavirus (SARS-Cov-2) outside of Wuhan, China: retrospective case series." BMJ 368: m606.

Xu, Z., L. Shi, Y. Wang, J. Zhang, L. Huang, C. Zhang, S. Liu, P. Zhao, H. Liu, L. Zhu, Y. Tai, C. Bai, T. Gao, J. Song, P. Xia, J. Dong, J. Zhao and F. S. Wang (2020). "Pathological findings of COVID-19 associated with acute respiratory distress syndrome." Lancet Respir Med 8(4): 420-422.

Xue, C., Y. Shen, X. Li, B. Li, S. Zhao, J. Gu, Y. Chen, B. Ma, J. Wei, Q. Han and R. C. Zhao (2018). "Exosomes Derived from Hypoxia-Treated Human Adipose Mesenchymal Stem Cells Enhance Angiogenesis Through the PKA Signaling Pathway." Stem Cells Dev 27(7): 456-465.

Xue, M., Z. Sun, M. Shao, J. Yin, Z. Deng, J. Zhang, L. Xing, X. Yang, B. Chen, Z. Dong, Y. Han, S. Sun, Y. Wang, C. Yao, X. Chu, C. Tong and Z. Song (2015). "Diagnostic and prognostic utility of tissue factor for severe sepsis and sepsis-induced acute lung injury." J Transl Med 13: 172.

Yan, S. B., J. D. Helterbrand, D. L. Hartman, T. J. Wright and G. R. Bernard (2001). "Low levels of protein C are associated with poor outcome in severe sepsis." Chest 120(3): 915-922.

Yanagi, S., H. Tsubouchi, A. Miura, N. Matsumoto and M. Nakazato (2015). "Breakdown of Epithelial Barrier Integrity and Overdrive Activation of Alveolar Epithelial Cells in the Pathogenesis of Acute Respiratory Distress Syndrome and Lung Fibrosis." Biomed Res Int 2015: 573210.

Yanez-Mo, M., P. R. Siljander, Z. Andreu, A. B. Zavec, F. E. Borras, E. I. Buzas, K. Buzas, E. Casal, F. Cappello, J. Carvalho, E. Colas, A. Cordeiro-da Silva, S. Fais, J. M. Falcon-Perez, I. M. Ghobrial, B. Giebel, M. Gimona, M. Graner, I. Gursel, M. Gursel, N. H. Heegaard, A. Hendrix, P. Kierulf, K. Kokubun, M. Kosanovic, V. Kralj-Iglic, E. M. Kramer-Albers, S. Laitinen, C. Lasser, T. Lener, E. Ligeti, A. Line, G. Lipps, A. Llorente, J. Lotvall, M. Mancek-Keber, A. Marcilla, M. Mittelbrunn, I. Nazarenko, E. N. Nolte-'t Hoen, T. A. Nyman, L. O'Driscoll, M. Olivan, C. Oliveira, E. Pallinger, H. A. Del Portillo, J. Reventos, M. Rigau, E. Rohde, M. Sammar, F. Sanchez-Madrid, N. Santarem, K. Schallmoser, M. S. Ostenfeld, W. Stoorvogel, R. Stukelj, S. G. Van der Grein, M. H. Vasconcelos, M. H. Wauben and O. De Wever (2015). "Biological properties of extracellular vesicles and their physiological functions." J Extracell Vesicles 4: 27066.

Yang, C. Y., C. S. Chen, G. T. Yiang, Y. L. Cheng, S. B. Yong, M. Y. Wu and C. J. Li (2018). "New Insights into the Immune Molecular Regulation of the Pathogenesis of Acute Respiratory Distress Syndrome." Int J Mol Sci 19(2).

Yang, J. X., N. Zhang, H. W. Wang, P. Gao, Q. P. Yang and Q. P. Wen (2015). "CXCR4 receptor overexpression in mesenchymal stem cells facilitates treatment of acute lung injury in rats." J Biol Chem 290(4): 1994-2006.

Yang, X., D. Coriolan, V. Murthy, K. Schultz, D. T. Golenbock and D. Beasley (2005). "Proinflammatory phenotype of vascular smooth muscle cells: role of efficient Toll-like receptor 4 signaling." Am J Physiol Heart Circ Physiol 289(3): H1069-1076.

Yehya, N. (2019). "Lessons learned in acute respiratory distress syndrome from the animal laboratory." Ann Transl Med 7(19): 503.

Yi, X., X. Wei, H. Lv, Y. An, L. Li, P. Lu, Y. Yang, Q. Zhang, H. Yi and G. Chen (2019). "Exosomes derived from microRNA-30b-3p-overexpressing mesenchymal stem cells protect against lipopolysaccharide-induced acute lung injury by inhibiting SAA3." Exp Cell Res 383(2): 111454.

Yin, Q., D. Jiang, L. Li, Y. Yang, P. Wu, Y. Luo, R. Yang and D. Li (2017). "LPS Promotes Vascular Smooth Muscle Cells Proliferation Through the TLR4/Rac1/Akt Signalling Pathway." Cell Physiol Biochem 44(6): 2189-2200.

Yoshida, T., V. Torsani, S. Gomes, R. R. De Santis, M. A. Beraldo, E. L. Costa, M. R. Tucci, W. A. Zin, B. P. Kavanagh and M. B. Amato (2013). "Spontaneous effort causes occult pendelluft during mechanical ventilation." Am J Respir Crit Care Med 188(12): 1420-1427.

Zambon, M. and J. L. Vincent (2008). "Mortality rates for patients with acute lung injury/ARDS have decreased over time." Chest 133(5): 1120-1127.

Zapol, W. M. and M. T. Snider (1977). "Pulmonary hypertension in severe acute respiratory failure." N Engl J Med 296(9): 476-480.

Zarbock, A., K. Singbartl and K. Ley (2006). "Complete reversal of acid-induced acute lung injury by blocking of platelet-neutrophil aggregation." J Clin Invest 116(12): 3211-3219.

Zemans, R. L. and M. A. Matthay (2004). "Bench-to-bedside review: the role of the alveolar epithelium in the resolution of pulmonary edema in acute lung injury." Crit Care 8(6): 469-477.

Zeyed, Y. F., J. A. Bastarache, M. A. Matthay and L. B. Ware (2012). "The severity of shock is associated with impaired rates of net alveolar fluid clearance in clinical acute lung injury." Am J Physiol Lung Cell Mol Physiol 303(6): L550-555.

Zhai, P., Y. Ding, X. Wu, J. Long, Y. Zhong and Y. Li (2020). "The epidemiology, diagnosis and treatment of COVID-19." Int J Antimicrob Agents 55(5): 105955.

Zhang, H., F. He, P. Li, P. R. Hardwidge, N. Li and Y. Peng (2021). "The Role of Innate Immunity in Pulmonary Infections." Biomed Res Int 2021: 6646071.

Zhang, H. C., X. B. Liu, S. Huang, X. Y. Bi, H. X. Wang, L. X. Xie, Y. Q. Wang, X. F. Cao, J. Lv, F. J. Xiao, Y. Yang and Z. K. Guo (2012). "Microvesicles derived from human umbilical cord mesenchymal stem cells stimulated by hypoxia promote angiogenesis both in vitro and in vivo." Stem Cells Dev 21(18): 3289-3297.

Zhang, J., L. Terreni, M. G. De Simoni and A. J. Dunn (2001). "Peripheral interleukin-6 administration increases extracellular concentrations of serotonin and the evoked release of serotonin in the rat striatum." Neurochem Int 38(4): 303-308.

Zhang, L., Z. Wang, F. Xu, Y. Ren, H. Wang, D. Han, J. Lyu and H. Yin (2021). "The Role of Glucocorticoids in the Treatment of ARDS: A Multicenter Retrospective Study Based on the eICU Collaborative Research Database." Front Med (Lausanne) 8: 678260.

Zhang, W., X. Zhou, Q. Yao, Y. Liu, H. Zhang and Z. Dong (2017). "HIF-1-mediated production of exosomes during hypoxia is protective in renal tubular cells." Am J Physiol Renal Physiol 313(4): F906-F913.

Zhang, X., J. Chen, M. Xue, Y. Tang, J. Xu, L. Liu, Y. Huang, Y. Yang, H. Qiu and F. Guo (2019). "Overexpressing p130/E2F4 in mesenchymal stem cells facilitates the repair of injured alveolar epithelial cells in LPS-induced ARDS mice." Stem Cell Res Ther 10(1): 74.

Zhao, L., H. Luo, X. Li, T. Li, J. He, Q. Qi, Y. Liu and Z. Yu (2017). "Exosomes Derived from Human Pulmonary Artery Endothelial Cells Shift the Balance between Proliferation and Apoptosis of Smooth Muscle Cells." Cardiology 137(1): 43-53.

Zheng, J. (2020). "SARS-CoV-2: an Emerging Coronavirus that Causes a Global Threat." Int J Biol Sci 16(10): 1678-1685.

Zheng, Y., J. Liu, P. Chen, L. Lin, Y. Luo, X. Ma, J. Lin, Y. Shen and L. Zhang (2021). "Exosomal miR-22-3p from human umbilical cord blood-derived mesenchymal stem cells protects against lipopolysaccharid-induced acute lung injury." Life Sci 269: 119004.

Zhou, X., Z. Cheng, L. Luo, Y. Zhu, W. Lin, Z. Ming, W. Chen and Y. Hu (2021). "Incidence and impact of disseminated intravascular coagulation in COVID-19 a systematic review and meta-analysis." Thromb Res 201: 23-29.

Zhou, Y., P. Li, A. J. Goodwin, J. A. Cook, P. V. Halushka, E. Chang and H. Fan (2018). "Exosomes from Endothelial Progenitor Cells Improve the Outcome of a Murine Model of Sepsis." Mol Ther 26(5): 1375-1384.

Zhou, Y., P. Li, A. J. Goodwin, J. A. Cook, P. V. Halushka, E. Chang, B. Zingarelli and H. Fan (2019). "Exosomes from endothelial progenitor cells improve outcomes of the lipopolysaccharide-induced acute lung injury." Crit Care 23(1): 44.

Zhu, L. P., T. Tian, J. Y. Wang, J. N. He, T. Chen, M. Pan, L. Xu, H. X. Zhang, X. T. Qiu, C. C. Li, K. K. Wang, H. Shen, G. G. Zhang and Y. P. Bai (2018). "Hypoxia-elicited mesenchymal stem cell-derived exosomes facilitates cardiac repair through miR-125b-mediated prevention of cell death in myocardial infarction." Theranostics 8(22): 6163-6177.

Zhu, Y. G., X. M. Feng, J. Abbott, X. H. Fang, Q. Hao, A. Monsel, J. M. Qu, M. A. Matthay and J. W. Lee (2014). "Human mesenchymal stem cell microvesicles for treatment of Escherichia coli endotoxin-induced acute lung injury in mice." Stem Cells 32(1): 116-125.

Zitnik, R. J., N. L. Whiting and J. A. Elias (1994). "Glucocorticoid inhibition of interleukin-1-induced interleukin-6 production by human lung fibroblasts: evidence for transcriptional and post-transcriptional regulatory mechanisms." Am J Respir Cell Mol Biol 10(6): 643-650.

ANNEX I

Table 1. Clean data Proteomics

											Normalized abundance							
											NMX				HPX			
Accession	Peptide count	Unique peptides	Confidence score	Anova (p)	q Value	Max fold change	Power	Highest mean condition	Mass	Description	1_LM_NMX23_L1	3_LM_NMX14_L2	5_LM_NMX15_L3	7_LM_NMX25_L4	2_LM_HPX23_L5	4_LM_HPX14_L6	6_LM_HPX15_L7	8_LM_HPX25_L8
AGM1	2,00	2,00	108,14	0,02	1,00	1,41	1,00	HPX	60270,00	Phosphoacetylglucosamine mutase GN=PGM3	4,18E+04	1,99E+04	3,77E+04	5,40E+04	4,95E+04	2,71E+04	6,35E+04	7,67E+04
TPBG	2,00	2,00	72,99	0,08	1,00	1,92	0,85	HPX	46573,00	Trophoblast glycoprotein GN=TPBG	8,53E+04	4,25E+04	2,26E+05	3,12E+04	9,39E+04	1,19E+05	3,79E+05	1,47E+05
PABP1	2,00	2,00	86,53	0,05	1,00	1,63	0,90	HPX	70854,00	Polyadenylate-binding protein 1 GN=PABPC1	7,77E+04	7,78E+04	1,28E+05	8,24E+04	1,19E+05	1,78E+05	2,06E+05	9,23E+04
ARL8B	3,00	3,00	148,73	0,00	1,00	1,12	1,00	HPX	21753,00	ADP-ribosylation factor-like protein 8B GN=ARL8B	9,14E+04	1,66E+05	1,06E+05	7,18E+04	1,02E+05	1,86E+05	1,22E+05	7,86E+04
K1C18	4,00	3,00	207,14	0,08	1,00	1,46	1,00	HPX	48029,00	Keratin, type I cytoskeletal 18 GN=KRT18	3,47E+05	4,14E+05	4,37E+05	1,05E+05	7,27E+05	5,58E+05	4,59E+05	1,52E+05
COCA1	67,00	67,00	3721,95	0,00	1,00	1,27	1,00	NMX	334138,00	Collagen alpha-1(XII) chain GN=COL12A1	2,28E+06	1,69E+06	3,08E+06	3,62E+06	1,67E+06	1,30E+06	2,35E+06	3,10E+06
FCL	2,00	2,00	69,19	0,10	1,00	1,35	0,62	HPX	36098,00	GDP-L-fucose synthase GN=TSTA3	3,47E+04	3,55E+04	4,89E+04	5,13E+04	6,37E+04	3,86E+04	7,09E+04	5,75E+04
EGLN	9,00	9,00	519,95	0,07	1,00	1,33	1,00	HPX	71559,00	Endoglin GN=ENG	6,83E+05	5,91E+05	2,00E+06	5,16E+05	1,03E+06	9,68E+05	2,53E+06	5,25E+05
CTR1	3,00	3,00	212,64	0,03	1,00	1,32	1,00	HPX	68449,00	High affinity cationic amino acid transporter 1 GN=SLC7A1	3,64E+05	4,55E+05	5,54E+05	3,81E+05	4,84E+05	4,95E+05	7,96E+05	5,46E+05
FBLN1	**6,00**	**6,00**	**357,47**	**0,03**	**1,00**	**1,76**	**0,95**	**NMX**	**81268,00**	**Fibulin-1 GN=FBLN1**	**7,98E+05**	**5,10E+05**	**3,69E+05**	**4,73E+05**	**3,44E+05**	**2,54E+05**	**2,40E+05**	**3,84E+05**
GIPC1	2,00	2,00	114,97	0,02	1,00	1,25	1,00	HPX	36141,00	PDZ domain-containing protein GIPC1 GN=GIPC1	1,19E+05	1,01E+05	1,69E+05	4,72E+04	1,46E+05	1,33E+05	1,93E+05	7,20E+04
PGM1	5,00	5,00	258,00	0,07	1,00	1,29	1,00	HPX	61696,00	Phosphoglucomutase-1 GN=PGM1	5,26E+04	6,45E+04	9,74E+04	1,36E+05	8,78E+04	7,49E+04	1,07E+05	1,81E+05
HBB	2,00	2,00	87,63	0,00	1,00	1,25	1,00	HPX	16102,00	Hemoglobin subunit beta GN=HBB	8,99E+06	9,83E+06	6,43E+06	2,68E+07	1,19E+07	1,16E+07	8,53E+06	3,32E+07
RL3	3,00	3,00	166,26	0,09	1,00	1,28	0,48	HPX	46365,00	60S ribosomal protein L3 GN=RPL3	1,71E+05	2,46E+05	2,09E+05	2,39E+05	2,88E+05	3,12E+05	2,19E+05	2,85E+05
ILK	10,00	10,00	452,40	0,05	1,00	1,31	1,00	HPX	51899,00	Integrin-linked protein kinase GN=ILK	2,21E+05	2,37E+05	3,33E+05	4,78E+05	3,68E+05	2,64E+05	4,38E+05	5,88E+05
ITB5	3,00	3,00	136,95	0,02	1,00	1,28	1,00	HPX	91303,00	Integrin beta-5 GN=ITGB5	2,44E+05	1,53E+05	2,52E+05	1,43E+05	3,17E+05	2,22E+05	2,81E+05	1,92E+05
PLAK	16,00	11,00	839,40	0,05	1,00	1,20	1,00	HPX	82434,00	Junction plakoglobin GN=JUP	4,50E+05	4,70E+05	7,96E+05	3,08E+05	5,15E+05	5,02E+05	9,80E+05	4,38E+05
K22E	**10,00**	**7,00**	**611,11**	**0,04**	**1,00**	**1,59**	**0,98**	**NMX**	**65678,00**	**Keratin, type II cytoskeletal 2 epidermal GN=KRT2**	**8,61E+05**	**1,06E+06**	**6,54E+05**	**7,87E+05**	**3,55E+05**	**8,95E+05**	**4,30E+05**	**4,35E+05**
FIBB	5,00	5,00	165,21	0,10	1,00	1,24	1,00	NMX	56577,00	Fibrinogen beta chain GN=FGB	4,10E+04	9,22E+04	4,03E+04	4,16E+05	4,14E+04	8,32E+04	3,22E+04	3,19E+05
RASN;RASH	3,00	3,00	157,07	0,06	1,00	1,20	1,00	HPX	21501,00	GTPase NRas GN=NRAS	2,28E+05	2,39E+05	4,51E+05	2,43E+05	3,35E+05	2,73E+05	4,83E+05	2,98E+05
VP37B	3,00	3,00	158,67	0,10	1,00	1,25	0,99	NMX	31345,00	Vacuolar protein sorting-associated protein 37B GN=VPS37B	6,80E+04	1,29E+05	9,73E+04	5,54E+04	5,63E+04	1,07E+05	6,28E+04	5,44E+04
RSSA	2,00	2,00	120,12	0,07	1,00	1,17	0,94	HPX	32947,00	40S ribosomal protein SA GN=RPSA	1,43E+05	2,07E+05	1,48E+05	1,67E+05	1,79E+05	2,24E+05	1,96E+05	1,76E+05
LAMC1	9,00	9,00	472,13	0,02	1,00	1,37	1,00	NMX	183191,00	Laminin subunit gamma-1 GN=LAMC1	6,53E+05	3,10E+05	3,22E+05	3,22E+05	4,17E+05	2,56E+05	2,45E+05	2,56E+05
ALBU	5,00	5,00	329,74	0,06	1,00	1,27	1,00	NMX	71317,00	Serum albumin GN=ALB	8,12E+06	1,02E+07	3,29E+06	2,09E+07	5,48E+06	8,82E+06	3,12E+06	1,62E+07
DNSL1	2,00	2,00	129,55	0,06	1,00	1,32	0,95	NMX	34214,00	Deoxyribonuclease-1-like 1 GN=DNASE1L1	3,10E+05	2,63E+05	4,43E+05	2,66E+05	2,03E+05	1,78E+05	3,26E+05	2,65E+05
ARF1	8,00	4,00	470,26	0,09	1,00	1,16	1,00	HPX	20741,00	ADP-ribosylation factor 1 GN=ARF1	1,69E+06	1,64E+06	2,86E+06	1,73E+06	2,01E+06	2,11E+06	2,79E+06	2,24E+06
LOXL2	10,00	10,00	581,06	0,09	1,00	1,33	0,97	NMX	88778,00	Lysyl oxidase homolog 2 GN=LOXL2	3,03E+06	2,40E+06	1,74E+06	1,45E+06	2,00E+06	1,52E+06	1,58E+06	1,38E+06
PAPS2	6,00	6,00	280,59	0,04	1,00	1,50	1,00	HPX	70027,00	Bifunctional 3'-phosphoadenosine 5'-phosphosulfate synthase 2 GN=PAPSS2	2,97E+05	2,42E+05	6,14E+05	1,99E+05	6,19E+05	3,89E+05	7,65E+05	2,55E+05
PGBM	67,00	67,00	4314,14	0,01	1,00	1,43	1,00	NMX	479253,00	Basement membrane-specific heparan sulfate proteoglycan core protein GN=HSPG2	5,09E+06	3,33E+06	2,92E+06	2,36E+06	3,08E+06	2,36E+06	2,42E+06	1,73E+06
PROF1	3,00	3,00	125,30	0,03	1,00	1,31	0,50	HPX	15216,00	Profilin-1 GN=PFN1	3,24E+05	3,37E+05	3,02E+05	3,30E+05	4,29E+05	3,71E+05	4,66E+05	4,29E+05
RALA	5,00	5,00	235,71	0,04	1,00	1,20	1,00	HPX	23723,00	Ras-related protein Ral-A GN=RALA	1,15E+06	1,24E+06	1,70E+06	8,47E+05	1,22E+06	1,68E+06	2,03E+06	9,94E+05
H12;H1T	2,00	2,00	96,08	0,10	1,00	1,18	1,00	NMX	21352,00	Histone H1.2 GN=HIST1H1C	7,54E+04	4,35E+05	6,39E+04	7,59E+04	5,03E+04	4,05E+05	5,70E+04	4,06E+04
ARPC3	3,00	3,00	105,81	0,11	1,00	1,41	0,44	HPX	20761,00	Actin-related protein 2/3 complex subunit 3 GN=ARPC3	2,05E+05	2,17E+05	3,19E+05	2,74E+05	4,42E+05	2,40E+05	4,14E+05	3,37E+05
AGRIN	10,00	10,00	500,83	0,11	1,00	1,47	0,89	NMX	225246,00	Agrin GN=AGRN	5,68E+05	2,08E+05	2,37E+05	1,97E+05	3,23E+05	1,86E+05	2,21E+05	9,57E+04
K2C1	19,00	15,00	1244,38	0,11	1,00	1,46	0,43	NMX	66170,00	Keratin, type II cytoskeletal 1 GN=KRT1	2,93E+06	3,25E+06	2,09E+06	2,78E+06	1,15E+06	2,87E+06	1,77E+06	1,79E+06
NID2	14,00	11,00	701,08	0,11	1,00	1,47	1,00	NMX	153952,00	Nidogen-2 GN=NID2	2,92E+06	1,21E+06	9,64E+05	1,05E+06	1,45E+06	9,61E+05	8,86E+05	8,70E+05
RS9	6,00	6,00	282,65	0,11	1,00	1,19	0,94	HPX	22635,00	40S ribosomal protein S9 GN=RPS9	3,85E+05	7,57E+05	4,46E+05	5,49E+05	5,98E+05	7,82E+05	5,09E+05	6,50E+05
NEP	11,00	11,00	654,21	0,11	1,00	1,15	1,00	HPX	86144,00	Neprilysin GN=MME	3,48E+05	7,24E+05	4,43E+05	4,26E+05	3,58E+05	8,72E+05	4,57E+05	5,47E+05
GGT1	2,00	2,00	70,42	0,11	1,00	1,27	0,78	NMX	61714,00	Gamma-glutamyltranspeptidase 1 GN=GGT1	2,96E+05	3,10E+05	4,30E+05	3,04E+05	2,65E+05	2,66E+05	3,63E+05	1,64E+05
K1C19	5,00	4,00	263,96	0,12	1,00	1,09	1,00	HPX	44079,00	Keratin, type I cytoskeletal 19 GN=KRT19	3,08E+05	3,49E+05	2,77E+05	2,43E+05	3,64E+05	3,62E+05	3,18E+05	2,44E+05
THY1	3,00	3,00	340,24	0,12	1,00	1,12	1,00	HPX	18151,00	Thy-1 membrane glycoprotein GN=THY1	1,63E+07	1,25E+07	3,90E+07	1,36E+07	2,13E+07	1,27E+07	4,25E+07	1,49E+07
ARF4	7,00	4,00	378,15	0,12	1,00	1,18	0,94	HPX	20612,00	ADP-ribosylation factor 4 GN=ARF4	1,40E+06	1,25E+06	2,21E+06	1,21E+06	1,66E+06	1,84E+06	2,14E+06	1,53E+06
LHPL2	2,00	2,00	63,19	0,12	1,00	1,06	1,00	HPX	25154,00	Lipoma HMGIC fusion partner-like 2 protein GN=LHFPL2 PE=2 SV=2	1,59E+05	4,17E+05	2,33E+05	1,36E+05	1,72E+05	4,12E+05	2,53E+05	1,60E+05
STK25;STK24	2,00	2,00	77,49	0,12	1,00	1,12	1,00	HPX	48310,00	Serine/threonine-protein kinase 25 GN=STK25	5,82E+04	4,37E+04	8,26E+04	8,87E+04	7,16E+04	4,72E+04	9,94E+04	8,71E+04

SC31A	2,00	2,00	79,87	0,12	1,00	1,18	0,86	HPX	133900,00	Protein transport protein Sec31A GN=SEC31A	8,34E+04	1,11E+05	1,39E+05	1,37E+05	1,29E+05	1,25E+05	1,48E+05	1,53E+05
RL28	2,00	2,00	69,42	0,12	1,00	1,22	0,93	HPX	15795,00	60S ribosomal protein L28 GN=RPL28	5,94E+04	1,27E+05	5,52E+04	7,65E+04	7,90E+04	1,33E+05	9,36E+04	8,33E+04
LYOX	2,00	2,00	80,33	0,13	1,00	1,67	0,51	NMX	47599,00	Protein-lysine 6-oxidase GN=LOX	1,62E+05	3,14E+05	1,67E+05	3,33E+05	1,06E+05	6,59E+04	6,52E+04	3,46E+05
MPZL 1	2,00	2,00	88,55	0,13	1,00	1,27	0,71	HPX	29235,00	Myelin protein zero-like protein 1 GN=MPZL1	1,85E+05	3,27E+05	2,63E+05	1,60E+05	2,86E+05	3,02E+05	4,04E+05	2,00E+05
TFR1	10,00	10,00	558,43	0,13	1,00	1,14	0,44	HPX	85274,00	Transferrin receptor protein 1 GN=TFRC	6,75E+05	9,30E+05	8,34E+05	7,83E+05	9,30E+05	9,96E+05	8,91E+05	8,41E+05
SATT	3,00	3,00	161,90	0,13	1,00	1,21	0,44	NMX	56087,00	Neutral amino acid transporter A GN=SLC1A4	6,06E+05	5,38E+05	6,99E+05	5,76E+05	6,30E+05	4,68E+05	5,19E+05	3,81E+05
PSA	2,00	2,00	131,62	0,14	1,00	1,16	0,23	HPX	103895,00	Puromycin-sensitive aminopeptidase GN=NPEPPS	1,57E+05	1,68E+05	1,69E+05	1,80E+05	2,09E+05	1,66E+05	2,14E+05	1,89E+05
ITA5	11,00	11,00	599,30	0,14	1,00	1,12	0,99	HPX	115605,00	Integrin alpha-5 GN=ITGA5	6,83E+05	8,99E+05	9,53E+05	6,87E+05	6,51E+05	1,01E+06	1,14E+06	8,17E+05
RB11B	5,00	5,00	243,34	0,15	1,00	1,28	0,54	HPX	24588,00	Ras-related protein Rab-11B GN=RAB11B	5,49E+05	9,30E+05	4,94E+05	4,04E+05	8,81E+05	8,31E+05	8,25E+05	5,10E+05
S38A2	4,00	4,00	329,18	0,15	1,00	1,17	0,99	NMX	56332,00	Sodium-coupled neutral amino acid transporter 2 GN=SLC38A2	7,85E+05	2,20E+06	1,71E+06	1,37E+06	6,90E+05	1,99E+06	1,15E+06	1,35E+06
RS13	4,00	4,00	133,92	0,15	1,00	1,20	0,81	HPX	17212,00	40S ribosomal protein S13 GN=RPS13	2,88E+05	4,31E+05	2,53E+05	2,40E+05	4,02E+05	4,68E+05	3,51E+05	2,31E+05
RL7	3,00	3,00	142,86	0,15	1,00	1,58	0,60	HPX	29264,00	60S ribosomal protein L7 GN=RPL7	1,45E+05	3,16E+05	2,40E+05	1,35E+05	3,83E+05	5,30E+05	2,72E+05	1,39E+05
GOGA 7	2,00	2,00	123,96	0,15	1,00	1,39	0,63	HPX	16042,00	Golgin subfamily A member 7 GN=GOLGA7	2,03E+05	3,32E+05	3,62E+05	1,15E+05	2,95E+05	3,59E+05	4,25E+05	3,26E+05
K1C10	20,00	19,00	1622,98	0,16	1,00	1,43	0,36	NMX	59020,00	Keratin, type I cytoskeletal 10 GN=KRT10	1,46E+06	1,68E+06	1,19E+06	1,51E+06	9,06E+05	1,73E+06	9,20E+05	5,12E+05
IGSF8	4,00	4,00	222,54	0,16	1,00	1,04	1,00	NMX	65621,00	Immunoglobulin superfamily member 8 GN=IGSF8	3,30E+05	3,79E+05	4,45E+05	2,81E+05	3,38E+05	3,54E+05	4,22E+05	2,68E+05
MOXD 1	2,00	2,00	94,43	0,16	1,00	1,21	1,00	HPX	70520,00	DBH-like monooxygenase protein 1 GN=MOXD1	1,01E+05	1,02E+05	1,89E+05	3,26E+05	1,50E+05	1,00E+05	2,00E+05	4,19E+05
ACTC	22,00	12,00	1564,22	0,16	1,00	1,21	0,79	NMX	42334,00	Actin, alpha cardiac muscle 1 GN=ACTC1	2,35E+07	3,39E+07	1,53E+07	2,55E+07	2,59E+07	2,26E+07	1,16E+07	2,09E+07
NPTN	6,00	6,00	277,05	0,16	1,00	1,38	0,46	HPX	44702,00	Neuroplastin GN=NPTN	7,77E+05	9,05E+05	1,26E+06	4,05E+05	1,06E+06	8,65E+05	1,67E+06	1,01E+06
CYBR1	3,00	3,00	127,39	0,17	1,00	1,13	1,00	HPX	31735,00	Cytochrome b reductase 1 GN=CYBRD1	2,47E+05	4,68E+05	2,92E+05	9,25E+04	3,48E+05	4,28E+05	3,53E+05	1,15E+05
RS2	3,00	3,00	132,07	0,18	1,00	1,19	0,61	HPX	31590,00	40S ribosomal protein S2 GN=RPS2	2,48E+05	4,11E+05	3,24E+05	4,51E+05	3,70E+05	5,33E+05	3,10E+05	4,89E+05
NID1	3,00	2,00	138,98	0,18	1,00	1,54	0,99	NMX	139142,00	Nidogen-1 GN=NID1	2,00E+05	7,22E+04	4,40E+04	1,14E+05	1,05E+05	5,72E+04	5,15E+04	6,46E+04
GSTP1	3,00	3,00	166,01	0,19	1,00	1,16	0,62	HPX	23569,00	Glutathione S-transferase P GN=GSTP1	2,84E+05	5,00E+05	3,62E+05	2,54E+05	4,13E+05	4,48E+05	4,61E+05	3,07E+05
PVR	2,00	2,00	97,36	0,19	1,00	1,11	0,99	HPX	45787,00	Poliovirus receptor GN=PVR	2,41E+05	2,62E+05	5,50E+05	2,38E+05	2,44E+05	2,74E+05	5,98E+05	3,22E+05
BST1	5,00	5,00	228,20	0,19	1,00	1,12	0,86	HPX	36328,00	ADP-ribosyl cyclase/cyclic ADP-ribose hydrolase 2 GN=BST1	6,07E+05	5,89E+05	9,89E+05	7,56E+05	6,99E+05	5,92E+05	1,00E+06	1,01E+06
RTN4	6,00	6,00	379,17	0,20	1,00	1,26	0,89	HPX	130250,00	Reticulon-4 GN=RTN4	1,73E+06	3,15E+06	1,53E+06	9,03E+05	3,07E+06	3,56E+06	1,47E+06	1,10E+06
PLP2	2,00	2,00	108,39	0,20	1,00	1,13	0,95	HPX	17022,00	Proteolipid protein 2 GN=PLP2	3,45E+05	7,01E+05	2,86E+05	3,07E+05	4,80E+05	6,24E+05	3,99E+05	3,55E+05
NIBL1	5,00	5,00	257,94	0,20	1,00	1,14	0,90	NMX	84598,00	Niban-like protein 1 GN=FAM129B	4,91E+05	4,41E+05	9,44E+05	4,70E+05	5,17E+05	3,23E+05	7,65E+05	4,47E+05
COPA	2,00	2,00	108,93	0,20	1,00	1,28	0,22	HPX	139797,00	Coatomer subunit alpha GN=COPA	3,22E+04	3,21E+04	3,81E+04	5,97E+04	4,24E+04	5,18E+04	6,52E+04	4,87E+04
CN37	4,00	4,00	301,16	0,21	1,00	1,64	0,26	NMX	47948,00	2',3'-cyclic-nucleotide 3'-phosphodiesterase GN=CNP	2,49E+05	3,57E+05	8,38E+05	3,86E+05	2,91E+05	2,08E+05	3,06E+05	3,15E+05
RAB7 A	7,00	7,00	385,36	0,21	1,00	1,10	1,00	NMX	23760,00	Ras-related protein Rab-7a GN=RAB7A	8,42E+05	2,06E+06	8,22E+05	7,81E+05	6,35E+05	1,88E+06	8,08E+05	7,71E+05
SYRC	2,00	2,00	118,65	0,21	1,00	1,21	0,36	HPX	76129,00	Arginine--tRNA ligase, cytoplasmic GN=RARS	1,65E+05	1,39E+05	2,73E+05	2,53E+05	2,26E+05	2,39E+05	2,39E+05	3,02E+05
SC23A	2,00	2,00	136,70	0,21	1,00	1,19	0,73	HPX	87018,00	Protein transport protein Sec23A GN=SEC23A	8,27E+04	5,78E+04	1,88E+05	9,33E+04	1,25E+05	9,75E+04	1,89E+05	8,95E+04
CO1A 1	15,00	15,00	853,10	0,21	1,00	1,33	0,70	NMX	139883,00	Collagen alpha-1(I) chain GN=COL1A1	2,22E+06	5,32E+05	1,00E+06	1,11E+06	1,42E+06	2,77E+05	1,36E+06	5,93E+05
PLOD 1	4,00	4,00	208,28	0,21	1,00	1,19	1,00	HPX	84068,00	Procollagen-lysine,2-oxoglutarate 5-dioxygenase 1 GN=PLOD1	3,66E+05	4,75E+05	4,03E+05	5,49E+05	3,34E+05	6,05E+05	4,45E+05	7,52E+05
ITB1	23,00	23,00	1512,44	0,21	1,00	1,08	0,92	HPX	91664,00	Integrin beta-1 GN=ITGB1	1,10E+07	1,26E+07	1,90E+07	1,17E+07	1,12E+07	1,31E+07	1,98E+07	1,48E+07
RS24	2,00	2,00	101,65	0,22	1,00	1,12	0,89	HPX	15413,00	40S ribosomal protein S24 GN=RPS24	7,35E+04	1,61E+05	8,76E+04	6,53E+04	1,02E+05	1,45E+05	1,14E+05	7,31E+04
CSPG4	20,00	20,00	1019,54	0,22	1,00	1,26	0,59	NMX	251067,00	Chondroitin sulfate proteoglycan 4 GN=CSPG4	4,00E+05	3,22E+05	6,50E+05	7,81E+05	4,85E+05	1,87E+05	3,99E+05	6,33E+05
RL6	4,00	4,00	176,61	0,22	1,00	1,27	0,27	HPX	32765,00	60S ribosomal protein L6 GN=RPL6	1,59E+05	2,77E+05	1,50E+05	1,93E+05	3,17E+05	2,91E+05	1,88E+05	1,95E+05
NRP2	8,00	8,00	372,35	0,22	1,00	1,02	1,00	NMX	106160,00	Neuropilin-2 GN=NRP2	2,74E+05	2,41E+05	3,60E+05	2,53E+05	2,74E+05	2,29E+05	3,49E+05	2,54E+05
ITA3	15,00	15,00	954,71	0,22	1,00	1,11	1,00	HPX	117735,00	Integrin alpha-3 GN=ITGA3	4,05E+06	4,26E+06	6,68E+06	2,36E+06	4,69E+06	4,43E+06	6,57E+06	3,52E+06
NOTC 2	7,00	7,00	406,29	0,22	1,00	1,31	0,56	NMX	279082,00	Neurogenic locus notch homolog protein 2 GN=NOTCH2	1,65E+05	2,81E+05	4,49E+05	2,06E+05	1,96E+05	2,28E+05	2,71E+05	1,45E+05
HBA	5,00	5,00	301,84	0,23	1,00	1,26	0,66	HPX	15305,00	Hemoglobin subunit alpha GN=HBA1	6,84E+06	1,32E+07	7,18E+06	1,95E+07	1,34E+07	1,40E+07	7,02E+06	2,46E+07
MMP 14	5,00	5,00	249,57	0,23	1,00	1,11	0,99	HPX	66194,00	Matrix metalloproteinase-14 GN=MMP14	3,88E+05	1,05E+06	3,35E+05	2,46E+05	3,87E+05	1,06E+06	4,06E+05	3,91E+05
XPO2	3,00	2,00	224,60	0,23	1,00	1,24	0,69	HPX	111145,00	Exportin-2 GN=CSE1L	4,13E+04	1,58E+04	7,10E+04	2,69E+04	7,62E+04	2,35E+04	5,69E+04	3,54E+04
CD63	3,00	3,00	173,23	0,23	1,00	1,21	0,66	HPX	26474,00	CD63 antigen GN=CD63	3,43E+06	5,79E+06	2,38E+06	1,74E+06	3,77E+06	5,74E+06	4,62E+06	2,02E+06
5NTD	19,00	18,00	1226,47	0,23	1,00	1,19	0,58	HPX	63898,00	5'-nucleotidase GN=NT5E	2,85E+06	2,66E+06	5,02E+06	1,97E+06	2,52E+06	3,41E+06	5,75E+06	3,18E+06
MRGR F	2,00	2,00	116,77	0,24	1,00	1,08	1,00	NMX	39172,00	Mas-related G-protein coupled receptor member F GN=MRGPRF PE=2 SV=1	3,75E+05	5,25E+05	4,57E+05	1,59E+05	3,86E+05	4,58E+05	4,00E+05	1,58E+05
PLEC	30,00	27,00	1341,41	0,24	1,00	1,20	0,69	HPX	533462,00	Plectin GN=PLEC	1,23E+06	1,12E+06	8,08E+05	3,55E+05	1,11E+06	1,14E+06	1,35E+06	6,03E+05
TIMP3	8,00	8,00	413,21	0,24	1,00	1,24	0,52	HPX	24813,00	Metalloproteinase inhibitor 3 GN=TIMP3	1,00E+06	1,27E+06	2,79E+06	2,10E+06	1,46E+06	1,53E+06	2,31E+06	3,56E+06
CTL1	5,00	5,00	353,08	0,25	1,00	1,10	0,77	HPX	74793,00	Choline transporter-like protein 1 GN=SLC44A1	4,48E+05	3,76E+05	5,43E+05	3,35E+05	4,17E+05	4,56E+05	6,36E+05	3,55E+05

F234A	2,00	2,00	123,59	0,25	1,00	1,10	0,99	NMX	60249,00	Protein FAM234A GN=FAM234A	2,79E+05	1,57E+05	3,33E+05	1,25E+05	2,21E+05	1,28E+05	3,32E+05	1,30E+05
CD151	2,00	2,00	117,83	0,25	1,00	1,33	0,39	NMX	29132,00	CD151 antigen GN=CD151	2,63E+06	2,70E+06	6,63E+06	2,82E+06	3,02E+06	2,42E+06	4,48E+06	1,18E+06
RAC2	5,00	2,00	200,41	0,25	1,00	1,14	0,52	HPX	21814,00	Ras-related C3 botulinum toxin substrate 2 GN=RAC2	4,45E+05	5,81E+05	5,52E+05	3,68E+05	5,14E+05	5,35E+05	7,72E+05	4,04E+05
ARC1B	3,00	3,00	141,17	0,25	1,00	1,22	0,35	HPX	41722,00	Actin-related protein 2/3 complex subunit 1B GN=ARPC1B	1,53E+05	1,15E+05	2,12E+05	2,19E+05	2,76E+05	1,33E+05	2,04E+05	2,39E+05
1A01	5,00	2,00	275,11	0,25	1,00	1,11	0,95	NMX	41105,00	HLA class I histocompatibility antigen, A-1 alpha chain GN=HLA-A	4,05E+05	4,78E+05	4,34E+05	5,24E+05	3,15E+05	3,90E+05	3,38E+05	6,11E+05
XPO1	2,00	2,00	140,90	0,25	1,00	1,24	0,88	HPX	124447,00	Exportin-1 GN=XPO1	1,08E+05	5,19E+04	1,91E+05	1,20E+05	1,37E+05	1,31E+05	1,67E+05	1,50E+05
CAN1	3,00	3,00	102,21	0,25	1,00	1,19	0,36	HPX	82465,00	Calpain-1 catalytic subunit GN=CAPN1	1,16E+05	1,42E+05	9,29E+04	6,81E+04	1,68E+05	1,17E+05	1,24E+05	8,71E+04
DLG1	3,00	3,00	118,86	0,26	1,00	1,09	1,00	NMX	100678,00	Disks large homolog 1 GN=DLG1	2,11E+05	1,06E+05	4,13E+05	1,95E+05	2,10E+05	8,93E+04	3,46E+05	2,02E+05
#####	3,00	2,00	100,03	0,26	1,00	1,24	0,26	HPX	49652,00	Septin-11 GN=SEPT11	9,98E+04	1,21E+05	9,64E+04	9,98E+04	1,64E+05	1,52E+05	1,17E+05	8,49E+04
PEF1	2,00	2,00	119,70	0,26	1,00	1,28	0,43	HPX	30646,00	Peflin GN=PEF1	1,00E+05	5,88E+04	1,03E+05	7,48E+04	9,81E+04	5,62E+04	1,41E+05	1,34E+05
EPHA 2	23,00	22,00	1368,89	0,26	1,00	1,31	0,21	NMX	109679,00	Ephrin type-A receptor 2 GN=EPHA2	1,10E+06	1,51E+06	2,40E+06	1,53E+06	1,37E+06	1,24E+06	1,63E+06	7,73E+05
VPS35	2,00	2,00	109,59	0,26	1,00	1,41	0,19	NMX	92447,00	Vacuolar protein sorting-associated protein 35 GN=VPS35	9,05E+04	1,73E+05	8,19E+04	9,76E+04	9,53E+04	9,38E+04	9,07E+04	3,57E+04
MOT1	4,00	4,00	160,44	0,27	1,00	1,15	0,99	HPX	54593,00	Monocarboxylate transporter 1 GN=SLC16A1	2,54E+05	2,65E+05	4,12E+05	2,04E+05	3,11E+05	2,49E+05	5,43E+05	2,06E+05
SERPH	6,00	6,00	422,12	0,27	1,00	1,20	0,95	NMX	46525,00	Serpin H1 GN=SERPINH1	3,38E+05	1,34E+06	2,89E+05	4,20E+05	4,06E+05	1,03E+06	2,10E+05	3,36E+05
MUC1 8	3,00	3,00	138,98	0,27	1,00	1,08	0,66	HPX	72532,00	Cell surface glycoprotein MUC18 GN=MCAM	2,97E+05	2,79E+05	3,83E+05	2,24E+05	3,65E+05	2,75E+05	3,74E+05	2,57E+05
PRS10	3,00	3,00	108,87	0,27	1,00	1,13	0,48	HPX	44430,00	26S protease regulatory subunit 10B GN=PSMC6	1,13E+05	1,42E+05	2,34E+05	1,78E+05	1,75E+05	1,65E+05	2,05E+05	2,11E+05
PGS1	2,00	2,00	105,72	0,28	1,00	1,30	0,17	NMX	42027,00	Biglycan GN=BGN	3,27E+05	1,72E+05	1,86E+05	1,58E+05	1,64E+05	1,39E+05	1,81E+05	1,66E+05
PLS3	6,00	6,00	401,93	0,28	1,00	1,18	1,00	NMX	32369,00	Phospholipid scramblase 3 GN=PLSCR3	8,96E+05	1,39E+06	2,12E+06	7,33E+05	8,76E+05	1,30E+06	1,46E+06	7,36E+05
RHOA	10,00	3,00	627,22	0,28	1,00	1,14	0,37	HPX	22096,00	Transforming protein RhoA GN=RHOA	7,12E+05	7,94E+05	1,20E+06	8,01E+05	1,07E+06	8,07E+05	1,35E+06	7,79E+05
SYG	8,00	8,00	368,44	0,28	1,00	1,07	0,93	HPX	83854,00	Glycine--tRNA ligase GN=GARS	4,10E+05	3,23E+05	5,89E+05	6,82E+05	4,03E+05	3,99E+05	6,76E+05	6,66E+05
ACOC	4,00	4,00	236,27	0,28	1,00	1,19	0,48	HPX	98850,00	Cytoplasmic aconitate hydratase GN=ACO1	1,49E+05	2,93E+05	2,85E+05	4,66E+05	2,61E+05	3,34E+05	2,45E+05	5,81E+05
CA2D 1	4,00	4,00	280,19	0,28	1,00	1,17	0,84	NMX	125630,00	Voltage-dependent calcium channel subunit alpha-2/delta-1 GN=CACNA2D1	2,92E+05	2,56E+05	6,04E+05	3,54E+05	3,00E+05	2,35E+05	4,06E+05	3,43E+05
PTK7	7,00	7,00	451,48	0,29	1,00	1,15	0,22	HPX	119799,00	Inactive tyrosine-protein kinase 7 GN=PTK7	5,01E+05	5,03E+05	5,01E+05	5,12E+05	5,17E+05	4,54E+05	6,84E+05	6,55E+05
PLXA1	4,00	2,00	207,68	0,30	1,00	1,12	0,72	HPX	214126,00	Plexin-A1 GN=PLXNA1	2,28E+05	1,40E+05	4,31E+05	2,06E+05	2,03E+05	1,87E+05	4,43E+05	2,88E+05
NSF	2,00	2,00	78,61	0,30	1,00	1,09	0,92	NMX	83055,00	Vesicle-fusing ATPase GN=NSF	1,02E+05	1,49E+05	1,91E+05	2,14E+05	9,72E+04	1,62E+05	1,66E+05	1,80E+05
CO9	2,00	2,00	111,32	0,30	1,00	1,09	0,87	NMX	64615,00	Complement component C9 GN=C9	2,28E+06	2,74E+06	1,94E+06	5,07E+06	1,42E+06	2,37E+06	1,92E+06	5,30E+06
RFTN1	4,00	4,00	148,77	0,31	1,00	1,30	0,17	NMX	63677,00	Raftlin GN=RFTN1	4,38E+05	5,93E+05	1,03E+06	7,73E+05	5,75E+05	4,74E+05	7,32E+05	3,97E+05
TTYH3	3,00	3,00	218,60	0,31	1,00	1,13	0,47	NMX	58477,00	Protein tweety homolog 3 GN=TTYH3	8,44E+05	7,48E+05	7,33E+05	4,09E+05	5,72E+05	7,85E+05	6,50E+05	4,04E+05
GDN	9,00	9,00	525,27	0,31	1,00	1,19	0,97	NMX	44202,00	Glia-derived nexin GN=SERPINE2	2,73E+06	8,31E+05	2,95E+06	1,04E+06	2,49E+06	7,65E+05	1,96E+06	1,13E+06
H4	5,00	5,00	330,55	0,31	1,00	1,02	1,00	NMX	11360,00	Histone H4 GN=HIST1H4A	1,24E+06	1,10E+07	6,62E+05	2,60E+06	7,38E+05	1,16E+07	6,87E+05	2,08E+06
K1C9	10,00	10,00	520,35	0,31	1,00	1,41	0,12	NMX	62255,00	Keratin, type I cytoskeletal 9 GN=KRT9	1,23E+06	7,96E+05	9,17E+05	6,29E+05	2,71E+05	1,17E+06	7,17E+05	3,68E+05
RECK	7,00	7,00	457,42	0,32	1,00	1,06	0,77	NMX	111460,00	Reversion-inducing cysteine-rich protein with Kazal motifs GN=RECK	2,91E+05	3,15E+05	3,39E+05	2,19E+05	2,58E+05	2,64E+05	3,81E+05	1,90E+05
E41L2	4,00	4,00	220,05	0,32	1,00	1,21	0,34	NMX	113032,00	Band 4.1-like protein 2 GN=EPB41L2	2,65E+05	2,31E+05	5,17E+05	4,04E+05	3,24E+05	2,04E+05	3,51E+05	2,95E+05
PSMD 3	4,00	4,00	153,36	0,32	1,00	1,33	0,10	NMX	61054,00	26S proteasome non-ATPase regulatory subunit 3 GN=PSMD3	1,69E+05	2,54E+05	3,15E+05	3,51E+05	2,24E+05	2,29E+05	1,88E+05	1,76E+05
VIME	20,00	20,00	1176,94	0,32	1,00	1,26	0,10	HPX	53676,00	Vimentin GN=VIM	2,29E+06	3,49E+06	3,63E+06	2,98E+06	4,84E+06	2,96E+06	3,83E+06	3,96E+06
RL24	3,00	3,00	173,33	0,32	1,00	1,16	0,22	HPX	17882,00	60S ribosomal protein L24 GN=RPL24	1,47E+05	2,11E+05	1,95E+05	2,70E+05	2,35E+05	2,30E+05	1,71E+05	3,15E+05
UGDH	6,00	6,00	264,63	0,33	1,00	1,19	0,25	HPX	55674,00	UDP-glucose 6-dehydrogenase GN=UGDH	2,71E+05	3,74E+05	5,55E+05	6,36E+05	4,93E+05	4,12E+05	4,64E+05	8,05E+05
SULF1	2,00	2,00	90,34	0,33	1,00	1,20	0,74	HPX	102388,00	Extracellular sulfatase Sulf-1 GN=SULF1	1,56E+05	7,32E+04	9,66E+04	2,95E+05	1,23E+05	9,87E+04	1,23E+05	4,00E+05
DPP4	21,00	21,00	1062,74	0,34	1,00	1,16	0,46	NMX	88907,00	Dipeptidyl peptidase 4 GN=DPP4	2,11E+06	2,95E+06	5,02E+06	5,11E+06	2,23E+06	2,46E+06	3,12E+06	5,30E+06
PLXB2	15,00	14,00	904,72	0,34	1,00	1,34	0,11	NMX	207734,00	Plexin-B2 GN=PLXNB2	1,44E+06	1,70E+06	8,84E+05	9,16E+05	5,83E+05	1,06E+06	7,89E+05	1,26E+06
LDHB	7,00	7,00	357,24	0,34	1,00	1,18	0,21	HPX	36900,00	L-lactate dehydrogenase B chain GN=LDHB	8,98E+05	8,38E+05	1,43E+06	1,20E+06	1,37E+06	8,20E+05	1,24E+06	1,75E+06
CLIC1	9,00	9,00	526,08	0,35	1,00	1,19	0,09	NMX	27248,00	Chloride intracellular channel protein 1 GN=CLIC1	1,66E+06	2,11E+06	2,13E+06	1,54E+06	1,91E+06	1,45E+06	1,30E+06	1,60E+06
LAMP 1	4,00	3,00	176,20	0,35	1,00	1,11	0,98	HPX	45367,00	Lysosome-associated membrane glycoprotein 1 GN=LAMP1	2,19E+05	3,32E+05	2,72E+05	2,07E+05	2,41E+05	4,04E+05	3,18E+05	1,83E+05
PARV A	6,00	3,00	375,56	0,35	1,00	1,24	0,20	HPX	42274,00	Alpha-parvin GN=PARVA	2,70E+05	1,82E+05	5,37E+05	4,55E+05	2,47E+05	4,48E+05	6,33E+05	4,63E+05
GPC6	2,00	2,00	214,28	0,35	1,00	1,17	0,30	NMX	63721,00	Glypican-6 GN=GPC6	6,96E+05	3,56E+05	7,45E+05	5,24E+05	4,88E+05	3,64E+05	5,43E+05	5,89E+05
RADI	10,00	2,00	476,45	0,35	1,00	1,07	0,74	NMX	68635,00	Radixin GN=RDX	4,59E+05	2,60E+05	5,44E+05	3,87E+05	4,73E+05	2,19E+05	4,37E+05	4,08E+05
TLDC1	4,00	4,00	175,30	0,35	1,00	1,09	0,45	HPX	51588,00	TLD domain-containing protein 1 GN=TLDC1	2,02E+05	1,67E+05	3,65E+05	2,03E+05	2,06E+05	2,47E+05	3,48E+05	2,18E+05
GFPT1	3,00	3,00	135,00	0,35	1,00	1,08	0,96	HPX	79555,00	Glutamine--fructose-6-phosphate aminotransferase [isomerizing] 1 GN=GFPT1	1,46E+05	2,51E+05	1,34E+05	4,62E+05	2,21E+05	2,48E+05	2,11E+05	3,90E+05

DPYL3;DPYS	3,00	2,00	143,77	0,35	1,00	1,20	0,12	HPX	62323,00	Dihydropyrimidinase-related protein 3 GN=DPYSL3	1,21E+05	1,48E+05	1,36E+05	1,09E+05	2,00E+05	1,20E+05	1,72E+05	1,23E+05
CEMIP	7,00	7,00	330,58	0,35	1,00	1,21	0,96	HPX	154440,00	Cell migration-inducing and hyaluronan-binding protein GN=CEMIP	5,68E+05	3,84E+05	5,74E+05	7,09E+05	6,78E+05	3,53E+05	5,67E+05	1,10E+06
ADA10	7,00	7,00	291,76	0,35	1,00	1,10	0,58	NMX	86140,00	Disintegrin and metalloproteinase domain-containing protein 10 GN=ADAM10	5,23E+05	8,93E+05	6,93E+05	5,18E+05	4,82E+05	8,35E+05	7,61E+05	3,17E+05
RS4X	6,00	6,00	322,60	0,35	1,00	1,13	0,15	HPX	29807,00	40S ribosomal protein S4, X isoform GN=RPS4X	4,36E+05	7,92E+05	7,38E+05	5,95E+05	7,33E+05	8,59E+05	6,68E+05	6,43E+05
PGFRB	8,00	7,00	488,73	0,35	1,00	1,07	0,84	HPX	124973,00	Platelet-derived growth factor receptor beta GN=PDGFRB	9,14E+05	2,76E+05	7,21E+05	4,28E+05	7,61E+05	3,51E+05	8,03E+05	5,89E+05
AHNK	29,00	28,00	1316,23	0,35	1,00	1,26	0,37	NMX	629213,00	Neuroblast differentiation-associated protein AHNAK GN=AHNAK	8,89E+05	9,48E+05	2,08E+06	6,28E+05	1,09E+06	7,08E+05	1,21E+06	5,87E+05
TSP1	38,00	34,00	2422,49	0,36	1,00	1,17	0,85	NMX	133291,00	Thrombospondin-1 GN=THBS1	1,16E+07	2,77E+06	1,65E+07	7,69E+06	7,24E+06	2,54E+06	1,44E+07	8,90E+06
MINK1	5,00	2,00	179,50	0,36	1,00	1,10	0,29	HPX	150413,00	Misshapen-like kinase 1 GN=MINK1	5,55E+04	5,66E+04	7,76E+04	3,68E+04	5,67E+04	5,29E+04	8,43E+04	5,62E+04
RL18	5,00	5,00	229,34	0,36	1,00	1,15	0,20	HPX	21735,00	60S ribosomal protein L18 GN=RPL18	3,70E+05	8,02E+05	4,23E+05	5,59E+05	6,60E+05	8,15E+05	4,83E+05	5,07E+05
HEXB	2,00	2,00	86,72	0,36	1,00	1,33	0,96	HPX	63527,00	Beta-hexosaminidase subunit beta GN=HEXB	3,34E+04	1,82E+05	3,41E+04	5,71E+04	3,48E+04	2,51E+05	2,78E+04	9,56E+04
AT1A1	23,00	23,00	1455,71	0,37	1,00	1,11	0,59	NMX	114135,00	Sodium/potassium-transporting ATPase subunit alpha-1 GN=ATP1A1	2,07E+06	1,90E+06	3,75E+06	1,49E+06	2,04E+06	2,05E+06	3,36E+06	8,49E+05
PLXD1	3,00	2,00	171,43	0,37	1,00	1,23	0,28	HPX	215293,00	Plexin-D1 GN=PLXND1	1,30E+05	2,28E+05	1,73E+05	2,11E+05	1,53E+05	2,25E+05	1,58E+05	3,74E+05
#####	4,00	3,00	202,58	0,37	1,00	1,17	0,14	HPX	50933,00	Septin-7 GN=SEPT7	1,70E+05	1,65E+05	3,10E+05	2,40E+05	3,06E+05	1,90E+05	2,48E+05	2,90E+05
SNAA	2,00	2,00	104,97	0,37	1,00	1,13	0,22	HPX	33667,00	Alpha-soluble NSF attachment protein GN=NAPA	1,74E+05	1,87E+05	2,15E+05	1,90E+05	1,78E+05	1,67E+05	2,50E+05	2,73E+05
CCD80	6,00	6,00	264,19	0,37	1,00	1,15	0,27	NMX	108505,00	Coiled-coil domain-containing protein 80 GN=CCDC80	2,52E+05	1,29E+05	2,19E+05	2,84E+05	1,80E+05	1,22E+05	2,67E+05	1,99E+05
CALD1	5,00	4,00	211,25	0,37	1,00	1,08	0,35	NMX	93232,00	Caldesmon GN=CALD1	2,92E+05	4,35E+05	3,22E+05	2,74E+05	3,27E+05	3,90E+05	3,03E+05	2,00E+05
SAHH	8,00	8,00	436,84	0,37	1,00	1,10	0,23	HPX	48255,00	Adenosylhomocysteinase GN=AHCY	2,61E+05	3,82E+05	2,89E+05	4,73E+05	3,94E+05	3,49E+05	3,10E+05	4,99E+05
EF1G	7,00	7,00	412,62	0,37	1,00	1,09	0,63	HPX	50429,00	Elongation factor 1-gamma GN=EEF1G	8,84E+05	6,10E+05	1,51E+06	8,56E+05	1,13E+06	8,49E+05	1,21E+06	1,01E+06
2AAA	6,00	6,00	277,67	0,38	1,00	1,15	0,17	HPX	66065,00	Serine/threonine-protein phosphatase 2A 65 kDa regulatory subunit A alpha isoform GN=PPP2R1A	1,62E+05	1,50E+05	3,44E+05	1,36E+05	2,46E+05	1,65E+05	2,57E+05	2,39E+05
SYEP	3,00	3,00	99,88	0,38	1,00	1,13	0,98	HPX	172080,00	Bifunctional glutamate/proline--tRNA ligase GN=EPRS	3,62E+04	5,21E+04	5,17E+04	7,30E+04	3,35E+04	6,44E+04	5,01E+04	9,23E+04
NRP1	10,00	10,00	705,76	0,38	1,00	1,11	0,35	HPX	104323,00	Neuropilin-1 GN=NRP1	1,05E+06	1,18E+06	1,57E+06	7,73E+05	8,83E+05	1,36E+06	1,81E+06	1,03E+06
RL26L	2,00	2,00	60,24	0,38	1,00	1,15	0,25	HPX	17246,00	60S ribosomal protein L26-like 1 GN=RPL26L1	1,48E+05	3,05E+05	2,37E+05	1,10E+05	2,79E+05	2,92E+05	2,12E+05	1,36E+05
SYVC	4,00	4,00	216,16	0,38	1,00	1,16	0,19	HPX	141642,00	Valine--tRNA ligase GN=VARS	6,18E+04	6,96E+04	1,17E+05	6,12E+04	1,10E+05	7,93E+04	1,11E+05	5,80E+04
ANXA5	20,00	19,00	1354,58	0,40	1,00	1,05	0,98	HPX	35971,00	Annexin A5 GN=ANXA5	6,72E+06	1,02E+07	1,44E+07	8,52E+06	8,91E+06	1,02E+07	1,32E+07	9,65E+06
GNAQ	6,00	3,00	261,26	0,40	1,00	1,07	0,22	NMX	42400,00	Guanine nucleotide-binding protein G(q) subunit alpha GN=GNAQ	3,06E+05	3,53E+05	3,87E+05	2,78E+05	2,31E+05	3,14E+05	3,84E+05	3,04E+05
PDIA4	6,00	6,00	319,83	0,40	1,00	1,07	0,88	HPX	73229,00	Protein disulfide-isomerase A4 GN=PDIA4	1,49E+05	3,92E+05	9,87E+04	1,54E+05	2,07E+05	3,87E+05	9,53E+04	1,62E+05
TR10B	3,00	3,00	153,91	0,40	1,00	1,15	0,30	NMX	48874,00	Tumor necrosis factor receptor superfamily member 10B GN=TNFRSF10B	9,88E+04	2,80E+05	2,25E+05	1,27E+05	1,20E+05	2,71E+05	1,84E+05	5,81E+04
DSG2	8,00	7,00	403,72	0,40	1,00	1,04	1,00	HPX	123016,00	Desmoglein-2 GN=DSG2	4,28E+05	6,03E+05	8,49E+05	4,10E+05	5,14E+05	6,06E+05	7,76E+05	4,77E+05
AP2B1	4,00	4,00	194,00	0,40	1,00	1,36	0,09	HPX	105398,00	AP-2 complex subunit beta GN=AP2B1	1,61E+05	1,51E+05	2,65E+05	2,16E+05	3,92E+05	2,80E+05	2,53E+05	1,54E+05
MYO1B	17,00	17,00	775,78	0,40	1,00	1,20	0,14	NMX	132928,00	Unconventional myosin-Ib GN=MYO1B	6,63E+05	7,50E+05	1,35E+06	7,19E+05	8,04E+05	7,23E+05	7,86E+05	5,74E+05
S38A1	2,00	2,00	123,22	0,40	1,00	1,04	0,98	HPX	54639,00	Sodium-coupled neutral amino acid transporter 1 GN=SLC38A1	1,09E+05	2,41E+05	1,12E+05	6,97E+04	1,06E+05	2,32E+05	1,37E+05	7,64E+04
ITB3	5,00	5,00	233,57	0,40	1,00	1,08	0,40	HPX	90194,00	Integrin beta-3 GN=ITGB3	1,23E+05	2,36E+05	1,11E+05	2,42E+05	1,43E+05	1,98E+05	1,68E+05	2,60E+05
HSP7C	21,00	17,00	1450,92	0,41	1,00	1,19	0,12	NMX	71082,00	Heat shock cognate 71 kDa protein GN=HSPA8	5,00E+06	3,27E+06	2,60E+06	2,80E+06	2,84E+06	3,11E+06	2,68E+06	2,89E+06
PYGL	4,00	2,00	205,84	0,41	1,00	1,03	0,94	HPX	97486,00	Glycogen phosphorylase, liver form GN=PYGL	1,52E+05	1,26E+05	2,35E+05	4,73E+05	2,01E+05	1,66E+05	2,17E+05	4,36E+05
CAD11	2,00	2,00	73,89	0,41	1,00	1,05	0,62	HPX	88367,00	Cadherin-11 GN=CDH11 PE=2 SV=2	2,49E+05	2,86E+05	4,79E+05	3,24E+05	2,79E+05	2,74E+05	4,61E+05	3,86E+05
TBB6	14,00	3,00	926,84	0,41	1,00	1,16	0,09	HPX	50281,00	Tubulin beta-6 chain GN=TUBB6	1,81E+05	3,21E+05	4,56E+05	3,13E+05	3,93E+05	3,31E+05	3,82E+05	3,62E+05
RL15	3,00	3,00	132,65	0,42	1,00	1,12	0,09	HPX	24245,00	60S ribosomal protein L15 GN=RPL15	1,43E+05	2,08E+05	1,78E+05	1,99E+05	2,33E+05	2,14E+05	1,67E+05	2,01E+05
NEK7;NEK6	2,00	2,00	86,26	0,42	1,00	1,15	0,19	HPX	34985,00	Serine/threonine-protein kinase Nek7 GN=NEK7	8,25E+04	1,27E+05	1,60E+05	7,86E+04	1,49E+05	1,38E+05	1,54E+05	7,40E+04
IF4G1	2,00	2,00	114,84	0,42	1,00	1,13	0,18	NMX	176124,00	Eukaryotic translation initiation factor 4 gamma 1 GN=EIF4G1	3,35E+05	4,41E+05	6,29E+05	6,04E+05	4,03E+05	3,51E+05	4,37E+05	5,84E+05
CALM	3,00	3,00	189,46	0,43	1,00	1,08	0,23	HPX	16827,00	Calmodulin GN=CALM1	3,82E+05	3,66E+05	5,49E+05	5,87E+05	5,36E+05	3,54E+05	5,86E+05	5,62E+05
TS101	3,00	3,00	138,96	0,43	1,00	1,12	0,19	HPX	44088,00	Tumor susceptibility gene 101 protein GN=TSG101	1,20E+05	1,70E+05	9,43E+04	5,74E+04	9,57E+04	1,73E+05	1,23E+05	1,04E+05
CD81	4,00	4,00	438,27	0,43	1,00	1,11	0,13	HPX	26476,00	CD81 antigen GN=CD81	1,97E+07	2,27E+07	2,49E+07	1,56E+07	1,72E+07	2,29E+07	2,86E+07	2,35E+07
AT2B1	16,00	6,00	1194,89	0,44	1,00	1,10	0,65	NMX	139637,00	Plasma membrane calcium-transporting ATPase 1 GN=ATP2B1	3,70E+05	6,92E+05	7,79E+05	5,07E+05	3,88E+05	6,05E+05	5,98E+05	5,43E+05

EMIL1	9,00	8,00	531,19	0,44	1,00	1,05	0,77	NMX	107913,00	EMILIN-1 GN=EMILIN1	2,39E+05	1,40E+05	3,95E+05	3,64E+05	1,73E+05	1,32E+05	3,74E+05	4,07E+05
CAB39	3,00	2,00	166,85	0,44	1,00	1,08	0,80	HPX	40015,00	Calcium-binding protein 39 GN=CAB39	1,58E+05	1,22E+05	2,71E+05	1,85E+05	1,62E+05	1,13E+05	2,84E+05	2,36E+05
H2A1B	3,00	2,00	209,25	0,44	1,00	1,00	0,84	HPX	14127,00	Histone H2A type 1-B/E GN=HIST1H2AB	7,89E+05	7,67E+06	4,33E+05	2,50E+06	5,40E+05	9,02E+06	4,96E+05	1,39E+06
ZYX	4,00	4,00	258,88	0,44	1,00	1,57	0,12	NMX	62436,00	Zyxin GN=ZYX	1,29E+05	1,53E+05	5,92E+05	1,67E+05	2,61E+05	9,22E+04	2,02E+05	1,06E+05
LEG1	2,00	2,00	61,18	0,44	1,00	1,17	0,12	HPX	15048,00	Galectin-1 GN=LGALS1	1,35E+05	1,97E+05	1,85E+05	2,33E+05	2,10E+05	1,45E+05	2,14E+05	3,09E+05
FLNB	26,00	17,00	1478,87	0,44	1,00	1,07	0,26	NMX	280157,00	Filamin-B GN=FLNB	1,17E+06	9,63E+05	1,06E+06	7,44E+05	1,28E+06	9,76E+05	7,60E+05	6,70E+05
RS14	3,00	3,00	152,83	0,44	1,00	1,22	0,08	HPX	16434,00	40S ribosomal protein S14 GN=RPS14	8,48E+04	2,12E+05	1,42E+05	1,31E+05	2,27E+05	1,80E+05	1,38E+05	1,48E+05
GELS	8,00	8,00	395,40	0,44	1,00	1,17	0,19	NMX	86043,00	Gelsolin GN=GSN	4,98E+05	9,97E+05	7,03E+05	1,09E+06	6,64E+05	7,34E+05	5,54E+05	8,70E+05
FLOT1	4,00	4,00	212,52	0,44	1,00	1,10	0,28	HPX	47554,00	Flotillin-1 GN=FLOT1	6,92E+04	1,34E+05	5,35E+04	1,04E+05	7,76E+04	1,06E+05	6,50E+04	1,48E+05
COF1	4,00	4,00	254,78	0,44	1,00	1,23	0,08	NMX	18719,00	Cofilin-1 GN=CFL1	5,87E+05	9,71E+05	1,00E+06	9,11E+05	9,20E+05	4,98E+05	6,62E+05	7,43E+05
S39AA	3,00	3,00	104,57	0,45	1,00	1,16	0,23	NMX	94928,00	Zinc transporter ZIP10 GN=SLC39A10	1,35E+05	1,21E+05	3,05E+05	1,47E+05	1,32E+05	8,94E+04	2,03E+05	1,86E+05
GNA11	9,00	6,00	417,42	0,46	1,00	1,11	0,12	NMX	42382,00	Guanine nucleotide-binding protein subunit alpha-11 GN=GNA11	9,97E+05	9,92E+05	8,76E+05	6,21E+05	6,98E+05	8,08E+05	9,69E+05	6,72E+05
RS16	3,00	3,00	123,06	0,46	1,00	1,13	0,10	HPX	16549,00	40S ribosomal protein S16 GN=RPS16	2,64E+05	5,02E+05	4,14E+05	4,01E+05	4,78E+05	5,49E+05	3,57E+05	4,06E+05
NECT2	3,00	3,00	106,67	0,46	1,00	1,22	0,46	HPX	58162,00	Nectin-2 GN=NECTIN2	1,35E+05	1,56E+05	1,28E+05	7,73E+04	1,79E+05	1,61E+05	2,04E+05	6,04E+04
SCRB2	2,00	2,00	91,59	0,46	1,00	1,10	0,11	HPX	54712,00	Lysosome membrane protein 2 GN=SCARB2	3,09E+05	5,25E+05	5,23E+05	3,69E+05	4,74E+05	5,70E+05	4,22E+05	4,32E+05
CD47	2,00	2,00	79,37	0,46	1,00	1,03	0,96	HPX	35590,00	Leukocyte surface antigen CD47 GN=CD47	4,03E+05	6,63E+05	5,97E+05	3,87E+05	4,11E+05	6,39E+05	6,60E+05	3,91E+05
1433B	10,00	6,00	669,15	0,46	1,00	1,36	0,09	NMX	28179,00	14-3-3 protein beta/alpha GN=YWHAB	3,23E+05	3,77E+05	9,68E+05	4,31E+05	5,70E+05	2,81E+05	4,12E+05	2,81E+05
CTNA1	28,00	28,00	1683,02	0,46	1,00	1,68	0,17	NMX	100693,00	Catenin alpha-1 GN=CTNNA1	1,62E+06	1,18E+06	8,03E+06	1,49E+06	2,47E+06	7,73E+05	2,55E+06	1,53E+06
CD44	8,00	8,00	537,70	0,47	1,00	1,04	0,97	HPX	82001,00	CD44 antigen GN=CD44	5,79E+06	5,85E+06	1,13E+07	7,45E+06	6,25E+06	5,84E+06	1,24E+07	7,05E+06
ITA6	5,00	5,00	206,28	0,47	1,00	1,17	0,15	HPX	127724,00	Integrin alpha-6 GN=ITGA6	1,05E+05	1,55E+05	1,58E+05	9,79E+04	8,61E+04	1,47E+05	2,12E+05	1,57E+05
CAN2	6,00	6,00	312,17	0,47	1,00	1,30	0,07	NMX	80800,00	Calpain-2 catalytic subunit GN=CAPN2	2,87E+05	4,84E+05	6,42E+05	4,91E+05	4,99E+05	3,73E+05	2,72E+05	3,26E+05
S10A6	3,00	3,00	117,97	0,48	1,00	1,29	0,08	HPX	10230,00	Protein S100-A6 GN=S100A6	2,68E+05	5,64E+05	3,91E+05	2,55E+05	7,73E+05	3,73E+05	4,49E+05	3,13E+05
TERA	15,00	15,00	795,46	0,48	1,00	1,15	0,11	NMX	89950,00	Transitional endoplasmic reticulum ATPase GN=VCP	4,72E+05	8,47E+05	4,91E+05	6,93E+05	6,64E+05	6,80E+05	3,94E+05	4,42E+05
DYHC1	55,00	55,00	3010,42	0,48	1,00	1,14	0,07	NMX	534809,00	Cytoplasmic dynein 1 heavy chain 1 GN=DYNC1H1	8,50E+05	8,77E+05	8,62E+05	1,21E+06	8,55E+05	9,80E+05	8,45E+05	6,35E+05
STXB1	2,00	2,00	83,72	0,49	1,00	1,04	0,86	HPX	67925,00	Syntaxin-binding protein 1 GN=STXBP1	2,41E+04	3,40E+04	5,52E+04	4,14E+04	3,38E+04	3,67E+04	4,76E+04	4,36E+04
CO1A2	5,00	5,00	249,79	0,49	1,00	1,09	0,17	NMX	129749,00	Collagen alpha-2(I) chain GN=COL1A2	3,38E+05	1,31E+05	1,83E+05	2,29E+05	3,31E+05	6,35E+04	3,07E+05	1,10E+05
EVA1B	2,00	2,00	172,74	0,49	1,00	1,23	0,24	NMX	18476,00	Protein eva-1 homolog B GN=EVA1B	3,96E+05	4,35E+05	6,93E+05	2,12E+05	4,11E+05	3,54E+05	3,81E+05	2,62E+05
RS15A	2,00	2,00	67,12	0,49	1,00	1,13	0,10	HPX	14944,00	40S ribosomal protein S15a GN=RPS15A	3,50E+05	5,95E+05	6,19E+05	4,13E+05	6,46E+05	6,16E+05	6,06E+05	3,70E+05
PFKAP	10,00	10,00	553,98	0,49	1,00	1,06	0,23	HPX	86454,00	ATP-dependent 6-phosphofructokinase, platelet type GN=PFKP	4,40E+05	5,30E+05	6,03E+05	4,34E+05	5,40E+05	5,16E+05	6,80E+05	3,98E+05
G6PI	6,00	6,00	282,94	0,50	1,00	1,09	0,12	HPX	63335,00	Glucose-6-phosphate isomerase GN=GPI	3,27E+05	4,27E+05	7,01E+05	4,50E+05	5,38E+05	3,90E+05	6,33E+05	5,11E+05
PTTG	2,00	2,00	96,85	0,50	1,00	1,09	0,21	NMX	21109,00	Pituitary tumor-transforming gene 1 protein-interacting protein GN=PTTG1IP	1,21E+06	2,83E+06	6,90E+05	9,92E+05	4,72E+05	2,85E+06	5,89E+05	1,32E+06
TKT	2,00	2,00	114,03	0,50	1,00	1,05	0,34	HPX	68519,00	Transketolase GN=TKT	8,32E+04	5,28E+04	1,32E+05	6,69E+04	1,10E+05	6,14E+04	1,13E+05	6,83E+04
BGH3	6,00	6,00	347,88	0,50	1,00	1,02	0,96	HPX	75261,00	Transforming growth factor-beta-induced protein ig-h3 GN=TGFBI	3,05E+05	2,99E+05	4,38E+05	1,95E+06	2,08E+05	3,24E+05	3,82E+05	2,14E+06
VINC	27,00	26,00	1588,62	0,50	1,00	1,05	0,26	HPX	124292,00	Vinculin GN=VCL	7,59E+05	5,72E+05	2,17E+06	1,15E+06	1,31E+06	7,10E+05	1,65E+06	1,19E+06
K2C8	13,00	12,00	697,65	0,50	1,00	1,13	0,07	NMX	53671,00	Keratin, type II cytoskeletal 8 GN=KRT8	2,16E+06	3,37E+06	2,75E+06	2,57E+06	3,09E+06	2,34E+06	2,00E+06	2,13E+06
#####	6,00	6,00	320,94	0,51	1,00	1,19	0,08	NMX	41689,00	Septin-2 GN=SEPT2	2,70E+05	3,23E+05	5,31E+05	4,44E+05	4,20E+05	2,55E+05	3,47E+05	2,99E+05
ML12A	2,00	2,00	112,17	0,51	1,00	1,23	0,07	NMX	19839,00	Myosin regulatory light chain 12A GN=MYL12A	3,31E+05	4,23E+05	6,31E+05	5,37E+05	5,68E+05	3,97E+05	3,25E+05	2,70E+05
PDC6I	19,00	19,00	1194,83	0,51	1,00	1,06	0,45	NMX	96590,00	Programmed cell death 6-interacting protein GN=PDCD6IP	6,94E+05	1,30E+06	8,26E+05	5,45E+05	6,37E+05	1,24E+06	6,67E+05	6,23E+05
LAMA4	3,00	3,00	143,46	0,51	1,00	1,50	0,15	NMX	205020,00	Laminin subunit alpha-4 GN=LAMA4	1,93E+05	3,60E+04	5,29E+04	1,18E+05	6,77E+04	4,24E+04	7,18E+04	8,45E+04
RS3A	5,00	5,00	189,28	0,51	1,00	1,07	0,10	NMX	30154,00	40S ribosomal protein S3a GN=RPS3A	4,51E+05	6,41E+05	5,02E+05	5,25E+05	5,31E+05	5,63E+05	3,65E+05	5,19E+05
ANX11	8,00	8,00	501,73	0,52	1,00	1,04	0,19	NMX	54697,00	Annexin A11 GN=ANXA11	1,03E+06	1,09E+06	1,47E+06	1,08E+06	1,15E+06	1,04E+06	1,32E+06	9,69E+05
MFGM	24,00	24,00	2061,52	0,52	1,00	1,18	0,32	NMX	43894,00	Lactadherin GN=MFGE8	3,95E+07	6,40E+07	5,62E+07	2,12E+07	4,31E+07	4,10E+07	4,43E+07	2,52E+07
CSPG2	15,00	15,00	900,43	0,52	1,00	1,62	0,50	NMX	374585,00	Versican core protein GN=VCAN	7,19E+06	3,62E+06	1,29E+06	3,44E+05	2,89E+06	2,58E+06	1,83E+06	3,82E+05
TMEM2	3,00	2,00	149,79	0,52	1,00	1,27	0,45	HPX	155702,00	Transmembrane protein 2 GN=TMEM2	6,97E+04	5,60E+04	8,25E+04	3,88E+04	8,53E+04	4,44E+04	1,47E+05	3,71E+04
EHD4	18,00	13,00	1021,74	0,53	1,00	1,05	0,27	HPX	61365,00	EH domain-containing protein 4 GN=EHD4	1,12E+06	7,10E+05	1,92E+06	6,81E+05	1,36E+06	6,93E+05	1,59E+06	1,00E+06
FINC	68,00	68,00	4863,65	0,53	1,00	1,17	0,10	NMX	266052,00	Fibronectin GN=FN1	3,65E+07	1,75E+07	3,62E+07	5,44E+07	1,85E+07	1,83E+07	6,04E+07	2,61E+07
RS18	3,00	3,00	138,64	0,53	1,00	1,08	0,12	HPX	17708,00	40S ribosomal protein S18 GN=RPS18	2,08E+05	4,84E+05	2,72E+05	4,00E+05	3,73E+05	4,64E+05	2,80E+05	3,56E+05
NCKP1	5,00	5,00	262,04	0,53	1,00	1,07	0,31	HPX	130018,00	Nck-associated protein 1 GN=NCKAP1	1,23E+05	1,36E+05	2,18E+05	3,35E+05	1,79E+05	1,17E+05	2,38E+05	3,36E+05
ITA4	15,00	15,00	686,48	0,53	1,00	1,09	0,22	NMX	116252,00	Integrin alpha-4 GN=ITGA4	8,68E+05	7,38E+05	1,74E+06	9,63E+05	7,66E+05	6,13E+05	1,35E+06	1,23E+06
TCPH	8,00	8,00	450,47	0,53	1,00	1,13	0,07	HPX	59842,00	T-complex protein 1 subunit eta GN=CCT7	2,53E+05	3,16E+05	3,73E+05	3,16E+05	4,70E+05	3,17E+05	3,19E+05	3,20E+05
TLN1	41,00	41,00	2747,13	0,53	1,00	1,42	0,12	NMX	271766,00	Talin-1 GN=TLN1	4,49E+05	6,67E+05	1,38E+06	2,62E+06	9,06E+05	4,90E+05	6,12E+05	1,59E+06
ITIH3	2,00	2,00	87,50	0,54	1,00	1,13	0,12	NMX	100072,00	Inter-alpha-trypsin inhibitor heavy chain H3 GN=ITIH3	8,47E+05	1,25E+06	6,52E+05	5,37E+05	5,17E+05	1,10E+06	5,52E+05	7,43E+05
KCY	2,00	2,00	106,29	0,54	1,00	1,17	0,16	NMX	22436,00	UMP-CMP kinase GN=CMPK1	4,14E+04	4,72E+04	1,07E+05	9,27E+04	5,45E+04	4,02E+04	6,34E+04	8,85E+04

FLOT2	3,00	3,00	172,21	0,54	1,00	1,00	1,00	NMX	47434,00	Flotillin-2 GN=FLOT2	1,71E+05	2,19E+05	2,14E+05	3,23E+05	9,66E+04	2,09E+05	1,65E+05	4,56E+05
TRFL	2,00	2,00	90,28	0,54	1,00	1,29	0,36	HPX	80014,00	Lactotransferrin GN=LTF	1,06E+06	1,47E+06	7,00E+05	2,13E+06	8,90E+05	1,35E+06	8,07E+05	3,89E+06
MVP	22,00	22,00	1277,51	0,54	1,00	1,07	0,52	NMX	99551,00	Major vault protein GN=MVP	2,80E+06	4,91E+06	1,49E+06	3,53E+06	2,71E+06	4,91E+06	1,64E+06	2,64E+06
CDC42	5,00	4,00	304,46	0,54	1,00	1,04	0,28	HPX	21587,00	Cell division control protein 42 homolog GN=CDC42	9,84E+05	1,04E+06	2,10E+06	1,28E+06	1,33E+06	1,11E+06	1,96E+06	1,20E+06
MYL6; MYL6 B	4,00	4,00	205,93	0,55	1,00	1,21	0,08	HPX	17090,00	Myosin light polypeptide 6 GN=MYL6	2,66E+05	1,05E+06	3,82E+05	4,79E+05	9,81E+05	8,20E+05	3,74E+05	4,49E+05
VDAC 2	3,00	3,00	120,79	0,55	1,00	1,29	0,15	HPX	32060,00	Voltage-dependent anion-selective channel protein 2 GN=VDAC2	1,03E+05	2,25E+05	5,16E+04	9,95E+04	2,82E+05	1,97E+05	5,12E+04	8,85E+04
GBB2	8,00	4,00	546,62	0,55	1,00	1,03	0,25	HPX	38048,00	Guanine nucleotide-binding protein G(I)/G(S)/G(T) subunit beta-2 GN=GNB2	1,03E+06	1,11E+06	2,70E+06	9,62E+05	1,46E+06	1,04E+06	2,21E+06	1,26E+06
ANO6	2,00	2,00	76,80	0,55	1,00	1,11	0,17	NMX	107180,00	Anoctamin-6 GN=ANO6	1,97E+05	1,64E+05	3,94E+05	2,61E+05	1,66E+05	1,81E+05	2,71E+05	2,97E+05
TCPD	6,00	6,00	428,76	0,56	1,00	1,06	0,07	HPX	58401,00	T-complex protein 1 subunit delta GN=CCT4	5,06E+05	6,77E+05	7,83E+05	7,34E+05	7,26E+05	6,81E+05	6,68E+05	7,96E+05
ACSL4	3,00	3,00	146,65	0,56	1,00	1,05	0,19	HPX	80220,00	Long-chain-fatty-acid--CoA ligase 4 GN=ACSL4	1,93E+05	4,07E+05	4,36E+05	2,53E+05	2,97E+05	4,00E+05	3,39E+05	3,18E+05
CO6A 2	18,00	17,00	1115,20	0,56	1,00	1,12	0,33	HPX	109709,00	Collagen alpha-2(VI) chain GN=COL6A2	8,56E+05	9,07E+06	6,34E+05	1,18E+06	5,92E+05	8,91E+06	7,70E+05	2,88E+06
6PGD	9,00	9,00	432,59	0,56	1,00	1,21	0,07	NMX	53619,00	6-phosphogluconate dehydrogenase, decarboxylating GN=PGD	2,05E+05	4,30E+05	3,67E+05	3,49E+05	3,96E+05	2,91E+05	2,11E+05	2,21E+05
S10AB	6,00	6,00	412,40	0,56	1,00	1,08	0,09	NMX	11847,00	Protein S100-A11 GN=S100A11	1,11E+06	1,32E+06	1,79E+06	1,45E+06	1,20E+06	1,04E+06	1,31E+06	1,72E+06
GRP7 8	14,00	12,00	906,83	0,56	1,00	1,18	0,16	NMX	72402,00	78 kDa glucose-regulated protein GN=HSPA5	4,14E+05	1,66E+06	4,11E+05	5,31E+05	7,17E+05	1,23E+06	2,42E+05	3,76E+05
SYIC	5,00	5,00	195,26	0,56	1,00	1,06	0,10	HPX	145718,00	Isoleucine--tRNA ligase, cytoplasmic GN=IARS	1,55E+05	2,50E+05	2,66E+05	2,85E+05	2,20E+05	2,96E+05	2,19E+05	2,79E+05
RHOG	5,00	4,00	310,97	0,57	1,00	1,18	0,07	NMX	21751,00	Rho-related GTP-binding protein RhoG GN=RHOG	3,34E+05	5,54E+05	7,40E+05	4,40E+05	4,82E+05	4,02E+05	4,42E+05	4,29E+05
ANXA 6	30,00	29,00	1961,34	0,57	1,00	1,03	0,24	HPX	76168,00	Annexin A6 GN=ANXA6	4,37E+06	5,00E+06	8,39E+06	4,75E+06	5,01E+06	5,09E+06	7,10E+06	6,00E+06
FLNA	62,00	55,00	3651,18	0,57	1,00	1,07	0,09	NMX	283301,00	Filamin-A GN=FLNA	3,28E+06	2,58E+06	3,56E+06	2,84E+06	4,45E+06	2,74E+06	2,50E+06	1,76E+06
TPP2	2,00	2,00	76,51	0,57	1,00	1,03	0,22	NMX	139745,00	Tripeptidyl-peptidase 2 GN=TPP2	5,49E+04	5,38E+04	7,26E+04	1,03E+05	4,40E+04	6,00E+04	5,28E+04	1,18E+05
FRIH	2,00	2,00	91,29	0,57	1,00	1,59	0,71	NMX	21383,00	Ferritin heavy chain GN=FTH1	8,86E+04	1,74E+05	1,75E+05	9,74E+05	1,26E+05	1,84E+05	1,38E+05	4,40E+05
HPLN 1	7,00	7,00	347,21	0,57	1,00	1,42	0,13	NMX	40767,00	Hyaluronan and proteoglycan link protein 1 GN=HAPLN1 PE=2 SV=2	1,17E+06	6,77E+05	9,16E+05	1,73E+05	4,76E+05	4,19E+05	8,53E+05	3,23E+05
PLCD3	2,00	2,00	89,21	0,57	1,00	1,06	0,08	HPX	90115,00	1-phosphatidylinositol 4,5-bisphosphate phosphodiesterase delta-3 GN=PLCD3	1,40E+05	1,46E+05	1,58E+05	1,51E+05	1,60E+05	1,25E+05	1,58E+05	1,87E+05
RL14	2,00	2,00	103,29	0,57	1,00	1,09	0,08	HPX	23531,00	60S ribosomal protein L14 GN=RPL14	2,17E+05	3,77E+05	2,31E+05	2,73E+05	3,69E+05	3,41E+05	2,29E+05	2,60E+05
SDCB1	2,00	2,00	274,95	0,57	1,00	1,15	0,14	HPX	32595,00	Syntenin-1 GN=SDCBP	3,52E+05	5,86E+05	3,41E+05	1,66E+05	2,45E+05	7,88E+05	3,43E+05	2,87E+05
ESYT1	2,00	2,00	83,36	0,58	1,00	1,17	0,12	HPX	123293,00	Extended synaptotagmin-1 GN=ESYT1	1,04E+05	1,73E+05	1,07E+05	1,07E+05	1,82E+05	2,11E+05	9,80E+04	8,49E+04
APOM	3,00	3,00	129,81	0,58	1,00	1,15	0,07	HPX	21582,00	Apolipoprotein M GN=APOM	3,44E+05	3,49E+05	3,38E+05	3,96E+05	6,03E+05	3,84E+05	3,29E+05	3,19E+05
RL8	3,00	3,00	134,91	0,58	1,00	1,14	0,07	HPX	28235,00	60S ribosomal protein L8 GN=RPL8	1,33E+05	3,41E+05	2,66E+05	2,66E+05	3,49E+05	3,05E+05	2,08E+05	2,85E+05
MAM C2	4,00	4,00	161,04	0,58	1,00	1,16	0,22	NMX	78589,00	MAM domain-containing protein 2 GN=MAMDC2 PE=2 SV=3	9,16E+04	2,55E+05	6,15E+04	6,27E+04	6,12E+04	2,01E+05	5,24E+04	9,16E+04
GT251	2,00	2,00	91,23	0,58	1,00	1,22	0,09	NMX	71933,00	Procollagen galactosyltransferase 1 GN=COLGALT1	1,20E+04	4,56E+04	4,49E+04	3,59E+04	1,59E+04	4,27E+04	1,41E+04	4,10E+04
CO3	7,00	7,00	278,91	0,58	1,00	1,18	1,00	NMX	188569,00	Complement C3 GN=C3	6,64E+05	5,45E+05	2,03E+05	1,56E+06	5,78E+05	5,03E+05	2,57E+05	1,17E+06
MOT4	4,00	4,00	258,22	0,58	1,00	1,03	0,29	HPX	50064,00	Monocarboxylate transporter 4 GN=SLC16A3	1,45E+06	1,74E+06	3,46E+06	2,25E+06	1,88E+06	1,67E+06	3,03E+06	2,57E+06
CDC37	2,00	2,00	97,40	0,58	1,00	1,09	0,07	HPX	44953,00	Hsp90 co-chaperone Cdc37 GN=CDC37	1,12E+05	1,27E+05	2,74E+05	1,51E+05	2,23E+05	1,50E+05	1,78E+05	1,73E+05
TSN9	2,00	2,00	100,08	0,58	1,00	1,13	0,08	HPX	27559,00	Tetraspanin-9 GN=TSPAN9	9,04E+05	6,51E+05	6,71E+05	3,75E+05	6,20E+05	6,27E+05	1,13E+06	5,62E+05
RAB8 A	4,00	2,00	258,22	0,58	1,00	1,03	0,28	HPX	23824,00	Ras-related protein Rab-8A GN=RAB8A	1,33E+05	2,29E+05	3,59E+05	2,15E+05	2,04E+05	2,48E+05	3,02E+05	2,10E+05
ANXA 7	6,00	6,00	298,21	0,58	1,00	1,07	0,07	HPX	52991,00	Annexin A7 GN=ANXA7	2,21E+05	3,22E+05	3,76E+05	2,85E+05	3,49E+05	2,87E+05	3,59E+05	2,91E+05
PDIA3	13,00	12,00	716,48	0,58	1,00	1,13	0,10	NMX	57146,00	Protein disulfide-isomerase A3 GN=PDIA3	6,27E+05	1,44E+06	7,96E+05	6,12E+05	9,34E+05	1,10E+06	4,75E+05	5,61E+05
ANXA 1	17,00	17,00	1188,46	0,59	1,00	1,03	0,32	HPX	38918,00	Annexin A1 GN=ANXA1	5,98E+06	6,91E+06	1,16E+07	4,55E+06	7,69E+06	7,03E+06	9,05E+06	6,01E+06
CD59	4,00	4,00	224,07	0,59	1,00	1,10	0,10	HPX	14795,00	CD59 glycoprotein GN=CD59	2,07E+06	1,96E+06	2,52E+06	1,48E+06	1,63E+06	1,93E+06	3,17E+06	2,05E+06
HSP74	2,00	2,00	70,21	0,59	1,00	1,08	0,62	HPX	95127,00	Heat shock 70 kDa protein 4 GN=HSPA4	6,31E+05	1,13E+06	4,43E+05	1,47E+06	7,24E+05	9,93E+05	4,26E+05	1,83E+06
TSP2	12,00	8,00	619,45	0,59	1,00	1,34	0,07	NMX	133785,00	Thrombospondin-2 GN=THBS2	5,58E+05	1,49E+05	3,86E+05	2,09E+05	1,52E+05	1,93E+05	3,67E+05	2,58E+05
EDIL3	27,00	27,00	1813,96	0,59	1,00	1,05	0,14	HPX	55098,00	EGF-like repeat and discoidin I-like domain-containing protein 3 GN=EDIL3	9,49E+06	9,64E+06	1,48E+07	4,85E+06	1,29E+07	7,94E+06	1,27E+07	7,23E+06
LAMP 2	2,00	2,00	112,56	0,59	1,00	1,07	0,07	HPX	45503,00	Lysosome-associated membrane glycoprotein 2 GN=LAMP2	2,69E+05	3,16E+05	2,85E+05	2,00E+05	2,29E+05	3,32E+05	2,82E+05	3,05E+05
PLOD 2	8,00	8,00	378,46	0,59	1,00	1,03	0,15	HPX	85373,00	Procollagen-lysine,2-oxoglutarate 5-dioxygenase 2 GN=PLOD2	3,42E+05	1,28E+06	4,94E+05	4,64E+05	6,38E+05	1,06E+06	4,44E+05	5,16E+05
A2MG	6,00	3,00	357,79	0,60	1,00	1,07	0,13	NMX	164613,00	Alpha-2-macroglobulin GN=A2M	6,24E+07	3,80E+07	2,19E+07	1,01E+08	2,61E+07	3,51E+07	2,62E+07	1,21E+08
RL13	4,00	4,00	184,09	0,60	1,00	1,05	0,19	NMX	24304,00	60S ribosomal protein L13 GN=RPL13	1,87E+05	3,25E+05	1,84E+05	3,31E+05	2,27E+05	3,13E+05	1,39E+05	2,98E+05
DAF	3,00	3,00	89,78	0,60	1,00	1,01	0,42	HPX	42400,00	Complement decay-accelerating factor GN=CD55	3,60E+05	5,41E+05	9,54E+05	3,91E+05	4,78E+05	5,00E+05	8,54E+05	4,42E+05

CTNB1	15,00	10,00	894,01	0,60	1,00	1,02	0,38	NMX	86069,00	Catenin beta-1 GN=CTNNB1	8,23E+05	5,89E+05	9,99E+05	6,99E+05	6,91E+05	5,34E+05	1,16E+06	6,74E+05
LYN	3,00	3,00	135,01	0,60	1,00	1,03	0,16	HPX	58993,00	Tyrosine-protein kinase Lyn GN=LYN	2,47E+05	2,71E+05	3,27E+05	1,82E+05	2,33E+05	2,62E+05	3,27E+05	2,37E+05
MEST	2,00	2,00	78,95	0,60	1,00	1,12	0,08	NMX	38863,00	Mesoderm-specific transcript homolog protein GN=MEST PE=2 SV=2	1,18E+05	1,01E+05	1,96E+05	1,01E+05	5,68E+04	1,67E+05	1,42E+05	9,50E+04
ADT2; ADT1	4,00	4,00	140,61	0,60	1,00	1,17	0,08	HPX	33059,00	ADP/ATP translocase 2 GN=SLC25A5	2,58E+05	4,15E+05	2,76E+05	5,13E+05	5,50E+05	5,05E+05	2,09E+05	4,45E+05
SYCC	2,00	2,00	104,67	0,61	1,00	1,04	0,19	NMX	86103,00	Cysteine--tRNA ligase, cytoplasmic GN=CARS	1,18E+05	6,36E+04	1,25E+05	9,13E+04	8,82E+04	6,14E+04	1,35E+05	9,63E+04
TRXR1	6,00	6,00	413,60	0,61	1,00	1,09	0,07	HPX	71832,00	Thioredoxin reductase 1, cytoplasmic GN=TXNRD1	5,04E+05	7,69E+05	8,51E+05	6,56E+05	8,93E+05	7,58E+05	7,71E+05	6,00E+05
FMNL 2	4,00	4,00	188,23	0,61	1,00	1,03	0,24	NMX	123699,00	Formin-like protein 2 GN=FMNL2	2,58E+05	2,66E+05	3,77E+05	4,24E+05	2,29E+05	3,00E+05	3,38E+05	4,17E+05
ENPL	19,00	18,00	1005,32	0,61	1,00	1,13	0,13	HPX	92696,00	Endoplasmin GN=HSP90B1	4,89E+05	1,60E+06	5,73E+05	4,54E+05	1,02E+06	1,61E+06	4,64E+05	4,28E+05
ARRD 1	3,00	3,00	103,79	0,61	1,00	1,04	0,22	HPX	46352,00	Arrestin domain-containing protein 1 GN=ARRDC1	1,29E+05	1,38E+05	1,85E+05	2,67E+04	1,00E+05	2,06E+05	1,46E+05	4,70E+04
BASP1	7,00	7,00	470,89	0,61	1,00	1,09	0,13	NMX	22680,00	Brain acid soluble protein 1 GN=BASP1	1,60E+06	1,28E+06	3,18E+06	1,81E+06	2,13E+06	9,51E+05	2,37E+06	1,79E+06
H2B1 B	5,00	4,00	355,90	0,61	1,00	1,08	0,46	HPX	13942,00	Histone H2B type 1-B GN=HIST1H2BB	5,32E+05	3,54E+06	4,25E+05	1,52E+06	3,38E+05	4,62E+06	4,90E+05	1,06E+06
PAI1	9,00	9,00	388,34	0,61	1,00	1,01	0,43	HPX	45088,00	Plasminogen activator inhibitor 1 GN=SERPINE1	1,60E+06	1,09E+06	2,69E+06	3,62E+06	1,18E+06	1,07E+06	2,29E+06	4,55E+06
AMPN	31,00	31,00	1888,03	0,62	1,00	1,07	0,70	NMX	109870,00	Aminopeptidase N GN=ANPEP	2,08E+06	2,15E+06	3,89E+06	1,53E+06	2,22E+06	1,97E+06	3,17E+06	1,66E+06
AT2B4	23,00	13,00	1617,14	0,62	1,00	1,14	0,25	NMX	139030,00	Plasma membrane calcium-transporting ATPase 4 GN=ATP2B4	1,30E+06	2,01E+06	3,75E+06	1,89E+06	1,64E+06	1,68E+06	2,55E+06	1,96E+06
CTND 1	12,00	11,00	704,74	0,62	1,00	1,08	0,16	NMX	108674,00	Catenin delta-1 GN=CTNND1	6,91E+05	6,47E+05	1,32E+06	1,06E+06	8,66E+05	5,96E+05	1,09E+06	9,01E+05
EZRI	18,00	10,00	1019,76	0,62	1,00	1,16	0,11	NMX	69484,00	Ezrin GN=EZR	2,89E+06	1,42E+06	4,66E+06	1,75E+06	3,34E+06	1,28E+06	2,50E+06	2,10E+06
TCPZ	8,00	8,00	398,71	0,63	1,00	1,14	0,06	HPX	58444,00	T-complex protein 1 subunit zeta GN=CCT6A	2,12E+05	3,55E+05	4,61E+05	3,35E+05	5,29E+05	3,48E+05	3,34E+05	3,38E+05
PGK1	10,00	10,00	618,63	0,63	1,00	1,13	0,08	NMX	44985,00	Phosphoglycerate kinase 1 GN=PGK1	1,12E+06	1,94E+06	2,10E+06	2,42E+06	1,66E+06	1,54E+06	1,70E+06	1,82E+06
FA5	3,00	2,00	209,89	0,63	1,00	1,04	0,17	HPX	252686,00	Coagulation factor V GN=F5	1,86E+05	2,78E+05	2,10E+05	3,32E+05	2,33E+05	2,86E+05	1,85E+05	3,41E+05
ANXA 4	9,00	7,00	537,93	0,64	1,00	1,04	0,07	NMX	36088,00	Annexin A4 GN=ANXA4	7,22E+05	6,48E+05	8,18E+05	7,09E+05	5,79E+05	7,65E+05	7,84E+05	6,61E+05
MRP1	2,00	2,00	87,33	0,64	1,00	1,03	0,14	HPX	172907,00	Multidrug resistance-associated protein 1 GN=ABCC1	7,59E+04	8,78E+04	1,32E+05	1,00E+05	7,43E+04	9,86E+04	1,16E+05	1,20E+05
IF4A1	12,00	12,00	686,33	0,64	1,00	1,06	0,06	HPX	46353,00	Eukaryotic initiation factor 4A-I GN=EIF4A1	5,90E+05	7,80E+05	9,05E+05	8,86E+05	8,99E+05	7,08E+05	8,25E+05	9,07E+05
FLNC	28,00	21,00	1520,79	0,64	1,00	1,09	0,06	NMX	293407,00	Filamin-C GN=FLNC	8,10E+05	1,11E+06	1,18E+06	9,72E+05	1,29E+06	9,04E+05	8,74E+05	6,72E+05
MACF 1	3,00	3,00	127,77	0,64	1,00	1,05	0,08	HPX	843033,00	Microtubule-actin cross-linking factor 1, isoforms 1/2/3/5 GN=MACF1	7,05E+04	7,70E+04	1,24E+05	1,22E+05	1,15E+05	7,74E+04	1,14E+05	1,08E+05
RL4	3,00	3,00	149,43	0,64	1,00	1,11	0,08	HPX	47953,00	60S ribosomal protein L4 GN=RPL4	3,92E+05	5,59E+05	4,91E+05	8,38E+05	6,84E+05	5,22E+05	3,87E+05	9,30E+05
COR1 C	7,00	7,00	412,20	0,64	1,00	1,12	0,09	HPX	53899,00	Coronin-1C GN=CORO1C	4,92E+05	4,25E+05	1,06E+06	3,47E+05	1,02E+06	5,26E+05	7,42E+05	3,13E+05
PP2BA	3,00	3,00	142,56	0,65	1,00	1,11	0,07	HPX	59335,00	Serine/threonine-protein phosphatase 2B catalytic subunit alpha isoform GN=PPP3CA	6,94E+04	1,51E+05	1,09E+05	2,73E+05	2,13E+05	1,01E+05	1,29E+05	2,25E+05
MYOF	50,00	45,00	2625,02	0,65	1,00	1,09	0,08	NMX	236100,00	Myoferlin GN=MYOF	1,28E+06	1,28E+06	2,05E+06	9,80E+05	1,39E+06	1,55E+06	1,31E+06	8,82E+05
4F2	20,00	20,00	1222,12	0,65	1,00	1,07	0,18	HPX	68180,00	4F2 cell-surface antigen heavy chain GN=SLC3A2	3,75E+06	4,04E+06	5,45E+06	3,98E+06	3,08E+06	4,23E+06	6,30E+06	4,73E+06
ALDO A	7,00	7,00	464,36	0,66	1,00	1,17	0,06	HPX	39851,00	Fructose-bisphosphate aldolase A GN=ALDOA	9,73E+05	1,67E+06	1,38E+06	1,07E+06	2,23E+06	1,20E+06	1,63E+06	9,08E+05
CPNE3	2,00	2,00	72,38	0,66	1,00	1,04	0,08	HPX	60947,00	Copine-3 GN=CPNE3	2,13E+05	2,08E+05	3,24E+05	2,05E+05	2,79E+05	1,92E+05	2,76E+05	2,41E+05
STXB3	4,00	4,00	194,24	0,66	1,00	1,02	0,20	HPX	68633,00	Syntaxin-binding protein 3 GN=STXBP3	1,55E+05	1,70E+05	3,43E+05	1,76E+05	1,95E+05	1,56E+05	3,10E+05	1,97E+05
DDX3 X	3,00	3,00	165,05	0,66	1,00	1,06	0,06	HPX	73597,00	ATP-dependent RNA helicase DDX3X GN=DDX3X	5,30E+04	5,58E+04	8,15E+04	6,29E+04	7,26E+04	7,46E+04	6,20E+04	5,94E+04
TGM2	9,00	9,00	500,95	0,66	1,00	1,04	0,08	HPX	78420,00	Protein-glutamine gamma-glutamyltransferase 2 GN=TGM2	1,35E+06	1,60E+06	2,52E+06	2,09E+06	1,98E+06	1,63E+06	2,01E+06	2,22E+06
COPG 1	2,00	2,00	127,59	0,67	1,00	1,02	0,07	HPX	98967,00	Coatomer subunit gamma-1 GN=COPG1	1,29E+05	5,70E+04	2,52E+05	1,90E+05	1,58E+05	1,59E+05	1,66E+05	1,56E+05
HEG1	6,00	6,00	319,00	0,67	1,00	1,07	0,14	HPX	149023,00	Protein HEG homolog 1 GN=HEG1	2,98E+05	2,56E+05	4,88E+05	1,56E+05	4,18E+05	1,95E+05	4,76E+05	1,94E+05
BASI	10,00	10,00	862,95	0,67	1,00	1,05	0,12	NMX	42573,00	Basigin GN=BSG	5,42E+06	5,86E+06	1,06E+07	7,25E+06	5,55E+06	5,21E+06	8,36E+06	8,57E+06
RSU1	3,00	3,00	159,29	0,67	1,00	1,04	0,18	HPX	31521,00	Ras suppressor protein 1 GN=RSU1	1,68E+05	1,28E+05	4,59E+05	3,83E+05	2,57E+05	1,15E+05	3,77E+05	4,39E+05
TSN4	2,00	2,00	123,24	0,67	1,00	1,26	0,08	NMX	26841,00	Tetraspanin-4 GN=TSPAN4	1,68E+06	2,11E+06	4,55E+05	1,18E+05	2,76E+05	1,71E+06	1,37E+06	9,67E+04
CAV1	3,00	3,00	210,06	0,67	1,00	1,23	0,06	NMX	20630,00	Caveolin-1 GN=CAV1	4,75E+05	1,17E+06	1,42E+06	7,47E+05	8,94E+05	9,86E+05	5,65E+05	6,54E+05
RAB6 A	3,00	2,00	129,03	0,68	1,00	1,15	0,07	NMX	23692,00	Ras-related protein Rab-6A GN=RAB6A	1,09E+05	2,27E+05	2,91E+05	2,11E+05	1,76E+05	2,00E+05	2,07E+05	1,46E+05
CD276	2,00	2,00	99,96	0,68	1,00	1,01	0,13	HPX	57941,00	CD276 antigen GN=CD276	2,20E+05	5,40E+05	4,11E+05	1,76E+05	2,56E+05	5,30E+05	3,07E+05	2,73E+05
GNAI2	15,00	9,00	970,79	0,68	1,00	1,07	0,17	NMX	40995,00	Guanine nucleotide-binding protein G(i) subunit alpha-2 GN=GNAI2	2,98E+06	3,43E+06	6,77E+06	3,42E+06	3,60E+06	2,96E+06	5,50E+06	3,44E+06
RL12	2,00	2,00	120,39	0,68	1,00	1,26	0,09	HPX	17979,00	60S ribosomal protein L12 GN=RPL12	2,00E+05	3,58E+05	7,24E+04	9,85E+04	4,31E+05	2,98E+05	1,39E+05	5,27E+04
DIP2B	3,00	3,00	155,20	0,68	1,00	1,02	0,22	NMX	173606,00	Disco-interacting protein 2 homolog B GN=DIP2B	1,07E+05	1,21E+05	1,65E+05	1,16E+05	1,03E+05	1,32E+05	1,52E+05	1,12E+05
CAPZB	2,00	2,00	76,51	0,68	1,00	1,14	0,06	NMX	31616,00	F-actin-capping protein subunit beta GN=CAPZB	1,92E+05	2,22E+05	6,03E+05	1,86E+05	5,34E+05	1,86E+05	2,49E+05	8,83E+04
S39AE	3,00	3,00	191,69	0,68	1,00	1,10	0,08	NMX	54918,00	Zinc transporter ZIP14 GN=SLC39A14	5,05E+05	9,47E+05	1,33E+06	8,61E+05	6,92E+05	9,65E+05	1,09E+06	5,65E+05
TAGL2	3,00	3,00	203,40	0,68	1,00	1,04	0,06	HPX	22548,00	Transgelin-2 GN=TAGLN2	2,12E+05	3,85E+05	5,68E+05	4,00E+05	4,24E+05	3,46E+05	4,67E+05	3,90E+05

MYH10	11,00	2,00	693,41	0,69	1,00	1,32	0,06	HPX	229827,00	Myosin-10 GN=MYH10	8,61E+04	1,86E+05	2,06E+05	1,90E+05	4,11E+05	1,93E+05	1,78E+05	1,03E+05
TPIS	2,00	2,00	145,86	0,69	1,00	1,07	0,07	NMX	31057,00	Triosephosphate isomerase GN=TPI1	1,87E+05	2,31E+05	2,24E+05	3,32E+05	2,60E+05	1,66E+05	2,05E+05	2,84E+05
TBB5	23,00	4,00	1630,11	0,69	1,00	1,04	0,07	HPX	50095,00	Tubulin beta chain GN=TUBB	1,69E+06	3,58E+06	2,70E+06	3,13E+06	2,70E+06	3,33E+06	2,25E+06	3,24E+06
LG3BP	18,00	18,00	1451,49	0,69	1,00	1,17	0,08	NMX	66202,00	Galectin-3-binding protein GN=LGALS3BP	1,70E+07	2,08E+07	9,65E+06	5,44E+06	8,00E+06	1,91E+07	9,90E+06	8,07E+06
ITIH2	7,00	7,00	470,40	0,69	1,00	1,14	0,15	NMX	106853,00	Inter-alpha-trypsin inhibitor heavy chain H2 GN=ITIH2	2,46E+07	3,41E+07	1,05E+07	4,80E+06	1,23E+07	3,43E+07	1,28E+07	5,51E+06
DNM1L	2,00	2,00	173,36	0,69	1,00	1,10	0,06	HPX	82339,00	Dynamin-1-like protein GN=DNM1L	5,07E+04	5,61E+04	1,48E+05	5,70E+04	1,21E+05	1,00E+05	7,57E+04	4,81E+04
IF5A1	2,00	2,00	152,57	0,70	1,00	1,09	0,07	HPX	17049,00	Eukaryotic translation initiation factor 5A-1 GN=EIF5A	1,88E+05	1,59E+05	3,77E+05	1,88E+05	3,77E+05	1,52E+05	2,61E+05	2,08E+05
AL1A1	2,00	2,00	84,00	0,70	1,00	1,19	0,06	NMX	55454,00	Retinal dehydrogenase 1 GN=ALDH1A1	1,25E+05	2,93E+05	2,36E+05	4,14E+05	2,46E+05	2,08E+05	1,52E+05	2,95E+05
ARF6	5,00	4,00	258,15	0,70	1,00	1,01	0,18	HPX	20183,00	ADP-ribosylation factor 6 GN=ARF6	3,39E+05	4,07E+05	7,52E+05	4,07E+05	4,55E+05	4,42E+05	5,95E+05	4,24E+05
UPAR	5,00	5,00	435,24	0,70	1,00	1,11	0,09	NMX	38607,00	Urokinase plasminogen activator surface receptor GN=PLAUR	6,64E+05	7,44E+05	1,92E+06	1,05E+06	7,77E+05	5,81E+05	1,27E+06	1,34E+06
HNRPQ	2,00	2,00	107,56	0,70	1,00	1,08	0,06	HPX	69788,00	Heterogeneous nuclear ribonucleoprotein Q GN=SYNCRIP	3,41E+04	6,19E+04	4,67E+04	7,45E+04	7,58E+04	5,26E+04	4,36E+04	6,27E+04
NP1L1	3,00	3,00	89,83	0,70	1,00	1,08	0,08	NMX	45631,00	Nucleosome assembly protein 1-like 1 GN=NAP1L1	1,55E+05	2,51E+05	1,67E+05	3,61E+05	2,43E+05	1,78E+05	1,28E+05	3,14E+05
RAP2C	5,00	2,00	277,54	0,71	1,00	1,14	0,06	NMX	20959,00	Ras-related protein Rap-2c GN=RAP2C	2,22E+04	3,49E+04	1,01E+04	9,06E+03	4,76E+03	1,22E+04	3,97E+04	1,04E+04
CALR	6,00	6,00	337,63	0,71	1,00	1,13	0,07	HPX	48283,00	Calreticulin GN=CALR	2,61E+05	9,68E+05	3,68E+05	5,61E+05	6,89E+05	9,94E+05	2,39E+05	5,23E+05
CO6A3	89,00	88,00	5867,86	0,71	1,00	1,20	0,15	HPX	345167,00	Collagen alpha-3(VI) chain GN=COL6A3	1,55E+06	2,12E+07	1,50E+06	1,67E+06	1,09E+06	2,40E+07	1,10E+06	4,97E+06
1433Z	11,00	8,00	841,25	0,71	1,00	1,12	0,06	NMX	27899,00	14-3-3 protein zeta/delta GN=YWHAZ	1,93E+06	2,76E+06	3,83E+06	3,79E+06	3,31E+06	2,17E+06	2,64E+06	2,90E+06
RAB8B	4,00	2,00	181,46	0,71	1,00	1,00	0,77	HPX	23740,00	Ras-related protein Rab-8B GN=RAB8B	6,79E+04	1,24E+05	1,74E+05	1,17E+05	9,57E+04	1,26E+05	1,45E+05	1,17E+05
TPM2;TPM1	3,00	3,00	199,75	0,71	1,00	1,16	0,06	NMX	32945,00	Tropomyosin beta chain GN=TPM2	3,59E+05	3,66E+05	9,23E+05	1,00E+06	1,22E+06	3,03E+05	4,18E+05	3,43E+05
CLIC4	10,00	10,00	643,07	0,72	1,00	1,19	0,07	NMX	28982,00	Chloride intracellular channel protein 4 GN=CLIC4	1,32E+06	9,84E+05	3,56E+06	1,65E+06	2,13E+06	9,00E+05	1,78E+06	1,53E+06
PRDX6	8,00	8,00	474,36	0,72	1,00	1,04	0,85	NMX	25133,00	Peroxiredoxin-6 GN=PRDX6	1,32E+06	1,41E+06	2,31E+06	2,11E+06	1,43E+06	1,49E+06	1,98E+06	1,97E+06
MOES	26,00	18,00	1705,14	0,72	1,00	1,06	0,20	NMX	67892,00	Moesin GN=MSN	7,47E+06	3,92E+06	1,06E+07	5,25E+06	8,07E+06	3,99E+06	8,05E+06	5,51E+06
GNAI3	8,00	2,00	417,79	0,72	1,00	1,10	0,08	NMX	41076,00	Guanine nucleotide-binding protein G(k) subunit alpha GN=GNAI3	9,25E+04	1,30E+05	2,27E+05	1,45E+05	1,33E+05	1,18E+05	1,80E+05	1,11E+05
CD109	6,00	6,00	289,95	0,72	1,00	1,02	0,10	HPX	162500,00	CD109 antigen GN=CD109	3,65E+05	1,66E+05	6,83E+05	2,01E+05	4,27E+05	1,43E+05	5,13E+05	3,59E+05
RAB10	6,00	4,00	348,88	0,72	1,00	1,01	0,09	HPX	22755,00	Ras-related protein Rab-10 GN=RAB10	8,23E+05	9,91E+05	1,75E+06	1,03E+06	1,10E+06	1,17E+06	1,45E+06	9,39E+05
HXK1	3,00	3,00	144,89	0,73	1,00	1,27	0,06	HPX	103561,00	Hexokinase-1 GN=HK1	3,89E+04	9,13E+04	6,52E+04	5,78E+04	1,34E+05	1,06E+05	3,88E+04	4,40E+04
TARSH	8,00	8,00	375,17	0,73	1,00	1,09	0,23	NMX	119253,00	Target of Nesh-SH3 GN=ABI3BP	4,10E+05	7,69E+05	1,96E+05	5,21E+04	2,46E+05	7,38E+05	2,82E+05	4,77E+04
UCHL1	2,00	2,00	84,57	0,73	1,00	1,09	0,06	NMX	25151,00	Ubiquitin carboxyl-terminal hydrolase isozyme L1 GN=UCHL1	2,79E+05	5,26E+05	5,38E+05	3,87E+05	5,17E+05	3,04E+05	4,93E+05	2,68E+05
FAT1	6,00	6,00	303,70	0,73	1,00	1,05	0,47	NMX	509379,00	Protocadherin Fat 1 GN=FAT1	1,88E+05	9,90E+04	3,42E+05	1,79E+05	1,87E+05	9,97E+04	2,85E+05	1,96E+05
GANAB	5,00	5,00	236,60	0,73	1,00	1,06	0,06	HPX	107263,00	Neutral alpha-glucosidase AB GN=GANAB	1,07E+05	2,23E+05	2,14E+05	1,84E+05	1,93E+05	2,49E+05	1,39E+05	1,92E+05
OX2G	3,00	3,00	140,23	0,73	1,00	1,09	0,11	NMX	31643,00	OX-2 membrane glycoprotein GN=CD200	7,16E+05	5,34E+05	1,76E+06	5,77E+05	7,68E+05	3,87E+05	1,34E+06	7,80E+05
RS5	2,00	2,00	179,40	0,73	1,00	1,09	0,06	NMX	23033,00	40S ribosomal protein S5 GN=RPS5	1,99E+05	4,37E+05	4,17E+05	2,51E+05	3,59E+05	4,33E+05	2,24E+05	1,77E+05
STOM	8,00	8,00	523,26	0,74	1,00	1,04	0,07	NMX	31882,00	Erythrocyte band 7 integral membrane protein GN=STOM	9,48E+05	1,52E+06	9,75E+05	8,90E+05	1,28E+06	1,31E+06	9,28E+05	6,67E+05
PI4KA	2,00	2,00	166,07	0,74	1,00	1,11	0,22	NMX	239244,00	Phosphatidylinositol 4-kinase alpha GN=PI4KA	2,16E+04	2,89E+03	3,74E+04	2,45E+04	1,57E+04	7,90E+03	3,15E+04	2,28E+04
CO4A	2,00	2,00	110,60	0,74	1,00	1,12	0,42	HPX	194261,00	Complement C4-A GN=C4A	6,64E+04	1,07E+05	6,64E+04	2,33E+05	7,33E+04	9,21E+04	6,12E+04	3,03E+05
PCBP2	3,00	2,00	139,74	0,74	1,00	1,08	0,05	HPX	38955,00	Poly(rC)-binding protein 2 GN=PCBP2	1,43E+05	2,49E+05	3,09E+05	2,74E+05	3,35E+05	2,74E+05	2,64E+05	1,84E+05
PSMD6	3,00	3,00	147,21	0,75	1,00	1,14	0,05	NMX	45787,00	26S proteasome non-ATPase regulatory subunit 6 GN=PSMD6	7,89E+04	1,36E+05	1,89E+05	1,65E+05	1,42E+05	1,28E+05	1,16E+05	1,12E+05
CAND1	5,00	5,00	255,19	0,75	1,00	1,03	0,08	HPX	137999,00	Cullin-associated NEDD8-dissociated protein 1 GN=CAND1	1,39E+05	7,55E+04	1,90E+05	1,61E+05	1,22E+05	1,02E+05	1,53E+05	2,05E+05
UGPA	3,00	3,00	118,03	0,75	1,00	1,09	0,06	NMX	57076,00	UTP--glucose-1-phosphate uridylyltransferase GN=UGP2	1,03E+05	1,44E+05	1,42E+05	2,00E+05	1,66E+05	1,26E+05	1,13E+05	1,37E+05
VDAC1	2,00	2,00	91,57	0,75	1,00	1,17	0,05	NMX	30868,00	Voltage-dependent anion-selective channel protein 1 GN=VDAC1	9,69E+04	2,34E+05	1,55E+05	3,33E+05	2,75E+05	2,19E+05	9,30E+04	1,11E+05
GBG12	3,00	3,00	227,37	0,75	1,00	1,07	0,10	NMX	8115,00	Guanine nucleotide-binding protein G(I)/G(S)/G(O) subunit gamma-12 GN=GNG12	3,08E+06	3,10E+06	7,24E+06	3,41E+06	3,30E+06	2,59E+06	5,70E+06	4,20E+06
PICAL	3,00	3,00	179,48	0,75	1,00	1,17	0,07	NMX	70881,00	Phosphatidylinositol-binding clathrin assembly protein GN=PICALM	2,16E+05	1,54E+05	5,66E+05	2,20E+05	3,03E+05	1,41E+05	3,00E+05	2,44E+05
ESTD	2,00	2,00	88,45	0,75	1,00	1,05	0,05	HPX	31956,00	S-formylglutathione hydrolase GN=ESD	1,90E+05	1,46E+05	3,02E+05	1,82E+05	1,87E+05	2,22E+05	1,81E+05	2,76E+05
AT1B3	4,00	4,00	245,02	0,76	1,00	1,03	0,07	NMX	31834,00	Sodium/potassium-transporting ATPase subunit beta-3 GN=ATP1B3	1,55E+06	1,78E+06	2,24E+06	2,22E+06	1,48E+06	2,02E+06	2,45E+06	1,66E+06

XPP1	2,00	2,00	98,93	0,76	1,00	1,05	0,08	NMX	70558,00	Xaa-Pro aminopeptidase 1 GN=XPNPEP1	5,72E+04	5,59E+04	8,94E+04	9,61E+04	6,77E+04	5,65E+04	6,86E+04	9,28E+04
PHB2	2,00	2,00	131,12	0,76	1,00	1,19	0,08	HPX	33276,00	Prohibitin-2 GN=PHB2	7,90E+04	1,90E+05	2,58E+04	9,61E+04	1,91E+05	1,90E+05	2,80E+04	5,50E+04
RL22	2,00	2,00	94,23	0,76	1,00	1,02	0,06	NMX	14835,00	60S ribosomal protein L22 GN=RPL22	1,45E+05	1,89E+05	3,09E+05	1,03E+05	3,40E+05	1,99E+05	1,30E+05	5,96E+04
PXDN	28,00	28,00	1658,50	0,76	1,00	1,15	0,06	NMX	167793,00	Peroxidasin homolog GN=PXDN	3,12E+06	8,85E+05	1,37E+06	2,38E+06	1,02E+06	9,70E+05	2,80E+06	1,95E+06
PYGB	6,00	4,00	408,34	0,77	1,00	1,06	0,07	NMX	97319,00	Glycogen phosphorylase, brain form GN=PYGB	2,94E+05	3,33E+05	4,90E+05	6,48E+05	4,20E+05	2,86E+05	3,42E+05	6,20E+05
CPNS1	3,00	3,00	221,05	0,77	1,00	1,13	0,05	NMX	28469,00	Calpain small subunit 1 GN=CAPNS1	1,66E+05	2,01E+05	4,05E+05	3,27E+05	3,76E+05	1,93E+05	2,52E+05	1,56E+05
KINH	5,00	5,00	317,44	0,77	1,00	1,04	0,06	HPX	110358,00	Kinesin-1 heavy chain GN=KIF5B	3,01E+05	3,27E+05	4,10E+05	3,80E+05	4,30E+05	2,98E+05	3,72E+05	3,68E+05
MAP1B	4,00	4,00	258,24	0,78	1,00	1,08	0,05	HPX	271665,00	Microtubule-associated protein 1B GN=MAP1B	2,11E+05	3,68E+05	3,47E+05	2,37E+05	4,39E+05	3,57E+05	2,41E+05	2,24E+05
RL18A	2,00	2,00	70,60	0,78	1,00	1,00	0,15	HPX	21034,00	60S ribosomal protein L18a GN=RPL18A	1,24E+05	1,10E+05	1,31E+05	2,28E+05	1,39E+05	1,22E+05	1,19E+05	2,15E+05
HS90B	17,00	7,00	931,47	0,79	1,00	1,05	0,05	HPX	83554,00	Heat shock protein HSP 90-beta GN=HSP90AB1	8,16E+05	9,24E+05	1,51E+06	9,50E+05	1,34E+06	1,27E+06	9,82E+05	8,33E+05
PRS6A	2,00	2,00	76,87	0,79	1,00	1,12	0,05	NMX	49458,00	26S protease regulatory subunit 6A GN=PSMC3	8,11E+04	1,41E+05	1,68E+05	1,92E+05	1,42E+05	1,24E+05	1,18E+05	1,38E+05
COR1B	2,00	2,00	74,09	0,79	1,00	1,06	0,05	NMX	54885,00	Coronin-1B GN=CORO1B	5,60E+04	8,95E+04	1,13E+05	1,01E+05	1,37E+05	7,41E+04	8,06E+04	4,57E+04
RAP1B	5,00	3,00	339,98	0,79	1,00	1,02	0,08	HPX	21040,00	Ras-related protein Rap-1b GN=RAP1B	4,20E+06	3,21E+06	7,81E+06	4,62E+06	4,31E+06	4,27E+06	7,85E+06	3,79E+06
TSN14	2,00	2,00	140,99	0,79	1,00	1,05	0,08	NMX	31355,00	Tetraspanin-14 GN=TSPAN14	1,71E+05	3,62E+05	2,88E+05	1,58E+05	1,85E+05	3,56E+05	2,05E+05	1,84E+05
RS27A	5,00	5,00	225,28	0,79	1,00	1,08	0,13	NMX	18296,00	Ubiquitin-40S ribosomal protein S27a GN=RPS27A	7,52E+06	1,57E+07	8,74E+06	4,99E+06	7,97E+06	1,27E+07	7,13E+06	6,29E+06
MYO1C	25,00	25,00	1377,13	0,79	1,00	1,03	0,07	NMX	122461,00	Unconventional myosin-Ic GN=MYO1C	9,97E+05	1,13E+06	1,67E+06	1,39E+06	1,18E+06	1,01E+06	1,42E+06	1,42E+06
CD82	7,00	7,00	466,48	0,79	1,00	1,02	0,07	HPX	30233,00	CD82 antigen GN=CD82	1,36E+06	2,56E+06	2,07E+06	1,13E+06	1,38E+06	2,71E+06	1,59E+06	1,58E+06
PSB1	3,00	3,00	119,33	0,79	1,00	1,03	0,36	HPX	26700,00	Proteasome subunit beta type-1 GN=PSMB1	5,28E+05	5,55E+05	4,19E+05	9,51E+05	4,63E+05	5,00E+05	4,01E+05	1,16E+06
SERA	2,00	2,00	87,60	0,80	1,00	1,09	0,06	HPX	57356,00	D-3-phosphoglycerate dehydrogenase GN=PHGDH	4,75E+04	7,84E+04	7,26E+04	1,37E+05	1,02E+05	7,69E+04	4,47E+04	1,41E+05
1433T	9,00	6,00	596,30	0,80	1,00	1,10	0,06	NMX	28032,00	14-3-3 protein theta GN=YWHAQ	4,43E+05	5,22E+05	9,82E+05	9,67E+05	7,12E+05	4,72E+05	6,89E+05	7,78E+05
GTR1	8,00	8,00	476,51	0,80	1,00	1,05	0,09	HPX	54391,00	Solute carrier family 2, facilitated glucose transporter member 1 GN=SLC2A1	5,83E+06	8,07E+06	5,17E+06	8,80E+06	6,62E+06	7,10E+06	4,59E+06	1,09E+07
TCPA	9,00	9,00	536,56	0,80	1,00	1,07	0,05	NMX	60819,00	T-complex protein 1 subunit alpha GN=TCP1	2,99E+05	4,81E+05	5,40E+05	5,57E+05	4,58E+05	4,70E+05	3,82E+05	4,36E+05
CALX	9,00	9,00	605,75	0,81	1,00	1,03	0,06	NMX	67982,00	Calnexin GN=CANX	5,33E+05	1,30E+06	7,28E+05	8,76E+05	9,22E+05	1,33E+06	4,56E+05	6,19E+05
GPX3	2,00	2,00	67,56	0,81	1,00	1,15	0,11	HPX	25765,00	Glutathione peroxidase 3 GN=GPX3	5,04E+04	1,08E+05	7,64E+04	2,26E+05	4,87E+04	6,41E+04	6,98E+04	3,49E+05
PAPP1	5,00	5,00	250,49	0,81	1,00	1,01	0,12	HPX	185645,00	Pappalysin-1 GN=PAPPA	2,14E+05	1,24E+05	3,29E+05	6,54E+04	1,45E+05	1,44E+05	3,86E+05	6,16E+04
PCBP1	3,00	2,00	129,15	0,81	1,00	1,05	0,05	NMX	37987,00	Poly(rC)-binding protein 1 GN=PCBP1	1,80E+05	3,29E+05	2,61E+05	2,73E+05	3,39E+05	2,62E+05	2,28E+05	1,61E+05
UBA1	5,00	5,00	379,26	0,81	1,00	1,05	0,06	HPX	118858,00	Ubiquitin-like modifier-activating enzyme 1 GN=UBA1	3,76E+05	4,90E+05	4,77E+05	5,58E+05	5,19E+05	3,96E+05	4,14E+05	6,59E+05
PTX3	16,00	14,00	1107,06	0,81	1,00	1,02	0,06	NMX	42519,00	Pentraxin-related protein PTX3 GN=PTX3	3,15E+07	3,06E+07	1,07E+07	2,78E+06	1,00E+07	4,01E+07	1,76E+07	6,40E+06
CAZA1	3,00	2,00	153,09	0,81	1,00	1,06	0,06	HPX	33073,00	F-actin-capping protein subunit alpha-1 GN=CAPZA1	1,33E+05	1,48E+05	2,40E+05	2,44E+05	2,35E+05	1,22E+05	1,84E+05	2,66E+05
CD9	3,00	3,00	229,93	0,81	1,00	1,17	0,08	HPX	25969,00	CD9 antigen GN=CD9	7,23E+06	7,48E+06	1,20E+07	3,35E+06	4,60E+06	1,31E+07	1,44E+07	3,13E+06
TSN3	2,00	2,00	71,55	0,81	1,00	1,03	0,18	NMX	28797,00	Tetraspanin-3 GN=TSPAN3 PE=2 SV=1	1,47E+05	5,45E+05	1,61E+05	6,84E+04	1,28E+05	5,21E+05	1,50E+05	9,96E+04
EHD2	19,00	17,00	1130,76	0,81	1,00	1,02	0,08	HPX	61294,00	EH domain-containing protein 2 GN=EHD2	2,56E+06	1,66E+06	5,14E+06	2,69E+06	2,64E+06	1,56E+06	4,20E+06	3,85E+06
RS3	6,00	6,00	321,39	0,81	1,00	1,05	0,05	HPX	26842,00	40S ribosomal protein S3 GN=RPS3	5,63E+05	9,99E+05	9,63E+05	7,91E+05	1,04E+06	9,85E+05	6,41E+05	8,13E+05
MPCP	2,00	2,00	84,26	0,81	1,00	1,16	0,06	HPX	40525,00	Phosphate carrier protein, mitochondrial GN=SLC25A3	1,77E+05	4,42E+05	2,11E+05	2,47E+05	4,65E+05	4,48E+05	1,29E+05	2,09E+05
SC22B	2,00	2,00	129,05	0,81	1,00	1,00	0,06	HPX	24806,00	Vesicle-trafficking protein SEC22b GN=SEC22B	1,02E+05	3,32E+05	2,83E+05	2,05E+05	2,03E+05	3,22E+05	2,46E+05	1,53E+05
SYAC	2,00	2,00	64,62	0,82	1,00	1,01	0,07	HPX	107484,00	Alanine--tRNA ligase, cytoplasmic GN=AARS	7,32E+04	1,11E+05	1,04E+05	1,27E+05	9,21E+04	9,73E+04	1,00E+05	1,30E+05
CYFP1	11,00	11,00	652,09	0,82	1,00	1,03	0,13	NMX	146742,00	Cytoplasmic FMR1-interacting protein 1 GN=CYFIP1	2,34E+05	1,71E+05	6,08E+05	3,88E+05	3,10E+05	1,84E+05	4,92E+05	3,73E+05
LAMB1	13,00	13,00	864,72	0,82	1,00	1,02	0,06	HPX	205150,00	Laminin subunit beta-1 GN=LAMB1	1,34E+06	4,62E+05	9,41E+05	3,70E+05	9,25E+05	9,62E+05	9,51E+05	3,24E+05
CXA1	3,00	3,00	209,66	0,82	1,00	1,03	0,05	NMX	43494,00	Gap junction alpha-1 protein GN=GJA1	4,14E+05	4,71E+05	3,82E+05	3,42E+05	4,26E+05	3,52E+05	4,05E+05	3,83E+05
EIF3F	2,00	2,00	125,13	0,82	1,00	1,15	0,05	NMX	37654,00	Eukaryotic translation initiation factor 3 subunit F GN=EIF3F	7,33E+04	7,49E+04	1,85E+05	1,51E+05	1,31E+05	8,58E+04	1,09E+05	9,66E+04
UAP1	4,00	4,00	199,47	0,82	1,00	1,15	0,05	NMX	59131,00	UDP-N-acetylhexosamine pyrophosphorylase GN=UAP1	1,38E+05	3,11E+05	4,43E+05	3,70E+05	2,75E+05	2,25E+05	2,76E+05	3,19E+05
ITAV	21,00	21,00	1044,39	0,83	1,00	1,03	0,06	NMX	117048,00	Integrin alpha-V GN=ITGAV	1,34E+06	1,54E+06	2,12E+06	1,38E+06	1,19E+06	1,50E+06	1,77E+06	1,74E+06
HTRA1	8,00	8,00	423,88	0,83	1,00	1,01	0,08	NMX	52167,00	Serine protease HTRA1 GN=HTRA1	1,09E+06	3,03E+05	8,29E+05	7,91E+05	7,82E+05	3,89E+05	8,41E+05	9,56E+05
RAB5C	4,00	2,00	258,52	0,83	1,00	1,08	0,05	NMX	23696,00	Ras-related protein Rab-5C GN=RAB5C	3,81E+05	6,04E+05	8,34E+05	6,86E+05	6,21E+05	5,78E+05	5,97E+05	5,18E+05
LAMA5	14,00	14,00	648,22	0,83	1,00	1,47	0,06	NMX	412023,00	Laminin subunit alpha-5 GN=LAMA5	1,14E+06	7,98E+04	1,84E+05	8,63E+04	4,46E+05	2,13E+05	2,73E+05	8,05E+04
CLMP	2,00	2,00	74,24	0,84	1,00	1,00	0,21	NMX	41597,00	CXADR-like membrane protein GN=CLMP	1,22E+05	1,40E+05	1,93E+05	1,18E+05	1,31E+05	1,34E+05	1,82E+05	1,24E+05
ACTB	25,00	12,00	2234,55	0,84	1,00	1,07	0,05	NMX	42052,00	Actin, cytoplasmic 1 GN=ACTB	3,68E+07	5,90E+07	8,29E+07	6,79E+07	8,79E+07	4,15E+07	4,51E+07	5,54E+07
MRCKA	2,00	2,00	106,38	0,84	1,00	1,02	0,06	HPX	199349,00	Serine/threonine-protein kinase MRCK alpha GN=CDC42BPA	3,47E+04	3,58E+04	9,42E+04	3,26E+04	6,00E+04	4,40E+04	7,39E+04	2,35E+04

ANXA2	23,00	23,00	1640,83	0,84	1,00	1,01	0,05	NMX	38808,00	Annexin A2 GN=ANXA2	2,12E+07	2,45E+07	4,94E+07	2,34E+07	3,24E+07	2,28E+07	3,33E+07	2,84E+07
WDR1	9,00	9,00	434,48	0,85	1,00	1,05	0,05	HPX	66836,00	WD repeat-containing protein 1 GN=WDR1	9,00E+05	1,32E+06	1,75E+06	1,79E+06	1,91E+06	9,66E+05	1,41E+06	1,76E+06
CO6A1	23,00	23,00	1860,99	0,85	1,00	1,07	0,10	NMX	109602,00	Collagen alpha-1(VI) chain GN=COL6A1	1,27E+06	1,40E+07	1,06E+06	1,74E+06	1,13E+06	1,22E+07	6,65E+05	3,00E+06
ENOA	14,00	14,00	814,86	0,85	1,00	1,05	0,05	NMX	47481,00	Alpha-enolase GN=ENO1	2,14E+06	3,38E+06	3,56E+06	2,18E+06	3,87E+06	2,16E+06	2,46E+06	2,24E+06
RS8	4,00	4,00	232,39	0,85	1,00	1,09	0,05	NMX	24475,00	40S ribosomal protein S8 GN=RPS8	3,60E+05	9,82E+05	5,09E+05	8,46E+05	6,98E+05	8,02E+05	3,76E+05	5,91E+05
ACTN1	41,00	28,00	2431,04	0,85	1,00	1,02	0,06	HPX	103563,00	Alpha-actinin-1 GN=ACTN1	2,14E+06	1,52E+06	3,10E+06	3,47E+06	3,58E+06	1,65E+06	2,41E+06	2,84E+06
CD166	5,00	5,00	247,24	0,85	1,00	1,07	0,05	NMX	65745,00	CD166 antigen GN=ALCAM	9,75E+05	1,52E+06	1,81E+06	1,01E+06	1,34E+06	1,12E+06	1,31E+06	1,20E+06
FERM2	18,00	18,00	975,82	0,85	1,00	1,05	0,69	NMX	78438,00	Fermitin family homolog 2 GN=FERMT2	1,39E+06	5,77E+05	3,04E+06	1,56E+06	1,50E+06	7,12E+05	2,47E+06	1,55E+06
HYOU1	2,00	2,00	132,18	0,85	1,00	1,27	0,05	NMX	111494,00	Hypoxia up-regulated protein 1 GN=HYOU1	1,59E+04	1,66E+05	7,24E+04	2,77E+04	7,06E+04	1,09E+05	1,56E+04	2,61E+04
EF2	26,00	26,00	1376,11	0,85	1,00	1,02	0,06	NMX	96246,00	Elongation factor 2 GN=EEF2	1,34E+06	1,33E+06	3,14E+06	1,78E+06	2,02E+06	1,43E+06	2,19E+06	1,80E+06
RINI	6,00	6,00	380,34	0,85	1,00	1,04	0,05	HPX	51766,00	Ribonuclease inhibitor GN=RNH1	2,51E+05	4,09E+05	3,63E+05	4,21E+05	5,02E+05	3,44E+05	3,41E+05	3,20E+05
PUR9	4,00	4,00	207,89	0,85	1,00	1,02	0,05	HPX	65089,00	Bifunctional purine biosynthesis protein PURH GN=ATIC	1,45E+05	2,04E+05	2,37E+05	2,60E+05	2,29E+05	1,75E+05	1,92E+05	2,68E+05
IQGA1	25,00	25,00	1539,66	0,85	1,00	1,05	0,05	NMX	189761,00	Ras GTPase-activating-like protein IQGAP1 GN=IQGAP1	7,11E+05	8,97E+05	1,27E+06	1,11E+06	1,26E+06	7,41E+05	7,78E+05	1,03E+06
CLH1	38,00	38,00	2239,84	0,85	1,00	1,05	0,05	NMX	193260,00	Clathrin heavy chain 1 GN=CLTC	1,63E+06	2,00E+06	2,88E+06	2,37E+06	2,50E+06	2,28E+06	2,08E+06	1,60E+06
STAT1	2,00	2,00	71,58	0,85	1,00	1,10	0,05	NMX	87850,00	Signal transducer and activator of transcription 1-alpha/beta GN=STAT1	8,60E+04	1,85E+05	2,22E+05	1,85E+05	1,56E+05	1,70E+05	1,59E+05	1,29E+05
KCC2D	2,00	2,00	151,91	0,85	1,00	1,08	0,05	NMX	56961,00	Calcium/calmodulin-dependent protein kinase type II subunit delta GN=CAMK2D	2,01E+05	2,93E+05	4,71E+05	3,20E+05	3,03E+05	3,03E+05	3,30E+05	2,55E+05
GAPR1	2,00	2,00	142,33	0,86	1,00	1,02	0,05	NMX	17322,00	Golgi-associated plant pathogenesis-related protein 1 GN=GLIPR2	1,28E+05	1,73E+05	2,83E+05	1,34E+05	2,72E+05	1,17E+05	2,17E+05	9,87E+04
DAG1	2,00	2,00	131,26	0,86	1,00	1,05	0,06	NMX	97723,00	Dystroglycan GN=DAG1	2,14E+05	2,76E+05	4,18E+05	3,73E+05	2,97E+05	2,54E+05	3,16E+05	3,49E+05
SYK	2,00	2,00	94,53	0,86	1,00	1,02	0,05	NMX	68461,00	Lysine--tRNA ligase GN=KARS	1,10E+05	7,76E+04	1,04E+05	1,02E+05	1,11E+05	9,10E+04	7,81E+04	1,06E+05
IMB1	6,00	6,00	384,13	0,86	1,00	1,02	0,05	NMX	98420,00	Importin subunit beta-1 GN=KPNB1	4,04E+05	7,48E+05	4,98E+05	5,04E+05	5,08E+05	6,75E+05	3,64E+05	5,56E+05
RAP2B	5,00	2,00	275,40	0,86	1,00	1,02	0,08	NMX	20719,00	Ras-related protein Rap-2b GN=RAP2B	3,80E+05	5,35E+05	6,78E+05	5,00E+05	3,97E+05	5,36E+05	5,76E+05	5,41E+05
PDCD6	3,00	3,00	152,85	0,87	1,00	1,01	0,07	HPX	21912,00	Programmed cell death protein 6 GN=PDCD6	5,26E+05	3,93E+05	6,07E+05	5,31E+05	4,64E+05	3,98E+05	6,34E+05	5,91E+05
G6PD	5,00	5,00	219,25	0,87	1,00	1,02	0,05	HPX	59675,00	Glucose-6-phosphate 1-dehydrogenase GN=G6PD	2,92E+05	3,91E+05	3,29E+05	4,23E+05	3,95E+05	3,54E+05	2,91E+05	4,19E+05
ITA11	6,00	6,00	283,20	0,87	1,00	1,04	0,05	NMX	134527,00	Integrin alpha-11 GN=ITGA11	2,01E+05	2,19E+05	1,28E+05	1,41E+05	2,01E+05	1,43E+05	1,71E+05	1,45E+05
SYFB	2,00	2,00	82,96	0,87	1,00	1,02	0,05	HPX	66701,00	Phenylalanine--tRNA ligase beta subunit GN=FARSB	5,80E+04	8,25E+04	1,07E+05	8,77E+04	1,05E+05	7,31E+04	7,38E+04	9,16E+04
ACTZ	4,00	4,00	247,48	0,87	1,00	1,07	0,05	HPX	42701,00	Alpha-centractin GN=ACTR1A	1,49E+05	2,01E+05	2,37E+05	2,92E+05	3,64E+05	1,68E+05	1,83E+05	2,28E+05
ATL1	3,00	3,00	102,59	0,87	1,00	1,00	0,07	NMX	199271,00	ADAMTS-like protein 1 GN=ADAMTSL1	4,33E+04	5,11E+04	8,11E+04	1,36E+05	4,27E+04	4,05E+04	1,14E+05	1,13E+05
SC11A	2,00	2,00	126,23	0,87	1,00	1,05	0,05	HPX	20612,00	Signal peptidase complex catalytic subunit SEC11A GN=SEC11A	4,89E+04	1,09E+05	7,57E+04	6,16E+04	8,97E+04	1,13E+05	5,48E+04	5,17E+04
LRP1	23,00	23,00	1116,40	0,88	1,00	1,07	0,09	HPX	523150,00	Prolow-density lipoprotein receptor-related protein 1 GN=LRP1	5,35E+05	4,53E+05	6,29E+05	1,03E+06	3,80E+05	4,52E+05	6,04E+05	1,38E+06
GBB1	6,00	2,00	395,28	0,88	1,00	1,08	0,06	NMX	38151,00	Guanine nucleotide-binding protein G(I)/G(S)/G(T) subunit beta-1 GN=GNB1	1,76E+06	1,77E+06	4,22E+06	1,60E+06	2,09E+06	1,54E+06	3,11E+06	1,94E+06
TAGL	11,00	11,00	612,83	0,88	1,00	1,03	0,07	NMX	22653,00	Transgelin GN=TAGLN	7,27E+05	5,50E+05	1,48E+06	1,01E+06	8,36E+05	5,08E+05	1,21E+06	1,11E+06
HSPB1	3,00	3,00	139,81	0,88	1,00	1,01	0,05	HPX	22826,00	Heat shock protein beta-1 GN=HSPB1	3,03E+05	5,45E+05	6,55E+05	6,93E+05	5,49E+05	4,41E+05	4,68E+05	7,58E+05
GCN1	2,00	2,00	89,22	0,89	1,00	1,20	0,05	NMX	294967,00	eIF-2-alpha kinase activator GCN1 GN=GCN1	3,91E+04	8,71E+03	8,89E+04	4,14E+04	4,08E+04	4,29E+04	2,66E+04	3,85E+04
ATPB	6,00	6,00	300,23	0,89	1,00	1,02	0,05	HPX	56525,00	ATP synthase subunit beta, mitochondrial GN=ATP5B	2,08E+05	4,18E+05	2,06E+05	1,94E+05	4,24E+05	3,38E+05	1,40E+05	1,48E+05
AAAT	10,00	10,00	728,31	0,89	1,00	1,04	0,06	HPX	57018,00	Neutral amino acid transporter B(0) GN=SLC1A5	7,71E+06	4,46E+06	9,56E+06	7,25E+06	6,39E+06	4,14E+06	1,04E+07	9,16E+06
SEPR	11,00	11,00	528,30	0,89	1,00	1,01	0,06	HPX	88341,00	Prolyl endopeptidase FAP GN=FAP	7,95E+05	6,61E+05	1,37E+06	1,10E+06	5,10E+05	8,04E+05	1,27E+06	1,39E+06
ARPC4	4,00	4,00	209,35	0,89	1,00	1,03	0,05	HPX	19768,00	Actin-related protein 2/3 complex subunit 4 GN=ARPC4	6,63E+05	6,53E+05	9,94E+05	9,99E+05	1,12E+06	6,34E+05	7,92E+05	8,48E+05
EHD1	30,00	18,00	1755,73	0,89	1,00	1,05	0,07	NMX	60646,00	EH domain-containing protein 1 GN=EHD1	2,70E+06	1,68E+06	6,62E+06	2,46E+06	3,27E+06	1,66E+06	5,00E+06	2,91E+06
TCPE	6,00	6,00	281,67	0,89	1,00	1,02	0,05	HPX	60089,00	T-complex protein 1 subunit epsilon GN=CCT5	1,83E+05	2,45E+05	3,19E+05	1,98E+05	3,06E+05	2,46E+05	2,14E+05	1,96E+05
CH60	7,00	7,00	373,31	0,89	1,00	1,06	0,05	HPX	61187,00	60 kDa heat shock protein, mitochondrial GN=HSPD1	1,61E+05	3,57E+05	1,46E+05	2,20E+05	3,60E+05	2,65E+05	1,15E+05	1,97E+05
SYTC	2,00	2,00	95,12	0,89	1,00	1,07	0,05	NMX	84294,00	Threonine--tRNA ligase, cytoplasmic GN=TARS	8,30E+04	1,00E+05	1,77E+05	1,05E+05	1,32E+05	1,11E+05	8,45E+04	1,08E+05
APMAP	3,00	3,00	106,67	0,90	1,00	1,05	0,05	HPX	46622,00	Adipocyte plasma membrane-associated protein GN=APMAP	9,29E+04	2,24E+05	2,01E+05	1,77E+05	2,09E+05	2,72E+05	1,11E+05	1,39E+05
EIFCL	3,00	3,00	109,28	0,90	1,00	1,03	0,05	HPX	106091,00	Eukaryotic translation initiation factor 3 subunit C-like protein GN=EIF3CL PE=3 SV=1	3,09E+04	4,91E+04	5,16E+04	6,32E+04	6,55E+04	3,62E+04	4,36E+04	5,47E+04

SNP23	2,00	2,00	89,46	0,90	1,00	1,00	0,05	HPX	23682,00	Synaptosomal-associated protein 23 GN=SNAP23	1,19E+05	2,02E+05	2,94E+05	1,14E+05	2,69E+05	1,39E+05	1,93E+05	1,32E+05
1A02	8,00	7,00	477,54	0,90	1,00	1,01	0,11	NMX	41181,00	HLA class I histocompatibility antigen, A-2 alpha chain GN=HLA-A	1,04E+06	1,38E+06	1,35E+06	7,28E+05	1,11E+06	1,22E+06	1,16E+06	9,33E+05
APOE	4,00	4,00	128,96	0,90	1,00	1,00	0,05	NMX	36246,00	Apolipoprotein E GN=APOE	6,74E+05	1,08E+06	1,37E+06	1,55E+06	8,86E+05	9,19E+05	8,75E+05	1,97E+06
RAI3	3,00	3,00	244,36	0,90	1,00	1,02	0,06	NMX	40624,00	Retinoic acid-induced protein 3 GN=GPRC5A	1,34E+06	1,45E+06	2,76E+06	9,97E+05	1,45E+06	1,22E+06	2,44E+06	1,30E+06
TBB2A	20,00	2,00	1498,60	0,91	1,00	1,06	0,05	NMX	50274,00	Tubulin beta-2A chain GN=TUBB2A	1,45E+06	3,59E+06	2,33E+06	2,39E+06	2,76E+06	2,37E+06	1,51E+06	2,57E+06
GNAS 1	9,00	8,00	496,17	0,91	1,00	1,02	0,05	NMX	111697,00	Guanine nucleotide-binding protein G(s) subunit alpha isoforms XLas GN=GNAS	9,53E+05	1,23E+06	2,14E+06	1,37E+06	1,35E+06	1,18E+06	1,75E+06	1,31E+06
PRDX 1	7,00	5,00	243,60	0,91	1,00	1,04	0,07	NMX	22324,00	Peroxiredoxin-1 GN=PRDX1	2,10E+06	1,60E+06	8,01E+05	1,17E+06	1,50E+06	1,47E+06	1,22E+06	1,27E+06
FARP1	10,00	10,00	524,79	0,91	1,00	1,07	0,06	NMX	119300,00	FERM, RhoGEF and pleckstrin domain-containing protein 1 GN=FARP1	4,39E+05	3,27E+05	1,21E+06	3,35E+05	5,96E+05	2,97E+05	8,70E+05	4,08E+05
TCPG	14,00	14,00	884,83	0,91	1,00	1,03	0,05	NMX	61066,00	T-complex protein 1 subunit gamma GN=CCT3	3,98E+05	5,88E+05	5,91E+05	6,54E+05	5,17E+05	5,63E+05	5,01E+05	5,91E+05
FSCN1	7,00	7,00	419,23	0,91	1,00	1,07	0,05	NMX	55123,00	Fascin GN=FSCN1	4,46E+05	3,73E+05	1,01E+06	5,56E+05	7,60E+05	3,58E+05	5,42E+05	5,62E+05
THRB	8,00	8,00	513,32	0,91	1,00	1,16	0,06	HPX	71475,00	Prothrombin GN=F2	8,28E+05	1,50E+06	1,62E+06	5,30E+06	1,39E+06	1,16E+06	1,04E+06	7,17E+06
CAP1	10,00	9,00	593,93	0,91	1,00	1,04	0,05	NMX	52325,00	Adenylyl cyclase-associated protein 1 GN=CAP1	6,37E+05	6,92E+05	1,35E+06	9,87E+05	1,31E+06	6,61E+05	8,05E+05	7,41E+05
RL7A	3,00	3,00	159,76	0,91	1,00	1,02	0,05	HPX	30148,00	60S ribosomal protein L7a GN=RPL7A	2,63E+05	6,36E+05	3,86E+05	2,85E+05	5,00E+05	5,55E+05	2,79E+05	2,65E+05
RAB2 A	2,00	2,00	112,67	0,91	1,00	1,05	0,05	NMX	23702,00	Ras-related protein Rab-2A GN=RAB2A	2,53E+05	4,68E+05	5,37E+05	4,32E+05	3,59E+05	4,12E+05	3,74E+05	4,62E+05
FPRP	11,00	11,00	528,09	0,91	1,00	1,03	0,06	HPX	99464,00	Prostaglandin F2 receptor negative regulator GN=PTGFRN	2,57E+05	3,86E+05	4,51E+05	1,51E+05	3,38E+05	4,09E+05	4,08E+05	1,26E+05
ITA2	27,00	27,00	1609,85	0,91	1,00	1,04	0,07	NMX	130468,00	Integrin alpha-2 GN=ITGA2	1,56E+06	2,27E+06	5,92E+06	3,29E+06	1,74E+06	2,27E+06	4,55E+06	4,03E+06
ICAM 1	15,00	15,00	776,57	0,91	1,00	1,04	0,06	NMX	58587,00	Intercellular adhesion molecule 1 GN=ICAM1	5,45E+06	5,82E+06	9,91E+06	4,94E+06	5,69E+06	5,52E+06	8,17E+06	5,85E+06
GDIB	11,00	11,00	688,59	0,91	1,00	1,07	0,06	NMX	51087,00	Rab GDP dissociation inhibitor beta GN=GDI2	1,35E+06	6,07E+05	2,27E+06	8,66E+05	1,03E+06	8,44E+05	1,78E+06	1,12E+06
HS90A	19,00	11,00	1065,29	0,91	1,00	1,04	0,05	HPX	85006,00	Heat shock protein HSP 90-alpha GN=HSP90AA1	8,02E+05	1,19E+06	1,49E+06	1,29E+06	1,78E+06	1,00E+06	1,03E+06	1,13E+06
RLA0	3,00	3,00	186,22	0,92	1,00	1,01	0,05	NMX	34423,00	60S acidic ribosomal protein P0 GN=RPLP0	3,35E+05	5,47E+05	4,61E+05	5,12E+05	5,71E+05	5,43E+05	3,36E+05	3,79E+05
GBB4	3,00	2,00	206,32	0,92	1,00	1,05	0,05	NMX	38284,00	Guanine nucleotide-binding protein subunit beta-4 GN=GNB4	1,97E+05	2,12E+05	5,61E+05	2,25E+05	2,64E+05	1,80E+05	4,02E+05	2,95E+05
1433E	12,00	9,00	633,08	0,92	1,00	1,04	0,05	NMX	29326,00	14-3-3 protein epsilon GN=YWHAE	1,71E+06	2,30E+06	3,13E+06	3,16E+06	2,79E+06	1,92E+06	2,52E+06	2,67E+06
ARPC2	10,00	10,00	459,95	0,92	1,00	1,06	0,05	HPX	34426,00	Actin-related protein 2/3 complex subunit 2 GN=ARPC2	4,29E+05	4,50E+05	7,83E+05	3,74E+05	8,37E+05	4,10E+05	6,15E+05	2,93E+05
#####	2,00	2,00	77,51	0,92	1,00	1,03	0,05	HPX	65646,00	Septin-9 GN=SEPT9	9,92E+04	1,19E+05	1,47E+05	1,40E+05	1,82E+05	1,07E+05	1,18E+05	1,16E+05
RL27A	3,00	3,00	144,43	0,92	1,00	1,00	0,05	HPX	16665,00	60S ribosomal protein L27a GN=RPL27A	3,10E+05	6,46E+05	3,53E+05	5,04E+05	5,35E+05	5,76E+05	3,23E+05	3,86E+05
TBA4A	14,00	2,00	933,48	0,93	1,00	1,11	0,06	HPX	50634,00	Tubulin alpha-4A chain GN=TUBA4A	1,80E+05	4,76E+05	2,57E+05	2,10E+06	2,59E+05	2,59E+05	2,96E+05	2,53E+06
MARC S	4,00	4,00	329,03	0,93	1,00	1,05	0,05	HPX	31707,00	Myristoylated alanine-rich C-kinase substrate GN=MARCKS	7,99E+05	7,07E+05	1,00E+06	7,78E+05	1,10E+06	4,85E+05	1,02E+06	8,62E+05
RAB21	3,00	3,00	143,87	0,93	1,00	1,02	0,05	NMX	24731,00	Ras-related protein Rab-21 GN=RAB21	4,90E+05	5,24E+05	8,35E+05	4,79E+05	4,47E+05	5,24E+05	7,21E+05	5,90E+05
LDHA	10,00	10,00	666,53	0,93	1,00	1,08	0,05	NMX	36950,00	L-lactate dehydrogenase A chain GN=LDHA	9,04E+05	1,10E+06	2,49E+06	2,05E+06	1,86E+06	9,46E+05	1,52E+06	1,73E+06
PPIA	4,00	4,00	199,16	0,93	1,00	1,01	0,05	NMX	18229,00	Peptidyl-prolyl cis-trans isomerase A GN=PPIA	5,46E+05	8,26E+05	7,60E+05	1,08E+06	7,90E+05	5,15E+05	7,45E+05	1,15E+06
MYH9	68,00	58,00	4632,03	0,93	1,00	1,01	0,05	HPX	227646,00	Myosin-9 GN=MYH9	2,50E+06	4,62E+06	3,65E+06	4,79E+06	4,32E+06	4,63E+06	2,54E+06	4,29E+06
RAN	3,00	3,00	165,54	0,93	1,00	1,03	0,05	NMX	24579,00	GTP-binding nuclear protein Ran GN=RAN	2,10E+05	3,65E+05	4,63E+05	4,96E+05	3,40E+05	3,66E+05	3,65E+05	4,11E+05
CSKP	4,00	4,00	158,58	0,94	1,00	1,00	0,06	HPX	105968,00	Peripheral plasma membrane protein CASK GN=CASK	3,02E+05	1,62E+05	3,64E+05	2,25E+05	2,70E+05	1,59E+05	3,69E+05	2,58E+05
GRP7 5	2,00	2,00	110,77	0,94	1,00	1,01	0,05	HPX	73920,00	Stress-70 protein, mitochondrial GN=HSPA9	2,73E+05	5,14E+05	2,18E+05	2,15E+05	3,61E+05	4,56E+05	2,31E+05	1,79E+05
VAT1	11,00	11,00	723,90	0,94	1,00	1,01	0,05	NMX	42122,00	Synaptic vesicle membrane protein VAT-1 homolog GN=VAT1	8,79E+05	1,12E+06	1,81E+06	1,42E+06	1,28E+06	1,00E+06	1,41E+06	1,47E+06
TRFM	3,00	3,00	157,70	0,94	1,00	1,03	0,06	HPX	81760,00	Melanotransferrin GN=MELTF	2,88E+05	3,46E+05	4,09E+05	3,01E+05	2,81E+05	3,65E+05	4,90E+05	2,50E+05
PGAM 1	3,00	3,00	162,55	0,94	1,00	1,05	0,05	NMX	28900,00	Phosphoglycerate mutase 1 GN=PGAM1	5,83E+05	9,27E+05	1,47E+06	1,11E+06	1,18E+06	6,66E+05	9,83E+05	1,05E+06
PDIA1	13,00	12,00	605,83	0,94	1,00	1,03	0,05	HPX	57480,00	Protein disulfide-isomerase GN=P4HB	1,85E+05	8,46E+05	3,55E+05	3,80E+05	5,57E+05	7,96E+05	1,88E+05	2,85E+05
1433F	7,00	4,00	402,08	0,94	1,00	1,00	0,05	NMX	28372,00	14-3-3 protein eta GN=YWHAH	3,45E+05	4,60E+05	4,89E+05	4,70E+05	4,50E+05	3,85E+05	3,55E+05	5,67E+05
ARP2	6,00	5,00	303,18	0,95	1,00	1,04	0,05	HPX	45017,00	Actin-related protein 2 GN=ACTR2	5,37E+05	6,91E+05	1,06E+06	8,08E+05	1,25E+06	6,33E+05	7,93E+05	5,53E+05
GTR3	3,00	3,00	188,23	0,95	1,00	1,05	0,05	NMX	54345,00	Solute carrier family 2, facilitated glucose transporter member 3 GN=SLC2A3	4,40E+05	1,57E+06	8,67E+05	7,88E+05	6,76E+05	1,39E+06	5,12E+05	9,21E+05
RAB23	5,00	5,00	309,57	0,95	1,00	1,04	0,06	NMX	26871,00	Ras-related protein Rab-23 GN=RAB23	2,79E+05	2,92E+05	7,70E+05	3,13E+05	3,46E+05	2,89E+05	6,32E+05	3,19E+05
PSMD 1	2,00	2,00	73,81	0,95	1,00	1,01	0,05	HPX	106795,00	26S proteasome non-ATPase regulatory subunit 1 GN=PSMD1	1,04E+05	1,73E+05	8,86E+04	1,03E+05	1,08E+05	1,53E+05	7,47E+04	1,36E+05
PSMD 2	7,00	7,00	384,59	0,95	1,00	1,02	0,05	NMX	100877,00	26S proteasome non-ATPase regulatory subunit 2 GN=PSMD2	2,28E+05	3,19E+05	4,07E+05	4,39E+05	3,23E+05	3,34E+05	3,09E+05	4,03E+05
RAB35	4,00	2,00	250,31	0,95	1,00	1,06	0,05	NMX	23296,00	Ras-related protein Rab-35 GN=RAB35	1,59E+05	2,43E+05	4,51E+05	2,05E+05	2,44E+05	2,64E+05	3,26E+05	1,63E+05

RAB1A	7,00	5,00	334,05	0,95	1,00	1,05	0,05	NMX	22891,00	Ras-related protein Rab-1A GN=RAB1A	1,53E+06	2,95E+06	3,45E+06	2,30E+06	2,28E+06	2,77E+06	2,63E+06	2,08E+06
EF1A1	10,00	10,00	633,04	0,95	1,00	1,04	0,05	HPX	50451,00	Elongation factor 1-alpha 1 GN=EEF1A1	6,33E+06	1,14E+07	7,52E+06	6,51E+06	1,07E+07	9,87E+06	7,88E+06	4,45E+06
PLST	21,00	19,00	1229,52	0,96	1,00	1,03	0,05	HPX	71279,00	Plastin-3 GN=PLS3	1,31E+06	9,46E+05	2,26E+06	1,49E+06	2,67E+06	8,04E+05	1,43E+06	1,28E+06
SYSC	2,00	2,00	106,25	0,96	1,00	1,01	0,05	HPX	59253,00	Serine--tRNA ligase, cytoplasmic GN=SARS	1,32E+05	1,40E+05	1,71E+05	1,97E+05	1,67E+05	1,38E+05	1,37E+05	2,02E+05
PSD11	4,00	4,00	157,04	0,96	1,00	1,00	0,05	NMX	47719,00	26S proteasome non-ATPase regulatory subunit 11 GN=PSMD11	1,85E+05	2,80E+05	2,96E+05	3,73E+05	2,79E+05	2,60E+05	2,17E+05	3,75E+05
ATPA	8,00	8,00	444,66	0,96	1,00	1,06	0,05	HPX	59828,00	ATP synthase subunit alpha, mitochondrial GN=ATP5A1	3,81E+05	6,96E+05	3,68E+05	3,83E+05	7,25E+05	6,45E+05	2,29E+05	3,31E+05
TENA	3,00	3,00	108,80	0,96	1,00	1,29	0,05	NMX	246345,00	Tenascin GN=TNC	1,43E+04	1,02E+04	1,27E+04	9,43E+04	2,11E+04	1,03E+04	1,49E+04	5,59E+04
RL9	2,00	2,00	100,36	0,96	1,00	1,04	0,05	HPX	21964,00	60S ribosomal protein L9 GN=RPL9	2,11E+05	3,56E+05	3,87E+05	2,78E+05	4,46E+05	3,66E+05	1,90E+05	2,78E+05
BMP1	3,00	3,00	113,84	0,96	1,00	1,00	0,05	HPX	113516,00	Bone morphogenetic protein 1 GN=BMP1	1,51E+05	3,42E+04	8,93E+04	1,34E+05	8,50E+04	4,80E+04	8,13E+04	1,96E+05
RHG01	3,00	3,00	120,86	0,96	1,00	1,03	0,05	NMX	50461,00	Rho GTPase-activating protein 1 GN=ARHGAP1	1,42E+05	2,44E+05	3,43E+05	2,83E+05	2,63E+05	1,90E+05	2,45E+05	2,89E+05
SPTB2	6,00	6,00	286,65	0,97	1,00	1,03	0,05	HPX	275237,00	Spectrin beta chain, non-erythrocytic 1 GN=SPTBN1	7,11E+04	9,56E+04	1,25E+05	1,01E+05	1,54E+05	8,56E+04	7,99E+04	8,54E+04
ANKH	3,00	3,00	221,41	0,97	1,00	1,07	0,05	HPX	54719,00	Progressive ankylosis protein homolog GN=ANKH	2,01E+05	4,66E+04	1,17E+05	6,94E+04	1,68E+05	4,26E+04	2,05E+05	4,99E+04
TCPB	7,00	7,00	476,52	0,97	1,00	1,02	0,05	NMX	57794,00	T-complex protein 1 subunit beta GN=CCT2	2,89E+05	5,08E+05	4,85E+05	5,11E+05	5,60E+05	4,03E+05	3,72E+05	4,17E+05
CPNE1	3,00	3,00	131,71	0,97	1,00	1,00	0,05	NMX	59649,00	Copine-1 GN=CPNE1	2,16E+05	2,01E+05	2,86E+05	1,65E+05	2,57E+05	1,90E+05	2,56E+05	1,62E+05
RRAS	7,00	4,00	395,38	0,97	1,00	1,02	0,06	NMX	23637,00	Ras-related protein R-Ras GN=RRAS	1,19E+06	1,72E+06	2,55E+06	1,53E+06	1,45E+06	1,66E+06	2,14E+06	1,57E+06
RRAS2	9,00	6,00	532,96	0,97	1,00	1,02	0,06	NMX	23613,00	Ras-related protein R-Ras2 GN=RRAS2	5,68E+05	8,19E+05	1,21E+06	7,28E+05	6,92E+05	7,91E+05	1,02E+06	7,47E+05
LAT1	5,00	5,00	249,31	0,97	1,00	1,02	0,05	NMX	55659,00	Large neutral amino acids transporter small subunit 1 GN=SLC7A5	1,39E+06	1,95E+06	2,54E+06	1,61E+06	1,86E+06	1,56E+06	2,18E+06	1,72E+06
CKAP4	10,00	10,00	555,95	0,97	1,00	1,06	0,05	HPX	66097,00	Cytoskeleton-associated protein 4 GN=CKAP4	2,89E+05	7,93E+05	4,43E+05	3,83E+05	5,03E+05	8,86E+05	4,48E+05	1,86E+05
PSD13	4,00	3,00	166,17	0,98	1,00	1,02	0,05	NMX	43203,00	26S proteasome non-ATPase regulatory subunit 13 GN=PSMD13	9,52E+04	1,41E+05	1,37E+05	1,99E+05	1,45E+05	1,29E+05	1,25E+05	1,60E+05
G3P	12,00	11,00	971,35	0,98	1,00	1,03	0,05	NMX	36201,00	Glyceraldehyde-3-phosphate dehydrogenase GN=GAPDH	6,30E+06	1,01E+07	1,30E+07	1,33E+07	1,17E+07	7,85E+06	9,64E+06	1,22E+07
ACTN4	26,00	12,00	1529,54	0,98	1,00	1,02	0,05	HPX	105245,00	Alpha-actinin-4 GN=ACTN4	1,13E+06	8,54E+05	1,66E+06	1,95E+06	2,18E+06	8,13E+05	1,21E+06	1,50E+06
CTL2	7,00	7,00	386,81	0,98	1,00	1,01	0,05	HPX	81610,00	Choline transporter-like protein 2 GN=SLC44A2	6,46E+05	6,93E+05	7,30E+05	4,10E+05	5,82E+05	7,47E+05	7,96E+05	3,85E+05
ITA1	7,00	7,00	332,42	0,98	1,00	1,10	0,05	HPX	132304,00	Integrin alpha-1 GN=ITGA1	2,03E+05	1,28E+05	3,34E+05	6,89E+05	2,03E+05	1,34E+05	2,44E+05	9,08E+05
MDHM	3,00	3,00	157,06	0,99	1,00	1,10	0,05	HPX	35937,00	Malate dehydrogenase, mitochondrial GN=MDH2	1,62E+05	2,00E+05	1,74E+05	1,90E+05	3,53E+05	1,87E+05	1,16E+05	1,43E+05
1433G	7,00	3,00	516,14	0,99	1,00	1,05	0,05	NMX	28456,00	14-3-3 protein gamma GN=YWHAG	3,20E+05	5,95E+05	8,22E+05	7,38E+05	7,24E+05	4,78E+05	5,99E+05	5,65E+05
NB5R3	3,00	3,00	101,04	0,99	1,00	1,01	0,05	HPX	34441,00	NADH-cytochrome b5 reductase 3 GN=CYB5R3	1,65E+05	3,04E+05	2,56E+05	2,57E+05	3,10E+05	3,07E+05	1,65E+05	2,07E+05
CAD13	5,00	5,00	278,22	0,99	1,00	1,00	0,05	HPX	78694,00	Cadherin-13 GN=CDH13	5,78E+05	7,34E+05	8,16E+05	6,36E+05	6,26E+05	5,86E+05	8,38E+05	7,19E+05
SURF4	3,00	3,00	199,77	0,99	1,00	1,01	0,05	NMX	30602,00	Surfeit locus protein 4 GN=SURF4	3,03E+05	4,31E+05	6,35E+05	3,96E+05	4,88E+05	5,47E+05	3,28E+05	3,80E+05
HS71A	8,00	3,00	441,10	0,99	1,00	1,00	0,05	HPX	70294,00	Heat shock 70 kDa protein 1A GN=HSPA1A	1,16E+05	1,22E+05	1,76E+05	1,65E+05	1,93E+05	1,12E+05	1,35E+05	1,40E+05
CADH2	6,00	6,00	481,06	0,99	1,00	1,03	0,05	HPX	100203,00	Cadherin-2 GN=CDH2	8,34E+05	7,70E+05	1,40E+06	9,20E+05	8,10E+05	6,09E+05	1,52E+06	1,11E+06
PPIB	3,00	3,00	167,72	0,99	1,00	1,04	0,05	NMX	23785,00	Peptidyl-prolyl cis-trans isomerase B GN=PPIB	1,52E+05	6,98E+05	2,92E+05	1,49E+05	3,67E+05	5,78E+05	1,61E+05	1,33E+05
PDIA6	3,00	3,00	186,03	0,99	1,00	1,13	0,05	HPX	48490,00	Protein disulfide-isomerase A6 GN=PDIA6	4,95E+04	2,03E+05	9,97E+04	4,25E+04	1,48E+05	2,28E+05	3,14E+04	4,09E+04
PYRG1	4,00	4,00	170,40	1,00	1,00	1,02	0,05	HPX	67332,00	CTP synthase 1 GN=CTPS1	1,33E+05	1,72E+05	2,01E+05	2,37E+05	2,30E+05	1,36E+05	1,35E+05	2,59E+05
ACLY	19,00	19,00	1137,02	1,00	1,00	1,01	0,05	NMX	121674,00	ATP-citrate synthase GN=ACLY	8,90E+05	1,12E+06	1,50E+06	1,57E+06	1,15E+06	1,03E+06	1,23E+06	1,63E+06
EGFR	3,00	3,00	109,49	1,00	1,00	1,00	0,05	NMX	137612,00	Epidermal growth factor receptor GN=EGFR	9,65E+04	1,47E+05	1,84E+05	1,58E+05	1,07E+05	1,63E+05	1,87E+05	1,27E+05
ARP3	11,00	11,00	606,45	1,00	1,00	1,03	0,05	NMX	47797,00	Actin-related protein 3 GN=ACTR3	8,02E+05	1,07E+06	1,93E+06	1,29E+06	1,65E+06	8,59E+05	1,11E+06	1,35E+06
FAS	15,00	15,00	789,92	1,00	1,00	1,03	0,05	NMX	275877,00	Fatty acid synthase GN=FASN	7,77E+05	4,62E+05	9,52E+05	3,74E+05	7,83E+05	6,75E+05	6,50E+05	3,73E+05
PRDX2	3,00	2,00	123,32	1,00	1,00	1,03	0,05	HPX	22049,00	Peroxiredoxin-2 GN=PRDX2	6,00E+04	8,18E+04	9,02E+04	6,51E+04	1,13E+05	6,47E+04	7,48E+04	5,26E+04
TCPQ	11,00	10,00	569,78	1,00	1,00	1,02	0,05	NMX	60153,00	T-complex protein 1 subunit theta GN=CCT8	2,93E+05	4,95E+05	5,82E+05	4,10E+05	5,62E+05	4,25E+05	4,01E+05	3,60E+05
RL30	2,00	2,00	124,48	1,00	1,00	1,01	0,05	NMX	12947,00	60S ribosomal protein L30 GN=RPL30	2,14E+05	4,24E+05	2,93E+05	3,75E+05	3,90E+05	3,19E+05	2,17E+05	3,70E+05
KPYM	22,00	22,00	1680,48	1,00	1,00	1,05	0,05	NMX	58470,00	Pyruvate kinase PKM GN=PKM	4,20E+06	6,94E+06	1,03E+07	7,11E+06	7,28E+06	6,08E+06	6,72E+06	7,15E+06
NNMT	5,00	5,00	287,59	1,00	1,00	1,03	0,05	NMX	30011,00	Nicotinamide N-methyltransferase GN=NNMT	2,81E+05	3,85E+05	6,58E+05	3,27E+05	4,34E+05	3,41E+05	5,25E+05	3,01E+05

Table 2. GO terms and KEGG pathways

PATHWAY	Enrichment FDR	Enrichement score (-log(FDR value)	nGenes	Pathway Genes	GENES
GO BIOLOGICAL COMPONENT					
Extracellular matrix organization	0,00	3	5	450	FBLN1 LAMC1 COL12A1 ITGB5 HSPG2
Locomotion	0,00	4	8	1982	ITGB5 LAMC1 FBLN1 KRT2 GIPC1 ILK PFN1 RALA
Supramolecular fiber organization	0,00	3	6	919	PFN1 ILK KRT2 ITGB5 COL12A1 HSPG2
Movement of cell or subcellular component	0,00	2	8	2271	ITGB5 LAMC1 FBLN1 KRT2 GIPC1 ARL8B ILK PFN1
Cell adhesion	0,00	2	7	1639	ILK HBB ITGB5 LAMC1 FBLN1 COL12A1 SLC7A1
Endoderm development	0,00	2	3	89	COL12A1 ITGB5 LAMC1
Tissue development	0,00	2	8	2220	COL12A1 LAMC1 HSPG2 KRT2 RALA PFN1 ILK ITGB5
Cell migration	0,00	2	7	1590	ITGB5 LAMC1 FBLN1 KRT2 GIPC1 ILK PFN1
GO CELLULAR COMPONENT					
Extracellular organelle	5,39E-07	6	11	2339	RALA FBLN1 ITGB5 PFN1 COL12A1 GIPC1 ARL8B LAMC1 HSPG2 KRT2 HBB
Extracellular exosome	5,39E-07	6	11	2314	RALA FBLN1 ITGB5 PFN1 COL12A1 GIPC1 ARL8B LAMC1 HSPG2 KRT2 HBB
Extracellular vesicle	5,39E-07	6	11	2337	RALA FBLN1 ITGB5 PFN1 COL12A1 GIPC1 ARL8B LAMC1 HSPG2 KRT2 HBB
Extracellular space	3,22E-07	6	11	3550	RALA FBLN1 ITGB5 PFN1 COL12A1 GIPC1 ARL8B LAMC1 HSPG2 KRT2 HBB
Focal adhesion	0,000193245	4	5	471	RALA ITGB5 PFN1 HSPG2 ILK
Cell-substrate junction	0,000193245	4	5	478	RALA ITGB5 PFN1 HSPG2 ILK
Vesicle	0,000193245	4	11	4396	RALA FBLN1 ITGB5 PFN1 COL12A1 GIPC1 ARL8B LAMC1 HSPG2 KRT2 HBB
Extracellular region	0,000259096	4	11	4658	RALA FBLN1 ITGB5 PFN1 COL12A1 GIPC1 ARL8B LAMC1 HSPG2 KRT2 HBB
Basement membrane	0,000491158	3	3	97	LAMC1 HSPG2 FBLN1
Endocytic vesicle	0,001798195	3	4	421	RALA GIPC1 ITGB5 HBB
GO MOLECULAR FUNCTION					
Extracellular matrix structural constituent	0,000802607	3	4	186	LAMC1 FBLN1 HSPG2 COL12A1
Cell adhesion molecule binding	0,001826081	3	5	577	PFN1 GIPC1 ITGB5 FBLN1 ILK
Integrin binding	0,004582361	2	3	152	ITGB5 FBLN1 ILK
Structural molecule activity	0,004582361	2	5	784	LAMC1 FBLN1 KRT2 HSPG2 COL12A1
Cytoskeletal protein binding	0,012310634	2	5	1050	PFN1 ARL8B GIPC1 KRT2 RALA
Adenylylsulfate kinase activity	0,014876583	2	1	2	PAPSS2
Sulfate adenylyltransferase activity	0,014876583	2	1	2	PAPSS2
Sulfate adenylyltransferase (ATP) activity	0,014876583	2	1	2	PAPSS2
Signaling receptor binding	0,014876583	2	6	1846	ITGB5 RALA FBLN1 ILK GIPC1 HSPG2
Myosin binding	0,014876583	2	2	76	GIPC1 RALA
KEGG PATHWAYS					
ECM-receptor interaction	0,00090492	3	3	88	HSPG2 ITGB5 LAMC1
Focal adhesion	0,005180783	2	3	200	ILK ITGB5 LAMC1
Salmonella infection	0,006556681	2	3	249	PFN1 ARL8B RALA
Sulfur metabolism	0,04576229	1	1	10	PAPSS2
Rap1 signaling pathway	0,04576229	1	2	210	PFN1 RALA
Regulation of actin cytoskeleton	0,04576229	1	2	217	ITGB5 PFN1
Shigellosis	0,04576229	1	2	246	ILK PFN1
Proteoglycans in cancer	0,04576229	1	2	202	HSPG2 ITGB5